

Molecular mechanisms of congenital limb malformations

Inaugural Dissertation

zur

Erlangung des Doktorgrades

Dr. nat. med.

der Medizinischen Fakultät

und

der Mathematisch-Naturwissenschaftlichen Fakultät

der Universität zu Köln



vorgelegt von

Dipl. Biol. Barbara Pawlik

aus Ratibor (Polen)

Köln, 2010

Gutachter: Prof. Dr. Gabriele Pfitzer
Prof. Dr. Peter Nürnberg

Tag der letzten mündlichen Prüfung: 18.10.2010

Contents

1. List of Publications.....	1
1.1 Main publications on human limb malformations	1
1.2 Publications derived from additional projects.....	2
2. Abstract.....	3
2. Zusammenfassung.....	4
3. Introduction	6
3.1 Vertebrate limb development	6
3.2 Signalling pathways important in limb development.....	8
3.2.1 The Shh signalling pathway	8
3.2.2 Fgf signalling.....	9
3.2.3 The canonical Wnt signalling pathway	10
3.2.3.1 Wnt signalling in limb development	12
3.2.3.2 Low-density lipoprotein receptor-related proteins 4 and 6 (Lrp4 & Lrp6)....	12
3.3 Human limb malformation syndromes.....	15
3.3.1 Phenotypes investigated in this study.....	17
3.3.1.1 Cenani-Lenz syndrome.....	17
3.3.1.2 Werner mesomelic syndrome.....	18
3.3.1.3 Split-hand/foot malformation	18
3.3.1.4 Bardet-Biedl syndrome	18
3.3.2 Molecular pathogenesis of SHH limb phenotypes	19
3.3.3 Limb phenotypes due to defective Wnt signalling.....	20
3.3.4 Molecular pathogenesis of split-hand/foot malformation (SHFM) phenotypes	21
3.3.5 Molecular pathogenesis of Bardet-Biedl (BBS) syndrome.....	22
4. Aims and major findings of this Ph.D thesis.....	22
4.1 Aims	22
4.2 Major findings	23
5. Main publications on human limb malformations with own contributions....	24
5.1 A Novel Familial BBS12 Mutation Associated with a Mild Phenotype: Implications for Clinical and Molecular Diagnostic Strategies. (Pawlik et al., 2010) Mol Syndromol (2010); 1:27-34.	24

5.2 LRP4 Mutations Alter Wnt/b-Catenin Signalling and Cause Limb and Kidney Malformations in Cenani-Lenz Syndrome. (Li et al., 2010) Am J Hum Genet (2010); 86(5):696-706.....	26
5.3 A specific mutation in the distant sonic hedgehog cis-regulator (ZRS) causes Werner mesomelic syndrome while complete ZRS duplications underlie Haas type polysyndactyly and preaxial polydactyly with or without triphalangeal thumb. (Wieczorek et al., 2010) Hum Mutat. (2010); 31(1):81-9.	29
5.4 Reduced LRP6-mediated WNT10B signalling in the pathogenesis of SHFM6. (Pawlik et al., submitted).....	31
5.5 Temtamy preaxial brachydactyly syndrome is caused by loss-of-function mutations in Chondroitin synthase 1, a potential target of BMP signalling (Li et al., 2010) in Press Am J Hum Genet (2010).....	34
6. Publications derived from additional projects during this Ph.d.....	37
6.1 A novel loss-of-function mutation in the GNS gene causes Sanfilippo syndrome type D. (Elçioglu et al., 2009) Genet Couns (2009); 20(2):133-9.	37
6.2 Mutation analysis of TMC1 identifies four new mutations and suggests an additional deafness gene at loci DFNA36 and DFNB7/11. (Hilgert et al., 2008) Clin Genet. (2008); 74(3):223-32.....	39
7. Conclusions	41
8. References	42
9. Appendix: Acknowledgements and Academic Curriculum Vitae	48

1. List of Publications

This Ph.D thesis is based on the following publications:

1.1 Main publications on human limb malformations

Pawlik B, Mir A, Iqbal H, Li Y, Nürnberg G, Becker C, Qamar R, Nürnberg P, Wollnik B. **A Novel Familial *BBS12* Mutation Associated with a Mild Phenotype: Implications for Clinical and Molecular Diagnostic Strategies.** Mol Syndromol (2010); 1:27-34.

Li Y*, **Pawlik B***, Elcioglu N, Aglan M, Kayserili H, Yigit G, Percin F, Goodman F, Nürnberg G, Cenani A, Urquhart J, Chung B, Ismail S, Amr K, Aslanger AD, Becker C, Netzer C, Scambler P, Eyaid W, Hamamy H, Clayton-Smith Y, Hennekam R, Nürnberg P, Herz J, Temtamy SA, Wollnik B. **LRP4 Mutations Alter Wnt/b-Catenin Signalling and Cause Limb and Kidney Malformations in Cenani-Lenz Syndrome.** Am J Hum Genet (2010); 86(5):696-706.

* These authors contributed equally to this work

Wieczorek D, **Pawlik B**, Li Y, Akarsu NA, Caliebe A, May KJ, Schweiger B, Vargas FR, Balci S, Gillessen-Kaesbach G, Wollnik B. **A specific mutation in the distant sonic hedgehog cis-regulator (ZRS) causes Werner mesomelic syndrome while complete ZRS duplications underlie Haas type polysyndactyly and preaxial polydactyly with or without triphalangeal thumb.** Hum Mutat. (2010); 31(1):81-9.

Pawlik B, Yigit G, Wollnik B. **Reduced LRP6-mediated WNT10B signalling in the pathogenesis of SHFM6.** (submitted)

Li Y, Laue K, Temtamy S, Aglan M, Kotan L.D, Yigit G, Husniye C, **Pawlik B**, Nürnberg G, Wakeling EL, Quarrell OW, Baessmann I, Lanktree MB, Yilmaz M, Hegele RA, Amr K, May KW, Nürnberg P, Topaloglu AK, Hammerschmidt M, Wollnik B. **Temtamy preaxial brachydactyly syndrome is caused by loss-of-function mutations in Chondroitin synthase 1, a potential target of BMP signalling.** In Press, Am J Hum Genet (2010).

1.2 Publications derived from additional projects

Elçioglu NH, **Pawlik B**, Colak B, Beck M, Wollnik B. **A novel loss-of-function mutation in the GNS gene causes Sanfilippo syndrome type D.** Genet Couns (2009); 20(2):133-9.

Hilgert N, Alasti F, Dieltjens N, **Pawlik B**, Wollnik B, Uyguner O, Delmaghani S, Weil D, Petit C, Danis E, Yang T, Pandelia E, Petersen MB, Goossens D, Favero JD, Sanati MH, Smith RJ, Van Camp G. **Mutation analysis of TMC1 identifies four new mutations and suggests an additional deafness gene at loci DFNA36 and DFNB7/11.** Clin Genet. (2008); 74(3):223-32.

2. Abstract

Congenital limb malformations occur in 1 in 500 to 1 in 1000 human live births and are diverse in their epidemiology, aetiology and anatomy. The molecular analysis of disturbed gene function in inherited limb malformations provides essential information for the understanding of physiological and pathophysiological limb development in humans as well as in other vertebrates. The following Ph.D thesis focussed on the identification and molecular characterisation of disease causing genes and their pathophysiological mechanism for selected human limb defects such as Cenani-Lenz syndrome (CLS), Werner mesomelic syndrome (WMS), Bardet-Biedl syndrome (BBS), Split hand/ foot malformation (SHFM) and Temtamy preaxial brachydactyly syndrome (TPBS).

In this context, we were able to identify novel limb specific genes and causative mutations in different components of evolutionary highly conserved pathways and, furthermore, to elucidate their role in physiological as well as in pathophysiological limb development. In detail, we found (i) alterations in the low-density-lipoprotein-related protein 4 (LRP4), an antagonistic receptor of Wnt signalling, causing the rare autosomal recessive CLS, (ii) specific mutations in the cis-acting limb-specific enhancer of the *sonic hedgehog* (*SHH*) gene being causative for WMS, and (iii) mutations in *CHSY1* to be responsible for TPBS. Furthermore, we could show that mutations in the ciliary protein BBS12 can cause a very mild BBS phenotype.

Moreover, we used in vitro studies to obtain insights into the molecular pathogenesis of these limb malformations. We studied the effect of five LRP4 mutants on the transduction and activation of canonical Wnt signalling by using a Dual-Luciferase Reporter Assay and showed that co-expression of each of the five missense mutations with LRP6 and WNT1 abolish the known antagonistic effect of LRP4 on LRP6-mediated activation of Wnt/ β -catenin signalling and thus conclude that homozygous *LRP4* mutations in CLS cause a loss of protein function.

Additionally, we functionally characterized the first autosomal recessive p.R332W mutation in the *WNT10b* gene causing SHFM6 and rise evidence that p.R332W causes loss of function of Lrp6-mediated Wnt signalling. In this regard we examined the role of the SHFM3 candidate gene *Fgf8* in altering Wnt signalling and demonstrated that *Fgf8* is a novel putative Wnt signalling antagonist which functions by direct interaction with Wnt10b. Hence, we present the first direct cross-talk between Fgf and Wnt signalling pathways and, therefore, physically link two important signalling pathways involved in limb initiation and outgrowth.

2. Zusammenfassung

Congenitale Extremitätenfehlbildungen treten mit einer Inzidenz von 1 in 500 bis zu 1 in 1000 Lebendgeburten auf und sind in ihrer Epidemiologie, Ätiologie und Anatomie sehr mannigfaltig. Die molekulare Analyse von krankheitsverursachenden Genen liefert wichtige Erkenntnisse über physiologische und pathophysiologische Mechanismen der Extremitätenentwicklung. Die nachfolgende Dissertation konzentriert sich auf die Identifikation und funktionelle Charakterisierung von krankheitsverursachenden Genen und ihren pathophysiologischen Mechanismen für ausgewählte humane Extremitätenfehlbildungen wie das Cenani-Lenz-Syndrom (CLS), das Werner mesomele Syndrom (WMS), das Bardet-Biedl-Syndrom, die Spalthand/Spaltfuß-Malformation sowie das Tentamy preaxiale Brachydaktylie-Syndrom (TPBS).

In diesem Zusammenhang ist es uns gelungen, neue extremitätenspezifische Gene und kausale Mutationen in verschiedenen Komponenten von evolutionär hoch konservierten Signalwegen zu identifizieren. Darüber hinaus konnten wir die physiologische und pathophysiologische Rolle jener Gene aufklären. Im Einzelnen fanden wir heraus, dass (i) Veränderungen im low-density-lipoprotein-related Protein 4 (LRP4), einem antagonistischen Rezeptor des Wnt Signalweges, ursächlich sind für das seltene, autosomal rezessive CLS, dass (ii) spezifische Mutationen im extremitätenspezifischen, cis-agierenden, regulatorischen Element des *sonic hedgehog* (*SHH*) Genes das WMS verursachen und dass (iii) Mutationen im *CHSY1*-Gen kausal sind für das TPBS. Des Weiteren konnten wir nachweisen, dass Mutationen im ziliären BBS12-Protein einen sehr mild ausgeprägten Phänotyp im BBS bewirken.

Im weiteren Verlauf des Projekts nutzten wir verschiedene *in vitro* Studien, um die molekulare Pathogenese der genannten Extremitätenfehlbildungen aufzuklären. Wir untersuchten den Effekt von fünf verschiedenen LRP4-Mutanten auf die Transduktion und Aktivierung des kanonischen Wnt Signalweges mittels eines Dual-Luciferase-Assays und konnten zeigen, dass die Ko-Expression jeder Mutante mit LRP6 und WNT1 den wildtypischen antagonistischen Effekt von LRP4 auf den kanonischen Wnt Signalweg aufhebt. Daher schlussfolgern wir, dass homozygote Mutationen im *LRP4*-Gen CLS verursachen und zu einem Funktionsverlust des LRP4-Proteins führen. Zusätzlich haben wir die erste rezessive p.R332W Wnt10b-Mutation, die ursächlich für SHFM ist, mittels eines Dual-Luciferase-Assays funktionell charakterisiert und nachgewiesen, dass die p.R332W Mutation zu einem Proteinfunktionsverlust des Lrp6-vermittelten Wnt Signalweges führt. In diesem Zusammenhang untersuchten wir ebenfalls die Rolle des Kandidatengens *Fgf8* für

SHFM3 im Wnt Signalweg. Mit Hilfe des Dual-Luciferase-Assays ist es uns gelungen, *Fgf8* als neuen Wnt Signalweg Antagonisten, der direkt an Wnt10b binden kann, zu identifizieren. Somit zeigen wir die erste direkte Interaktion zwischen dem Fgf und Wnt Signalweg und verbinden hierdurch zwei wichtige Signalwege miteinander, die an der Extremitätenentwicklung maßgeblich beteiligt sind.

3. Introduction

3.1 Vertebrate limb development

The genetic processes that control limb development in vertebrates are complex and still not fully understood. The current understanding of the molecular genetics of limb development was mainly achieved from (i) experiments manipulating genetic interactions of temporal and spatial expression of individual genes in vertebrates and invertebrates and (ii) identification of genes involved in congenital limb malformations in mouse and human and the subsequent functional analysis of the underlying pathogenesis.

The human limb buds are built on day 26 for the upper limb and day 28 for the lower limb by the activation of mesenchymal cells of the lateral mesodermal plate. During the onset of outgrowth, the distal border of the ectoderm thickens to form the apical ectodermal ridge (AER). The developing limb is characterized by three different compartments; the proximal stylopod, the middle zeugopod and the distal autopod and it is patterned into three axes; the proximal-distal (PD), the anterior-posterior (AP) and the dorsal-ventral (DV) axis. During human development the AP limb axis corresponds to the primary body axis and manifests itself in the skeletal morphology of the zeugopod with the radius/ulna in the upper limb and the tibia/fibula in the lower limb and in the distinct identities of the autopod developing into digits. The thumb has the most anterior and the little finger has the most posterior identity in the autopod.

The AER is an important organizing center for limb bud development and controls the outgrowth and the patterning of the PD limb bud axis (Saunders 1948). Initially, T-box family transcription factors *TBX4* and *TBX5* activate *FGF10* and *WNT3* (Barrow et al. 2003) to initiate the outgrowth of the limb bud (Rallis et al. 2003). T-box genes may modify the morphology of limbs by selectively inducing or repressing genes that are specific either for the forelimb or the hindlimb. For instance, *TBX5* can induce expression of the forelimb marker *HOX9* and repress the hindlimb marker *HOXC9* (Rodriguez-Esteban et al. 1999; Takeuchi et al. 1999). The *HOX* gene family is instrumental in proximal-distal patterning. *HOX* genes become up-regulated e.g. by retinoic acid (RA) in the limb bud and especially genes from the *HOX-A* and *HOX-D* clusters are involved in limb patterning (Yashiro et al. 2004). For instance, *HOXD9* is expressed across the whole limb during zeugopod development, but *HOXD13* is restricted to the posterior part of the limb. *HOXD10*, *-11* and *-12* are expressed in an overlapping pattern between *HOXD9* and *HOXD13*. This differential

expression creates the morphological differences between the radius and the ulna in the forelimb and the tibia and fibula in the hindlimb (Zakany and Duboule 2007).

The AP axis is patterned and controlled by the zone of polarising activity (ZPA), which consists of a collection of cells at the posterior border of the developing limb. The formation of the ZPA depends on the expression of *HOXB-8* and RA in the posterior mesoderm (Charite et al. 1994). The development of the AP axis is mainly mediated through the expression of *sonic hedgehog* (*SHH*), which is up-regulated in the ZPA through RA (Riddle et al. 1993). A complicated set of positive and negative feedback loops exists, in which e.g. SHH stimulates FGFs in the AER and FGFs in the AER activate SHH in the ZPA (Zuniga et al. 1999).

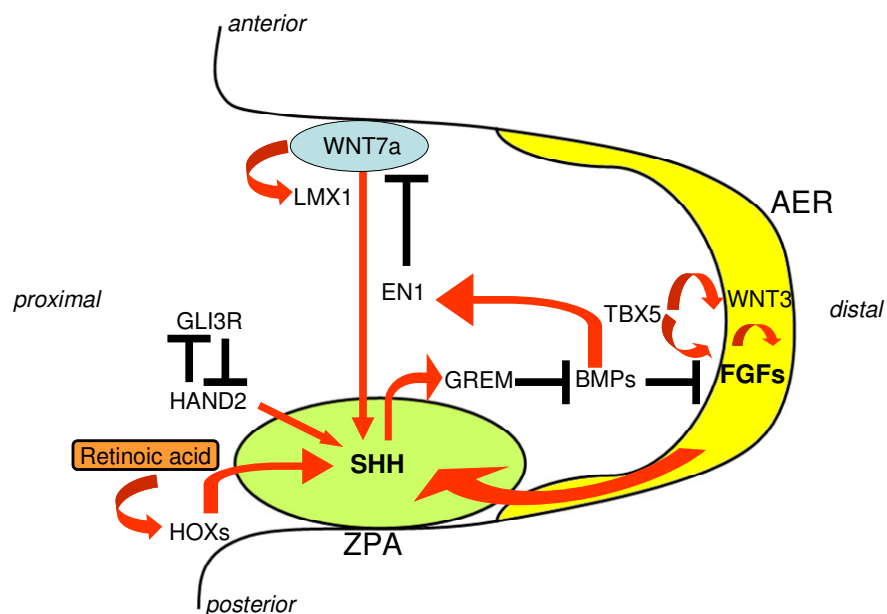


Figure 1: The developing limb bud with the relative position of the zone of polarizing Activity and the apical ectodermal ridge (AER). *TBX5* induces *WNT3* expression which itself triggers the expression of FGFs and thereby forms the AER. FGFs from the AER together with retinoic acid and different *HOX* genes induce the expression of *SHH* in the ZPA. The SHH signal is maintained by *WNT7a*, which itself is repressed by engrailed 1 (EN1).

WNT7a, which is one of the factors responsible for the preservation of the SHH signal in the ZPA, was shown to be mainly involved in the development of the DV axis by inducing the transcription factor *LMX1*, which specifies cells to the dorsal site. *WNT7a* itself is repressed by the transcription factor *engrailed 1*, which is induced by bone morphogenic proteins

(BMPs) from the ventral ectoderm (Dealy et al. 1993). BMPs, which are expressed in response to the SHH signal from the ZPA, act via cell surface bone morphogenic protein receptors (BMPRs) and are essential for the formation of bone and cartilage. For instance BMP2 plays a key role in osteoblast differentiation and induction of bone formation while BMP4 controls the formation of limbs from the mesoderm. Under the influence of SHH, BMP2 and BMP7 play a major role in digit identity and formation (Zou and Niswander 1996; Jena et al. 1997). Finally the temporal and spatial control of progressive skeletal development is monitored by SOX9 and RUNX2, which initiate the condensation and differentiation of chondroblasts in the developing limb (Weston et al. 2003).

3.2 Signalling pathways important in limb development

Vertebrate limb development results from a temporally and spatially co-ordinated expression of many different genes and pathways including the Shh-Gli, Fgf and Wnt signalling-pathway. Because defects in these pathways have dramatic and devastating effects on limb development the understanding and investigation of each of them is of high relevance. In the following, some of the most important signalling pathways for vertebrate limb development are described separately, although it has to be mentioned that in the limb bud a complex interaction between these pathways might exist, which forms different positive and negative feedback loops and thereby maintains the expression of a specific signal.

3.2.1 The Shh signalling pathway

In human development, the *SHH* gene is expressed in the gut, the neural tube and in the zone of polarizing activity in the posterior part of the limb bud (Odent et al. 1999). The elements of the Shh-Patched-Gli-pathway are highly conserved among species, indicating the essential role of this pathway during development.

In order to function in development patterning, the SHH protein first needs to be processed to an active N-terminal form, which is modified by the addition of cholesterol (Pepinsky et al. 1998; Williams et al. 1999). The SHH protein functions by binding to its 12-span transmembrane receptor proteins PATCHED-1 (PTCH-1) and PATCHED-2 (PTCH-2) (Stone et al. 1996). Without the SHH signal, PTCH-1 and PTCH-2 block downstream signal transduction through a physical interaction with the 7-span transmembrane protein SMOOTHENED (SMO). Binding of SHH to PTCHs results in the activation of GLI zinc

finger transcription factors which are normally inhibited by the suppressor-of-fused (SUFU). The activation of the intracellular signal transduction by SHH releases Gli1 which finally activates gene expression (Huangfu and Anderson 2006).

Genetic analysis in the transgenic mouse mutant Sasquatch (Ssq), which resembles a pre-axial polydactyly phenotype, showed initial evidence for the regulation of the *SHH* gene (Lettice et al. 2003). In the Ssq mouse, a random transgenic insertion of a HOXB1 human placental alkaline phosphatase construct on chromosome 5 displays extopic SHH expression at the anterior margin of the developing limb bud. The transgene insertion was physically linked to SHH, but is placed in intron 5 of the neighbouring gene *LMBR1* (limb-region homolog 1) located about 1 Mb away (Lettice et al. 2003). A cis-trans test showed that this 800 bp long highly conserved region, which was named zone of polarizing activity regulatory sequence (ZRS), acts as a cis enhancer to directly affect the expression of the *SHH* gene (Lettice et al. 2003). The authors concluded that the ZRS is responsible for initiation of SHH expression in limb bud development and that it also drives the posteriorly restricted spatial expression pattern (Lettice et al. 2003).

3.2.2 Fgf signalling

Fibroblast growth factors (FGFs) belong to a large family of highly conserved polypeptide growth factors which mediate a variety of cellular responses during embryonic development and in the adult organism. FGFs function by binding and activating their specific cell surface tyrosine kinase Fgf receptors (FGFRs) (Ornitz and Itoh 2001) and the Fgf signalling pathway itself is one of the most ubiquitous in biology. Ligand binding results in receptor dimerization and activation of intrinsic tyrosine kinases, leading to trans-phosphorylation of multiple tyrosine residues on the receptor. These residues then serve as docking sites for the recruitment of SH2 (src-homology-2) or PTB (phosphotyrosine binding) domains of adaptors, docking proteins or signalling enzymes (Dailey et al. 2005). Activated FGFRs then act as transducers for several downstream intracellular signalling pathways, including extracellular signal-regulated kinase (ERK), p38 mitogen-activated kinases, phospholipase C gamma, protein kinase C (PKC) and phosphatidylinositol 3-kinase (PI3K)(Klint and Claesson-Welsh 1999).

Fgf signalling is crucial for the PD outgrowth in human limb development. In the developing limb bud, the AER is positioned and induced by the expression of Fgf8 and Fgf10, followed by expression of Fgf4 (Niswander et al. 1993). A positive feedback loop, regulated by the

Wnt signalling pathway, is then established between Fgf8 and Fgf10, such that Fgf10 promotes Fgf8 expression and Fgf8 promotes Fgf10 expression (Agarwal et al. 2003). Further evidence for the importance of the pathway in limb development comes from a conditional knockout of Fgf4 and Fgf8. Mouse lacking these two gene products fails to form limbs (Sun et al. 2002).

3.2.3 The canonical Wnt signalling pathway

The Wnt signalling pathway is an evolutionary highly conserved pathway in metazoan animals that regulates fundamental aspects of cell fate determination, cell migration, cell polarity, neural patterning and organogenesis during embryonic development. The extra-cellular Wnt signal induces several intra-cellular signal transduction cascades such as the canonical or Wnt/ β -catenin-dependent pathway and the non-canonical or β -catenin-independent pathway which can be further split into the Planar Cell Polarity pathway and the Wnt/ Ca^{2+} pathway (Wodarz and Nusse 1998). Wnt proteins are secreted glycoproteins that bind to the N-terminal extra-cellular domain of the frizzled (Fz) receptor family and their expression during development is restricted both temporally and spatially (Yamaguchi 2001; He et al. 2004). Low-density-lipoprotein receptor-related protein 5/6 (LRP5/6) are required for mediating the Wnt signalling (He et al. 2004). Also Norrin and R-Spondin, which can bind to the LRP5/6 receptor, are capable of activating Wnt signalling independent of a Wnt signal (Kazanskaya et al. 2004; Xu et al. 2004). A key mechanism in regulating Wnt signalling is the presence of diverse numbers of secreted Wnt antagonists like dickkopf (DKK) proteins, wise, cerebrus, Wnt-inhibitor protein (WIF) or the Sost protein (Bouwmeester et al. 1996; Glinka et al. 1998; Itasaki et al. 2003; Semenov et al. 2005; Cadigan and Liu 2006).

The hallmark of the canonical Wnt pathway is the accumulation and translocation of cytoplasmic β -catenin into the nucleus. Without Wnt signalling, β -catenin is degraded by axin, adenomatosis polyposis coli (APC), protein phosphatase 2A (PP2A), glycogen synthase kinase 3 (GSK3) and casein kinase 1 α (CK1 α) (He et al. 2004; Gordon and Nusse 2006). Phosphorylation of β -catenin within this complex targets it for ubiquitilation and proteolytic destruction by the proteosomal machinery (He et al. 2004). After binding to the receptor complex, the Wnt signal is first transduced to cytoplasmic dishevelled (DSH) which is able to directly interact with Fz (Wallingford and Habas 2005). This induces the phosphorylation of LRP5/6 by CK1 and GSK3- β and allows the translocation of axin from the cytosol to the membrane. Axin now binds to the phosphorylated LRP5/6 and this triggers the stabilisation of

β -catenin via either sequestration and/or degradation of axin and allows the translocation of β -catenin to the nucleus where it complexes with LEF/TCT family members to mediate transcriptional activation of target genes (Mao et al. 2001b; He et al. 2004; Zeng et al. 2008). These target genes then control posterior patterning, heart, lung, kidney, skin and bone formation (Yamaguchi 2001; Logan and Nusse 2004; Clevers 2006).

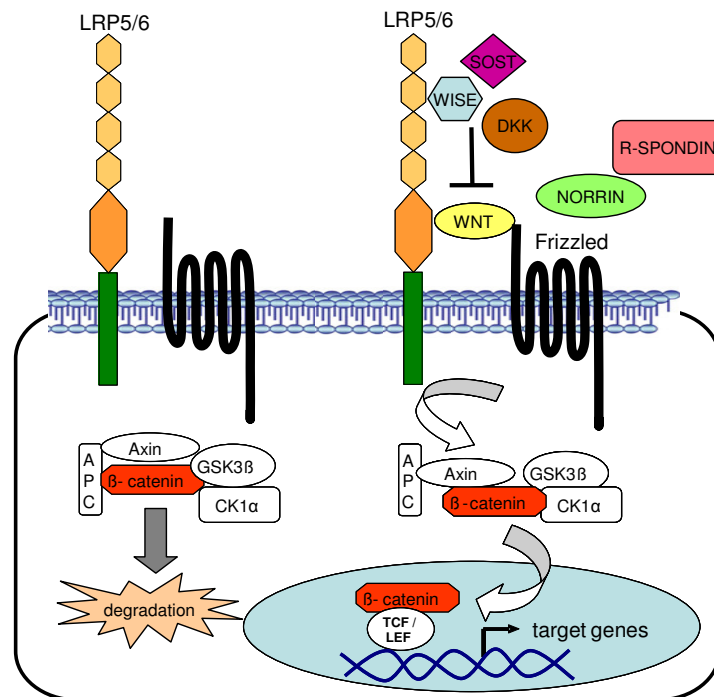


Figure 2: The canonical Wnt-signalling pathway. Without a ligand, β -catenin gets ubiquitinated and degraded. Binding of e.g. Wnts, NORRIN or R-SPONDIN2 results in the translocation of β -catenin to the nucleus where it binds to TCF/LEF and induces the expression of target genes. WISE, DKK and SOST are known inhibitors of canonical Wnt-signalling.

3.2.3.1 Wnt signalling in limb development

Wnt signalling plays a fundamental role in the developing limb bud and controls multiple processes such as limb patterning and limb morphogenesis. Several Wnt genes such as Wnt3, Wnt4, Wnt6, Wnt7a, Wnt7b, Wnt9b, Wnt10a, Wnt10b and Wnt16 are highly expressed in the ectoderm and AER during early limb development (Witte et al. 2009) and especially Wnt3 has been shown to be essential for limb initiation and AER induction (Barrow et al. 2003). Wnt3 in the developing limb bud triggers the expression of Fgf10 and Fgf8 and leads to a positive feedback loop between these three components which is required for AER maintenance and the proximal-distal limb outgrowth (Barrow et al. 2003). Furthermore, Wnt signalling is important for determining the dorsal-ventral limb identity (Galceran et al. 1999). Wnt7a is highly expressed in the dorsal limb ectoderm and is responsible for dorsal-ventral patterning by regulating the expression of Lmx1b, a factor which determines the dorsal mesodermal cell fate in the limb (Parr et al. 1993; Parr and McMahon 1995). In addition, Wnt7a signalling also regulates the expression of Shh in the ZPA and, since there is a positive feedback loop between Shh and Fgf4 in the AER (Laufer et al. 1994; Niswander et al. 1994), Wnt7a signalling also indirectly affects AP and DP patterning in the limb bud.

During late limb morphogenesis, Wnt signalling is determining the position and morphology of limb structures such as muscles, tendons and skeletal elements (Yang 2003). Wnt11 for instance is expressed in the periphery of the limb mesoderm and is involved in muscle fibre differentiation whereas Wnt5a triggers muscle fibre specification (Anakwe et al. 2003). Finally, Wnt signalling is also involved in bone formation by regulating chondrogenic differentiation from mesenchymal progenitors as well as osteoblast proliferation (Rudnicki and Brown 1997; Hartmann and Tabin 2001). While Wnt5a was found to promote chondrocyte differentiation in the distal limb bud (Yang et al. 2003), Wnt1, Wnt7a and Wnt14 are known inhibitors of chondrocyte differentiation (Hartmann and Tabin 2001).

3.2.3.2 Low-density lipoprotein receptor-related proteins 4 and 6 (Lrp4 & Lrp6)

The low-density lipoprotein receptor (Ldlr) superfamily consists of 10 structurally related proteins. Lrp1, Lrp1b, Lrp2, Ldlr, Vldlr, Lrp4, Lrp5, Lrp6, Lrp8 and Lrp12 are cell surface receptors with diverse biological functions such as lipid metabolism, protection against atherosclerosis, neurodevelopment, the transport of nutrients and vitamins and limb development (May et al. 2007).

Lrp4 or multiple EGF-like domain LDL receptor related protein 4 (Megf7) is associated with limb development and the formation of digits (May et al. 2007). Like all family members, Lrp4 exhibits a ligand binding type repeat, EGF-precursor homology domains, an O-glycosylation domain, a transmembrane domain, a cytoplasmatic tail and, similar to Lrp1, an NPxY sequence which mediates it to the endocytic machinery (Chen et al. 1990). LRP4 is expressed in migratory primordial germ cells in the hindgut, in spermatogonia of the neonatal, adult testis and in the immature oocytes and follicular cells in females (Yamaguchi et al. 2006). The Lrp4 knockout mouse is characterized by polysyndactyly of the fore and hind limbs, craniofacial and tooth abnormalities (Johnson et al. 2005). Johnson et al. could show that the loss of Lrp4 results in an abnormal expression of important signalling molecules like Fgf8, Shh, Bmp2, Bmp4 and Wnt7a, which are crucial for normal digit formation. Moreover, the authors demonstrate that Lrp4 is able to inhibit the Wnt-induced activation of the Luciferase Reporter in an activity assay, assuming that Lrp4 antagonizes the Lrp5/6 mediated activation of the pathway. LRP4 mutations causing syndactyly have so far been found in Holstein cattle (Duchesne et al. 2006).

Recently, Choi et al. showed that Lrp4 is also expressed in osteoblasts and that it regulates bone growth and turnover in vivo by binding sclerostin, an osteocyte secreted inhibitor of bone formation (Choi et al. 2009). The authors could also demonstrate that Lrp4 is a receptor for Dkk1, another inhibitor of Wnt/ β -catenin signalling. Finally, another group reported that Lrp4 is expressed in epithelial cells during tooth development and that it binds the Bmp antagonist Wise through its highly conserved EGF-like domain and thus acting as a modulator and integrator of Bmp and Wnt signalling during tooth morphogenesis (Ohazama et al. 2008).

Another prominent member of the Ldlr family is the *LRP6* gene located on human chromosome 12p13.3-p11.2 encoding the low-density lipoprotein receptor-related protein 6 (LRP6) (Brown et al. 1998). Lrp6 functions as a coreceptor for Wnt signal transduction by activating Wnt-frizzled signalling as well as Wnt-responsive genes. It could be shown that the extracellular domain of Lrp6 binds Wnt1 and thereby induces dorsal axis duplication and neural crest formation (Tamai et al. 2000). Furthermore, it could be elevated that Lrp6 is a specific, high-affinity receptor for Dkk1 and Dkk2 and that Dkk1 and Lrp6 interact antagonistically during embryonic head formation in *Xenopus laevis* (Mao et al. 2001a). Moreover, Semenov et al. found that human SOST protein antagonizes Wnt signalling by binding the extracellular domain of the LRP6 receptor and thereby disrupts the Wnt-induced frizzled LRP complex formation (Semenov et al. 2005). LRP6 itself gets phosphorylated via

the glycogen synthase kinase-3 (GSK3) and casein kinase-1 and this dual phosphorylation promotes the interaction of LRP6 with the scaffolding protein axin and the stabilization of β -catenin in Wnt signalling (Zeng et al. 2008).

Homozygous *Lrp6* null mice die at birth and exhibit a variety of severe developmental abnormalities, including the truncation of the axial skeleton, limb defects, microphthalmia, and malformations of the urogenital system (Pinson et al. 2000) (Kelly et al. 2004). Also in the *Lrp6*^{-/-} embryo, *Fgf8* expression is significantly reduced, suggesting that the AER is degenerated as a result of weakened canonical Wnt signalling (Pinson et al. 2000). A single human *LRP6* missense mutation has so far been identified and linked to a large Iranian family with early coronary artery disease and metabolic syndrome (Mani et al. 2007).

In conclusion, the *Lrp*-gene family is an evolutionary conserved multifunctional class of receptors acting in fundamental signal transduction pathways including BMP, TGF β , and canonical Wnt signalling with diverse physiological tasks.

3. 3 Human limb malformation syndromes

Congenital limb malformations belong to a rare group of genetically and clinically heterogeneous disorders with a very diverse spectrum in their epidemiology, aetiology and anatomy. Limb malformations manifest themselves as an isolated trait or as a part of a syndrome. Congenital hand and feet anomalies can be generally classified into malformations, deformations, disruptions and dysplasias. Malformations result as a structural defect in the embryo or fetus due to an abnormal development. Deformations are defined as a change from the normal size or shape of an anatomic structure due to mechanical forces that distort an otherwise normal structure. Disruptions are characterized by a destruction of a previously normally formed fetal body part due to external influences such as infections, and dysplasias refer to an abnormal formation of a body structure or tissue based on disturbed organogenesis. Furthermore, inherited hand anomalies are clinically grouped as polydactyilies, ectrodactyilies, brachydactyilies and syndactyilies.

Polydactyilies are distinguished by the appearance of supernumary digits or parts of them, which may be present as a complete duplication of a whole limb or as a duplication of single digits (Schwabe and Mundlos 2004). Preaxial polydactyly with extra digits located on the side of the hand of the thumb or postaxial polydactyly where the extra digit is found on the side of the hand or foot of the fifth digit are common isolated limb malformation traits. As a part of a syndrome, they may be detected in e.g. Smith-Lemli-Opitz syndrome, McKusick-Kaufmann syndrome, Bardet-Biedl syndrome or Greig cephalosynpolydactyly where the polydactyly is present both pre-and postaxial (Schwabe and Mundlos 2004). Another example is Pallister-Hall syndrome with a rare central or postaxial polydactyly.

Ectrodactyly involves the deficiency or absence of one or more central digits of the hand or foot with the absence of distal segments such as phalanges (aphalangia), fingers (adactyly) or the entire limb (acheiria). Ectrodactyilies often appear sporadically with only one hand or foot affected and most of the cases are considered to be non-genetic but due to disruptions in development. A prominent disease in the group of ectrodactyilies is split-hand/foot malformations, which may occur isolated or in combination with other features and which is phenotypically characterized by the deficiency of the central rays with a median cleft. Another example is Holt-Oram syndrome where a variable spectrum of the upper limb defects with shoulder girdle ranging from thumb hypoplasia to phocomelia is found (Schwabe and Mundlos 2004).

Brachydactyilies are defined by shortened digits and are classified on an anatomic and genetic background into five groups from A to E. Isolated brachydactyilies are often inherited in an

autosomal dominant manner and are characterized by a high degree of phenotypic variability. Brachydactylies can be also associated with a syndrome, for example Rubinstein-Taybi syndrome with short thumbs. A hallmark of type A brachydactylies is hypoplasia or aplasia of the middle phalanges in contrast to type B, where distal phalanges are missing, and where nail hypoplasia and distal or proximal symphalangism may be present. Type C brachydactylies are characterized by brachymesophalangy of the second, third and fifth fingers, hyperphalangy and shortening of the first metacarpals. Finally, a shortened distal phalanx of the thumbs is observed in type D brachydactylies and type E brachydactylies show a variable shortening of the metacarpals.

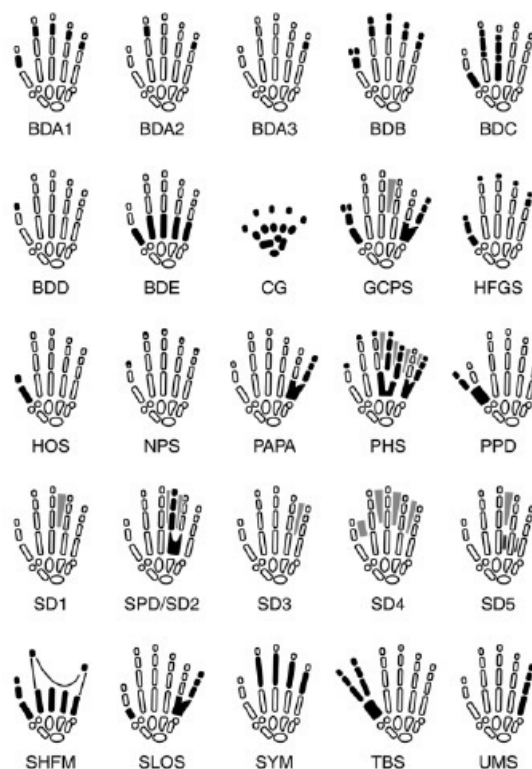


Figure 3: Schematic representation of congenital limb anomalies (Schwabe and Mundlos 2004).

The last and most frequent congenital limb malformation in Europe and North America are syndactylies, which are characterized by the fusion of the soft tissues of fingers and toes with or without bone fusion. Syndactylies are due to the lack of apoptosis in the interdigital mesenchyme and may also occur isolated or with other symptoms in a syndrome. The syndromal forms include Poland syndrome with symbrachydactyly, Saethre-Chotzen syndrome, Pfeiffer syndrome, and Fraser syndrome to mention only some of them. Isolated forms are grouped in categories from one to five according to the degree of affecting different

interdigital spaces (Schwabe and Mundlos 2004). A severe isolated syndactyly is syndactyly type IV (also known as Hass type syndactyly) where a total fusion of all fingers is observed.

3.3.1 Phenotypes investigated in this study

During this Ph.D study, cohorts of different human congenital limb patients were collected and the molecular cause of different defects such as Cenani-Lenz syndrome, Werner-mesomelic syndrome, split-hand/foot malformations and Bardet-Biedl syndrome were investigated. All these limb defects are due to mutations in different developmental genes, stages and pathways and therefore resemble an overview on the complex genetic concept necessary for proper limb development.

3.3.1.1 Cenani-Lenz syndrome

Cenani-Lenz Syndrome (CLS) was first described in 1967 by Cenani and Lenz (Cenani and Lenz 1967) in two brothers. CLS is a rare autosomal recessive disorder mainly characterized by total syndactyly of the hand and feet (so called spoon hands), bilateral radioulnar synostosis and metacarpal fusion. Additional features include mild facial dysmorphism such as a high broad, hypertelorism, a depressed nasal bridge, a short nose, a short prominent philtrum and malar hypoplasia (Temtamy et al. 2003). Also bilateral renal hypoplasia (Bacchelli et al. 2001) and oligodontia with flat head `screwdriver-shaped` incisors (Elliott et al. 2004) have been reported in some patients. The limb abnormalities in CLS closely resemble those found in the recessive mouse mutant `limb deformity` (ld) which is suffering from syndactyly, bone fusions, radioulnar and radiotarsal synostosis and renal malformations (Bacchelli et al. 2001). The ld mouse phenotype is a result of homozygous *Formin* mutations and, therefore, Formin and its downstream targets such as Gremlin were considered to be good candidate genes for human CLS. However, no alterations in either *FORMIN* or *GREMLIN* could be identified in CLS patients (Bacchelli et al. 2001), so the aetiology of this rare disorder was unknown at the initiation of this Ph.D thesis.

3.3.1.2 Werner mesomelic syndrome

Werner mesomelic syndrome (WMS), also known as tibial hypoplasia-polysyndactyly-triphalangeal thumb syndrome, was first reported by Werner in 1912 (Werner et al 1912). WMS is an autosomal dominant disorder with hypo- or aplasia of the tibiae resulting in short stature, preaxial polydactyly of the hands and feet and/or five-fingered hands and triphalangeal thumbs being distinctive features (Werner et al 1912). Triphalangeal thumb is a common autosomal dominant hand malformation, which can occur isolated or as a clinical feature of different syndromic conditions e.g. Holt Oram syndrome (Basson et al. 1997), lacrimo-auriculo-dento-digital syndrome (Rohmann et al. 2006) or Nager acrofacial dysostosis (McDonald and Gorski 1993). At the onset of this Ph.D thesis the molecular basis for WMS was unknown.

3.3.1.3 Split-hand/foot malformation

Split-hand/split foot malformation (SHFM), also known as ectrodactyly, is a congenital limb malformation involving the central rays of the autopod and characterized by syndactyly, median cleft of the hands and feet, aplasia and/or hypoplasia of the phalanges, metacarpals and metatarsals (Duijf et al. 2003). SHFM can manifest itself as an isolated entity or as a part of a syndrome and is phenotypically highly variable. Familial SHFM is often inherited in an autosomal dominant manner with reduced penetrance (Ozen et al. 1999), but also autosomal recessive (Gul and Oktenli 2002) as well as X-linked forms (Ahmad et al. 1987) are known. Recently the first autosomal recessive mutation in the *WNT10B* gene causing SHFM6 was identified in a large consanguineous family from Turkey (Ugur and Tolun 2008). *Wnt10b* is expressed throughout the mouse limb ectoderm from E.9.5 to E.15.5 (Witte et al. 2009) and a well-known regulator of osteoblastogenesis and bone mass (Bennett et al. 2005). However, the molecular pathophysiological mechanism of *WNT10B* mutations causing SHFM6 was unknown at the onset of this Ph.D study.

3.3.1.4 Bardet-Biedl syndrome

Bardet-Biedl syndrome (BBS) is an autosomal recessively inherited ciliopathy with red cone dystrophy, postaxial polydactyly, obesity, renal tract anomalies, learning difficulties or mental retardation and hypogonadism being distinct features (Beales et al. 1999). Postaxial

polydactyly with syndactylies and brachydactylies is observed in about 70% of all cases whereas other features such as hearing loss or dental anomalies are rare (Beales et al. 1999). In this study, we investigated a consanguineous family from Pakistan with postaxial polydactyly and late-onset retinal dysfunction. Adult affected individuals did not display any renal or genital anomalies, obesity, mental retardation or learning difficulties and did thus not fulfill the proposed clinical diagnostic criteria for BBS.

3.3.2 Molecular pathogenesis of SHH limb phenotypes

Components of the SHH-PTCH-GLI pathway, which plays a major role in anterior-posterior patterning of the limb, are known to cause severe congenital human limb disorders (Figure 4). Sporadic and inherited mutations in the human *SHH* gene itself are causative for holoprosencephaly, the most common structural malformation of the human forebrain characterized by cleft lip, absent olfactory bulbs, tracts and the corpus callosum, hypotelorism and/or a single cyclopic eye (Roessler et al. 1996).

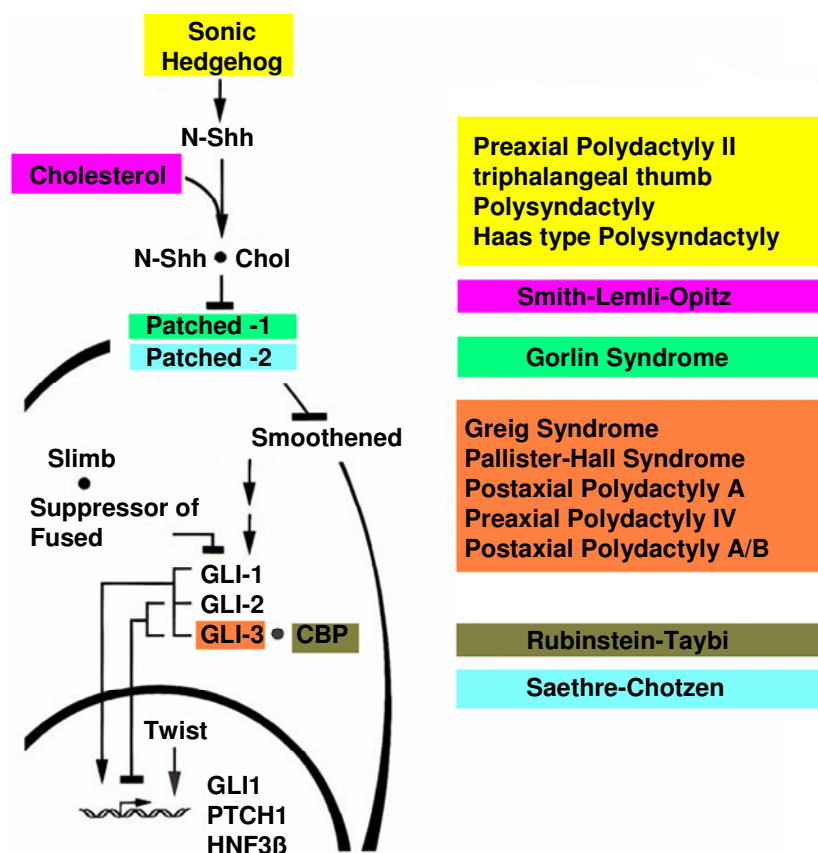


Figure 4: Human disorders associated with mutated elements of the SHH signalling pathway (Villavicencio et al. 2000).

Mutations in human *GLI3* have been detected in several types of limb malformation syndromes. Structural alterations such as translocations and deletions but also point mutations throughout the *GLI3* gene cause Greig Cephalopolysyndactyly syndrome, which manifests itself by syndactyly, preaxial polydactyly, broad thumbs and first toes, facial anomalies such as hypertelorism and frontal bossing (Vortkamp et al. 1991) whereas, *GLI3* frameshift and nonsense mutations cause the postaxial polydactyly syndactyly Pallister Hall syndrome (Kang et al. 1997). Recently, also frameshift, nonsense and missense *GLI3* mutations were shown to be responsible for human preaxial polydactyly type A, autosomal dominant preaxial polydactyly type IV and postaxial polydactyly type A/B (Radhakrishna et al. 1997).

Mutations in the zone of polarizing activity regulatory sequence (ZRS), a long-range limb-specific enhancer of *SHH*, have been identified in patients with preaxial polydactyly type II (PPD2) (Lettice et al. 2002; Li et al. 2009), triphalangeal thumb polysyndactyly (TPTPS) (Sun et al. 2008; Wu et al. 2009) and syndactyly type IV (SD4, Haas type polysyndactyly) (Sun et al. 2008).

3.3.3 Limb phenotypes due to defective Wnt signalling

Mutations of any element of the Wnt signalling pathway (Table 1) have been shown to cause a wide spectrum of limb malformations. For instance, mutations in *WNT3* have been found in the rare autosomal recessive disorder tetra-amelia, characterized by the absence of all four limbs (Niemann et al. 2004) and homozygous nucleotide changes in *WNT10B* lead to the scarce recessive split-hand/split foot malformation (Ugur and Tolun 2008). Furthermore, odonto-onycho-dermal-dysplasia which is characterized by hyperkeratosis and hyperhidrosis of the palms and soles, atrophic malar patches, hypodontia, conical teeth, onychodysplasia, and dry and sparse hair, is caused by a homozygous nonsense mutation in exon 3 of the *WNT10A* gene (Adaimy et al. 2007).

Also, alterations in Wnt signalling receptors are associated with different diseases. Loss-of-function and gain-of-function mutations in *LRP5*, which are associated with the regulation of bone mass and osteoporosis like in osteoporosis pseudoglioma syndrome (Gong et al. 2001), demonstrate the receptors' significance for proper bone development.

Gene	Human disease
WNT3	Tetra-amelia
WNT10A	Odonto-onycho-dermal-hypoplasia
WNT10B	Split-hand/foot malformation
LRP5	High bone mass, osteoporosis-pseudoglioma

Table 1: Human limb malformations with mutations in Wnt signalling components (MacDonald et al. 2009).

3.3.4 Molecular pathogenesis of split-hand/foot malformation (SHFM) phenotypes

SHFM is genetically very heterogenous and six loci have been described so far with autosomal dominant SHFM1 on 7q21-22, the X-linked form SHFM2 on Xq26, SHFM3 on 10q24, SHFM4 on 3q28, SHFM5 on chromosome 2q31 and the autosomal recessive SHFM6 on 12q13.11-13 (Scherer et al. 1994; Ianakiev et al. 2000; Goodman et al. 2002; Roscioli et al. 2004; Faiyaz-Ul-Haque et al. 2005; Ugur and Tolun 2008). SHFM1 is caused by chromosomal deletions on 7q21-22, which abolish the expression of the candidate genes *DLX5*, *DLX6* and *DSS1* in this region. However, no mutations in the coding region of these genes have been identified so far in any SHFM1 patient, indicating a putative long range enhancer in this region to cause the phenotype (Crackower et al. 1996). SHFM2 is due to translocations or X-chromosomal rearrangements on Xq26 which share the candidate genes *FGF13* and *TONDU* (Faiyaz-Ul-Haque et al. 2005). The SHFM3 locus is defined to a minimal 325-kb region on 10q24 containing the *BTRC* gene (Lyle et al. 2006), which is the human orthologue of *Drosophila* Slimb, an F-box/WD40 repeat protein and a regulator of the SHH and Wnt signalling pathway (Jiang and Struhl 1998). Also, only chromosomal rearrangements like duplications could be found in patients (Kano et al. 2005) but no mutations in the *BTRC* gene itself, again suggesting an regulatory element to cause the malformation. Mutations underlying SHFM4 have been detected in the *TP63* gene which has a fundamental role in embryonic development (Ianakiev et al. 2000). Finally, the critical SHFM5 interval includes the candidate genes *DLX1* and *DLX2*, two important genes expressed in the AER, but also here only deletions on 2q24-q31 could be identified in patients (Faiyaz-Ul-Haque et al. 2005).

3.3.5 Molecular pathogenesis of Bardet-Biedl (BBS) syndrome

Bardet-Biedl syndrome (BBS) is a genetically heterogeneous, pleiotropic ciliopathy disorder with recessive inheritance pattern but also triallelic and oligogenic inheritance are known (Katsanis et al. 2001). The incidence of BBS has been described with 1 in 150,000 to 175,000 individuals in European populations but populations with a high level of consanguinity or from geographically isolated regions show a much higher frequency of BBS (Farag and Teebi 1988). The 14 BBS genes (BBS1-BBS14 namely *BBS1*, *BBS2*, *ARL6*, *BBS4*, *BBS5*, *MKKS*, *BBS7*, *TTC8*, *BBS9*, *BBS10*, *TRIM32*, *BBS12*, *MKS1*, *CEP290*) identified to date account for over 75% of affected families (Zaghloul and Katsanis 2009), with *BBS1* and *BBS10* showing the highest frequency in families with European descent (Chiang et al. 2006; Stoetzel et al. 2007). Most of the known BBS genes are ciliary proteins with important functions in development and homeostasis of different tissues (Ross et al. 2005) and play a major role in signal transduction including fundamental biological pathways such as Wnt or SHH signalling (Marshall and Nonaka 2006; Saxena et al. 2007). Therefore, it is assumed that ciliary dysfunction and disturbance of the intraflagellar transport is the main pathophysiological mechanism leading to BBS (Katsanis et al. 2001).

4. Aims and major findings of this Ph.D thesis

4.1 Aims

The aim of the present Ph.D thesis was to identify novel key factors and new molecular mechanisms involved in physiological and pathophysiological processes during limb development. In order to identify novel genes and types of mutations, we wanted to focus on different human inherited limb malformations, such as Cenani-Lenz syndrome and Werner mesomelic syndrome, and used a combination of genome-wide linkage analysis, homozygosity mapping, positional cloning, and candidate gene approach to identify the disease causing genes. Furthermore, the intention was to investigate the encoded proteins and mutations of identified genes by in vitro studies to gain an insight into the molecular pathogenesis of these limb malformations and physiology of limb development.

4.2 Major findings

- (1) Mapping of the first locus for Cenani-Lenz syndrome (CLS) to chromosome 11p11.2 and identification of mutations in *LRP4* causing Cenani-Lenz syndrome (**Li et al., Am J Hum Genet (2010); 86(5):696-706**).
- (2) Screening of additional CLS patients and families and thus broadening the mutational spectrum of CLS mutations (**Li et al., Am J Hum Genet (2010); 86(5):696-706**).
- (3) Functional analysis of mutant LRP4 p.D137N, p.C160Y, p.D449N, p.D473N and p.D529N proteins. a) Dual-Luciferase Reporter Assays demonstrated that mutant proteins abolish the antagonistic LRP4 effect on LRP6-mediated activation of Wnt/ β -catenin signalling. b) Cell surface biotinylation displayed that mutant LRP4 receptors fail to be efficiently transported to the plasma membrane (**Li et al., Am J Hum Genet (2010); 86(5):696-706**).
- (4) Identification of point mutations within the sonic hedgehog (*SHH*) regulatory region (ZRS) causing Werner mesomelic syndrome (**Wieczorek et al., Hum Mutat. (2010); 31(1):81-9**).
- (5) Establishment of quantitative gene copy analysis and identification of duplications of the ZRS being responsible for polysyndactyly type IV Haas and triphalangeal thumbpolysyndactyly (TPTPS) (**Wieczorek et al., Hum Mutat. (2010); 31(1):81-9**).
- (6) Functional analysis of the *Wnt10b* p.R332W mutation causing autosomal recessive split-hand/foot malformation. Using Dual-Luciferase-Reporter-Assays we show that p.R332W causes a loss of function of Lrp6 mediated Wnt signalling (**Pawlik et al., submitted**).
- (7) Detection of the first direct cross-talk between Wnt and Fgf signalling pathways by indicating that Fgf8 is a novel potential Wnt signalling antagonist (**Pawlik et al., submitted**).
- (8) Mapping the Tentamy preaxial brachydactyly syndrome (TPBS) locus to 15q26 and identification of mutations in *CHSY1* causing TPBS (**Li et al., in Press, Am J Hum Genet (2010)**).
- (9) Identification of a novel nonsense *BBS12* mutation (p.S701X) in a Pakistani family diagnosed with postaxial polydactyly and late-onset dystrophy which causes a mild Bardet-Biedle syndrome (BBS) phenotype (**Pawlik et al., Mol Syndromol (2010); 1:27-34**).

5. Main publications on human limb malformations with own contributions

5.1 Pawlik B, Mir A, Iqbal H, Li Y, Nürnberg G, Becker C, Qamar R, Nürnberg P, Wollnik B. A Novel Familial BBS12 Mutation Associated with a Mild Phenotype: Implications for Clinical and Molecular Diagnostic Strategies. Mol Syndromol (2010); 1:27-34.

Abstract of the publication:

Bardet-Biedl syndrome (BBS) is an autosomal recessive disorder characterized by progressive retinal degeneration (rod-cone dystrophy), obesity, postaxial polydactyly, renal tract, genital anomalies, and learning difficulties or mental retardation. The phenotype of BBS is highly variable, and it has been suggested that the clinical diagnosis is established if at least four of the main manifestations are present in a patient. In this study, we investigated a consanguineous family from Pakistan with postaxial polydactyly and late-onset retinal dysfunction who did not fulfill all clinical diagnostic criteria for BBS.

In order to identify the disease causing gene we first conducted the Affymetrix GeneChip Human Mapping 10K Array (CCG, University of Cologne) and mapped the family to the *BBS12* locus on chromosome 4q27 to a critical region of 21,63 Mb between SNPs rs1390560 and rs1343812. The critical region on 4q27 was gene rich and contained approximately 80 known and predicted genes. In total, we tested 6 highly relevant candidate genes of this region: *FGF2*, *BBS7*, *BBS12*, *NUDT6*, *SPATA5*, and *SPRY1*. Finally sequencing of the coding exon 2 of *BBS12* in affected individuals identified a novel homozygous c.2103C >A mutation, which is predicted to insert a stop codon at position 701 of the BBS12 protein (p.S701X). This nonsense mutation is located at the very C-terminal end of the protein and the truncation leads to a loss of 10 amino acids. Co-segregation of the p.S701X mutation with the disease in the family could be confirmed. In addition, the mutation was not found in 147 healthy controls from Pakistan.

Thus we provide evidence for a very mild, familial BBS12 phenotype. Clinical diagnosis would have been missed when applying the suggested diagnostic criteria for BBS. Therefore, we propose the use of less strict diagnostic criteria in familial BBS cases that might also influence the molecular testing strategies of BBS.

Own contributions:

Initially, the index patient of the MR-10 family was subjected to a genome-wide scan using the Affymetrix GeneChip® Human Mapping 10K array (CCG, University of Cologne, group of Prof. Dr. P. Nürnberg). At first, I evaluated and interpreted the Affymetrix GeneChip data (Figure 1c, p.30). Genome Scan pointed out that the MR-10 family map to three possible loci on chromosome 4q27-4q31.22, 4q25.1-4q35.2 and 11q23.1-11q23.3, respectively (Figure 1c, p.30).

In order to identify the disease causing locus, I first performed fine mapping analysis using microsatellite markers and thereby excluded locus 4q25.1-4q35.2 and 11q23.1-11q23.3 and mapped the MR10 family to a critical region on 4q27-4q31.22 (Figure 1a, p.29). The critical region was gene rich and contained approximately 80 known and predicted genes (Figure 2a, p.32).

In total, I tested 6 highly relevant candidate genes for mutations in the index patient: *FGF2*, *BBS7*, *BBS12*, *NUDT6*, *SPATA5* and *SPRY*. I identified a novel homozygous c.2103C>A mutation in all affected family members which produces a stop codon at position 701 in the BBS12 protein (p.S701X) by sequencing the coding exon 2 of *BBS12* (Figure 2b, p.32).

I next confirmed co-segregation of the p.S701X mutation in the MR-10 family and finally established a PCR/enzyme digestion method using ApoI to test 147 healthy Pakistani control individuals (data not shown).

In the end, I arranged all figures for the publication and wrote the manuscript, which was published in Molecular Syndromology.

A Novel Familial *BBS12* Mutation Associated with a Mild Phenotype: Implications for Clinical and Molecular Diagnostic Strategies

B. Pawlik^{a,b} A. Mir^c H. Iqbal^c Y. Li^{a,b,d} G. Nürnberg^{e,f} C. Becker^{e,f}
R. Qamar^c P. Nürnberg^{a,d-f} B. Wollnik^{a,b,d}

^aCenter for Molecular Medicine Cologne (CMMC), University of Cologne, and ^bInstitute of Human Genetics, University Hospital Cologne, University of Cologne, Cologne, Germany; ^cDepartment of Biosciences, COMSATS Institute of Information Technology, Chak Shazad Campus, Islamabad, Pakistan; ^dCologne Excellence Cluster on Cellular Stress Responses in Aging-Associated Diseases (CECAD), University of Cologne, and ^eCologne Centre for Genomics, University of Cologne, and ^fInstitute of Genetics, University of Cologne, Cologne, Germany

Key Words

Bardet-Biedl syndrome · *BBS12* · Diagnostic criteria · Mild phenotype · Novel mutation

Abstract

Bardet-Biedl syndrome (BBS) is an autosomal recessively inherited ciliopathy mainly characterized by rod-cone dystrophy, postaxial polydactyly, obesity, renal tract anomalies, and hypogonadism. To date, 14 *BBS* genes, *BBS1* to *BBS14*, have been identified, accounting for over 75% of mutations in BBS families. In this study, we present a consanguineous family from Pakistan with postaxial polydactyly and late-onset retinal dysfunction. Adult affected individuals did not show any renal or genital anomalies, obesity, mental retardation or learning difficulties and did thus not fulfill the proposed clinical diagnostic criteria for BBS. We mapped the disease in this family to the *BBS12* locus on chromosome 4q27 and identified the novel homozygous p.S701X nonsense mutation in *BBS12* in all three affected individuals of this family. We conclude that *BBS12* mutations might cause a very mild phenotype, which is clinically not diagnosed by the current diagnostic criteria for BBS. Consequently, we suggest the use of less strict diagnostic criteria in familial BBS families with mild phenotypic expression.

Bardet-Biedl syndrome (BBS, MIM 209900) is an autosomal recessive disorder characterized by a wide spectrum of clinical features, of which the most common ones are progressive retinal degeneration (rod-cone dystrophy), obesity, postaxial polydactyly, renal tract and genital anomalies, and learning difficulties or mental retardation [Beales et al., 1999]. The phenotype of BBS is highly variable, and it has been suggested that the clinical diagnosis is established if at least four of the main manifestations are present in a patient. Clinical evaluation during early infancy remains difficult as not all of the main manifestations are congenital but may occur later during childhood. Congenital postaxial polydactyly including syndactyly and/or brachydactyly is present in approximately 70% of cases and may not affect all limbs. Developmental anomalies of the renal tract are also common and can lead to chronic renal failure [Harnett et al., 1988]. Further congenital symptoms, which can be diagnosed in early infancy, are genital anomalies such as vaginal atresia and hypoplasia of the uterus and hypogonadism in males. The appearance of a rod-cone dystrophy, which is also described as atypical retinitis pigmentosa

B.P. and A.M. contributed equally to this work.

KARGER

Fax +41 61 306 12 34
E-Mail karger@karger.ch
www.karger.com

© 2010 S. Karger AG, Basel
1661–8769/10/0011–0027\$26.00/0

Accessible online at:
www.karger.com/msy

Bernd Wollnik
Institute of Human Genetics and Center for Molecular Medicine Cologne (CMMC)
University Medical Faculty, University of Cologne
Kerpener Str. 34, DE-50931 Cologne (Germany)
Tel. +49 221 4788 6817, Fax +49 221 4788 6812, E-Mail bwollnik@uni-koeln.de

with early macular involvement, is characteristic in BBS patients and present in over 90% of patients [Green et al., 1989]. Typically, night blindness is one of the first symptoms at the end of the first decade and the progressive retinal degeneration often causes total blindness in the course of the second decade of life. Although mental retardation is not very common in BBS patients, learning difficulties are present in over half of the patients. Truncal and rhizomelic obesity develops in the majority of BBS patients before the end of puberty. Developmental delay might be present and poor motor coordination is described in a subset of patients. Other features such as hearing loss, dental anomalies, congenital heart defects, diabetes mellitus, and hepatic fibrosis are rare [Green et al., 1989; Beales et al., 1999].

The incidence of BBS has been estimated at 1 in 150,000 to 175,000 individuals in European populations. However, populations with a high level of consanguinity or from geographically isolated regions like Newfoundland show a much higher frequency [Frag and Teebi, 1988, 1989]. BBS is a genetically heterogeneous disorder and up to date 14 genes have been identified (*BBS1* to *BBS14*, namely *BBS1*, *BBS2*, *ARL6*, *BBS4*, *BBS5*, *MKKS*, *BBS7*, *TTC8*, *BBS9*, *BBS10*, *TRIM32*, *BBS12*, *MKS1*, *CEP290*) using traditional genome-wide mapping and positional cloning strategies in large consanguineous families or – more recently – computational comparative genomic expression methods [Katsanis et al., 2000; Mykytyn et al., 2001, 2002; Badano et al., 2003; Chiang et al., 2004; Fan et al., 2004; Li et al., 2004; Nishimura et al., 2005; Chiang et al., 2006; Stoetzel et al., 2006; Leitch et al., 2008]. While the majority of BBS patients do show a classical autosomal recessive inheritance pattern, triallelic and oligogenic inheritance was suggested in some families [Katsanis et al., 2001a]. Since then it has been suggested that genetic modifiers exist responsible for the clinical variability of phenotypic expression in BBS patients.

Mutations in *BBS1–14* account for over 75% of affected families [Zaghloul and Katsanis, 2009]. In families of European descent, mutations in *BBS1* and *BBS10* show the highest frequency accounting for approximately 20% of BBS mutations each [Chiang et al., 2006; Stoetzel et al., 2006]. The *BBS12* gene is the most recently identified gene and the encoded protein belongs to a novel branch of type 2 chaperonin superfamily, which includes also *BBS6* and *BBS10* [Stoetzel et al., 2007]. In general, most of the known *BBS* genes are highly conserved in ciliated organisms, such as *Chlamydomonas*, and are absent in non-ciliated ones such as *Arabidopsis* [Li et al., 2004]. There is molecular evidence that BBS proteins are part of primary

cilia structures arising from the basal body and playing an important role in development and homeostasis of various tissues, e.g. as mechanosensors in kidney epithelium and in the organization of photoreceptor cells of the retina [Ross et al., 2005; Badano et al., 2006a]. Cilia are microtubule-based eukaryotic organelles that project from the surface of human cells. Beside performing a wide variety of functions, they play a major role in extracellular signal transduction including important biological pathways such as wnt and hedgehog signalling [Marshall and Nonaka, 2006; Saxena et al., 2007]. It is suggested that ciliary dysfunction and disturbance of the intraflagellar transport represent the main pathophysiological mechanism leading to BBS [Katsanis et al., 2001b]. For this reason, BBS is regarded as a ciliopathy.

Here we report a novel *BBS12* mutation, p.S701X, found in three affected individuals of a consanguineous family from Pakistan clinically diagnosed with postaxial polydactyly and late-onset retinal dysfunction. Adult affected individuals did not show any renal and genital anomalies, obesity, learning difficulties or any other symptoms, thus indicating that mutations in *BBS12* can cause a very mild phenotype which is clinically not diagnosed by the current diagnostic criteria for BBS.

Material and Methods

MR-10 family: Index patient was referred to the hospital due to bilateral polydactyly and mild vision impairment. All affected family members were clinically examined including general physical examination, ophthalmological examination, X-rays of hands and feet, and abdominal ultrasound. The study was first approved by local institutional review boards of COMSATS Institute, Islamabad, Pakistan (CIIT Biosciences Review/Ethics Committee; A.S. 24112008), and followed the Declaration of Helsinki protocols. Afterwards, blood samples were taken after written informed consent was given and DNA was isolated using standard procedures.

Linkage Analysis

Genomic DNA of the index patient of the MR-10 family (IV-3) as well as DNAs of siblings and parents (fig. 1, individuals I-1, I-2, II-1, II-2, II-3, II-4, III-2, III-3, IV-1, IV-3, IV-4, IV-5, IV-6, IV-8) were subjected to a genome-wide mapping using the Affymetrix GeneChip Human Mapping 10K Array (Affymetrix, Santa Clara, CA). This 10K array comprises a total of 10,204 single-nucleotide polymorphisms (SNPs) with a mean intermarker distance of 258 kb, equivalent to 0.36 cM. Sample processing and labelling were performed in accordance with the manufacturer's instructions (Affymetrix Mapping 10K 2.0 Assay Manual). Genotypes were provided by the GeneChip DNA Analysis Software (v.4.1, Affymetrix). Non-parametric linkage analysis using all genotypes of a chromosome simultaneously was carried out with MERLIN.

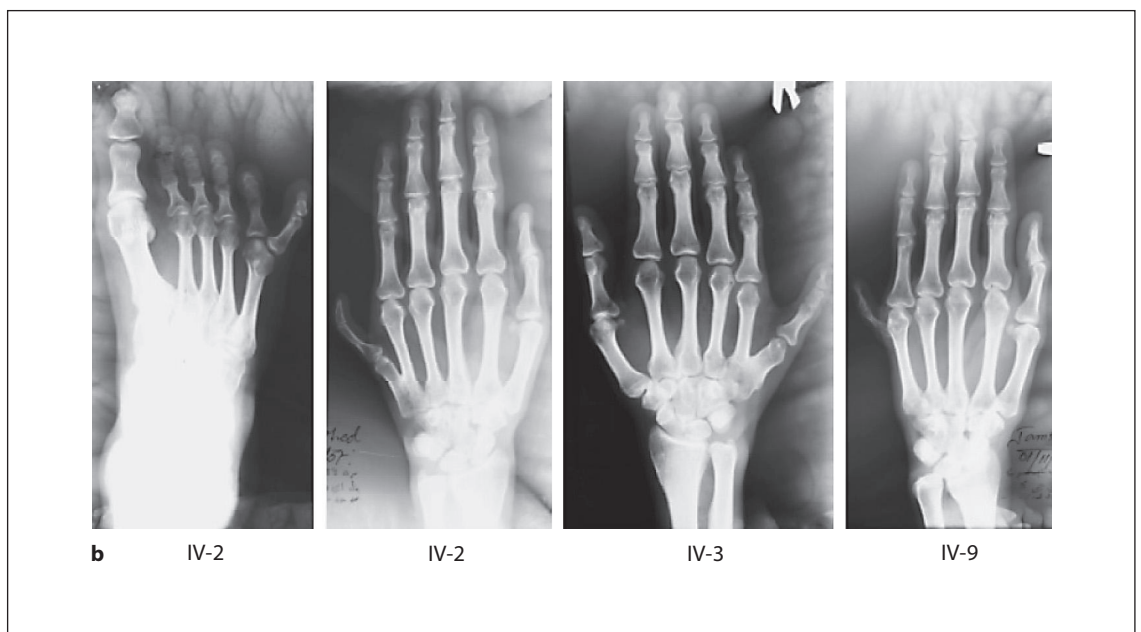
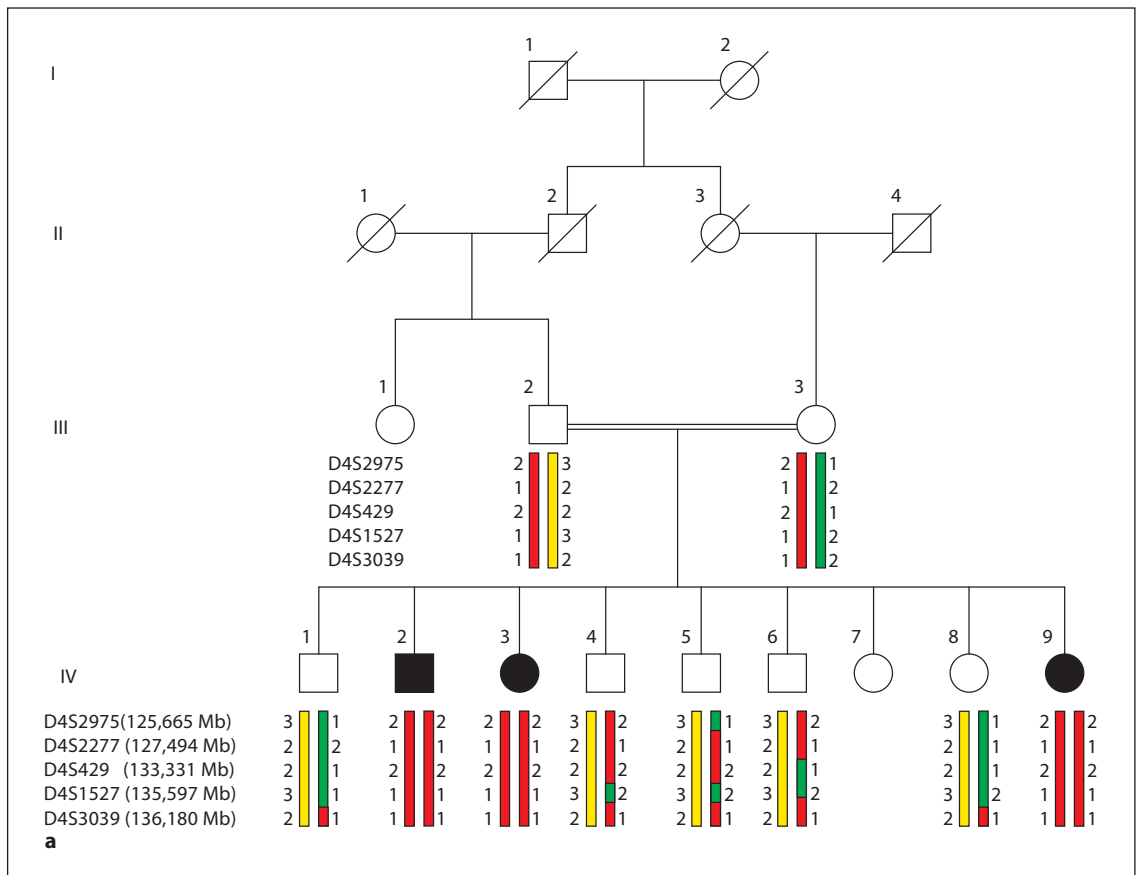


Fig. 1. MR-10 family maps to the *BBS12* locus on chromosome 4q27. **a** Pedigree of the MR-10 family and haplotypes of the 4q27 region. The disease-associated haplotype is shown in red. **b** X-rays of affected individuals showing the postaxial polydactyly of hands and feet.

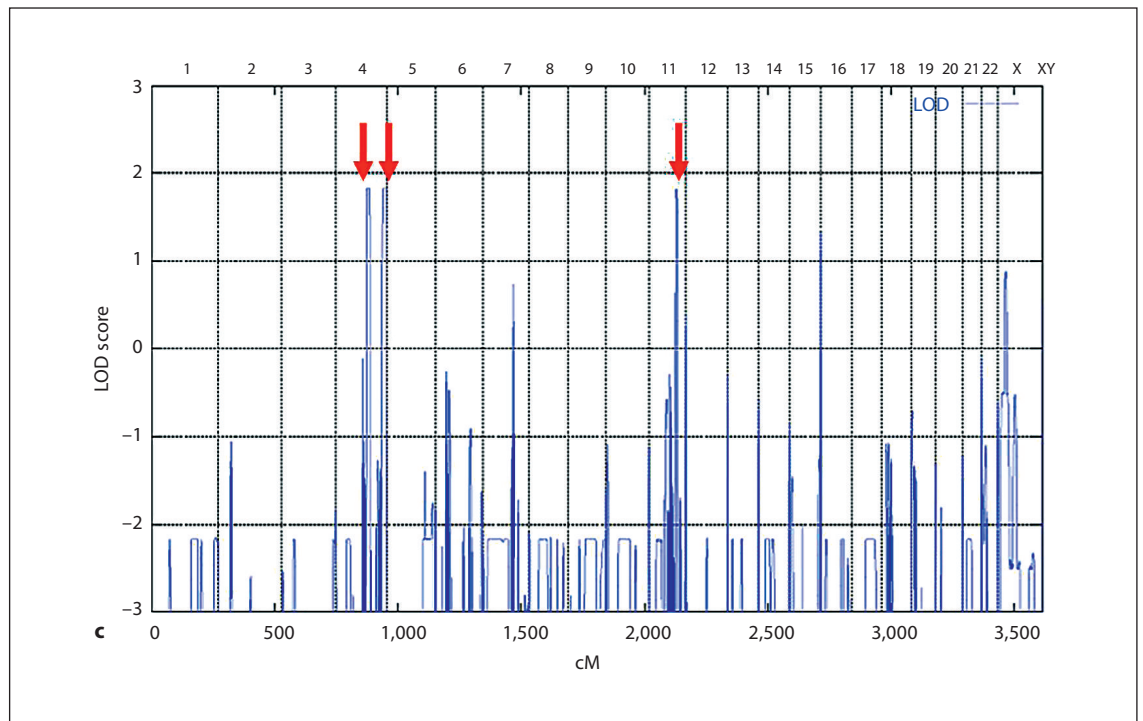


Fig. 1. Continued MR-10 family maps to the *BBS12* locus on chromosome 4q27. **c** Schematic view of genome-wide LOD score calculations. The arrows indicate regions of maximum LOD scores of 1.83.

Parametric linkage analysis was performed by the program ALLEGRO assuming autosomal recessive inheritance. For fine mapping analysis, available MR-10 family members were genotyped for the following markers: D4S2975, D4S2277, D4S429, D4S3039, D4S1527, D4S2920, D4S3047, D4S2921, D4S426, D11S480, D11S4122, D11S1885. Genomic localization and microsatellite sequences were obtained from the UCSC Genome Browser (<http://genome.ucsc.edu/>, build hg18, March 2006) and the ENSEMBL database (<http://www.ensembl.org>). Polymerase chain reaction (PCR) for fluorescent markers was performed on a DNA Engine Dyad Thermal Cycler (Bio-Rad, Germany) under standard PCR conditions, run on an ABI 3730 DNA Analyzer (Applied Biosystems, Germany), and evaluated with the GeneMarker 1.51 program (Soft Genetics LLC).

Mutation Analysis

The following genes of the critical region were tested for mutations in the index patient of family MR-10: *FGF2*, *BBS7*, *BBS12*, *NUDT6*, *SPATA5*, and *SPRY*. Primer sequences and PCR protocols are available upon request. The 2,144 bp of the coding sequence of exon 2 of the *BBS12* gene (123,873,307–123,885,548 Mb, UCSC Human Genome Browser, hg 18 assembly) was sequenced in the index patients (IV-2, IV-3, IV-9). 20 ng of genomic DNA from patients was used to amplify the 4 amplicons of exon 2 by a touchdown PCR protocol on a DNA Engine Dyad Thermal Cycler (Bio-Rad, Germany). PCR fragments were purified and directly sequenced from both sides using the ABI BigDye Terminator v1.1 Cycle Sequencing Kit and the ABI 3730 DNA Analyzer (Applied

Biosystems). Co-segregation of the mutation in the family was investigated by direct sequencing of all available family members and by a PCR/enzyme digestion method using *ApoI* (data not shown). In addition, the mutation was tested in 147 Pakistani control individuals by PCR/enzyme digestion method.

Results

Clinical Evaluation of the Family

The three affected individuals of family MR-10 from Pakistan (fig. 1a) were born to consanguineous parents (first-degree cousins). Congenital postaxial polydactyly of hands and feet were observed in various expressions (fig. 1b). In addition, progressive night blindness started between 13–15 years of age in all the patients. Individuals IV-2, IV-3, and IV-9 are now 30, 27, and 19 years old, respectively, and all of them have developed severe night blindness, while vision is only mildly impaired in daytime. Ophthalmological examination was performed and an atypical retinitis pigmentosa (RP, rod-cone dystrophy), myopia and astigmatism were diagnosed. Patients' history neither showed developmental delay in childhood nor mental retardation or learning difficulties. Obesity

Table 1. Clinical findings in three affected individuals of family MR-10 listed according to the clinical criteria for the diagnosis of BBS [Beales et al., 1999]

	IV-2	IV-3	IV-9
<i>Major criteria</i>			
Rod-cone dystrophy	+ (14 years)	+ (15 years)	+ (13 years)
Postaxial polydactyly	+	+	+
Truncal obesity	-	-	-
Hypogonadism	-	-	-
Renal anomalies	-	-	-
<i>Minor criteria</i>			
Speech disorder/delay	-	-	-
Development delay	-	-	-
Behaviour	normal	normal	normal
Ataxia/imbalance	-	-	-
Diabetes mellitus	-	-	-
Congenital heart defects	-	-	-
Liver disease	-	-	-
Hearing loss	-	-	-
Facial features	-	-	-
Situs inversus	-	-	-
Hirschsprung's disease	-	-	-
Polyuria/polydipsia	-	-	-
Hypodontia	+	+	+
Anosmia	-	-	-

was not present in all three affected individuals either. No organ anomaly was found in ultrasound; especially no renal tract abnormalities were seen. Furthermore, physical examination showed hypodontia but did not show any genital anomalies or additional symptoms. General neurological testing was normal. No signs for hypogonadism was present and individual IV-2 was fertile and had 4 children. A summary of clinical findings is listed in table 1. The initial diagnosis of an autosomal recessively inherited disorder characterized by postaxial polydactyly and atypical RP was given. It is of interest to note that a second, independent autosomal recessive disorder, namely non-syndromic mental retardation (MR), was present in the family, but none of the BBS patients was affected by MR (individuals IV-1, IV-5, IV-6, IV-8 had MR). The molecular basis of the independent MR phenotype will be analyzed in an upcoming study.

Linkage to the BBS12 Locus on 4q27 and Identification of a Novel BBS12 Mutation

In order to map the recessive disorder characterized by postaxial polydactyly and rod-cone dystrophy in the MR-10 family, we performed homozygosity mapping us-

ing the 10K array. Genome-wide LOD score calculations resulted in maximum LOD scores of 1.83 at three different chromosomal regions located on chromosome 4q27–4q31.22, 4q35.1–4q35.2, and 11q23.1–11q23.3, respectively (fig. 1c). Genotyping of additional microsatellite markers of these regions clearly excluded the two loci on 4q35.1–4q35.2 and 11q23.1–11q23.3 (data not shown). For locus 4q27–4q31.22, marker analysis confirmed homozygosity and the critical region was defined by SNPs rs1390560 (located at 122.07 Mb) and rs1343812 (143.70 Mb) (fig. 2a).

The 21.63-Mb critical region is gene rich and contains approximately 80 known and predicted genes. In total, we tested 6 highly relevant candidate genes of this region: *FGF2*, *BBS7*, *BBS12*, *NUDT6*, *SPATA5*, and *SPRY1*. Sequencing of the coding exon 2 of *BBS12* in affected individuals identified a novel homozygous c.2103C>A mutation (fig. 2b), which is predicted to insert a stop codon at position 701 of the BBS12 protein (p.S701X). This nonsense mutation is located at the very C-terminal end of the protein and the truncation leads to a loss of 10 amino acids (fig. 2c). Co-segregation of the p.S701X mutation with the disease in the family could be confirmed. All affected individuals were homozygous for the p.S701X mutation and parents were heterozygous carriers. In addition, the mutation was not found in 147 healthy controls from Pakistan.

We compared the localisation of this novel *BBS12* mutation with mutations described in the original gene identification study [Stoetzel et al., 2007]. The p.S701X mutation is located close to the C-terminus in the equatorial domain of the BBS12 protein (fig. 2b, c). Of the 17 pathogenic mutations described so far, which include missense, nonsense, and frameshift mutations, the p.S701X is the most C-terminal one.

Discussion

It is well known that a large clinical variability of phenotypic expression exists in Bardet-Biedl syndrome, both between and within families. In addition, clinical diagnosis is hampered by the fact that not all symptoms are congenital but may develop later during childhood or within the second decade of life. Therefore, especially in early infancy clinical diagnosis is often difficult. Diagnostic criteria for the clinical diagnosis of BBS have been suggested [Beales et al., 1999] that were modified by Tobin and Beales in 2007 using a sub-classification of symptoms in primary and secondary features [Tobin and

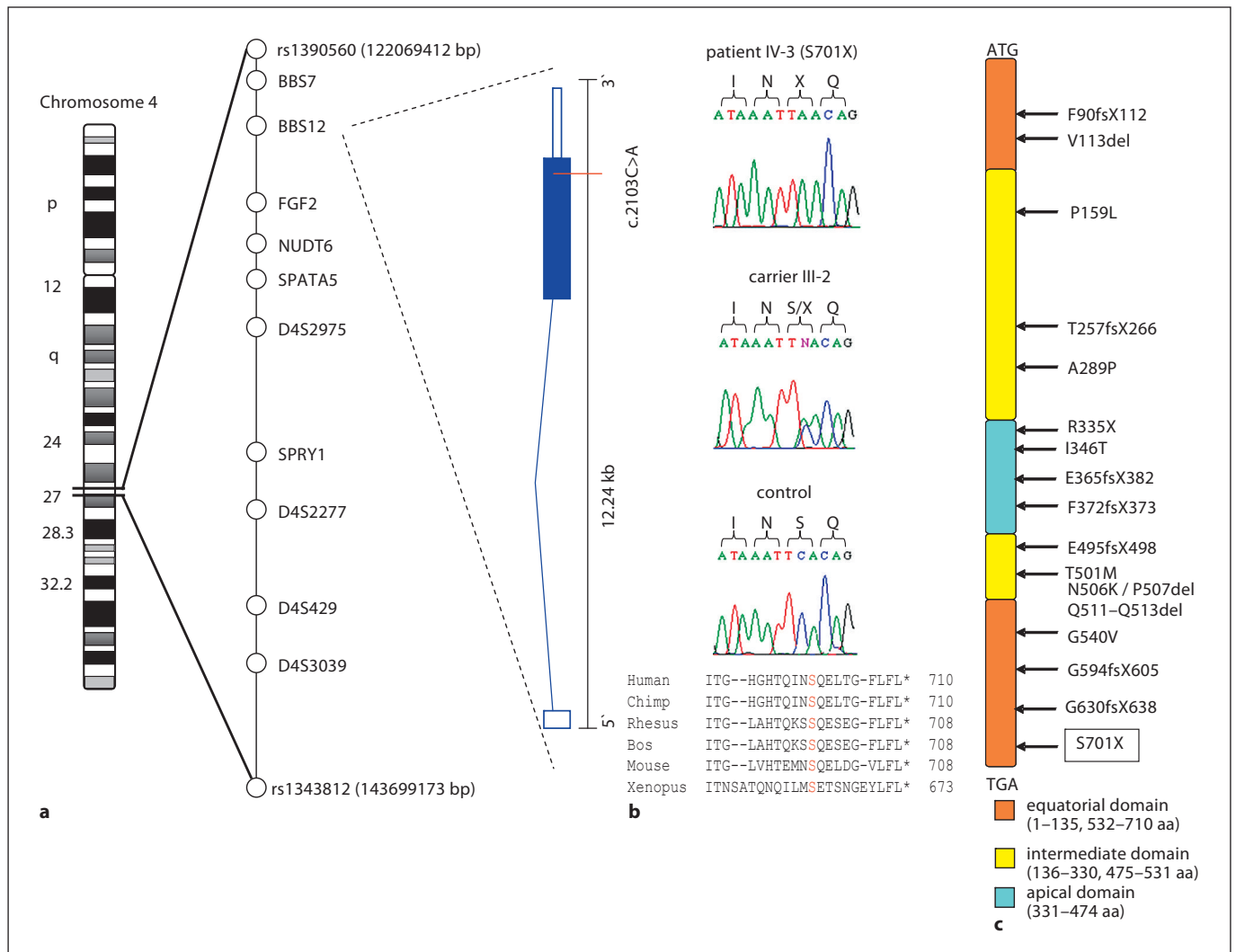


Fig. 2. Identification of the novel p.S701X mutation in *BBS12*. **a** Ideogram of chromosome 4 and localisation of the linked region on 4q27. SNPs defining the critical region, analysed markers, and tested candidate genes are listed within the critical region. Illustration of the genomic organisation and transcript composition of *BBS12*. The position of the c.2103C>A mutation is indicated. **b** Sequence chromatograms of c.2103C>A mutation in the index patient (IV-3), heterozygous carrier (III-2), and a healthy control. Amino-acid (aa) alignment of the truncated C-terminal end of *BBS12* proteins from different species. **c** Overview of *BBS12* protein structure and location of previously identified mutations.

Beales, 2007]. Primary features are rod-cone dystrophy, postaxial polydactyly, obesity, hypogonadism, and renal anomalies, whereas secondary features include speech disorder/delay, development delay, diabetes mellitus, congenital heart disease, liver disease, situs inversus and facial dysmorphism. It was suggested that the clinical diagnosis of BBS can be made in a patient if four primary features or three primary plus two secondary features are present. Using this classification, diagnosis would have

been missed in all three adult affected individuals in our family, because only 2 primary (polydactyly and rod-cone dystrophy) and 1 secondary criterion (hypodontia) are present. It is interesting to point out that this very mild form of BBS was present in all three affected individuals, suggesting a generally mild phenotypic expression of the disease in this particular family. Therefore, strict diagnostic criteria in BBS might lead to false-negative classification. For this reason, we propose that mo-

lecular genetic testing for BBS might be considered in familial forms even if the diagnostic criteria are not fulfilled. However, the phenotype observed in the three affected individuals of our family clearly represents symptoms known to be caused by dysfunction of cilia. Many human genetic disorders have been described which are collectively called the ciliopathies, and symptoms associated with ciliary dysfunction include alterations of left-right body axis, polydactyly, kidney, liver and pancreas anomalies, retinal degeneration and anosmia, neural tube defects as well as cognitive defects.

Using homozygosity mapping, we linked the disease in our family to the *BBS12* locus on chromosome 4q27 and identified the novel nonsense mutation p.S701X in *BBS12*. There is convincing evidence for a causative nature of this mutation: (i) genome-wide mapping identified only one homozygous locus in this consanguineous family, which could be confirmed by subsequent marker analysis; (ii) the mutation co-segregated with the disease in the family and was absent in 147 healthy and ethnically matched control chromosomes; (iii) the nonsense mutation is predicted to have a clear effect on the *BBS12* protein, truncating – even though – 10 amino acids from the conserved C-terminal end of the equatorial domain of the protein. It is estimated that *BBS12* mutations account for up to 5% of families with BBS [Stoetzel et al., 2007]. One frameshift mutation has yet been described to alter the equatorial domain of *BBS12*, namely p.G594fsX605 (fig. 2c).

Although clear genotype-phenotype correlations could not yet be established in BBS, mutations in *BBS3* seem to cause more often polydactyly of all four limbs, while patients with *BBS4* mutations more frequently show polydactyly only of the upper limbs. Moreover, *BBS2*-associated cases do not frequently suffer from obesity, whereas patients carrying *BBS3* mutations often develop early-onset obesity [Carmi et al., 1995; Beales et al.,

1997; Bruford et al., 1997]. Polygenic inheritance or genetic modifiers might be an explanation for phenotypic variability in BBS. Moreover, epistatic interactions might play an important role in phenotypic variability [Badano and Katsanis, 2002]. In this context, it was demonstrated that certain synergistic effects can modify the penetrance or expressivity of phenotype. Badano et al. reported some kind of evidence for a novel gene called *MGC1203*, which assists epistatically to *BBS1* mutations and also enhances the phenotype in a zebrafish model [Badano et al., 2006b].

No obvious phenotypic difference of *BBS12* patients compared to other *BBS* patients was reported in the original study, although no detailed information about the clinical presentation of the families was given [Stoetzel et al., 2007]. Nevertheless, our study showed that mutations in *BBS12* can cause a very mild phenotype that is clinically not diagnosed by the proposed diagnostic criteria. Only mild phenotypic effects of *BBS12* suppression were also reported in a zebrafish model [Stoetzel et al., 2007]. In the future, it will be interesting and necessary to further delineate the phenotypic expression in other *BBS12* families.

In conclusion, we provide evidence for a very mild, familial *BBS12* phenotype. Clinical diagnosis would have been missed when applying the suggested diagnostic criteria for BBS. For this reason, we propose the use of less strict diagnostic criteria in familial BBS cases that might also influence the molecular testing strategies of BBS.

Acknowledgements

We are grateful to the family for their participation in the study. This work was supported by the German Federal Ministry of Education and Research (BMBF) by grant number 01GM0880 to B.W.

References

- Badano JL, Katsanis N: Beyond Mendel: an evolving view of human genetic disease transmission. *Nat Rev Genet* 3:779–789 (2002).
- Badano JL, Ansley SJ, Leitch CC, Lewis RA, Lupski JR, Katsanis N: Identification of a novel Bardet-Biedl syndrome protein, BBS, that shares structural features with BBS1 and BBS2. *Am J Hum Genet* 72:650–658 (2003).
- Badano JL, Mitsuma N, Beales PL, Katsanis N: The ciliopathies: an emerging class of human genetic disorders. *Annu Rev Genomics Hum Genet* 7:125–148 (2006a).
- Badano JL, Leitch CC, Ansley SJ, May-Simera H, Lawson S, et al: Dissection of epistasis in oligogenic Bardet-Biedl syndrome. *Nature* 439:326–330 (2006b).
- Beales PL, Warner AM, Hitman GA, Thakker R, Flintner FA: Bardet-Biedl syndrome: a molecular and phenotypic study of 18 families. *J Med Genet* 34:92–98 (1997).
- Beales PL, Elcioglu N, Woolf AS, Parker D, Flintner FA: New criteria for improved diagnosis of Bardet-Biedl syndrome: results of a population survey. *J Med Genet* 36:437–446 (1999).

- Bruford EA, Riise R, Teague PW, Porter K, Thomson KL, et al: Linkage mapping in 29 Bardet-Biedl syndrome families confirms loci in chromosomal regions 11q13, 15q22.3–q23, and 16q21. *Genomics* 41:93–99 (1997).
- Carmi R, Elbedour K, Stone EM, Sheffield VC: Phenotypic differences among patients with Bardet-Biedl syndrome linked to three different chromosome loci. *Am J Med Genet* 59:199–203 (1995).
- Chiang AP, Nishimura D, Searby C, Elbedour K, Carmi R, et al: Comparative genomic analysis identifies an ADP-ribosylation factor-like gene as the cause of Bardet-Biedl syndrome (*BBS3*). *Am J Hum Genet* 75:475–484 (2004).
- Chiang AP, Beck JS, Yen HJ, Tayeh MK, Scheetz TE, et al: Homozygosity mapping with SNP arrays identifies *TRIM32*, an E3 ubiquitin ligase, as a Bardet-Biedl syndrome gene (*BBS11*). *Proc Natl Acad Sci USA* 103:6287–6292 (2006).
- Fan Y, Esmail MA, Ansley SJ, Blacque OE, Boerovitch K, et al: Mutations in a member of the Ras superfamily of small GTP-binding proteins causes Bardet-Biedl syndrome. *Nat Genet* 36:989–993 (2004).
- Farag TI, Teebi AS: Bardet-Biedl and Laurence-Moon syndromes in a mixed Arab population. *Clin Genet* 33:78–82 (1988).
- Farag TI, Teebi AS: High incidence of Bardet Biedl syndrome among the Bedouin. *Clin Genet* 36:463–464 (1989).
- Green JS, Parfrey PS, Harnett JD, Farid NR, Cramer BC, et al: The cardinal manifestations of Bardet-Biedl syndrome, a form of Laurence-Moon-Biedl syndrome. *N Engl J Med* 321:1002–1009 (1989).
- Harnett JD, Green JS, Cramer BC, Johnson G, Chafe L, et al: The spectrum of renal disease in Laurence-Moon-Biedl syndrome. *N Engl J Med* 319:615–618 (1988).
- Katsanis N, Beales PL, Woods MO, Lewis RA, Green JS, et al: Mutations in *MKKS* cause obesity, retinal dystrophy and renal malformations associated with Bardet-Biedl syndrome. *Nat Genet* 26:67–70 (2000).
- Katsanis N, Ansley SJ, Badano JL, Eichers ER, Lewis RA, et al: Triallelic inheritance in Bardet-Biedl syndrome, a Mendelian recessive disorder. *Science* 293:2256–2259 (2001a).
- Katsanis N, Lupski JR, Beales PL: Exploring the molecular basis of Bardet-Biedl syndrome. *Hum Mol Genet* 10:2293–2299 (2001b).
- Leitch CC, Zaghoul NA, Davis EE, Stoetzel C, Diaz-Font A, et al: Hypomorphic mutations in syndromic encephalocele genes are associated with Bardet-Biedl syndrome. *Nat Genet* 40:443–448 (2008).
- Li JB, Gerdes JM, Haycraft CJ, Fan Y, Teslovich TM, et al: Comparative genomics identifies a flagellar and basal body proteome that includes the *BBS5* human disease gene. *Cell* 117:541–552 (2004).
- Marshall WF, Nonaka S: Cilia: tuning in to the cell's antenna. *Curr Biol* 16:R604–R614 (2006).
- Mykytyn K, Braun T, Carmi R, Haider NB, Searby CC, et al: Identification of the gene that, when mutated, causes the human obesity syndrome *BBS4*. *Nat Genet* 28:188–191 (2001).
- Mykytyn K, Nishimura DY, Searby CC, Shastri M, Yen HJ, et al: Identification of the gene (*BBS1*) most commonly involved in Bardet-Biedl syndrome, a complex human obesity syndrome. *Nat Genet* 31:435–438 (2002).
- Nishimura DY, Swiderski RE, Searby CC, Berg EM, Ferguson AL, et al: Comparative genomics and gene expression analysis identifies *BBS9*, a new Bardet-Biedl syndrome gene. *Am J Hum Genet* 77:1021–1033 (2005).
- Ross AJ, May-Simera H, Eichers ER, Kai M, Hill J, et al: Disruption of Bardet-Biedl syndrome ciliary proteins perturbs planar cell polarity in vertebrates. *Nat Genet* 37:1135–1140 (2005).
- Saxena R, Voight BF, Lyssenko V, Burt NP, de Bakker PI, et al: Genome-wide association analysis identifies loci for type 2 diabetes and triglyceride levels. *Science* 316:1331–1336 (2007).
- Stoetzel C, Laurier V, Davis EE, Muller J, Rix S, et al: *BBS10* encodes a vertebrate-specific chaperonin-like protein and is a major *BBS* locus. *Nat Genet* 38:521–524 (2006).
- Stoetzel C, Muller J, Laurier V, Davis EE, Zaghoul NA, et al: Identification of a novel *BBS* gene (*BBS12*) highlights the major role of a vertebrate-specific branch of chaperonin-related proteins in Bardet-Biedl syndrome. *Am J Hum Genet* 80:1–11 (2007).
- Tobin JL, Beales PL: Bardet-Biedl syndrome: beyond the cilium. *Pediatr Nephrol* 22: 926–936 (2007).
- Zaghoul NA, Katsanis N: Mechanistic insights into Bardet-Biedl syndrome, a model ciliopathy. *J Clin Invest* 119:428–437 (2009).

5.2 Li Y*, Pawlik B*, Elcioglu N, Aglan M, Kayserili H, Yigit G, Percin F, Goodman F, Nürnberg G, Cenani A, Urquhart J, Chung B, Ismail S, Amr K, Aslanger AD, Becker C, Netzer C, Scambler P, Eyaid W, Hamamy H, Clayton-Smith Y, Hennekam R, Nürnberg P, Herz J, Temtamy SA, Wollnik B. LRP4 Mutations Alter Wnt/b-Catenin Signalling and Cause Limb and Kidney Malformations in Cenani-Lenz Syndrome. Am J Hum Genet (2010); 86(5):696-706.

* These authors contributed equally to this work

Abstract of the publication:

The autosomal recessive Cenani-Lenz syndrome (CLS) is a rare congenital disorder characterized by fusion and disorganization of metacarpal and phalangeal bones, radius and ulnar shortening, radioulnar synostosis, and severe syndactyly of hands and feet. To identify the genetic cause of CLS, we initially genotyped six CLS families with different origin using the Affymetrix GeneChip Human Mapping 10K Array (CCG, University of Cologne) and mapped the CLS1 locus to chromosome 11p11.2 to a 19.7 Mb critical region between SNPs rs1346671 and rs490192. The gene encoding the low-density lipoprotein receptor 4 (*LRP4*) was considered as an excellent positional and functional candidate gene because *Lrp4* knockout mouse displays polysyndactyly of the fore and hind limbs, craniofacial and tooth abnormalities.

We sequenced the coding region of all 39 exons of the *LRP4* gene and identified homozygous mutations in affected individuals in each of the six families. We found one donor splice-site mutation, c.547p1G>A (intron 6, CL-1), and five missense mutations: c.479G>A (p.C160Y, exon 5, CL-2), c.409G>A (p.D137N, exon 4, CL-3), c.1417C>T (p.L473F, exon 12, CL-4), c.1585G>A (p.D529N, exon 13, CL-5), c.1345G>A (p.D449N, exon 12, CL-6). All missense mutations are located in the extracellular domain of LRP4 within highly conserved regions. Furthermore we continued the molecular analysis of *LRP4* in eight additional CLS families and detected that the p.D529N mutation as well as the p.D137N are Turkish and Egypt founder mutations. Additionally we found two further missense mutations: c.1382A>C (p.T461P, exon 11) and c.3049T>C (p.C1017R, exon 22). We further identified compound-heterozygous splice-site mutations (c.200-9G>A and c.49566G>C) which caused aberrant spliced LRP4 transcripts (r.199_200insGATTCAG and r.4952_4987del) in a typically affected fetus with CLS. Finally we confirmed that the mutations, which co-segregated with

the disease, were present neither in unaffected family members nor in ethnically matched control individuals.

To investigate the molecular pathophysiological mechanism of LRP4 mutations leading to CLS we analyzed the effect of five missense mutations (p.D137N, p.C160Y, p.L473F, p.D449N, and p.D529N) on the transduction and activation of canonical Wnt signalling by using a Dual-Luciferase Reporter Assay in transiently transfected HEK293T cells. We could show that WNT1 was able to significantly activate LRP6-mediated β -catenin signalling and that additional co-expression of wt LRP4 potently antagonized this activation while the co-expression of each of the five missense mutations abolished the antagonistic LRP4 effect on LRP6-mediated activation of Wnt/ β -catenin signalling. Moreover, we could demonstrate by cell-surface biotinylation that mutant LRP4 receptors failed to be efficiently transported to the plasma membrane.

Own contributions:

Genome wide mapping analysis in five CLS families was carried out by the group of Prof. Dr. P. Nürnberg (CCG, University of Cologne). A combined parametric LOD score of 7.46 was obtained on chromosome 11p11.2 – q13.1 (Figure 1b, p.3). Fine mapping analysis of the initial five CLS families was performed by Dr. Yun Li (Figure 1c, p. 3).

In order to functionally characterize the LRP4 mutations found in our CLS patients, I first generated five different mouse mutant LRP4 constructs (C160Y, D137N, L473F, D529N and D449N) by site directed mutagenesis on *pcDNA3.1/V5-His-TOPO* expression vector. Mutations corresponded to five homozygous missense mutations identified by Dr. Yun Li in patients with CLS (Figure 2a, p.6).

For transient expression studies, I transfected HEK293T cells using Lipofectamine 2000. Then I conducted expression analysis of the mutant proteins by Western Blot analysis and showed that all mutant LRP4 proteins are transcribed and expressed (Figure 5a, p.9).

Next, I established a Dual-Luciferase Reporter Assay in order to determine the pathophysiological mechanism of the mutants. Consistent with earlier findings, co-expression of LRP6 and WNT1 significantly activated LRP6-mediated β -catenin signalling and additional co-expression of LRP4 antagonized this activation. In contrast, co-expression of each of the five LRP4 missense mutations abolished the observed antagonistic LRP4 effect on LRP6-mediated activation of Wnt/ β -catenin signalling (Figure 5a, p.9). Therefore, I could

demonstrate that homozygous LRP4 mutations cause a loss of protein function and that this is the underlying pathophysiology of CLS (Figure 5a, b, c, p.9).

Moreover, I established and performed a Biotinylation Assay of wt and mutant LRP4 proteins. I could show by Western Blot analysis that mutant LRP4 proteins were not detectable in the plasma membrane (Figure 5b, p.9). In order to confirm a mis-localisation of the LRP4 mutants I also performed immunofluorescence with specific antibodies (data not shown).

Furthermore, I sequenced the *LRP4* gene for additional CLS patients and identified the p.E97X, the p.T416P and the p.C1017R mutations in different patients of diverse origins (Figure 2a, p.6, p.E97X not published yet). In addition I re-sequenced the identified mutations in independent experiments, tested them for co-segregation within the families, and screened at least 100 healthy control individuals.

Finally, I accomplished fine mapping analysis using microsatellite markers for different families diagnosed with CLS and detected the founder mutations, p.D529N and p.D137N, in Turkish and Egypt CLS patients, respectively (Figure 3a, b, c,d, p.7).

At last, I constructed the figures concerning the functional data for the publication (Figure 5a, b, c, p. 9), prepared Table 1 in discussion with clinicians (p.4-5) and critically read the paper before its submission to the American Journal of Human Genetics.

Unpublished data:

I also analysed and interpreted Next Generation Sequencing (NGS) data from targeted regions of a consanguineous CLS patient from Saudi-Arabia who had no mutation in the *LRP4* gene and who was linked by the GeneChip® Human Mapping 10K SNP Array (CCG, University of Cologne) to three putative loci on chromosomes 5q12.3-5q13.3, 5q21.2-5q22.2 and 11p15.3-11p15.1. The complete critical regions were subject to NGS. In the beginning, a priority list of possible disease causing alterations in different genes on each chromosome had been developed. Then I started to confirm the NGS data by sequencing several alterations in distinct candidate genes in these regions. So far screening the patient for alterations in *FCHO2*, *EPB41C4A*, *ABCA13*, *RAD17*, *FER*, *NUCB2*, *GRB10*, *APC*, *SOX6* and *TRIM26* found by NGS has not revealed the causative mutation in this family.

LRP4 Mutations Alter Wnt/ β -Catenin Signaling and Cause Limb and Kidney Malformations in Cenani-Lenz Syndrome

Yun Li,^{1,2,18} Barbara Pawlik,^{1,2,18} Nursel Elcioglu,^{3,18} Mona Aglan,⁴ Hülya Kayserili,⁵ Gökhan Yigit,^{1,2} Ferda Percin,⁶ Frances Goodman,⁷ Gudrun Nürnberg,^{1,8,9} Asim Cenani,¹⁰ Jill Urquhart,¹¹ Boi-Dinh Chung,^{2,9} Samira Ismail,⁴ Khalda Amr,⁴ Ayca D. Aslanger,⁵ Christian Becker,^{8,9} Christian Netzer,^{1,2,9} Pete Scambler,¹² Wafaa Eyaid,¹³ Hanan Hamamy,¹⁴ Jill Clayton-Smith,¹¹ Raoul Hennekam,^{7,15} Peter Nürnberg,^{1,8,9,16} Joachim Herz,¹⁷ Samia A. Temtamy,⁴ and Bernd Wollnik^{1,2,16,*}

Cenani-Lenz syndrome (CLS) is an autosomal-recessive congenital disorder affecting distal limb development. It is characterized mainly by syndactyly and/or oligodactyly and is now shown to be commonly associated with kidney anomalies. We used a homozygosity-mapping approach to map the CLS1 locus to chromosome 11p11.2-q13.1. By sequencing candidate genes, we identified recessive *LRP4* mutations in 12 families with CLS. *LRP4* belongs to the low-density lipoprotein (LDL) receptor-related proteins (LRPs), which are essential for various developmental processes. *LRP4* is known to antagonize *LRP6*-mediated activation of canonical Wnt signaling, a function that is lost by the identified mutations. Our findings increase the spectrum of congenital anomalies associated with abnormal lipoprotein receptor-dependent signaling.

Introduction

Spatial and temporal activation of canonical Wnt/ β -catenin signaling is an essential developmental process during organogenesis and tissue regeneration.¹ Wnt ligands bind to their specific coreceptors, such as frizzled and low-density lipoprotein-related proteins 5 and 6 (*LRP5* [MIM 603506], *LRP6* [MIM 603507]), leading to a stabilization of β -catenin and transcriptional activation.² Alteration of the *LRP5/6* signaling pathway has been described in cancer development and human diseases.^{1,3,4} *LRP4* (MIM 604270) is another member of the low-density lipoprotein receptor family, but has an antagonistic effect on *LRP5/6* signaling. Recent results of GWAS in bone mineral density⁵ and the finding that *Lrp4* serves as a receptor for sclerostin regulating bone metabolism in mice⁶ highlight the importance of *LRP4* in the regulation of bone mineral density and the development of osteoporosis. In mice, *Lrp4* dysfunction also causes syndactyly.⁷

The genetic identification of factors regulating limb formation provided important insights into the role of major signaling pathways, such as sonic-hedgehog (SHH) and fibroblast growth factor (FGF), during limb develop-

ment.^{8,9} Cenani-Lenz syndrome (CLS [MIM 212780]) is an autosomal-recessive congenital anomaly affecting mainly distal limb development. CLS is characterized by fusion and disorganization of metacarpal and phalangeal bones, radius and ulnar shortening, radioulnar synostosis, and severe syndactyly of hands and feet.^{10,11} Kidney hypoplasia has been described in one patient with CLS,¹² but is not yet regarded as an associated trait.

Here, we map the CLS1 locus to chromosome 11p11.2-q13.1 and identify mutations in the *LRP4* gene in 12 CLS families. We show that *LRP4* function is required for the physiological regulation of Wnt signaling, and we identify mutations that cause loss of *LRP4* function, which is important for normal limb and kidney development. Therefore, loss of human *LRP4* function causes syndactyly, synostosis, and renal agenesis in Cenani-Lenz syndrome.

Material and Methods

Subjects

All subjects or their legal representatives gave written informed consent for participation in the study. The study was performed in accordance to the Declaration of Helsinki protocols and

¹Center for Molecular Medicine Cologne (CMMC), University of Cologne, 50931 Cologne, Germany; ²Institute of Human Genetics, University of Cologne, 50931 Cologne, Germany; ³Department of Pediatric Genetics, Marmara University Hospital, 34668 Istanbul, Turkey; ⁴Departments of Clinical and Molecular Genetics, Division of Human Genetics & Genome Research, National Research Centre, 12311 Cairo, Egypt; ⁵Medical Genetics Department, Istanbul Medical Faculty, Istanbul University, 34094 Istanbul, Turkey; ⁶Department of Medical Genetics, Faculty of Medicine, Gazi University, 06500 Ankara, Turkey; ⁷Clinical and Molecular Genetics Unit, Institute of Child Health, Great Ormond Street Hospital for Children, University College London, London WC1N 3JH, UK; ⁸Cologne Center for Genomics, University of Cologne, 50931 Cologne, Germany; ⁹Institute for Genetics, University of Cologne, 50674 Cologne, Germany; ¹⁰GETAM, Cerrahpasa Medical School, Istanbul University, 34452 Istanbul, Turkey; ¹¹Genetic Medicine, Manchester Academic Health Science Centre, St Mary's Hospital, Oxford Road, Manchester M13 0JH, UK; ¹²Molecular Medicine Unit, Institute of Child Health, London WC1N 1EH, UK; ¹³Department of Pediatrics, King Fahad National Guard Hospital, King Abdul Aziz Medical City, Riyadh 11426, Saudi Arabia; ¹⁴Department of Genetic Medicine and Development, Geneva University Hospital, 1211 Geneva, Switzerland; ¹⁵Department of Pediatrics, Academic Medical Center, 1105 AZ Amsterdam, The Netherlands; ¹⁶Cologne Excellence Cluster on Cellular Stress Responses in Aging-Associated Diseases (CECAD), University of Cologne, 50674 Cologne, Germany; ¹⁷Department of Molecular Genetics, University of Texas Southwestern Medical Center, Dallas, TX 75390, USA

¹⁸These authors contributed equally to this work

*Correspondence: bwollnik@uni-koeln.de

DOI 10.1016/j.ajhg.2010.03.004. ©2010 by The American Society of Human Genetics. All rights reserved.

approved by the local institutional review boards. We collected peripheral blood samples from the affected children and parents, after informed consent was obtained, according to the protocols approved by the participating institutions. All of the research procedures followed were in accordance with the ethical standards of the responsible national and institutional committees on human subject research. Fourteen families with the clinical diagnosis of CLS were included in the study. In 12 of them, mutations were identified in *LRP4*. Clinical features of some of the families have already been published; see families CL-1,¹² CL-2,¹³ CL-3,¹⁴ CL-6,¹⁵ CL-7.¹⁶ DNA from participating family members was extracted from peripheral blood lymphocytes by standard extraction procedures.

Linkage Analysis

We performed genome-wide linkage analysis in six families (CL-1 to CL-6; not all family members could be initially included into the genome scan), using the Affymetrix GeneChip Human Mapping 10K Array (version 2.0). This version of the 10K Chip Array comprises a total of 10,204 SNPs with a mean intermarker distance of 258 kb, equivalent to 0.36 cM. Genotypes were called by the GeneChip DNA Analysis Software (GDAS version 2.0, Affymetrix). We verified sample genders by counting heterozygous SNPs on the X chromosome. Relationship errors were evaluated with the help of the program Graphical Relationship Representation.¹⁷ The program PedCheck was applied to detect Mendelian errors,¹⁸ and data for SNPs with such errors were removed from the data set. Non-Mendelian errors were identified by use of the program MERLIN,¹⁹ and unlikely genotypes for related samples were deleted. Nonparametric linkage analysis using all genotypes of a chromosome simultaneously was carried out with MERLIN. Parametric linkage analysis was performed by a modified version of the program GENEHUNTER 2.1²⁰ through stepwise use of a sliding window with sets of 150 or 300 SNPs. Haplotypes were reconstructed with GENEHUNTER 2.1 and presented graphically with HaploPainter.²¹ This program also reveals informative SNP markers as points of recombination between parental haplotypes. All data handling was performed with the use of the graphical user interface ALOHOMORA,²² developed at the Berlin Gene Mapping Center to facilitate linkage analysis with chip data.

Mutation Screening

We identified candidate genes in the critical region by using the ENSEMBL and UCSC human genome databases. We amplified the 38 exons of the *LRP4* gene (primers are listed in Table S1, available online) from DNA of index patients from all 14 families and sequenced the PCR products via the BigDye Terminator method on an ABI 3100 sequencer. We resequenced all identified mutations in independent experiments, tested for cosegregation within the families, and screened at least 200 healthy control individuals from Turkey, 150 from Pakistan, 50 from Germany, and 50 from Egypt for each mutation by PCR and/or restriction digestion or direct sequencing. We analyzed all identified alterations by using the server PolyPhen. The *LRP4* protein structure was analyzed with the server Pfam in order to determine different protein domains of *LRP4*.

cDNA Analysis

RNA was extracted from fresh whole-cell blood through use of the Paxgene Blood RNA system. After cDNA transcription, nested PCR was used to amplify *LRP4* cDNA (primers are listed

in Table S1). Primers were designed according to the reference sequence.

Generation of Lrp4 Constructs

Five *Lrp4* mutant constructs were generated by site-directed mutagenesis with the use of wild-type mouse *Lrp4* in the pcDNA3.1/V5-His-TOPO vector (Invitrogen, Karlsruhe, Germany) as template. The correct sequence of all PCR amplicons and constructs was confirmed by direct sequencing from both sides with the use of the ABI BigDye Terminator v1.1 Cycle Sequencing Kit and the ABI 3730 DNA Analyzer (Applied Biosystems, Foster City, CA, USA).

Cell Culture and Transfections

Human embryonic kidney (HEK)293T cells were cultured in Dulbecco's Modified Eagle Media (DMEM) containing 10% fetal bovine serum (FBS), amphotericin B, streptomycin, and penicillin. Cells were transfected with the use of Lipofectamine 2000 (Invitrogen, Karlsruhe, Germany) according to the manufacturer's instructions.

Luciferase Assay

One day before transfection, approx. 400,000 HEK293T cells were plated out in 12-well plates and grown up to 50% confluency in 10% FBS and DMEM. Transfections were performed in triplicate with the use of the TOP-Flash reporter system and the indicated expression plasmids with the following concentrations: 500 ng wild-type (WT) *Lrp4* or 500 ng mutants, 250 ng *Lrp6*, 250 ng *Wnt1*, 100 ng Topflash Vector, 5 ng Renilla (p-RL-TK). Cells were transfected with the use of Lipofectamine 2000 (Invitrogen, Karlsruhe, Germany) according to the manufacturer's instructions. Two days after transfection, cells were lysed and Luciferase activity was measured with the use of the Dual-Luciferase Reporter Assay Kit and a Glomax 96-microplate luminometer (Promega, Mannheim, Germany). Each transfection was also measured in triplicate.

Immunoblot

Immunoblot analysis was performed according to standard protocols. Detection of *LRP4* was conducted with a C-terminal *Lrp4* mouse monoclonal antibody (1:1000).

Cell-Surface Biotin-Labeling Assay

One day before the experiment, 50% confluent HEK293T cells were cotransfected with 1.5 μ g *LRP4*, WT or mutant, and 1.5 μ g insulin receptor (IR) in T75 cm² flasks. Biotinylation was carried out with the use of the Cell Surface Protein Isolation Kit (Pierce, Bonn, Germany) according to the manufacturer's instructions. Protein concentrations were measured with the use of the BCA Protein Assay Kit (Pierce). Immunoblot analysis was performed according to standard protocols. Detection of *LRP4* and IR was conducted with a C-terminal *LRP4* mouse monoclonal antibody (1:1000) and an insulin-receptor rabbit monoclonal antibody (Abcam, Berlin, Germany) (1:1000).

Results

Clinical Findings in CLS Families

We have examined 14 CLS families presenting with a variable expression of clinical symptoms. In twelve of them we identified the molecular basis of the disease (Figure 1A,

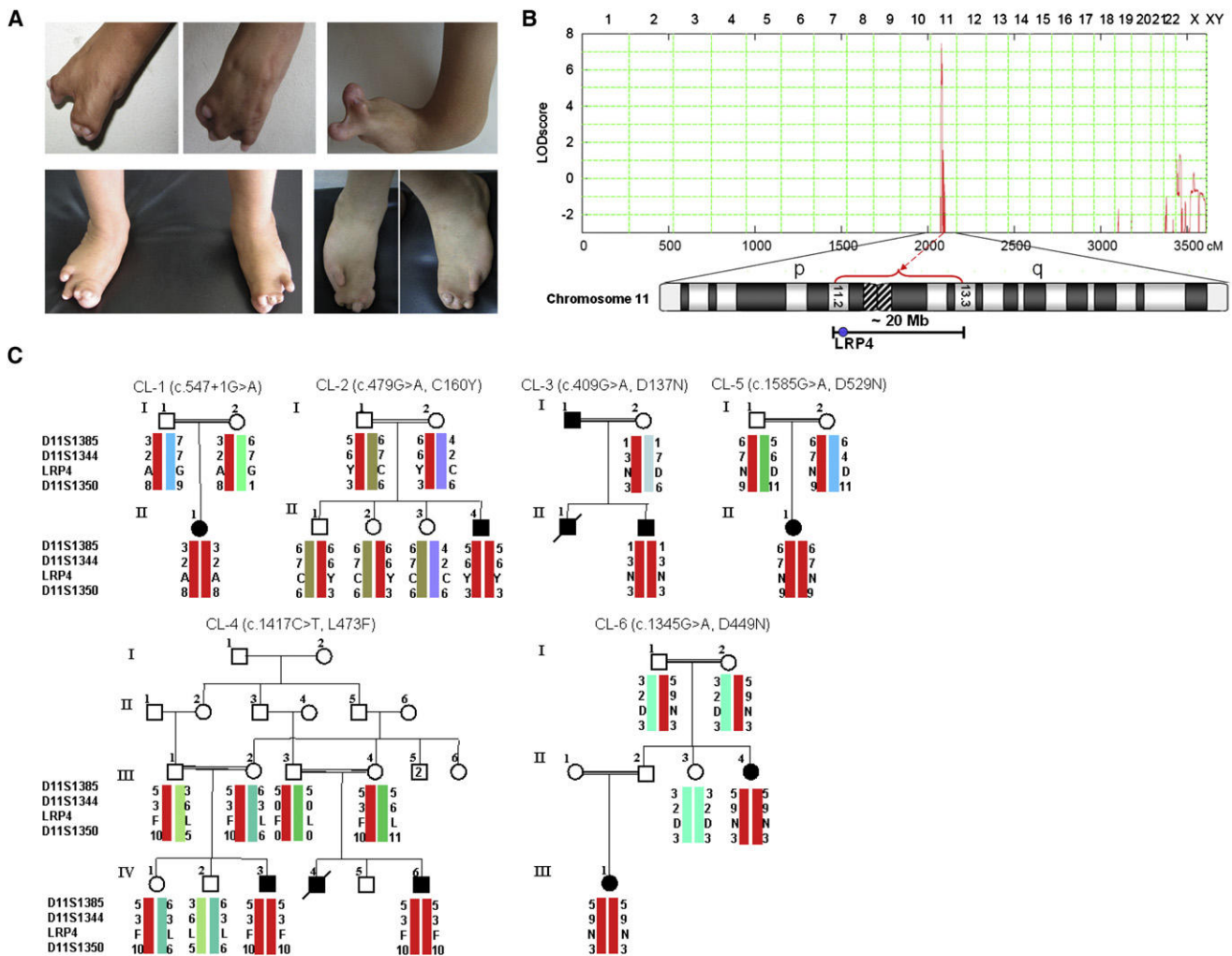


Figure 1. Clinical Findings in Families with CLS and Mapping of the CLS1 Locus

(A) Typical hand and feet anomalies seen in CLS patients.

(B) Graphical view of additive LOD-score calculations of genome-wide SNP mapping in families CL-1 to CL-6. Ideogram of chromosome 11 showing the localization of linked region.

(C) Haplotypes of CLS families included in the initial linkage analysis.

Table 1). We observed mild facial dysmorphism in the majority of CLS cases, with prominent forehead, hypertelorism, downslanting palpebral fissures, and micrognathia. Typical limb malformations included total to partial syndactyly of hands and feet, as well as distal bone malformations affecting the radius and ulna as well as the metacarpal and phalangeal bones (Figure 1A, Table 1). Interestingly, we also found kidney anomalies, including renal agenesis and hypoplasia, in over 50% of CLS families.

Mapping of the *CLS1* Locus and Identification of *LRP4* Mutations

Initially, we genotyped DNA samples from six CLS families (CL-1 to CL-6, Figure 1) by using the Affymetrix GeneChip Human Mapping 10K Array. Affected individuals were born to consanguineous parents in all families. A combined parametric LOD score of 7.46 was obtained for a single region located on chromosome 11p11.2-q13.1

between SNPs rs1346671 and rs490192 (Figure 1B), defining a shared critical interval of about 19.7 Mb. Subsequent analysis of microsatellite markers and inclusion of additional family members confirmed homozygous haplotypes for the linked region in all affected individuals (Figure 1C). We considered *LRP4* as a highly relevant positional and functional candidate gene. No additional gene from the critical region was tested. Sequencing of the 38 coding exons of *LRP4* (Table S1) revealed different homozygous mutations in affected individuals in each of the six families. The mutations cosegregated with the disease in the families and were not found in at least 250 healthy control individuals. We found one donor splice-site mutation, c.547+1G>A (intron 6, CL-1), and five missense mutations: c.479G>A (p.C160Y, exon 5, CL-2), c.409G>A (p.D137N, exon 4, CL-3), c.1417C>T (p.L473F, exon 12, CL-4), c.1585G>A (p.D529N, exon 13, CL-5), c.1345G>A (p.D449N, exon 12, CL-6) (Figure 2A). All missense

Table 1. Clinical Findings in CLS Families Carrying *LRP4* Mutations

Family Data	CL-1	CL-2	CL-3	CL-4	CL-5	CL-6	CL-7	CL-8	CL-9	CL-10	CL-11	CL-12
Consanguinity	+	+	+	+	+	+	+	+	+	+	-	+
No. of affected individuals	1	1	3	3	1	2	1	6	2	2	1	1
Mutation	c.547+1G>A	C160Y	D137N	L473F	D529N	D449N	T461P	C1017R	D529N	D529N	c.200-9G>A, c.4959G>C	D137N
Origin	Pakistan	Turkey	Egypt	Egypt	Turkey	Turkey	Pakistan	Jordan	Turkey	Turkey	Turkey	Egypt
Facial dysmorphism												
Prominent forehead	+	-	+	+	-	-	+	+	+	+	+	+
Hypertelorism	+	-	+	+	-	-	+	-	+	-	+	+
Downsl. palpebral fissures	-	-	+	+	-	-	-	+	-	-	-	+
Micro-, retrognathia	+	-	+	+	-	-	-	+	-	-	+	+
Teeth findings												
Hypodontia	-	-	-	-	-	-	-	-	+	-	?	?
Malar hypoplasia	+	-	+	+	-	-	+	+	-	-	+	+
Enamel hypoplasia	-	-	+	+	-	-	-	-	-	-	?	?
Early loss of permanent teeth	-	-	+	+	-	?	-	-	?	?	?	?
Upper limb findings												
Typical syndactyly	+	+/-	+	+	+	+	+/-	+	+	-	+	+
Short forearms	+	-	+	+	+	+	-	-	-	-	+	+
Radius-ulnar synostosis	+	-	+	+	+	+	-	-	?	?	+	+
Disorganized / missing metacarpals and phalanges	+	+	+	+	+	+	+	+	+	+	+	+
Fused metacarpals	+	+	+	+	+	+	-	+	+	+	+	+
Nail aplasia	+	+/-	+	+	+	+	+	+	+	-	+	+
Lower limb findings												
Syndactyly	2/3	2/3	+	+	2/3–2/5	+	+	1/2/3	R 2/3	2/3	1/2	+
Tibia-fibula synostosis	-	-	-	-	-	-	-	-	-	-	-	-

Table 1. Continued

Family Data	CL-1	CL-2	CL-3	CL-4	CL-5	CL-6	CL-7	CL-8	CL-9	CL-10	CL-11	CL-12
Disorganized / missing metatarsals and phalanges	-	-	+	+	+/-	-	+	+	+	-	-/+	+
Nail aplasia /partial	-	-	+	+	+/-	+	+	+	-/+	-	+	+
Kidney anomalies												
Agensis	-	-	-	-	-	-	unilateral	-	bilateral	bilateral	bilateral	-
Hypoplasia	bilateral	-	-	-	-	unilateral	-	unilateral	-	-	-	-
Ectopic localization	-	-	-	-	-	+	-	+	-	-	-	-
Additional findings												
Developmental delay	-	-	+	-	-	-	-	-	-	mild gross motor delay	?	?
Other		bilateral broad hallux valgus anomaly		hypoplastic scrotum	scoliosis, hemivertebrae, mixed-type hearing loss	duplicated distal phalanges of the first and second toe, congenital cataract	pulmonary stenosis, congenital hip dislocation	hypothyroidism	G1: died at first day of life due to bilateral renal agenesis	G2: medical abortion (20. GW), bilateral renal agenesis	medical abortion (20. GW)	pectus excavatum

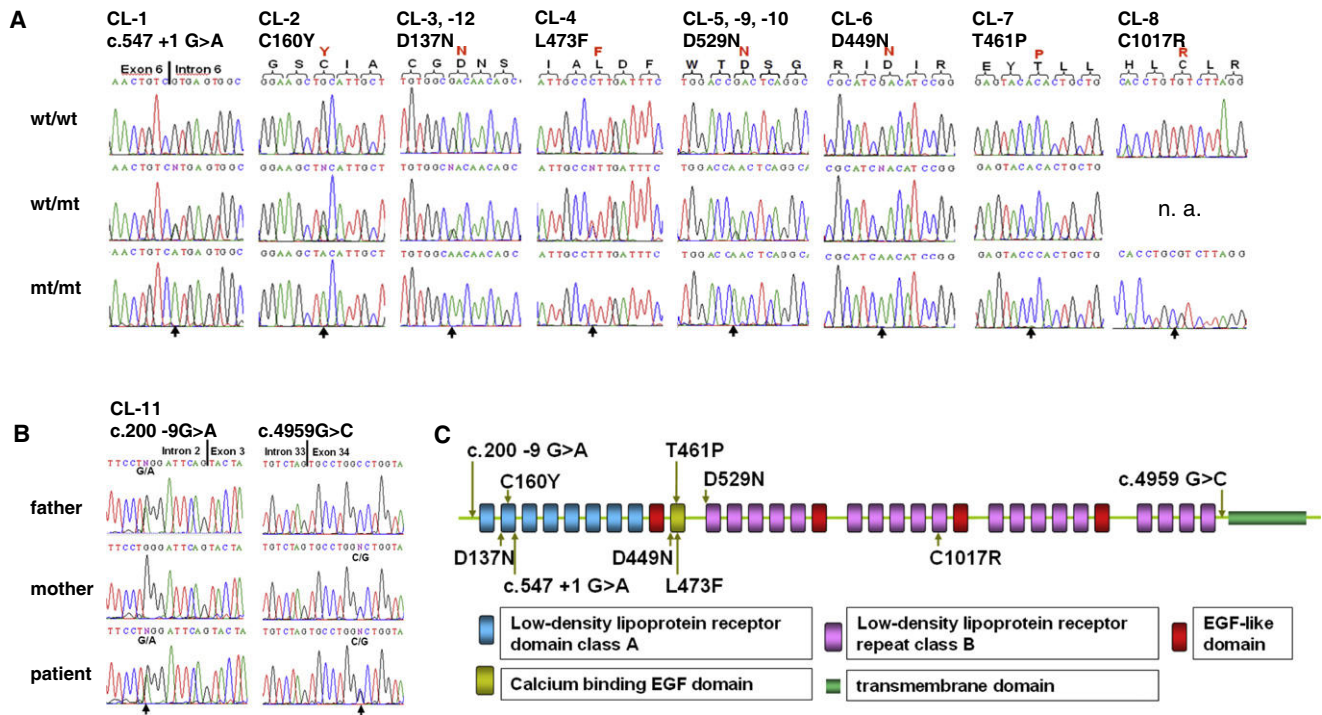


Figure 2. Mutations Identified in *LRP4*

(A) Electropherograms of identified homozygous *LRP4* mutations compared with heterozygous carrier and WT sequences (n.a., not available).

(B) Electropherograms of identified compound-heterozygous splice-site mutations in *LRP4* causing aberrant splicing and premature protein truncation.

(C) Schematic view of *LRP4* receptor domains and localization of identified CLS mutations.

mutations are located in the extracellular domains of *LRP4* within highly conserved regions, as shown by *LRP4* protein alignments of various species (Figure S1). p.C160Y and p.D137N mutations lie within the ligand-binding (class A) repeat-containing domain of the receptor, p.D449N and p.L473F are located within calcium-binding epidermal growth factor (EGF) repeats, and D529 is located within the YWTD domain (Figure 2C).

We continued the molecular analysis of *LRP4* in eight additional CLS families (Figures 3A and 3C). In families CL-9 and CL-10, we found the same homozygous p.D529N mutation as identified before in the CL-5 family. All three families originated from Turkey, and haplotype analysis confirmed that p.D529N is a common founder mutation in Turkish CLS patients (Figure 3C). It is also interesting to note that the p.D137N mutation is repeatedly found in CLS families from Egypt, as we could identify a second family, CL-12, carrying this mutation. p.D137N in both families was located on identical haplotypes (Figure 3D), suggesting that p.D137N is a founder mutation. Two additional missense mutations were found: c.1382A>C (p.T461P, exon 11, CL-7) in a Jordanian patient and c.3049T>C (p.C1017R, exon 22, CL-8) in a large CLS family from Pakistan with six affected family members (Figure 2B, Figure 3A). These mutations also cosegregated with the disease, were not found in matched controls, and were located in highly conserved regions (Figure S1).

Furthermore, no *LRP4* mutation was found in two other consanguineous CLS families, and haplotype analysis did not show homozygosity of the *LRP4* region in affected individuals from both families, supporting the idea of further locus heterogeneity (Figure 3B).

We found initial evidence for an impairment of *LRP4* function as the underlying pathomechanism of CLS by identifying compound-heterozygous splice-site mutations in a typically affected fetus with CLS. Both mutations, c.200-9G>A and c.4959G>C (Figure 2C), caused aberrantly spliced *LRP4* transcripts (r.199_200insGATTCAG and r.4952_4987del, respectively), and both mutations lead to a truncated protein (Figures 4A and 4B).

LRP4 Mutations Cause Loss of Protein Function

To investigate whether the identified missense mutations confer loss of function or whether they are functionally hypomorphic with biochemically detectable residual protein activity, we analyzed the effect of five missense mutations (p.D137N, p.C160Y, p.L473F, p.D449N, and p.D529N) on the transduction and activation of canonical Wnt signaling by using a Dual Luciferase Reporter Assay in transiently transfected HEK293T cells. Consistent with earlier findings,⁵ we found that WNT1 was able to significantly activate LRP6-mediated β -catenin signaling and that additional coexpression of *LRP4* potentially antagonized this activation (Figure 5A). In contrast, coexpression of

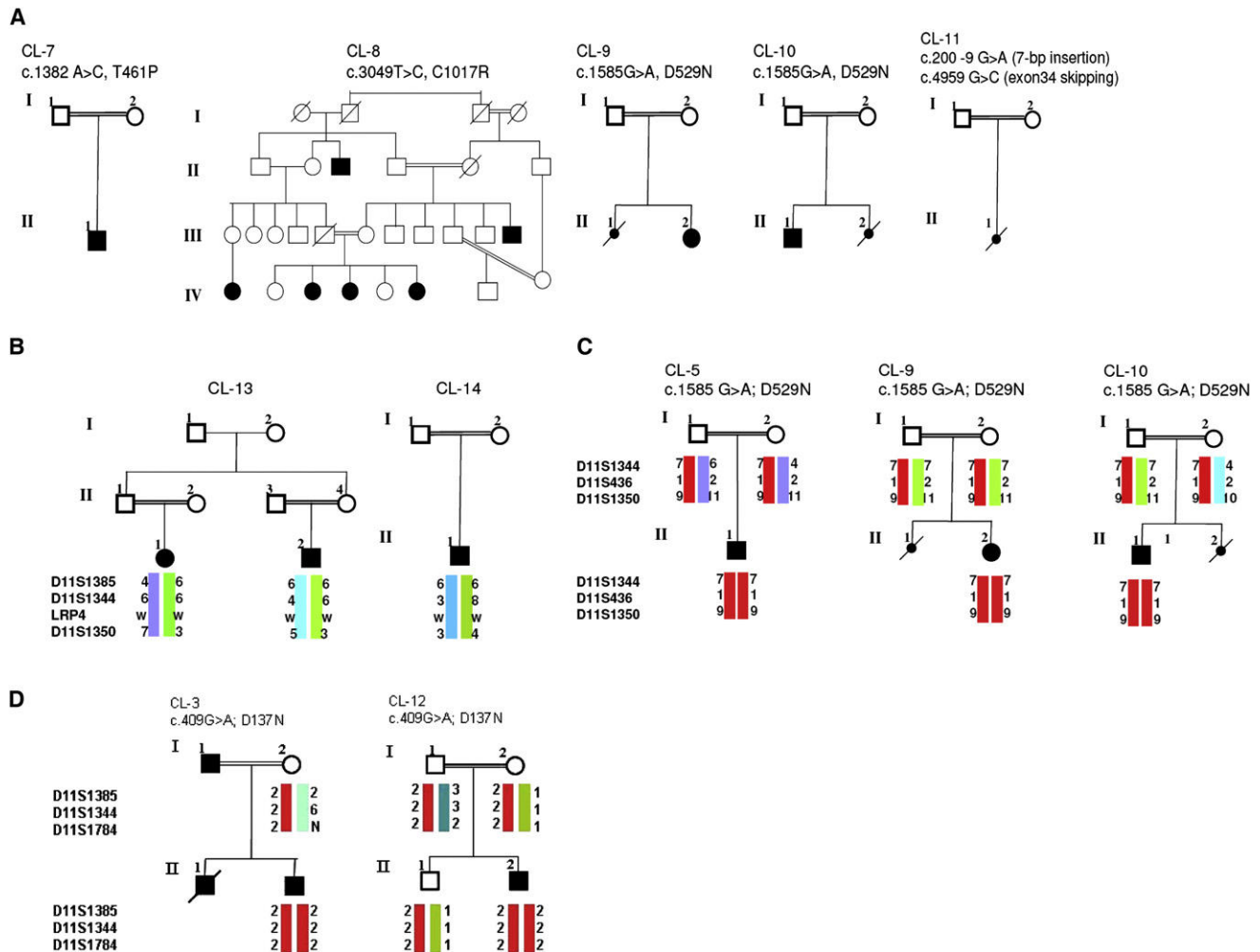


Figure 3. Additional CLS Families and Genetic Heterogeneity

(A) Pedigrees of additional CLS families.

(B) The *LRP4* locus was excluded in families CL-13 and CL-14 by haplotype analysis.

(C and D) Identification of an *LRP4* founder mutation, p.D529N, in three Turkish CLS families (C) and of p.D137N in two families from Egypt (D). Identical haplotypes are shown in red.

each of the five missense mutations abolished the observed antagonistic *LRP4* effect on *LRP6*-mediated activation of Wnt/ β -catenin signaling. Moreover, mutant *LRP4* receptors failed to be efficiently transported to the plasma membrane, as shown by cell-surface biotinylation (Figure 5B).

Discussion

We report the mapping of the *CLS1* locus to chromosome 11p11.2-q13.1 and present convincing evidence that mutations in the *LRP4* gene cause CLS. Clinical findings in our CLS patients showed that in addition to the well-described distal limb malformations (ranging from total to partial syndactyly and bone malformations of both hands and feet), patients presented with facial features such as prominent forehead, hypertelorism, downslanting palpebral fissures, and micrognathia. Previously, renal hypoplasia has been reported in only one case¹⁶ and was

therefore not regarded as an associated trait of CLS. Our finding that over 50% of CLS families present with renal agenesis and/or hypoplasia adds kidney anomalies to the clinical spectrum of CLS. In this context, it is interesting to note that a subpenetrant phenotype of kidney agenesis was observed in *Lrp4* homozygous null mice. In the *Lrp4*^{-/-} homozygous kidneys the ureteric budding is often delayed, resulting in insufficient stimulation of the mesenchyme. This results in destruction of pre-nephric mesenchymal structures, and no kidneys are formed (J. Herz, personal communication). These findings clearly show that *Lrp4* has an important function for kidney development in mice and humans.

Recently, murine *LRP4* was shown to serve as a coreceptor for agrin in the formation of the neuromuscular junction.²³ Mutations in genes encoding other members of this complex have been associated with akinetic and myasthenic syndromes in humans (MIM 288150 and MIM 254300).^{24,25} Given that we did not observe a clinically

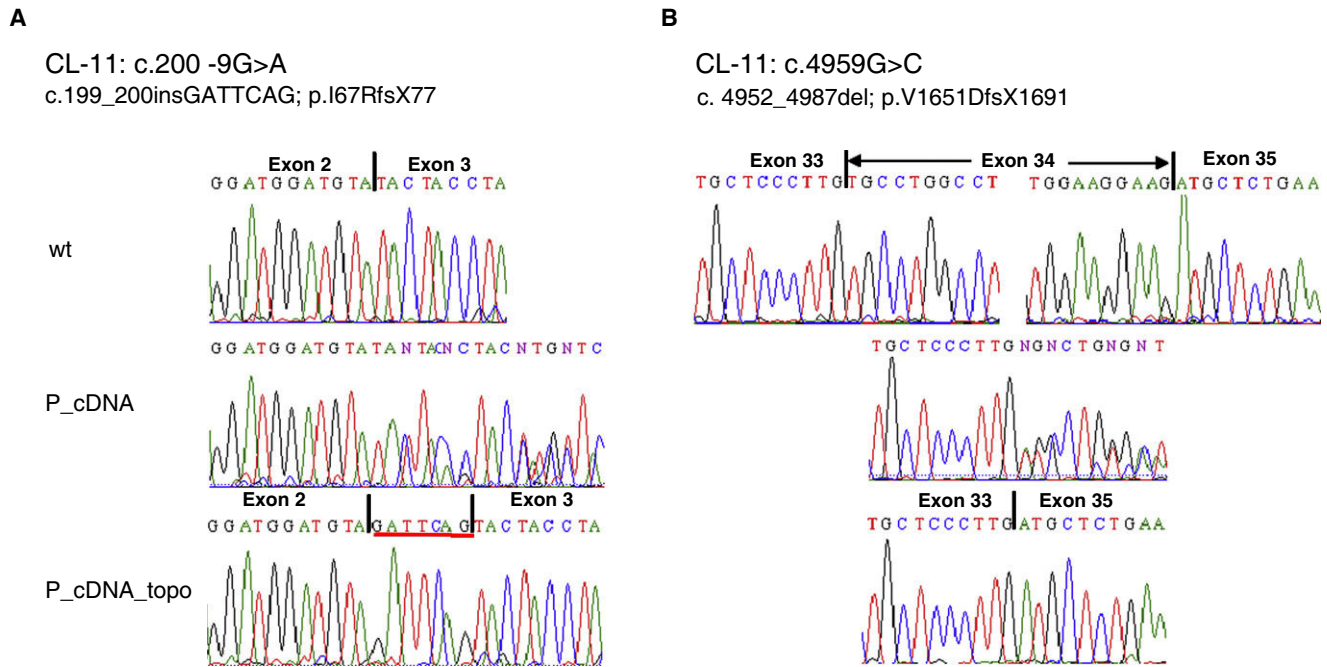


Figure 4. Splicing Effects of Mutations in Family CL-11

(A) Analysis of the heterozygous c.200-9G>A mutation. cDNA sequences of the exon 2-exon 3 boundary of wild-type (wt) and patient cDNA are shown (without [P_cDNA] and after subcloning via the TOPO-Vector system [P_cDNA_topo]).

(B) Analysis of the heterozygous c.4959G>C mutation. Electropherograms show the cDNA sequences of *LRP4* transcripts encoded by exon 33 to exon 35 of wild-type (wt), and skipping of exon 34 in the patient cDNA.

detectable neuromuscular phenotype in our CLS patients, the role of *LRP4* in the development and function of the neuromuscular junction in humans (as opposed to mice) will require further investigation. In the case that the *LRP4* mutations found in CLS patients are not complete loss-of-function mutations and do have minor residual functionality *in vivo*, there could be a different but overlapping phenotype caused by, for example, homozygous nonsense mutations or deletions in *LRP4*, and this could include neuromuscular symptoms.

The *LRP4* mutations identified in our study are frequently missense mutations, which are located in the large extracellular domain of *LRP4* within the ligand-binding (class A) repeat-containing domain, calcium-binding EGF repeats, and the YWTD domain of the receptor (Figure 2C). These changes might cause structural alterations of the extracellular *LRP4* domain that interfere with normal folding and thus prevent the efficient export of the protein through the secretory pathway, but this hypothesis has to be proven in future experimental studies. Our functional analysis of five of the missense mutations clearly demonstrated a functional impairment of *LRP4* mutant proteins. *LRP4* is important for control and modification of Wnt signaling by its antagonistic effect on *LRP6*-mediated activation of WNT signaling (Figure 5C). This antagonistic function is completely lost in four out of five *LRP4* mutants, as shown in our in a Dual Luciferase Reporter Assay. The p.D137N mutant seems to show some residual antagonistic function in the Reporter Assay experiment, and the biotinylation

experiments clearly demonstrated that p.D137N mutant protein is not getting to the cell surface. Whether a yet unknown function of *LRP4*, which is not dependent on its membrane integration, could be responsible for this residual function remains to be elucidated.

We also found that WNT1 was able to significantly activate *LRP6*-mediated β -catenin signaling, which is consistent with earlier findings.⁷ We demonstrated that the main reason for the loss-of-function effect is the failure of mutant *LRP4* receptors to be efficiently transported to the plasma membrane. In addition, the heterozygous splice-site mutations identified in the CL-11 fetus, c.200-9G>A and c.4959G>C, caused aberrantly spliced *LRP4* transcripts and premature protein truncations. Conclusively, we suggest complete or near-complete loss of *LRP4* function as the underlying pathogenetic mechanism of CLS. As a result, developmental limb and kidney malformations in patients occur through a mechanism that likely also involves excessive *LRP6*-mediated Wnt/ β -catenin activation (Figure 5C).

It has been previously shown that *Lrp4* dysfunction also causes polysyndactyly in mice⁷ and syndactyly with variable penetrance in bovines, termed mulefoot disease.²⁶ *Lrp4* was shown to be expressed in the apical ectodermal ridge (AER) in the developing limb bud,⁷ a structure important for coordination of patterning and growth of the distal limb.⁸ Various signaling molecules are secreted from the AER, such as sonic hedgehog (Shh), bone morphogenic proteins (Bmps), fibroblast growth factors (Fgfs), and Wnts,

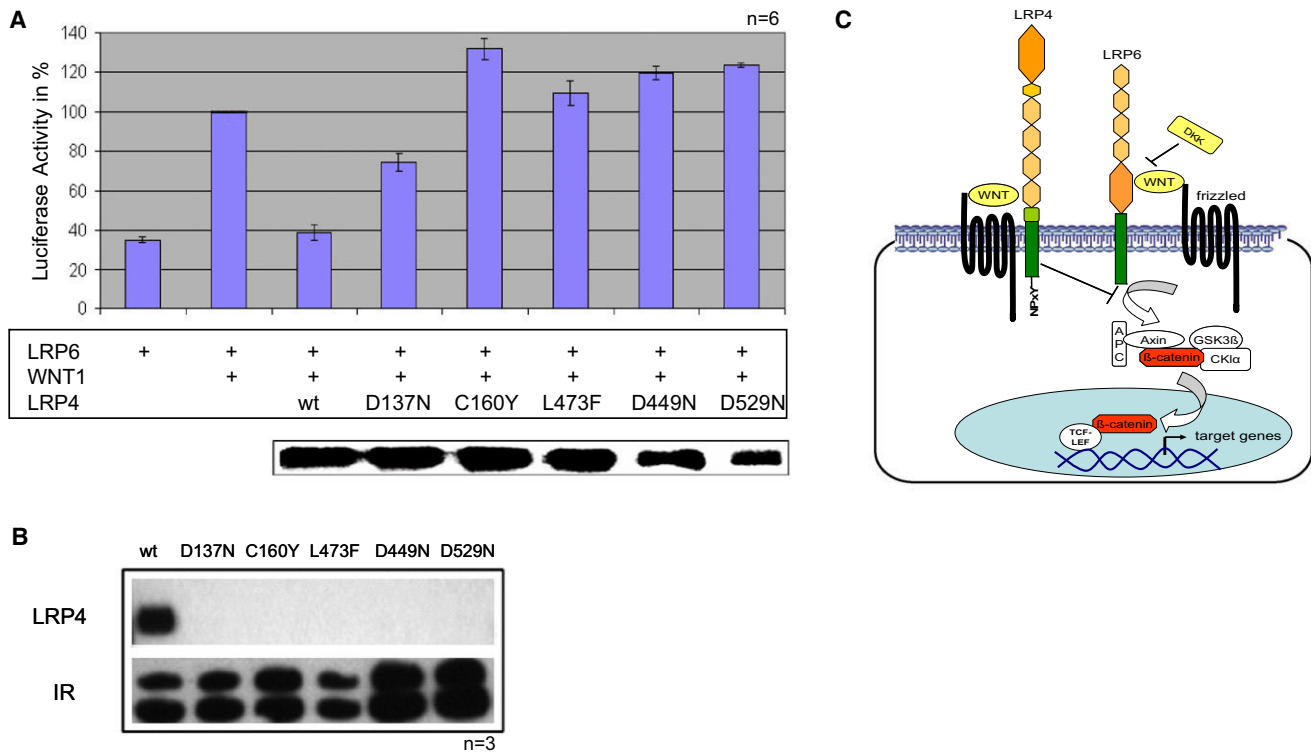


Figure 5. Functional Analysis of LRP4 Missense Mutations

(A) Results from the Dual Luciferase Reporter Assay after coexpression of LRP6, WNT1, and wild-type and mutant LRP4 in different combinations. Graph depicting the relative Luciferase activities (mean and standard deviations of six experiments, in triplicate each time). Comparable steady-state expression levels of wild-type and mutant LRP4 proteins are shown by immunoblotting of total lysates after measurement of luciferase activity.

(B) Compared to wild-type LRP4 and wild-type insulin receptor (IR), mutant LRP4 proteins are not detectable by cell-surface biotinylation. Results from three independent experiments are shown.

(C) Schematic representation of LRP4 function in LRP6-mediated activation of Wnt/ β -catenin signaling.

and the complex interactions of these signaling pathways are essential for normal limb development.^{27,28} Extensive analysis of the limb phenotype in *Lrp4*^{-/-} knockout mice showed that loss of *Lrp4* causes structural AER alterations as well as ectopic expression of different key signaling molecules (e.g., *Fgf8*, *Bmp4*, and *Shh*).⁷ Whether *Lrp6* expression was upregulated during limb development in the AER of *Lrp4*^{-/-} mice was not analyzed. Given the facts that (1) *Lrp4* was described as an integrator of Wnt and Bmp signaling,²⁹ (2) *Lrp4* has an antagonistic function on *Lrp6*-mediated Wnt/ β -catenin activation, and (3) *Lrp6* is critical for Wnt signaling during limb development in mice,³⁰ it is a reasonable working hypothesis that loss of LRP4 during limb development in CLS patients could lead to an overactivation of LRP6, which then causes altered Wnt signaling. Future approaches are needed to show that knocking down LRP4 expression upregulates Wnt/ β -catenin in vivo.

In two CLS families, we did not find *LRP4* mutations, and haplotype analysis did not show homozygosity in affected individuals born to consanguineous parents. In the CL-13 family with only a single affected individual, homozygosity is only an assumption due to parental con-

sanguinity, but lack of homozygosity does not completely exclude *LRP4* as causative gene. In the CL-14 family, haplotype analysis of microsatellite markers as well as results from 250K array analysis excluded common haplotypes in both affected individuals, suggesting further locus heterogeneity in CLS. Future identification of a causative gene(s) in these families will highlight additional key proteins for distal limb development.

We conclude that LRP4 function is required for the physiological regulation of Wnt signaling, which is important for normal limb and kidney development. Homozygous loss of human LRP4 function causes syndactyly, synostosis, and renal agenesis in Cenani-Lenz syndrome.

Supplemental Data

Supplemental Data include one figure and one table and can be found with this article online at <http://www.ajhg.org>.

Acknowledgments

We are thankful to all family members that participated in this study, to Bernhard Zabel for referral of patients, to Esther Milz

for excellent technical assistance, and to Christian Kubisch, Brunhilde Wirth, and Karin Boss for critical reading of the manuscript. This work was supported by the German Federal Ministry of Education and Research (BMBF) by grant numbers 01GM0880 (SKELNET) and 01GM0801 (E-RARE network CRANIRARE) to B.W. J.H. is supported by grants from the National Institutes of Health, the American Health Assistance Foundation, the Perot Family Foundation, and the Wolfgang-Paul Program of the Alexander-von-Humboldt Foundation. C.N. was supported by the German Research Foundation (DFG), grant NE826/3-2.

Received: January 17, 2010

Revised: March 10, 2010

Accepted: March 11, 2010

Published online: April 8, 2010

Web Resources

The URLs for data presented herein are as follows:

ENSEMBL, <http://www.ensembl.org>

Online Mendelian Inheritance in Man (OMIM), <http://www.ncbi.nlm.nih.gov/omim/>

Pfam Server, <http://pfam.sanger.ac.uk/>

PolyPhen, <http://coot.embl.de/PolyPhen>

UCSC Genome Browser, <http://www.genome.ucsc.edu>

References

- Clevers, H. (2006). Wnt/ β -catenin signaling in development and disease. *Cell* 127, 469–480.
- Gordon, M.D., and Nusse, R. (2006). Wnt signaling: multiple pathways, multiple receptors, and multiple transcription factors. *J. Biol. Chem.* 281, 22429–22433.
- Gong, Y., Slee, R.B., Fukui, N., Rawadi, G., Roman-Roman, S., Reginato, A.M., Wang, H., Cundy, T., Glorieux, F.H., Lev, D., et al. Osteoporosis-Pseudoglioma Syndrome Collaborative Group. (2001). LDL receptor-related protein 5 (LRP5) affects bone accrual and eye development. *Cell* 107, 513–523.
- Mani, A., Radhakrishnan, J., Wang, H., Mani, A., Mani, M.A., Nelson-Williams, C., Carew, K.S., Mane, S., Najmabadi, H., Wu, D., and Lifton, R.P. (2007). LRP6 mutation in a family with early coronary disease and metabolic risk factors. *Science* 315, 1278–1282.
- Styrkarsdottir, U., Halldorsson, B.V., Gretarsdottir, S., Gudbjartsson, D.F., Walters, G.B., Ingvarsson, T., Jonsdottir, T., Saemundsdottir, J., Snorraddottir, S., Center, J.R., et al. (2009). New sequence variants associated with bone mineral density. *Nat. Genet.* 41, 15–17.
- Choi, H.Y., Dieckmann, M., Herz, J., and Niemeier, A. (2009). Lrp4, a novel receptor for Dickkopf 1 and sclerostin, is expressed by osteoblasts and regulates bone growth and turnover in vivo. *PLoS ONE* 4, e7930.
- Johnson, E.B., Hammer, R.E., and Herz, J. (2005). Abnormal development of the apical ectodermal ridge and polysyndactyly in *Megf7*-deficient mice. *Hum. Mol. Genet.* 14, 3521–3538.
- Niswander, L. (2003). Pattern formation: old models out on a limb. *Nat. Rev. Genet.* 4, 133–143.
- Ingham, P.W., and Placzek, M. (2006). Orchestrating ontogenesis: variations on a theme by sonic hedgehog. *Nat. Rev. Genet.* 7, 841–850.
- Cenani, A., and Lenz, W. (1967). Total syndactyly and total radioulnar synostosis in 2 brothers. A contribution to the genetics of syndactyly. *Ztschr. Kinderheilk* 101, 181–190.
- Elçioğlu, N., Atasü, M., and Cenani, A. (1997). Dermatoglyphics in patients with Cenani-Lenz type syndactyly: studies in a new case. *Am. J. Med. Genet.* 70, 341–345.
- Bacchelli, C., Goodman, F.R., Scambler, P.J., and Winter, R.M. (2001). Cenani-Lenz syndrome with renal hypoplasia is not linked to FORMIN or GREMLIN. *Clin. Genet.* 59, 203–205.
- Seven, M., Yüksel, A., Ozkiliç, A., and Elçioğlu, N. (2000). A variant of Cenani-Lenz type syndactyly. *Genet. Couns.* 11, 41–47.
- Temtamy, S.A., Ismail, S., and Nemat, A. (2003). Mild facial dysmorphism and quasidominant inheritance in Cenani-Lenz syndrome. *Clin. Dysmorphol.* 12, 77–83.
- Percin, E.F., and Percin, S. (2003). Two unusual types of syndactyly in the same family; Cenani-Lenz type and “new” type versus severe type I syndactyly? *Genet. Couns.* 14, 313–319.
- Jarbhau, H., Hamamy, H., Al-Hadidy, A., and Ajlouni, K. (2008). Cenani-Lenz syndactyly with facial dysmorphism, hypothyroidism, and renal hypoplasia: a case report. *Clin. Dysmorphol.* 17, 269–270.
- Abecasis, G.R., Cherny, S.S., Cookson, W.O., and Cardon, L.R. (2001). GRR: graphical representation of relationship errors. *Bioinformatics* 17, 742–743.
- O’Connell, J.R., and Weeks, D.E. (1998). PedCheck: a program for identification of genotype incompatibilities in linkage analysis. *Am. J. Hum. Genet.* 63, 259–266.
- Abecasis, G.R., Cherny, S.S., Cookson, W.O., and Cardon, L.R. (2002). Merlin—rapid analysis of dense genetic maps using sparse gene flow trees. *Nat. Genet.* 30, 97–101.
- Strauch, K., Fimmers, R., Kurz, T., Deichmann, K.A., Wienker, T.F., and Baur, M.P. (2000). Parametric and nonparametric multipoint linkage analysis with imprinting and two-locus-trait models: application to mite sensitization. *Am. J. Hum. Genet.* 66, 1945–1957.
- Thiele, H., and Nürnberg, P. (2005). HaploPainter: a tool for drawing pedigrees with complex haplotypes. *Bioinformatics* 21, 1730–1732.
- Rüschendorf, F., and Nürnberg, P. (2005). ALOHOMORA: a tool for linkage analysis using 10K SNP array data. *Bioinformatics* 21, 2123–2125.
- Kim, N., Stiegler, A.L., Cameron, T.O., Hallock, P.T., Gomez, A.M., Huang, J.H., Hubbard, S.R., Dustin, M.L., and Burden, S.J. (2008). Lrp4 is a receptor for Agrin and forms a complex with MuSK. *Cell* 135, 334–342.
- Huzé, C., Bauché, S., Richard, P., Chevessier, F., Goillot, E., Gaudon, K., Ben Ammar, A., Chaboud, A., Grosjean, I., Lecuyer, H.A., et al. (2009). Identification of an agrin mutation that causes congenital myasthenia and affects synapse function. *Am. J. Hum. Genet.* 85, 155–167.
- Michalk, A., Stricker, S., Becker, J., Rupps, R., Pantzar, T., Mieratus, J., Botta, G., Naretto, V.G., Janetzki, C., Yaqoob, N., et al. (2008). Acetylcholine receptor pathway mutations explain various fetal akinesia deformation sequence disorders. *Am. J. Hum. Genet.* 82, 464–476.
- Johnson, E.B., Steffen, D.J., Lynch, K.W., and Herz, J. (2006). Defective splicing of *Megf7/Lrp4*, a regulator of distal limb

- development, in autosomal recessive mulefoot disease. *Genomics* 88, 600–609.
27. Capdevila, J., and Izpisua Belmonte, J.C. (2001). Patterning mechanisms controlling vertebrate limb development. *Annu. Rev. Cell Dev. Biol.* 17, 87–132.
28. Barrow, J.R., Thomas, K.R., Boussadia-Zahui, O., Moore, R., Kemler, R., Capecchi, M.R., and McMahon, A.P. (2003). Ectodermal Wnt3/beta-catenin signaling is required for the establishment and maintenance of the apical ectodermal ridge. *Genes Dev.* 17, 394–409.
29. Ohazama, A., Johnson, E.B., Ota, M.S., Choi, H.Y., Choi, H.J., Pornaveetus, T., Oommen, S., Itoh, N., Eto, K., Gritli-Linde, A., et al. (2008). Lrp4 modulates extracellular integration of cell signaling pathways in development. *PLoS ONE* 3, e4092.
30. Pinson, K.I., Brennan, J., Monkley, S., Avery, B.J., and Skarnes, W.C. (2000). *Nature* 28, 535–538.

5.3 Wieczorek D, Pawlik B, Li Y, Akarsu NA, Caliebe A, May KJ, Schweiger B, Vargas FR, Balci S, Gillessen-Kaesbach G, Wollnik B. A specific mutation in the distant sonic hedgehog cis-regulator (ZRS) causes Werner mesomelic syndrome while complete ZRS duplications underlie Haas type polysyndactyly and preaxial polydactyly with or without triphalangeal thumb. Hum Mutat. (2010); 31(1):81-9.

Abstract of the publication:

Werner mesomelic syndrome (WMS) is an autosomal dominant disorder characterized by hypo- or aplasia of the tibiae, preaxial polydactyly of the hands and feet and/or five fingered hands and triphalangeal thumbs. Triphalangeal thumb is a common hand malformation, which can occur isolated as autosomal dominant inherited, nonopposable triphalangeal thumb or as a clinical sign of well-characterized syndromic conditions; e.g., Holt-Oram syndrome. Recently, mutations in the zone of polarizing activity regulatory sequence (ZRS), a long-range limb-specific enhancer of the *sonic hedgehog* (*SHH*) gene, have been identified in patients with preaxial polydactyly type II (PPD2), triphalangeal thumb polysyndactyly (TPTPS), and syndactyly type IV (SD4, Haas type polysyndactyly). Thus, we regarded the ZRS enhancer, which lies within the intron 5 of the *LMBR1* gene, to be an excellent candidate gene for WMS.

Initially, we sequenced the ZRS within the index patients of one Turkish and another Brasil family with WMS. Furthermore we tested the enhancer in a sporadic female patient diagnosed with Haas type polysyndactyly and another family with TPTPS by using a quantitative PCR technique for the detection of Copy Number Variations (CPVs) of the ZRS.

We identified heterozygous single base pair alterations at position 404 of the ZRS in the Turkish index (404G>A) and in six affected individuals of the second Brasil family with WMS (404G>C). The mutations are affecting a highly conserved nucleotide position within the ZRS region and were absent in all tested healthy family members as well as in 100 Turkish control individuals. Moreover, based on the applied Δ Ct method, we detected ZRS duplications in the index patient with Haas type polysyndactyly and in eight affected individuals of the family with TPTPS. In contrast, unaffected family members from this family did not show any quantitative changes and the duplication was not detected in 35 Turkish controls.

Own contributions:

The patients' DNAs for this study was kindly provided Dr. Dagmar Wieczorek (Institut für Humangenetik, Universitätsklinikum, Essen). The complete molecular data presented in this paper were done by myself.

I started with primer design and PCR amplification of the 772 bp long ZRS-DNA-fragment in all affected family members. I could elucidate the molecular basis of WMS by identifying the 404G>A and the 404G>C mutation in distinct patients (Figure 4, p.4). I was able to confirm co-segregation of the mutations in the families by direct sequencing of all family members and by a PCR/enzyme digestion method using TaalI (data not shown). In addition, I performed control studies of 100 healthy Turkish control individuals. In conclusion, I could demonstrate that the 404G position of the ZRS is highly conserved among species using sequence alignment (Figure 4, p.4).

Next, I evaluated and interpreted the Array-CGH data (Figure 5, p.5) using genome databases. According to the CGH data I designed ZRS primers and probes for quantitative Real-Time PCR and performed TaqMan analysis with patients. After subsequent analysis of the qPCR data, I could detect duplications in one sporadic patient with Haas-type syndactyly and in eight affected family members of a family diagnosed with TPTPS. Furthermore these copy number changes were not present in 35 control individuals (Figure not shown).

Moreover, I designed ZRS containing constructs for FISH analysis by cloning ZRS-PCR fragments into *TOPO* vector and performed breakpoint PCR for the sporadic patient with type Haas syndactyly and for one patient of the family diagnosed with TPTPS.

Finally, I prepared all experimental figures (Figure 4, 5) for the publication and critically read the manuscript before its submission to Human Mutation.

Unpublished data:

Very recently I have been able to identify a novel ZRS mutation (405T>A) in a female WMS patient from Birmingham, UK. Promotor analysis of the ZRS transcription binding site predicted that the mutation might cause a loss of binding of the *PLZF* transcription factor. Because it is suggested that mutations in the ZRS cause a changed transcription factor-binding affinity and that this could be the disease-causing mechanism for triphalangeal thumb, I started to confirm this hypothesis for WMS by generating a mutant 405T>A construct on the wt mouse ZRS in the *pBGZ40/p1230* vector. A Band-Shift Assay with the mutant ZRS-DNA fragment and the purified PLZF transcription factor in the near future might show the importance of the ZRS in the pathophysiology of WMS.

A Specific Mutation in the Distant Sonic Hedgehog (*SHH*) *Cis*-Regulator (ZRS) Causes Werner Mesomelic Syndrome (WMS) While Complete ZRS Duplications Underlie Haas Type Polysyndactyly and Preaxial Polydactyly (PPD) With or Without Triphalangeal Thumb

Dagmar Wieczorek,^{1*} Barbara Pawlik,^{2,3} Yun Li,²⁻⁴ Nurten A. Akarsu,⁵ Almuth Caliebe,⁶ Klaus J.W. May,⁷ Bernd Schweiger,⁸ Fernando R. Vargas,^{9,10} Sevim Balci,¹¹ Gabriele Gillissen-Kaesbach,^{1,12} and Bernd Wollnik^{2-4*}

¹Institut für Humangenetik, Universitätsklinikum Essen, Essen, Germany; ²Institute for Human Genetics, University of Cologne, Cologne, Germany; ³Center for Molecular Medicine Cologne (CMMC), University of Cologne, Cologne, Germany; ⁴Cologne Excellence Cluster on Cellular Stress Responses in Aging-Associated Diseases (CECAD), University of Cologne, Cologne, Germany; ⁵Department of Medical Genetics, Hacettepe University Medical Faculty, Ankara, Turkey; ⁶Institut für Humangenetik, Christian-Albrechts-Universität zu Kiel, Kiel, Germany; ⁷Genomatix Software GmbH, München, Germany; ⁸Pädiatrische Radiologie, Institut für Diagnostische und Interventionelle Radiologie und Neuroradiologie, Universitätsklinikum Essen, Essen, Germany; ⁹Genetics and Molecular Biology Department, Universidade Federal do Estado do Rio de Janeiro, Rio de Janeiro, Brazil; ¹⁰Genetics Division, Instituto Nacional de Câncer, Rio de Janeiro, Brazil; ¹¹Clinical Genetics Unit, Hacettepe University Medical Faculty, Ankara, Turkey; ¹²Institut für Humangenetik, Universität zu Lübeck, Lübeck, Germany

Communicated by Iain McIntosh

Received 13 July 2009; accepted revised manuscript 29 September 2009.

Published online in Wiley InterScience (www.interscience.wiley.com). DOI 10.1002/humu.21142

ABSTRACT: Werner mesomelic syndrome (WMS) is an autosomal dominant disorder with unknown molecular etiology characterized by hypo- or aplasia of the tibiae in addition to the preaxial polydactyly (PPD) of the hands and feet and/or five-fingered hand with absence of thumbs. We show that point mutations of a specific nucleotide within the sonic hedgehog (*SHH*) regulatory region (ZRS) cause WMS. In a previously unpublished WMS family, we identified the causative G > A transition at position 404 of the ZRS, and in six affected family members of a second WMS family we found a 404G > C mutation of the ZRS. The 404G > A ZRS mutation is known as the “Cuban mutation” of PPD type II (PPD2). Interestingly, the index patient of that family had tibial hypoplasia as well. These data provide the first evidence that WMS is caused by a specific ZRS mutation, which leads to strong ectopic *SHH* expression. In contrast, we show that complete duplications of the ZRS region lead to type Haas polysyndactyly or triphalangeal thumb-polysyndactyly syndrome, but do not affect lower limb development. We suggest the term “ZRS-associated syndromes” and a clinical subclassification for the continuum of limb malformations caused by different molecular alterations of the ZRS.

Hum Mutat 30:1–9, 2009. © 2009 Wiley-Liss, Inc.

KEY WORDS: WMS; Haas polysyndactyly; triphalangeal thumb polysyndactyly syndrome; ZRS

Introduction

Triphalangeal thumb is a common hand malformation, which can occur isolated as autosomal dominant inherited, nonopposable triphalangeal thumb (MIM# 190600) or as a clinical sign of well-characterized syndromic conditions; e.g., Holt-Oram syndrome [Basson et al., 1997], lacrimo-auriculo-dento-digital syndrome [Rohmann et al., 2006], or Nager acrofacial dysostosis [McDonald and Gorski, 1993]. Recently, mutations in the zone of polarizing activity regulatory sequence (ZRS; MIM# 605522), a long-range limb-specific enhancer of the sonic hedgehog (*SHH*) gene (*HHG1*, *SMMCI*, *TPT*, *TPTPS*, *MCOPCB5*; MIM# 600725), have been identified in patients with preaxial polydactyly type II (PPD2) [Lettice et al., 2002, 2003; Li et al., 2009], triphalangeal thumb polysyndactyly (TPTPS; MIM# 174500) [Sun et al., 2008; Klopocki et al., 2008], and syndactyly type IV (SD4, Haas type polysyndactyly; MIM# 186200) [Sun et al., 2008; Wu et al., 2009; Furniss et al., in press]. The ZRS is located on human chromosome 7q36.3 within intron 5 of the *LMBR1* gene (ACHP, FLJ11665; MIM# 605522) [Lettice et al., 2003] and it has been shown that it regulates the timely and spatial expression of the *SHH* gene, which is located approximately 1 Mb downstream.

PPD2 is characterized by a triphalangeal thumb with or without preaxial polydactyly (PPD), sometimes leading to the appearance of a five-fingered hand. Characteristic clinical findings in TPTPS are triphalangeal thumb, syndactyly of hands, and pre- and postaxial polysyndactyly of the feet. Some patients show a more severe phenotype with complete syndactyly of all fingers giving a “cup-like” shape to the hands. This severe end of TPTPS, complete syndactyly with polydactyly, is the typical anomaly seen in patients with SD4. Werner mesomelic syndrome (WMS) (tibial hypoplasia-polysyndactyly-triphalangeal thumb, THPSTPT; MIM# 188770) was first described by Werner [1912] and the hallmark of this syndrome is the affection of tibia development leading to aplasia or hypoplasia of tibiae often accompanied with remarkable

*Correspondence to: Dagmar Wieczorek, Institut für Humangenetik, Universitätsklinikum Essen, Hufelandstr. 55, Essen 45122, Germany. E-mail: dagmar.wieczorek@uni-due.de; Bernd Wollnik, Institute of Human Genetics, University of Cologne, Kerpener Str. 34, 50931 Cologne, Germany. E-mail: bwollnik@uni-koeln.de

short stature. In addition, patients with Werner syndrome present with polydactyly of hands and feet and digitalization of the thumbs. The molecular basis for WMS is unknown.

We report on the molecular etiology of WMS in two families. Our results show that a specific point mutation in the ZRS is responsible for the abnormal development of tibiae seen in patients with WMS. In addition, we describe two different duplications of the ZRS region in a patient with Haas type polysyndactyly [Gillissen-Kaesbach and Majewski, 1991] and in a family with overlapping clinical signs of TPTPS and syndactyly type IV [Balci et al., 1999].

Materials and Methods

Mutation Analysis

The 772bp of the predicted ZRS region (156277329–156276557 Mb; University of California, Santa Cruz [UCSC] Human Genome Browser; <http://genome.ucsc.edu>; hg18 assembly; g.104811–105583 in reference sequence AC007097.4) was sequenced in the index patients of the families presented in our study after informed consent was obtained from the patients. Genomic DNA from patients was used to amplify the ZRS region by a touchdown PCR protocol on a DNA Engine Dyad Thermal Cycler (Bio-Rad, Munich, Germany). The following primers were used: 5'-CTGGCCAGTGTTTAAATGGT-3' (F1) and

5'-TGATCCATAACCAATTTCTAAG-3' (R1). PCR fragments were purified and directly sequenced from both sides using the ABI BigDye Terminator v3.1 Cycle Sequencing Kit and the ABI 3730 DNA Analyzer (Applied Biosystems, Darmstadt, Germany). Additional internal primers were used for sequencing, and primer sequences are available upon request. Cosegregation of the mutations in the families was confirmed by direct sequencing of all available family members and by a PCR/enzyme digestion method using *TaaI*. In addition, the mutations were not detected in 100 Turkish control individuals.

Array-Comparative Genomic Hybridization Analysis

Oligonucleotide array-comparative genomic hybridization (array-CGH) was performed on a Human Genome CGH Microarray 244A platform (Agilent Technologies, Santa Clara, CA). One microgram (1 µg) of the test DNA and 1 µg of reference DNA from a pool of 10 healthy donors with either male or female karyotype were hybridized using the manufacturer's protocol with slight modifications. Slides were scanned with a GenePix[®] 4000B microarray reader (Molecular Devices Corporation, Union City, CA) at a resolution of 5 µm/pixel. Signal intensities from the generated images were measured and evaluated with the Feature Extraction v9.1 and CGH Analytics v3.5 software packages, respectively (Agilent Technologies). Except for the *LMBR1* locus, statistically significant imbalances spanning a region of 10 sequential probes with a transformed log₂ ratio beyond 0.5 and mapping outside known copy number variations (CNVs) were

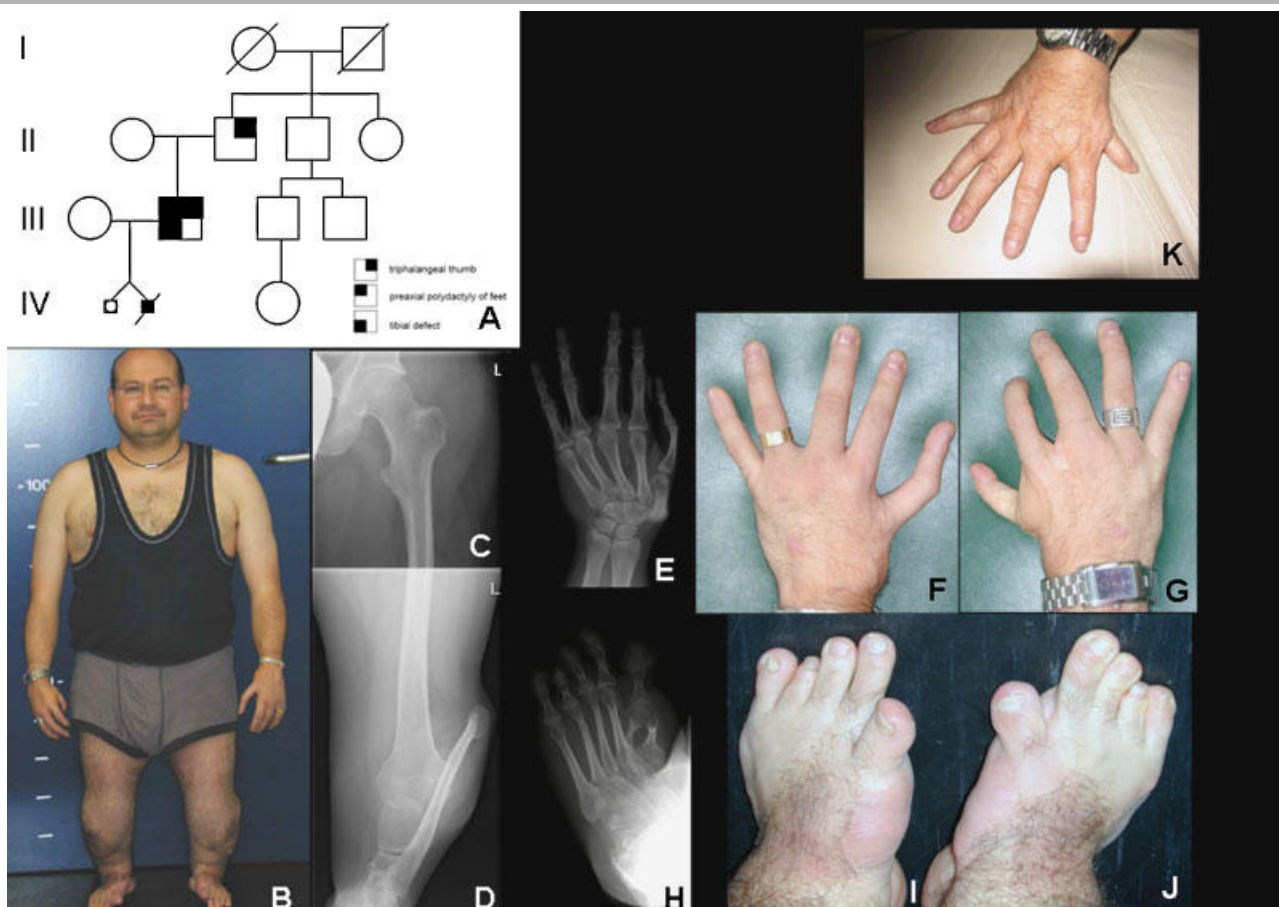


Figure 1. Family 1 with Werner mesomelic syndrome. **A:** Pedigree of Family 1. **B–J:** Index patient of Family 1 (Patient III/2). **K:** Right hand of father of the index patient (Patient II/2).

considered aberrant. The position of the array targets was mapped to the UCSC genome browser release March 2006.

Quantitative Real-Time PCR

We established a quantitative real-time polymerase chain reaction (qPCR) method for the detection of structural alterations of the ZRS region. Primers and probes located in the ZRS region and in the albumin gene (ALB) used as internal were designed using the Primer Express Software (Applied Biosystems) and were purchased from Applied Biosystems (ZRS forward primer: 5'-TGAGTGATTAAGGAAGTGCTGCTTAG-3'; reverse primer: 5'-GGCTTCCCTTTTGTCTGTGATTT-3' and probe: 5'-FAM-TGCGCATATTTGGC CTGTTTCTGG-BHQ-3'; ALB: forward primer 5'-CTTGTGGGCTGTAATCATCGTC TAG-3'; reverse primer: 5'-AGCTGCTGGTTCTCTTTCCTGAC-3' and probe 5'-VIC-CACACAAATCTCTC-MGB-3'). Each reaction was carried out in 20 μ l volume containing 10 μ l of 2 \times universal master mix buffer, 700 nM of the ZRS and ALB primers, and 400 nM of both ZRS and ALB probes. Ten nanograms (10 ng) of genomic DNA was used as templates. For detection of quantitative changes of DNA amounts, we used 5, 10, and 15 and 20 ng of DNA samples in separated replicates. Thermal cycling was performed for 2 min at 50°C, 10 min at 95°C, and then 40 cycles for 15 s at 95°C and for 1 min at 60°C. The threshold cycle parameter (Ct) was defined as the point at which the amplification plot—representing the fluorescence generated by cleavage of the probe as a function of the cycle number—passed a fixed threshold above baseline. Each replicate was normalized to ALB in order to obtain a Δ Ct (VIC dye Ct-FAM dye Ct). To imitate the Δ Ct created by one copy, two copies, and three copies of the ZRS gene, two control samples with different DNA amounts were used. All samples were then normalized to the calibrator to determine the $\Delta\Delta$ Ct (Δ Ct of each sample - Δ Ct of two copies).

Results

Clinical Reports

Family 1

The Turkish index patient was examined for diagnostic evaluation at the age of 43 years. He presented with short stature (height: 135 cm, -6.7 SD), shortening of forearms and PPD of both hands. The additional fingers were surgically removed and the residual state is five-fingered hands with a triphalangeal first ray on the left hand. The femora are mildly shortened and his lower legs are severely shortened. He had PPD of both feet (Fig. 1A-J). The clinical diagnosis WMS [Werner, 1912] was established. The index patient's father only presented with right-sided PPD of the hand (Fig. 1K). The index patient's wife was pregnant with twins after intracytoplasmic sperm injection (ICSI). Ultrasound examination in one of the fetuses revealed severely shortened legs with aplasia of fibulae and tibiae as well as syndactyly of the right hand. An elective feticide was done, the other child, a female, was born healthy. All other family members did not show any anomalies. DNA was available from Family Members III/2 and II/1-4.

Family 2

The clinical data of this family with WMS were published by Vargas et al. [1995]. Ten affected family members in three

generations were described. All affected patients presented with triphalangeal thumbs and PPD of the feet, two had tibial defects, and one duplicated fibulae. We add previously unpublished radiographs and clinical photographs of members of this family depicting severe hypoplasia of tibia and bowing of fibula in Patient II/3 (Fig. 2A), right-sided triphalangeal thumb in Patient III/9 (Fig. 2B), and radiographs of triphalangeal thumbs in Patient III/11 (Fig. 2C). DNA was available from Family Members II/3, III/9, III/11, III/16, and IV/7-9.

Family 3

The proposita, a sporadic female patient with Haas type polysyndactyly, was published by Gillessen-Kaesbach and Majewski [1991]. We examined her again as an adult woman.



Figure 2. Family 2 with Werner mesomelic syndrome published by Vargas et al. [1995]. **A:** Radiographs of the legs of Patient II/3 showing severe shortening of tibiae and bowing of fibulae. **B:** Hands of Patient III/9 with triphalangeal thumbs bilaterally. **C:** Hand radiographs of Patient III/11 showing triphalangeal thumbs bilaterally.

The photographs are depicting the primary state with complete cutaneous syndactyly of all fingers and polydactyly (Fig. 3A), the hands after 18 surgical corrections (Fig. 3B), and the feet with right-sided III–IV and left-sided IV–V skin syndactyly (Fig. 3C). There were no other congenital anomalies, and mental development was normal. DNA was available from the probanda and her healthy parents.

Family 4

This family with triphalangeal thumb-polysyndactyly syndrome was published by Balci et al. [1999]. The characteristic findings in this family were triphalangeal thumbs, webbing between the 3rd, 4th, and 5th fingers associated with bony synostosis in the distal phalanges of the same fingers, and pre- and postaxial polysyndactyly of feet. Some of the family members, especially Person 29 in this work, had clinical signs very similar to syndactyly type



Figure 3. Family 3. Patient with polysyndactyly type IV Haas, previously published by Gillessen-Kaesbach and Majewski [1991]. **A:** Complete syndactyly of left hand and partially surgically corrected right hand. **B:** Hands after 18 surgical corrections. **C:** Feet with right-sided III–IV syndactyly and left-sided IV/V syndactyly.

IV. DNA was available from the following Family Members: II/2, III/1, III/3, III/6, IV/1, IV/2, IV/6, and IV/8.

The research was reviewed and approved by the ethics committee of the medical faculty, University Duisburg-Essen, Germany.

A Specific Mutation in the ZRS Causes WMS

We used the reference sequence from the UCSC Human Genome Browser hg18 assembly to amplify the predicted ZRS region (according to Lettice and Hill [2005]) that is located in intron 5 of the *LMBR1* gene on chromosome 7q36.3. This region is highly conserved and single nucleotide changes as well as structural alterations were previously described to cause various distal limb malformations. Sequencing of the 772 bp of ZRS in the index patient of Family 1 revealed a heterozygous single-basepair alteration at position g.105213G>A in accordance with reference sequence AC007097.4 within the ZRS (named here 404G>A). This mutation affecting a highly conserved nucleotide position within the ZRS region (Fig. 4), was also present in the affected

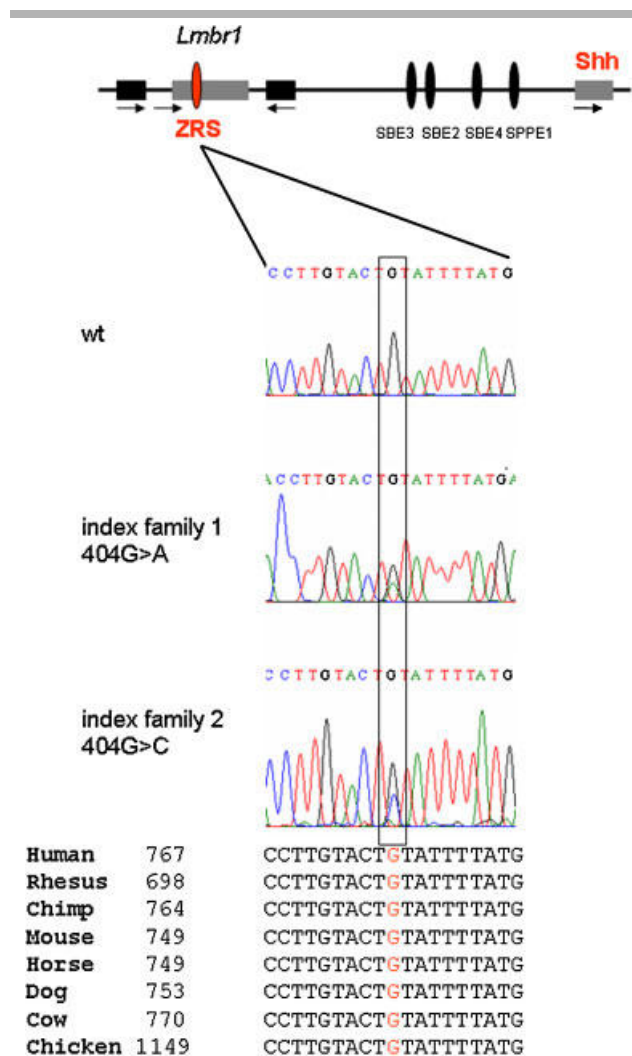


Figure 4. Molecular basis of Werner mesomelic syndrome. Chromatograms of index patients of Family 1 and 2 showing the 404G>A and 404G>C mutations in comparison to wild-type (wt) sequence. The location of the mutation in the ZRS within intron 5 of the *LMBR1* gene is indicated. Sequence alignment shows the high conservation of the altered 404G position.

father (Family 1, Patient II-2), and was absent in all tested healthy family members (II-1–4) and in 100 Turkish control individuals. The 404G>A mutation was previously described in a family from Cuba [Lettice et al., 2003] diagnosed with PPD phenotype, but evaluating the published clinical data of this family showed that the index patient had also tibial hypoplasia consistent with the diagnosis of WMS. Strikingly, we found the same nucleotide position mutated in six affected family members (II/3, III/9, III/11, III/16, and IV/7–9) of Family 2 with WMS. The highly-conserved guanine at position 404 of the ZRS was substituted by cytosine in the Brazilian family (404G>C). No ZRS point mutation was found in Families 3 and 4.

Duplications of ZRS Underlie Syndactyly Type IV and TPTPS

We used a qPCR technique for the detection of CNVs of the ZRS to test a previously described patient with syndactyly type IV (Family 3) and the Turkish index patient of Family 4 suffering from TPTPS. Based on the applied ΔC_t method we detected ZRS duplications in both index patients and subsequently in eight (II/2, III/1, III/3, III/6, IV/1, IV/2, IV/6, and IV/8) affected family members of Family 4. In contrast, unaffected individuals from this family did not show any quantitative changes (data not shown) and the duplication was not detected in 35 Turkish controls.

In the array-CGH analysis, the index patient of Family 3 showed an approximately 73-kb duplication involving parts of the *LMBR1* gene in 7q36.3. The aberration can be described as arr7q36.3(156,265,512x2,156,265,453–156,354,638x3,156,354,579–x2) (Fig. 5). In the index patient of Family 4 (Patient IV-2) a more centromeric breakpoint was observed. The 276-kb spanning

duplication, including the ZRS, can be described as arr7q36.3(156,061,302x2,156,088,827–156,354,638x3,156,354,579x2) (Fig. 5). Except for known CNVs no further abnormalities were detected. On the basis of these data, we tried to map the exact breakpoints of the duplications by the extensive use of long-range PCR experiments and various primer pair combinations. Due to the complex and repetitive nature of this genomic region, we were not able to determine the exact orientation of both duplications.

Discussion

ZRS and Its Role in the Development of Limb Buds

The SHH protein is expressed and secreted in the zone of polarizing activity (ZPA) in the early limb bud and its expression is regulated by the ZPA regulatory region (ZRS) a long-range *cis*-regulator of the *SHH* gene, which is located ~1 Mb away from the *SHH* gene and contains ~800 bp conserved from mammals to fish (Fig. 4) [Lettice et al., 2003]. SHH is a major determinant of cell fate and identity during early limb development, thereby controlling digit formation [Hill, 2007]. SHH is a secreted morphogenic protein expressed in a specific region in the posterior margin of the limb bud within the ZPA; it has been shown in different model organisms that disruption, ectopic expression, or changes in the timely expression of Shh can cause different types of distal limb anomalies [Maas and Fallon, 2005; Hill, 2007]. In human, PPD2 [Lettice et al., 2003; Furniss et al., 2008; Gurnett et al., 2007] is caused by point mutations of the ZRS. Transgenic assays revealed [Masuya et al., 2007] that some of these point mutations found in patients redirect Shh expression leading to an ectopic expression; e.g., at the anterior site of the limb bud. Very recently it was shown that TPTPS and Haas type

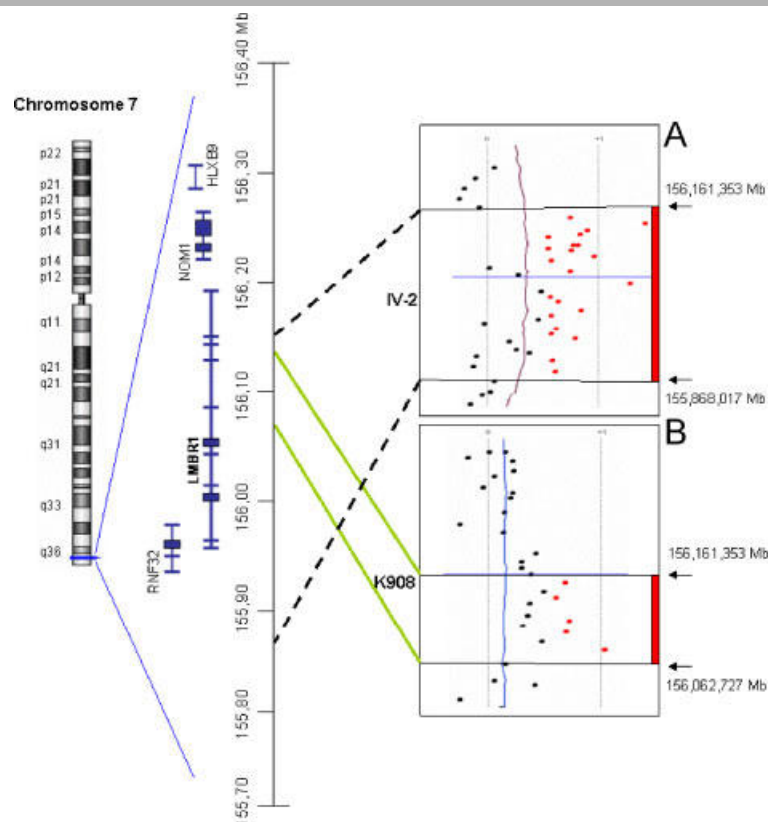


Figure 5. Array comparative genomic hybridization indicating a microduplication of 7q36.3 in Family 3 (A) and Family 4 (B).

Table 1. Comparison of Clinical Signs in Patients With Different ZRS Point Mutations

Reference	Lettice et al. [2003]	Furniss et al. [2008]	Lettice et al. [2003]	Lettice et al. [2003]	Semerici et al. [2009]	Present study	Present study; Vargas et al. [1995]	Lettice et al. [2003]; Zguricas et al. [1999]; Morales-Peralta [1994]	Gurnett et al. [2007]	Gurnett et al. [2007]; Dobbs et al. [2000]
Mutation ref.	105C>G;	295T>C;	305A>T;	323T>C;	396C>T;	404G>A;	404G>C;	404G>A;	621C>G;	739A>G;
AC007097.4	g.104914C>G	g.105104T>C	g.105114A>T	g.105132T>C	g.105205C>T	g.105213G>A	g.105213G>C	g.105213G>A	g.105430C>G	g.105548A>G
Syndrome clinical description	PPD	PPD	PPD	PPD	PPD	Werner mesomelic syndrome (THPTTS/PPD)	Werner mesomelic syndrome (THPTTS)	Werner mesomelic syndrome (PPD)	PPD	PPD
Hands affected	+	+	+	+	+	+	+	+	+	+
Triphalangeal thumb	+	+	+	+	+	+	+	+	+	+
Preaxial polydactyly	+	+	+	+	+	+	+	+	+	+
Postaxial polydactyly	-	-	-	-	-	-	-	-	-	-
Partial syndactyly	-	-	-	-	-	-	-	+	-	-
Complete syndactyly	-	-	-	-	-	-	-	-	-	-
Mirror hands	-	-	-	-	-	+	-	-	-	-
Arms affected	-	-	-	-	-	-	-	+	-	-
Radial dysplasia	-	-	-	-	-	-	-	+	-	-
Feet affected	-	-	-	-	-	+	+	-	-	-
Preaxial polydactyly	-	-	-	-	-	+	+	+	+	-
Postaxial polydactyly	-	-	-	-	-	-	-	-	-	-
Partial syndactyly	-	-	-	-	-	-	-	-	-	-
Complete syndactyly	-	-	-	-	-	-	-	-	-	-
Mirror feet	-	-	-	-	-	-	+	-	-	-
Legs affected	-	-	-	-	-	+	+	+	-	-
Tibial a-/hypoplasia	-	-	-	-	-	+	+	+	-	-
Fibula hypoplasia	-	-	-	-	-	+	+	-	-	-
Fibula duplication	-	-	-	-	-	-	+	-	-	-

Table 2. Comparison of Clinical Signs in Patients With Different ZRS Duplications

Size of duplication	73 kb	97 kb	131 kb	158 kb	235 kb	246 kb	276 kb	291 kb	398 kb	588 kb	Unknown
References	Present study; Gillessen-Kaesbach and Majewski [1991]	Wu et al. [2009]; Sato et al. [2007]	Sun et al. [2008]; Family 1	Sun et al. [2008]; Family 3	Sun et al. [2008]; Family 5	Sun et al. [2008]; Family 4	Present study; Balci et al. [1999]	Sun et al. [2008]; Family 2	Sun et al. [2008]; Family 6; Wang et al. [2007]	Kloppocki et al. [2008]	Furniss et al. [2009]
Clinical description	SD4	SD4+	TPTPS	TPTPS/SD4	TPTPS/SD4	TPTPS/SD4	SD4/TPTPS	TPTPS/SD4	TPTPS/SD4	TPTPS	SD4+
Hands affected	+	+	+	+	+	+	+	+	+	+	+
Triphalangeal thumb	-	-	+	+	+	+	+	+	+	+	+
Preaxial polydactyly	+	+	+	+	-	+	+	+	+	+	+
Postaxial polydactyly	-	+	+	-	-	-	-	-	+	+	-
Partial syndactyly	-	-	+	+	-	+	+	+	+	+	+
Complete syndactyly	+	+	-	+	+	+	+	+	-	-	-
Mirror hands	-	-	-	-	-	-	-	-	-	-	-
Arms affected	-	-	-	-	-	-	-	-	-	-	+
Radial dysplasia	-	-	-	-	-	-	-	-	-	-	-
Fixed flexion at wrist	-	-	-	-	-	-	-	-	-	-	+
Feet affected	+	+	-	-	-	-	+	+	-	+	+
Preaxial polydactyly	-	+	-	-	-	-	+	-	-	n.r.	+
Postaxial polydactyly	-	+	-	-	-	-	+	-	-	n.r.	-
Partial syndactyly	+	+	-	+	-	-	+	+	-	n.r.	+
Complete syndactyly	-	+	-	-	-	-	+	-	-	n.r.	-
Mirror feet	-	+	-	-	-	-	-	-	-	n.r.	+
Legs affected	-	-	-	-	-	-	-	-	-	-	-
Tibial a/hypoplasia	-	+	-	-	-	-	-	-	-	-	-
Fibula hypoplasia	-	-	-	-	-	-	-	-	-	-	-
Fibula duplication	-	-	-	-	-	-	-	-	-	-	-
Talipes	-	-	-	-	-	-	-	-	-	-	+

n.r., not recorded.

Table 3. Classification of ZRS-Associated Syndromes

	Mutational mechanism	Clinical outcome	Known malformation name	OMIM#
Type Ia	Point mutations in various positions of ZRS	Triphalangeal thumb polydactyly, hand involvement only	Preaxial polydactyly, type II: PPD II	174500
Type Ib	Point mutations at position 404 of ZRS	Triphalangeal thumb polydactyly-hypoplastic tibia	Werner mesomelic syndrome	188770
Type II	Duplications containing ZRS region	Complex polysyndactylies containing triphalangeal thumb	Triphalangeal thumb polysyndactyly (TPTPS) Haas type (syndactyly type IV)	Requires a new number 186200

polysyndactyly are caused by duplications of the ZRS, though the consequences on SHH expression are not yet known [Wu et al., 2009; Sun et al., 2008; Klopocki et al., 2008; Furniss et al., in press]. We now add WMS to these conditions caused by mutations within the ZRS.

Specific Point Mutations Affecting Position 404 of the ZRS Cause WMS

Our data provide genetic evidence that altering nucleotide position 404 of the ZRS underlies WMS. We found the 404G>A and 404G>C mutations in two families, respectively, and interestingly, though the 404G>A mutation was described as causative for PPD in this Cuban family, the Cuban index case did show tibial hypoplasia in addition consistent with the diagnosis of WMS. Table 1 summarizes the clinical and mutational data of patients described with PPD2 and WMS. Point mutations are scattered throughout the ZRS region, indicating the importance of the whole ZRS region in SHH regulation [Lettice et al., 2008]. No overt genotype–phenotype correlation is observed in PPD with specific respect to the location of point mutations, but mutations lead to highly variable Shh expression patterns during early limb development, dependent on the position and the sequence context of the mutation within the ZRS [Lettice et al., 2008; Hill, 2007]. It is striking that the mutation showing the strongest ectopic Shh expression in the reporter gene assay of the study of Lettice et al. [2008] was the 404G>A (“Cuban”) mutation. These functional data support our finding that specific alteration of position 404 leads to a more severe clinical phenotype with the affection of tibial development, namely WMS. It is not clear why the 404G>A and 404G>C Werner mutations have a stronger functional effect on Shh expression compared to other ZRS point mutations. Preliminary computational analysis of transcription factor binding sites within the affected region indicated that both 404G>A and 404G>C might lead to an increased binding probability of additional transcription factors (data not shown) [Cartharius et al., 2005; Werner et al., 2003]. Therefore, a specific change in transcription factor binding is an attractive working hypothesis for future studies aiming to identify the underlying molecular mechanism of altered Shh expression by Werner mutations.

In addition, it is still an open debate as to which factors are responsible for the reduced penetrance of WMS, as milder affected family members, e.g., the father of Patient 1, only presented with PPD2. One might discuss modifying factors or variations in the transcription factors.

Spectrum of ZRS-Associated Syndromes and Mutational Mechanisms

No systematic evaluation of ZRS phenotypes and mutations exists. Results of evaluation of clinical data of all families with ZRS mutations published so far ($n = 21$) are shown in Tables 1 and 2. In general, we observe an overt genotype–phenotype correlation: point mutations within the ZRS predominantly cause PPD2 and specific point mutations of position 404 are found in WMS, but

no point mutations are yet described in Haas type polysyndactyly or TPTPS.

The clinical spectrum of ZRS disorders is very similar, although clinically distinguishable: patients with PPD2 do not present with involvement of feet or lower extremities, whereas patients with WMS characteristically show tibial a-/hypoplasia and additional foot anomalies. In addition, patients with Haas type polysyndactyly or patients with TPTPS and a causative ZRS duplication identified mostly have involvement of feet and in some cases show lower limb anomalies.

The clinical spectrum and type of ZRS mutation being distinct, we suggest separating the OMIM numbers of PPD2 and TPTPS, which currently are summarized under a single OMIM number. In addition, not only is the molecular testing strategy different, but so is the impact on genetic counseling of patients on the expected clinical spectrum and prognosis.

The so-far-described duplications of the ZRS are of different sizes without recurrent breakpoints. There is no obvious genotype–phenotype correlation concerning the size of the duplications. All duplication patients do have similar clinical phenotypes, either SD4 or TPTPS. In some large families (e.g., Balci et al. [1999]) both phenotypes are present; thus, these two conditions are allelic expressions of the identical molecular cause. It will be interesting in the future to compare the expression profiles of SHH in patients with point mutations versus duplications.

Based on our detailed review of described ZRS mutations and phenotypes we suggest classifying ZRS-associated syndromes into two subtypes (Table 3): type I for point mutations and type II for duplications. Type I itself has two subdivisions, a and b. Table 3 is arbitrarily extensible as soon as new phenotypes evolve; e.g., the phenotypic consequences of ZRS deletions. In mice, the phenotype associated with a complete deletion of the ZRS region is acheiropodia, a limb truncation phenotype, which was published by Sagai et al. [2005]. To the best of our knowledge, a ZRS deletion and the resulting phenotype has not yet been described in human.

In summary, we identified the molecular basis of WMS. This autosomal dominant condition is caused by specific point mutations in the ZRS at position 404. In contrast to the hitherto existing literature, we could show that tibial a-/hypoplasia is not exclusively present in patients with duplication of the ZRS, but is also present in patients with WMS. In contrast, Haas type polysyndactyly (MIM# 186200) and TPTPS (MIM# 174500) are allelic and caused by duplications of the ZRS. We demonstrate that different mutational mechanisms affecting ZRS predispose to different phenotypic outcomes. Consequently, we suggest the generic term “ZRS-associated syndromes” for different limb malformations caused by alterations of the ZRS.

Acknowledgments

We thank Stanislas Lyonnet and Rainer König for sending DNA of further patients, Martin Erdel for performing fluorescent in situ hybridization

(FISH) analysis, Bernhard Horsthemke and Reiner Siebert for continuous support, and the patients and their families for taking part in this study. This study was supported by the German Federal Ministry of Education and Research (BMBF) grant 01GM0880 (to B.W.) within the rare disease network SKELNET.

References

- Balci S, Demirtas M, Civelek B, Piskin M, Sensoz O, Akarsu AN. 1999. Phenotypic variability of triphalangeal thumb-polysyndactyly syndrome linked to chromosome 7q36. *Am J Med Genet* 87:399–406.
- Basson CT, Bachinsky DR, Lin RC, Levi T, Elkins JA, Soultis J, Grayzel D, Kroumpouzou E, Traill TA, Leblanc-Straceski J, Renault B, Kucherlapati R, Seidman JG, Seidman CE. 1997. Mutations in human TBX5 [corrected] cause limb and cardiac malformation in Holt-Oram syndrome. *Nat Genet* 15:30–35.
- Cartharius K, Frech K, Grote K, Klocke B, Haltmeier M, Klingenhoff A, Frisch M, Bayerlein M, Werner T. 2005. MatInspector and beyond: promoter analysis based on transcription factor binding sites. *Bioinform* 21:2933–2942.
- Dobbs MB, Dietz FR, Gurnett CA, Morcuende JA, Steyers CM, Murray JC. 2000. Localization of dominantly inherited isolated triphalangeal thumb to chromosomal region 7q36. *J Orthop Res* 18:340–344.
- Furniss D, Lettice LA, Taylor IB, Critchley PS, Giele H, Hill RE, Wilkie AOM. 2008. A variant in the sonic hedgehog regulatory sequence (ZRS) is associated with triphalangeal thumb and deregulates expression in the developing limb. *Hum Mol Genet* 17:2417–2423.
- Furniss D, Kan S-H, Taylor IB, Johnson D, Critchley PS, Giele HP, Wilkie AOM. Genetic screening of 202 individuals with congenital limb malformations and requiring reconstructive surgery. *J Med Genet* (in press) [<http://dx.doi.org/doi:10.1136/jmg.2009.066027>].
- Gillessen-Kaesbach G, Majewski F. 1991. Bilateral complete polysyndactyly (type IV Haas). *Am J Med Genet* 38:29–31.
- Gurnett CA, Bowcock AM, Dietz FR, Morcuende JA, Murray JC, Dobbs MB. 2007. Two novel point mutations in the long-range SHH enhancer in three families with triphalangeal thumb and preaxial polydactyly. *Am J Med Genet A* 143A:27–32.
- Hill RA. 2007. How to make a zone of polarizing activity: Insights into limb development via the abnormality preaxial polydactyly. *Dev Growth Differ* 49:439–448.
- Klopocki E, Ott C-E, Benatar N, Ullmann R, Mundlos S, Lehmann K. 2008. A microduplication of the long range SHH limb regulator (ZRS) is associated with triphalangeal thumb-polysyndactyly syndrome. *J Med Genet* 45:370–375.
- Lettice LA, Horikoshi T, Heaney SJ, van Baren MJ, van der Linde HC, Breedveld GJ, Joosse M, Akarsu N, Oostra BA, Endo N, Shibata M, Suzuki M, Takahashi E, Shinka T, Nakahori Y, Ayusawa D, Nakabayashi K, Scherer SW, Heutink P, Hill RE, Noji S. 2002. Disruption of a long-range *cis*-acting regulator for Shh causes preaxial polydactyly. *Proc Natl Acad Sci USA* 99:7548–7553.
- Lettice LA, Heaney SJH, Purdie LA, Li L, de Beer P, Oostra BA, Goode D, Elgar G, Hill RE, de Graaff E. 2003. A long-range Shh enhancer regulates expression in the developing limb and fin and is associated with preaxial polydactyly. *Hum Mol Genet* 12:1725–1735.
- Lettice LA, Hill RE. 2005. Preaxial polydactyly, a model for defective long-range regulation in congenital abnormalities. *Curr Opin Genet Dev* 15:294–300.
- Lettice LA, Hill AE, Devenney PS, Hill RE. 2008. Point mutations in a distant sonic hedgehog *cis*-regulator generate a variable regulatory output responsible for preaxial polydactyly. *Hum Mol Genet* 17:978–985.
- Li H, Wang CY, Wang JX, Wu GS, Yu P, Yan XY, Chen YG, Zhao LH, Zhang YP. 2009. Mutation analysis of a large Chinese pedigree with congenital preaxial polydactyly. *Eur J Hum Genet* 17:604–610.
- Maas SA, Fallon JF. 2005. Single base pair change in the long-range Sonic hedgehog limb-specific enhancer is a genetic basis for preaxial polydactyly. *Dev Dyn* 232:345–348.
- Masuya H, Sezutsu H, Sakuraba Y, Sagai T, Hosoya M, Kaneda H, Miura I, Kobayashi K, Sumiyama K, Shimizu A, Nagano J, Yokoyama H, Kaneko S, Sakurai N, Okagaki Y, Noda T, Wakana S, Gondo Y, Shiroishi T. 2007. A series of ENU-induced single-base substitutions in a long-range *cis*-element altering Sonic hedgehog expression in the developing mouse limb bud. *Genomics* 89:207–214.
- McDonald MT, Gorski JL. 1993. Nager acrofacial dysostosis. *J Med Genet* 30:779–782.
- Morales-Peralta E. 1994. Absent tibia and polydactyly: a case report. *Bol Med Hosp Infant Mex* 51:295–297.
- Rohmann E, Brunner HG, Kayserili H, Uyguner O, Nürnberg G, Lew ED, Dobbie A, Eswarakumar VP, Uzumcu A, Ulubil-Emeroglu M, Leroy JG, Li Y, Becker C, Lehnerdt K, Cremers CW, Yüksel-Apak M, Nürnberg P, Kubisch C, Schlessinger J, van Bokhoven H, Wollnik B. 2006. Mutations in different components of FGF signaling in LADD syndrome. *Nat Genet* 38:414–417.
- Sagai T, Hosoya M, Mizushima Y, Tamura M, Shiroishi T. 2005. Elimination of a long-range *cis*-regulatory module causes complete loss of limb-specific Shh expression and truncation of the mouse limb. *Development* 132:797–803.
- Sato D, Liang D, Wu L, Pan Q, Xia K, Dai H, Wang H, Nishimura G, Yoshiura K, Xia J, Niikawa N. 2007. A syndactyly type IV locus maps to 7q36. *J Hum Genet* 52:561–564.
- Semerici CN, Demirkan F, Özdemir M, Biskin E, Akin B, Bagci H, Akarsu NA. 2009. Homozygous feature of isolated triphalangeal thumb-preaxial polydactyly linked to 7q36: no phenotypic difference between homozygotes and heterozygotes. *Clin Genet* 76:85–90.
- Sun M, Ma F, Zeng X, Liu Q, Zhao XL, Wu FX, Wu GP, Zhang ZF, Gu B, Zhao YF, Tian SH, Lin B, Kong XY, Zhang XL, Yang W, Lo WH, Zhang X. 2008. Triphalangeal thumb-polysyndactyly syndrome and syndactyly type IV are caused by genomic duplications involving the long-range, limb-specific SHH enhancer. *J Med Genet* 45:589–595.
- Vargas FR, Pontes RL, Llerena JC, de Almeida JC. 1995. Absent tibiae-polydactyly-triphalangeal thumbs with fibular dimelia: Variable expression of the Werner (McKusick 188770) syndrome? *Am J Med Genet* 55:261–264.
- Wang ZQ, Tian SH, Shi YZ, Zhou PT, Wang ZY, Shu RZ, Hu L, Kong X. 2007. A single C to T transition in intron 5 of LMBR1 gene is associated with triphalangeal thumb-polysyndactyly syndrome in a Chinese family. *Biochem Biophys Res Commun* 355:312–317.
- Werner P. 1912. Über einen seltenen Fall von Zwergwuchs (About a rare case of dwarfism). *Arch Gynakol* 104:278–300.[German]
- Werner T, Fessele S, Maier H, Nelson PJ. 2003. Computer modeling of promoter organization as a tool to study transcriptional coregulation. *FASEB J* 17:1228–1237.
- Wu L, Liang D, Niikawa N, Ma F, Sun M, Pan Q, Long Z, Zhou Z, Yoshiura K-I, Wang H, Sato D, Nishimura G, Dai H, Zhang X, Xia J. 2009. A ZRS duplication causes syndactyly type IV with tibial hypoplasia. *Am J Med Genet A* 149A:816–818.
- Zguricas J, Henk H, Morales-Peralta E, Breedveld G, Kuyt B, Mumcu EF, Bakker W, Arkasu N, Kay SPJ, Hovius SER, Heredero-Baute L, Ooswa BA, Heutink P. 1999. Clinical and genetic studies on 12 preaxial polydactyly families and refinement of the localisation of the gene responsible to a 1.9 cM region on chromosome 7q36. *J Med Genet* 36:32–40.

5.4 Pawlik B, Yigit G, Wollnik B. Reduced LRP6-mediated WNT10B signalling in the pathogenesis of SHFM6. (submitted)

Abstract of the publication:

Split-hand/foot malformation (SHFM) is a human congenital limb malformation characterized by an abnormal development of the central digit rays, with a deep median cleft and syndactyly of fingers and toes. SHFM can develop as an isolated condition or as a part of other syndromes and is phenotypically very variable. Familial SHFM is generally inherited in an autosomal dominant manner with reduced penetrance but also autosomal recessive forms as well as X-linked inheritance have been reported. SHFM is very heterogeneous and six different loci (SHFM1-SHFM6) have been described so far. Recent investigations report on the first autosomal recessive p.R332W mutation in the *WNT10b* gene causing SHFM6. However, the underlying molecular basis of the mutation leading to SHFM6 is still unknown.

In this study we functionally characterize the p.R332W mutation in *Wnt10b* leading to SHFM6. Therefore we first performed expression analysis by Western Blot and second conducted a Dual-Luciferase Assay with co-expression of Lrp6, Wnt1, Wnt10b wild-type (wt) and Wnt10b mutant p.R332W in transiently transfected HEK293T cells. We could show that mutant p.R332W Wnt10b is expressed but fails to activate canonical Wnt signalling. Furthermore we accomplished co-immunoprecipitation assay of wt and mutant p.R332W with Lrp6 and demonstrate that both wt and mutant Wnt10b protein interact with Lrp6 receptor. Interaction was confirmed by Western Blot analysis of Sulfo-SBED Biotin Label Transfer of human LRP6 protein and purified wt and p.R332W mutant protein. Hence, we conclude that the p.R332W *Wnt10b* mutation causes a loss of function of Lrp6 mediated Wnt signalling and that this is the pathophysiological mechanism leading to SHFM6.

We next examined the ability of the putative SHFM3 candidate gene *Fgf8* to alter Lrp6 mediated Wnt signalling by using a Dual-Luciferase Assay. Luciferase Assay after co-expression of Lrp6, Wnt10b (wt) and Flag-tagged *Fgf8* revealed that *Fgf8* reduces Wnt10b mediated Wnt signalling activation. We were also able to reveal that the Wnt signalling reduction is reversible by increasing the amount of wt Wnt10b. To exclude any unspecific signal reduction in our system we furthermore tested other small secreted proteins such as FGF21 and Bmp4. Dual-Luciferase-Reporter assay after co-expression of Lrp6, wt Wnt10b, GFP-tagged FGF21 and c-myc-tagged Bmp4 pointed out that FGF21 also reduces Wnt10b

mediated Wnt signalling activation while Bmp4 does not. To define the molecular basis of the signal reduction from the Luciferase Assay, we next conducted a co-immunoprecipitation assay. Flag-tagged Fgf8 was transiently co-expressed with either Wnt10b or Lrp6 in HEK293T cells and immunoprecipitated with specific antibodies. Western Blot analysis of co-immunoprecipitation Assay clearly showed that Flag-tagged Fgf8 interacts with Wnt10b while it does not interact with Lrp6 receptor. Thus the Fgf8 mediated canonical WNT signalling reduction results from the binding of Fgf8 to Wnt10b.

In conclusion, we show that the described SHFM6 mutation p.R332W in *WNT10B* is a loss-of-function mutation. We further provide evidence that Wnt10b can bind Lrp6 and activate Lrp6-mediated Wnt/ β -catenin signalling and that the mutant protein lost this ability. Moreover, we propose that Fgf8 has an additional yet unknown function as Wnt-antagonist by binding to Wnt10b. Therefore, we suggest a direct cross-talk between Fgf and Wnt signalling important during limb development and in the pathogenesis of SHFM

Own contribution:

All functional analyses described in the paper were performed by myself. The aim of this study was to functionally characterize the p.R332W mutation in the *WNT10b* gene leading to SHFM6. Therefore, I started with the generation of the mutant p.R332W *Wnt10b* expression plasmid by using site directed mutagenesis PCR on wt mouse *pcDNA3.1 Wnt10b* construct. I confirmed the insertion of the mutation by sequencing the fragment from both sides using the ABI BigDye Terminator v1.1 Cycle Sequencing Kit and the ABI 3730 DNA Analyzer (data not shown). Next, I constructed the expression plasmid for murine *Fgf8* by amplification of *Fgf8* from a full length mammalian gene collection and a cloning strategy into pCMV-SC-CF vector according to manufacturer's instructions.

Initially, I transfected HEK293T cells using Lipofectamine 2000 with wt and mutant *Wnt10b* expression construct and showed by Western Blot analysis that mutant p.R332W Wnt10b was expressed (Figure 1B). Then I implemented the Dual-Luciferase Assay with wt and mutant Wnt10b in order to investigate the mutant's ability to activate Lrp6 mediated canonical Wnt signalling. I was able to demonstrate that co-expression of Lrp6 and Wnt10b resulted in an activation of Wnt/ β -catenin signalling, while in contrast the p.R332W mutant lost the ability of activating Wnt signalling (Figure 1A).

Next, I conducted co-immunoprecipitation assays with wt and p.R332W *Wnt10b* with the Lrp6 receptor (Figure 1C, 1D) and confirmed both interaction by Western Blot analysis of

Sulfo-SBED Biotin Label Transfer of human LRP6 protein with purified wt and mutant Wnt10b protein (Figure 1E).

Taken together, I could exhibit that the p.R332W mutant is efficiently transcribed and translated, and, moreover, mutant Wnt10b protein can still bind to the Lrp6 receptor when transiently co-expressed in HEK293T cells but fails to activate canonical Wnt signalling and is therefore a loss-of-function mutation in the pathogenesis of SHFM6.

Furthermore, I used the Luciferase Assay to test the effect of murine *Fgf8* and human *FGF21* on the transduction and activation or inhibition on canonical Wnt signalling. The results showed that the putative SHFM3 candidate gene *Fgf8* as well as *FGF21* but not *Bmp4* reduce the *Wnt10b* mediated activation of canonical Wnt signalling (Figure 2, 3, 4A).

Finally, I performed a co-immunoprecipitation assay with murine Flag-tagged *Fgf8* and wt *Wnt10b* or *Lrp6* and specific antibodies. I was able to demonstrate by Western Blot analysis that Flag-tagged *Fgf8* interacts with *Wnt10b* while it does not interact with the *Lrp6* receptor (Figure 4B, 4C). Thus, I was able to show first evidence that different *Fgfs* might share a specific inhibitory effect on canonical Wnt/ β -catenin signalling.

I completed this study by preparing all figures (Figures 1-5) for the publication and by finally writing the first version of the manuscript.

Reduced LRP6-mediated WNT10B signalling in the pathogenesis of SHFM6

Barbara Pawlik^{1,2}, Gökhan Yigit^{1,2}, and Bernd Wollnik^{1,2,3}

¹Center for Molecular Medicine Cologne (CMMC) and ²Institute of Human Genetics,
University of Cologne, Cologne, Germany; ³Cologne Excellence Cluster on Cellular Stress
Responses in Aging-Associated Diseases (CECAD), University of Cologne, Cologne,
Germany

Correspondence:

Bernd Wollnik, MD

Center for Molecular Medicine Cologne (CMMC) and

Institute of Human Genetics; Kerpener Str. 34,

50931 Cologne, Germany

Phone: +49-221-478-86817; Fax: +49-221-478-86812;

Email: bwollnik@uni-koeln.de

Abstract

Split-hand/split-foot malformation (SHFM) is a congenital limb malformation characterized by an abnormal development of the central digit rays, deep median cleft and syndactyly of the affected hands and feet. A recent report described the first autosomal recessive inheritance of SHFM (SHFM6) caused by the homozygous p.R332W mutation in the *WNT10B* gene. However, the underlying molecular mechanism of this mutation is unknown. Here, we functionally characterized the described p.R332W mutation in *Wnt10b*. We show that the mutant protein is stable and still has the ability to bind to the low-density lipoprotein receptor-related protein 6 (Lrp6). In contrast to wild-type Wnt10b, the p.R332W mutant is not able to activate Lrp6-mediated Wnt signalling providing evidence for a reduced Wnt/ β -catenin signalling in the pathogenesis of SHFM. Moreover, we observed that Fgf8, likely involved in the pathogenesis of SHFM3, can bind Wnt10b and leads to a dosage-dependent suppression of Lrp6-mediated Wnt signalling. Our data give novel insights into the pathogenesis of SHFM6 and suggest a direct cross-talk between Wnt and Fgf signalling pathways.

Introduction

Split-hand/split-foot malformation (SHFM, MIM 183600, 313350, 600095, 605289, 606708, and 225300), also named ectrodactyly, is a complex congenital limb malformation involving the central rays of the autopod and characterized by syndactyly, median clefts of hands and/or feet, aplasia and/or hypoplasia of the phalanges, metacarpals and metatarsals (1). SHFM can occur as an isolated trait or as part of a more complex syndrome (2). Familial forms of SHFM are mainly inherited in an autosomal dominant manner (3), though autosomal recessive (4) and X-linked inheritance (5) have been described. SHFM is genetically heterogeneous with six loci described to date: SHFM1 located at 7q21-22 and structural alterations near *DLX5/6*, SHFM2 at Xq26 and no gene yet known, SHFM3 at 10q24 and duplications near *FGF8*, SHFM4 at 3q28 and mutations in *TP63*, SHFM5 at 2q31 and structural alterations near *EVX2* and the *HOXD* cluster (6-11). Recently, the first autosomal recessive locus was mapped in a large consanguineous family from Turkey to chromosome 12q13 (SHFM6) and, subsequently, a homozygous missense mutation in *WNT10B*, p.R332W, was identified in 12 affected and one unaffected family member (11). *WNT10B* consists of four coding exons and encodes a 389 amino acid protein, which is expressed throughout the mouse limb ectoderm during embryogenesis from day E.9.5 to E.15.5 (12). It was suggested that Wnt10b acts as an agonist in canonical Wnt signalling during various developmental processes (13).

The p.R332W alteration affects a highly conserved arginine in WNT10B and was not found in 200 healthy control individuals suggesting a causative nature of this missense mutation. No functional study was done and therefore, the functional consequences of the p.R332W WNT10B mutation as well as the pathophysiological mechanism underlying SHFM in the family are unknown.

In our study, we functionally characterized the Wnt10b p.R332W mutation. We show that wild-type Wnt10b can bind low-density lipoprotein receptor-related protein 6 (Lrp6) and activate canonical Wnt/ β -catenin signalling. In contrast, the p.R332W mutant is not able to

activate Lrp6-mediated Wnt signalling providing evidence for a reduced Wnt signalling in the pathogenesis of SHFM. Moreover, we demonstrated that Fgf8, likely involved in the pathogenesis of SHFM3, can bind Wnt10b and thereby alter Lrp6-mediated activation of Wnt signalling.

Material & Methods

Materials

Primers for site directed mutagenesis and sequencing of constructs were purchased from Metabion (Martinsried, Germany).

Plasmid Construction

Mutant *p.R332W Wnt10b* expression plasmid was generated using site directed mutagenesis PCR on wt mouse *Wnt10b* in the *pcDNA3.1* vector as template (kindly provided by Ormond MacDougald). Insertion of mutagenesis was confirmed by sequencing using the ABI BigDye Terminator v1.1 Cycle Sequencing Kit and the ABI 3730 DNA Analyzer (Applied Biosystems, Foster City; CA, USA). Expression plasmid for murine Fgf8 was generated by amplification of Fgf8 from a full length mammalian gene collection (Invitrogen, Karlsruhe, Germany) and cloning into *pCMV-SC-CF* vector (Agilent Technologies, La Jolla, CA, USA). Human *FGF21* in *pCMV6-AC-GFP* expression plasmid was purchased from OriGene (Darmstadt, Germany). Murine *Lrp6* in the *pcDNA3.1* expression vector was kindly provided by Matthew L. Warman and murine myc-tagged *Bmp4* in the *pcS2+* expression vector was a kind gift from N. Itasaki.

Cell Culture and Transfections

HEK293T cells were cultured in Dulbecco's Modified Eagle Media (DMEM) containing 10% fetal bovine serum (FBS, Gibco) and antibiotics. Cells were transfected using Lipofectamine 2000 (Invitrogen, Karlsruhe, Germany) according to manufacturer's instructions.

Dual Luciferase Reporter Assay

Luciferase Reporter assay was performed as described previously (13). In brief, HEK293T cells were plated out in 12-well plates, grown up to 50% confluency and transfected in

triplicates using the TOP-Flash reporter system and the indicated expression plasmids with the following concentrations: 100 ng Topflash vector, 5 ng Renilla (*p-RL-TK*), 750 ng Lrp6, 750 or 375 ng *Wnt10b*, 750 or 375 ng *Fgf8*, 750 or 375 ng *FGF21* and 750 or 375 ng *Bmp4*. Two days after transfection, cells were lysed and luciferase activity was measured using the Dual-Luciferase® Reporter Assay Kit by a Glomex™ 96-microplate luminometer (Promega, Mannheim, Germany). Each transfection was measured in triplicate.

Immunoprecipitation & Western Blot Analysis

Forty-eight hours after transfection, HEK293T cells were washed with cold PBS and solubilized using ice-cold lysis buffer containing 50mM HEPES, 150mM NaCl, 1% Triton X-100, 10% Glycerol, 10ug/ml Aprotinin, 5ug/ml Leupeptin, 1mM Na₃VO₄ and 1mM PMSF. Lysates were briefly centrifuged and total protein concentration of extracts was determined by BCA Protein Assay Kit (Pierce Protein Research Products, Thermo Fischer Scientific, Rockford, IL, USA). Equal amounts of total protein were incubated over night with protein A/G Plus-agarose (Santa Cruz Biotechnologies, Heidelberg, Germany) and the indicated antibodies [anti-Wnt10b (Abcam, Cambridge, UK), anti-Lrp6 (Abcam), anti-FLAG M2 (Stratagene, CA, US)]. After extensive washing, the immunoprecipitates were taken up in loading buffer, separated by 4-12% SDS-PAGE (Invitrogen, Germany) and blotted on nitrocellulose membrane (GE Healthcare, Freiburg, Germany). Immunoblots were blocked in 5% low-fat milk powder in Tris-buffered saline containing 0,2% Tween 20 and then probed with specific antibodies (1:1000 dilutions). Peroxidase conjugated secondary antibodies were purchased from Santa Cruz and blots were developed using an enhanced chemiluminescence system, ECL Plus (Amersham, UK), followed by exposure on autoradiographic film (GE Healthcare).

Sulfo-SBED Biotin Label Transfer

ProFound Sulfo-SBED Biotin Label Transfer Kit for Western Blot application was purchased from Pierce (Rockford, IL, USA). Label transfer and cross-linking were conducted according to manufacturer's instructions using 3 µg of human LRP6 protein (R&D Systems, Wiesbaden, Germany). Western blot analysis was accomplished using streptavidin-HRP (Pierce). Following detection, the membrane was stripped for 20 min using Restore™ Western Blot Stripping Buffer (Thermo Scientific, Bonn, Germany) according to manufacturer's instructions, washed three times with TBST and re-probed with anti-Lrp6 antibody (1:1000) and anti-Wnt10b (1:1000) antibodies.

Results

The p.R332W mutation in *Wnt10b* causes loss of protein function

Functional characterization of the described *WNT10B* mutation p.R332W is important (i) to provide additional evidence for the causative nature of this mutation in the molecular pathogenesis of SHFM6 and (ii) to gain insights into the pathophysiology of SHFM6. Therefore, we generated the p.R332W mutant by site directed mutagenesis PCR on wild-type (wt) *Wnt10b*. To analyze whether the homozygous missense mutation confers loss or gain of function we tested its transduction and activation of canonical WNT signalling using a Dual Luciferase Reporter Assay in transiently transfected HEK293T cells. Initially, we were able to demonstrate that – as previously described – Wnt1 significantly activates Lrp6-mediated Wnt/ β -catenin signalling (Fig. 1A). Also, co-expression of Lrp6 and Wnt10b resulted in a comparable activation of Wnt/ β -catenin signalling, while in contrast over expression of the p.R332W mutant did not lead to activation of Lrp6-mediated Wnt signalling. We showed that the p.R332W mutant is efficiently transcribed and translated, and, moreover, mutant Wnt10b protein can still bind to the Lrp6 receptor when transiently co-expressed in HEK293T cells using a co-immunoprecipitation approach (Fig. 1B, 1C, 1D). Furthermore, the interaction of wt and mutant Wnt10b with Lrp6 was confirmed by Western Blot analysis of a Sulfo-SBED Biotin Label Transfer assay (Fig. 1E). These findings clearly demonstrated that the p.R332W mutant is stable and although binding to the Lrp6 receptor, this interaction is no longer sufficient to activate Lrp6-mediated Wnt/ β -catenin signalling.

Fgf8 expression inhibits Wnt10b induced activation of Wnt/ β -catenin signalling

Fgf8 belongs to the fibroblast growth factor family and is a known key regulator of vertebrate limb development and essential for the induction of limb bud outgrowth and patterning. Interestingly, common duplications of the SHFM3 critical region occur physically nearby the chromosomal location of *FGF8* on 10q24 and, therefore, *FGF8* (among others) is regarded as

one of the candidate genes responsible for SHFM3, although no mutation in the coding region of *FGF8* has yet been identified in SHFM patients. We examined the potential role of Fgf8 in altering canonical WNT signalling by co-expression of Lrp6, Flag-tagged Fgf8 and Wnt10b in transiently transfected HEK293T cells. Co-expression of Fgf8 and Lrp6 alone did not have any effect on signalling while co-expression of Lrp6, Wnt10b and Fgf8 led to a significant reduction of relative luciferase activity as readout for Wnt/ β -catenin signalling (Fig. 2).

In order to determine the mechanism by which Fgf8 can inhibit Wnt10b induced Lrp6-mediated Wnt/ β -catenin signalling, we transfected HEK293T cells with different ratios of *Fgf8/Wnt10b* (1:1, 1:10 and 1:50) and observed that an increasing amount of Wnt10b rescued this inhibition suggesting either a competition of Fgf8/Wnt10b binding to Lrp6 binding or direct Fgf8/Wnt10b interaction (Fig. 3). To exclude any unspecific mechanism for this finding caused by the use of our cellular system and the overexpression of proteins, we tested the effects of two additional small secreted proteins, FGF21 and Bmp4. Dual Luciferase Reporter assay after co-expression of Lrp6, wt Wnt10b, GFP-tagged FGF21 and c-myc-tagged Bmp4 indeed indicated that also FGF21 reduces Lrp6-mediated Wnt10b signalling, while Bmp4 does not (Fig.4A). Thus, these data suggest that different Fgfs might share a specific inhibitory effect on canonical Wnt/ β -catenin signalling.

Fgf8 can bind Wnt10b: a putative cross-talk between both signalling pathways

An important hallmark of spatial and temporal activation of canonical Wnt/ β -catenin signalling during development is the ability of various secreted antagonists to down-regulate and suppress its activation. The results of our Luciferase-Reporter Assays demonstrated that co-expression of Fgf8 together with Wnt10b and Lrp6 results in a significant suppression of Wnt10b-induced canonical Wnt signalling. To define the molecular mechanism of Fgf8-mediated suppression, we conducted different co-immunoprecipitation experiments. Flag-tagged Fgf8 was transiently co-expressed in HEK293T cells with either Wnt10b or Lrp6 and

immunoprecipitated with specific antibodies. Western Blot analysis of co-immunoprecipitation assays clearly demonstrated that Fgf8 interacts with Wnt10b (Fig. 4B), while no direct interaction was observed between Fgf8 and the Lrp6 receptor (Fig. 4C). Thus, the Fgf8-mediated suppression of Wnt10b-activated canonical Wnt signalling likely results from a direct binding of Fgf8 to Wnt10b. As shown for other secreted Wnt antagonists, bound Wnt10b loses its ability to bind Lrp6 and, thereby, to activate the Wnt/ β -catenin signalling pathway.

Discussion

Pathophysiological mechanism of SHFM6

Recently, a homozygous missense mutation in the *WNT10b* gene was found to cause SHFM6 in a large consanguineous Turkish family (11), but the molecular mechanism and functional effects of the identified mutations remained unknown.

Previous studies on SHFM-related proteins suggested that alteration of the apical ectodermal ridge (AER) plays an important role in the development of SHFM (1). The formation and maintenance of the AER throughout limb development is a complex process, which depends on the orchestrated spatial and temporal expression of various transcription factors, secreted morphogens, and signalling proteins. The role of some of them has been defined in detail, such as signalling molecules belonging to the Fgf, Wnt, and Bmp families and their receptors (14-16). The Wnt signalling pathway is an evolutionary highly conserved pathway that regulates fundamental aspects of cell fate determination and cell migration in vertebrate limb development (reviewed by (17)). The canonical Wnt/ β -catenin pathway is activated by binding of specific Wnt ligands to their receptors, e. g. Lrp6 or frizzled (Fz) receptors. Binding of a Wnt to Lrp6 results in the stabilisation of cytosolic β -catenin, which then translocates to the nucleus where it associates with members of the Tcf/Lef family of transcription factors regulating the expression of target genes. In this study, we functionally characterized the described *WNT10B* missense mutation p.R332W and determined its impact on Wnt/ β -catenin signalling.

Initially, we showed for the first time that Wnt10b can bind Lrp6 and activate Wnt/ β -catenin signalling. Wnt10b itself is known to play a major role in the regulation of osteoblastogenesis and bone mass (18) as well as in the differentiation of epithelial cells in the hair follicle (19). Furthermore, it inhibits the development of white and brown adipose tissues (20). The finding that Wnt10b binds Lrp6 together with the fact that mutation in *WNT10B* cause limb malformation in SHFM6 suggests that Wnt10b/Lrp6 activation plays an essential role in

normal limb development, which is further supported by the finding that Wnt10b is expressed throughout the mouse limb ectoderm during embryogenesis from E.9.5 to E.15.5 (12). Wnt10b p.R332W mutant protein failed to activate the Lrp6-mediated Wnt signalling pathway in our *in vitro* system. It is interesting to note that distal limb malformations are also observed in a Lrp6 knockout mouse model (21). Since the crystal structure of Wnt10b protein is not available, we were unable to perform protein modelling of the mutant protein in order to predict possible steric hindrances caused by the mutation. Although overexpressed mutant protein was still able to bind to Lrp6, we suggest that this binding is either not efficient enough or takes place in an inappropriate way explaining the failure of Lrp6-mediated β -catenin activation.

Putative cross-talk between Fgf and Wnt signalling pathways

One key regulatory mechanism of Wnt signalling during development is the expression of various secreted Wnt antagonists, such as Dickkopf (DKK), Wise, Wnt-inhibitor protein (WIF) or Sost (22-26). One of the known mechanisms underlying this antagonistic function is the binding of these proteins directly to a specific Wnt, which then loses its ability to bind to its receptor. We now observed that Fgf8 is another putative Wnt antagonist (Fig. 5). Fgf8 does not directly bind to Lrp6, but to Wnt10b and this binding results in a dosage-dependent lack of Lrp6-mediated Wnt/ β -catenin activation. During limb bud formation and limb development, a tight regulation between Wnt and Fgf signalling is fundamental, e. g. to initiate and specify limb outgrowth and identity (27). However, an underlying cross-talk between both pathways was thought to exist only in an indirect manner (for example by inducing and regulating the expression of specific target genes).

We now provide the first link for a possible direct cross-talk between Fgf and Wnt pathways, although we admit that the evidence for this is based on *in vitro* data and has to be confirmed in the future in *in vivo* systems. In humans, *FGF8* is located in close proximity to the

frequently duplicated *SHFM3* region. Due to its known expression during limb bud formation and limb development (28, 29), several authors regard *FGF8* – beside others - as an excellent candidate gene for SHFM3. Dimitrov et al. suggested that duplications within the 10q24 region may alter a putative regulatory element of the *FGF8* gene (30) similarly to alterations of *SHH* expression by mutations or duplications of the ZRS region regulating the expression of *SHH* (31). Therefore, a physical interaction between both SHFM-related proteins Fgf8 and Wnt10b, as shown in our study, further supports a close balance and regulation of Fgf and Wnt signalling pathways during development of the median limb ray. Whether a specificity of Fgf/Wnt binding exists (which means that only specific Fgfs can bind to specific Wnts), remains to be elucidated in future experiments, though we were able to show that also FGF21 can bind to Wnt10b.

Furthermore, we excluded that Fgf/Wnt binding is a general *in vitro* artefact simply caused by overexpression of these small proteins by demonstrating that another small signalling molecule, Bmp4, does not cause any alteration of Wnt/ β -catenin signalling in our *in vitro* system.

In conclusion, we show that the described SHFM6 mutation p.R332W in *WNT10B* is a loss-of-function mutation. We further provide evidence that Wnt10b has the ability to bind Lrp6 and activate Lrp6-mediated Wnt/ β -catenin signalling and that the mutant protein lost this ability. Moreover, we propose that Fgf8 has an additional yet unknown function as a Wnt antagonist by binding to Wnt10b, a link for a direct cross-talk between Fgf and Wnt signalling important during limb development.

Acknowledgement

We are thankful to O. MacDougald for kindly providing the murine Wnt10B construct, M. L. Warman for the murine Lrp6 construct, N. Itasaki for the murine Bmp4 construct, and Karin Boss for critically reading the manuscript. This work was supported by the German Federal Ministry of Education and Research (BMBF) by grant number 01GM0880 (SKELNET) and 01GM0801 (E-RARE network CRANIRARE) to B.W.

References

1. Duijf, P. H., van Bokhoven, H. and Brunner, H. G. (2003) Pathogenesis of split-hand/split-foot malformation. *Hum Mol Genet*, **12**, Spec No 1, R51-60.
2. Elliott, A. M., Reed, M. H., Chudley, A. E., Chodirker, B. N. and Evans, J. A. (2006) Clinical and epidemiological findings in patients with central ray deficiency: split hand foot malformation (SHFM) in Manitoba, Canada. *Am J Med Genet A*, **140**, 1428-39.
3. Ozen, R. S., Baysal, B. E., Devlin, B., Farr, J. E., Gorry, M., Ehrlich, G. D. and Richard, C. W. (1999) Fine mapping of the split-hand/split-foot locus (SHFM3) at 10q24: evidence for anticipation and segregation distortion. *Am J Hum Genet*, **64**, 1646-54.
4. Gul, D. and Oktenli, C. (2002) Evidence for autosomal recessive inheritance of split hand/split foot malformation: a report of nine cases. *Clin Dysmorphol*, **11**, 183-6.
5. Ahmad, M., Abbas, H., Haque, S. and Flatz, G. (1987) X-chromosomally inherited split-hand/split-foot anomaly in a Pakistani kindred. *Hum Genet*, **75**, 169-73.
6. Scherer, S. W., Poorkaj, P., Massa, H., Soder, S., Allen, T., Nunes, M., Geshuri, D., Wong, E., Belloni, E., Little, S. *et al.* (1994) Physical mapping of the split hand/split foot locus on chromosome 7 and implication in syndromic ectrodactyly. *Hum Mol Genet*, **3**, 1345-54.
7. Ianakiev, P., Kilpatrick, M. W., Toudjarska, I., Basel, D., Beighton, P. and Tsipouras, P. (2000) Split-hand/split-foot malformation is caused by mutations in the p63 gene on 3q27. *Am J Hum Genet*, **67**, 59-66.
8. Goodman, F. R., Majewski, F., Collins, A. L. and Scambler, P. J. (2002) A 117-kb microdeletion removing HOXD9-HOXD13 and EVX2 causes synpolydactyly. *Am J Hum Genet*, **70**, 547-55.
9. Roscioli, T., Taylor, P. J., Bohlken, A., Donald, J. A., Masel, J., Glass, I. A. and Buckley, M. F. (2004) The 10q24-linked split hand/split foot syndrome (SHFM3): narrowing of the critical region and confirmation of the clinical phenotype. *Am J Med Genet A*, **124A**, 136-41.
10. Faiyaz-Ul-Haque, M., Zaidi, S. H., King, L. M., Haque, S., Patel, M., Ahmad, M., Siddique, T., Ahmad, W., Tsui, L. C. and Cohn, D. H. (2005) Fine mapping of the X-linked split-hand/split-foot malformation (SHFM2) locus to a 5.1-Mb region on Xq26.3 and analysis of candidate genes. *Clin Genet*, **67**, 93-7.
11. Ugur, S. A. and Tolun, A. (2008) Homozygous WNT10b mutation and complex inheritance in Split-Hand/Foot Malformation. *Hum Mol Genet*, **17**, 2644-53.
12. Witte, F., Dokas, J., Neuendorf, F., Mundlos, S. and Stricker, S. (2009) Comprehensive expression analysis of all Wnt genes and their major secreted antagonists during mouse limb development and cartilage differentiation. *Gene Expr Patterns*, **9**, 215-23.
13. Li, Y., Pawlik, B., Elcioglu, N., Aglan, M., Kayserili, H., Yigit, G., Percin, F., Goodman, F., Nurnberg, G., Cenani, A. *et al.* LRP4 mutations alter Wnt/beta-catenin signaling and cause limb and kidney malformations in Cenani-Lenz syndrome. *Am J Hum Genet*, **86**, 696-706.
14. Mariani, F. V., Ahn, C. P. and Martin, G. R. (2008) Genetic evidence that FGFs have an instructive role in limb proximal-distal patterning. *Nature*, **453**, 401-5.
15. Barham, G. and Clarke, N. M. (2008) Genetic regulation of embryological limb development with relation to congenital limb deformity in humans. *J Child Orthop*, **2**, 1-9.
16. Soshnikova, N., Zechner, D., Huelsken, J., Mishina, Y., Behringer, R. R., Taketo, M. M., Crenshaw, E. B., 3rd and Birchmeier, W. (2003) Genetic interaction between

- Wnt/beta-catenin and BMP receptor signaling during formation of the AER and the dorsal-ventral axis in the limb. *Genes Dev*, **17**, 1963-8.
17. MacDonald, B. T., Tamai, K. and He, X. (2009) Wnt/beta-catenin signaling: components, mechanisms, and diseases. *Dev Cell*, **17**, 9-26.
 18. Bennett, C. N., Longo, K. A., Wright, W. S., Suva, L. J., Lane, T. F., Hankenson, K. D. and MacDougald, O. A. (2005) Regulation of osteoblastogenesis and bone mass by Wnt10b. *Proc Natl Acad Sci U S A*, **102**, 3324-9.
 19. Ouji, Y., Yoshikawa, M., Moriya, K., Nishiofuku, M., Matsuda, R. and Ishizaka, S. (2008) Wnt-10b, uniquely among Wnts, promotes epithelial differentiation and shaft growth. *Biochem Biophys Res Commun*, **367**, 299-304.
 20. Longo, K. A., Wright, W. S., Kang, S., Gerin, I., Chiang, S. H., Lucas, P. C., Opp, M. R. and MacDougald, O. A. (2004) Wnt10b inhibits development of white and brown adipose tissues. *J Biol Chem*, **279**, 35503-9.
 21. Kelly, O. G., Pinson, K. I. and Skarnes, W. C. (2004) The Wnt co-receptors Lrp5 and Lrp6 are essential for gastrulation in mice. *Development*, **131**, 2803-15.
 22. Cadigan, K. M. and Liu, Y. I. (2006) Wnt signaling: complexity at the surface. *J Cell Sci*, **119**, 395-402.
 23. Glinka, A., Wu, W., Delius, H., Monaghan, A. P., Blumenstock, C. and Niehrs, C. (1998) Dickkopf-1 is a member of a new family of secreted proteins and functions in head induction. *Nature*, **391**, 357-62.
 24. Bouwmeester, T., Kim, S., Sasai, Y., Lu, B. and De Robertis, E. M. (1996) Cerberus is a head-inducing secreted factor expressed in the anterior endoderm of Spemann's organizer. *Nature*, **382**, 595-601.
 25. Itasaki, N., Jones, C. M., Mercurio, S., Rowe, A., Domingos, P. M., Smith, J. C. and Krumlauf, R. (2003) Wise, a context-dependent activator and inhibitor of Wnt signalling. *Development*, **130**, 4295-305.
 26. Semenov, M., Tamai, K. and He, X. (2005) SOST is a ligand for LRP5/LRP6 and a Wnt signaling inhibitor. *J Biol Chem*, **280**, 26770-5.
 27. Ng, J. K., Kawakami, Y., Buscher, D., Raya, A., Itoh, T., Koth, C. M., Rodriguez Esteban, C., Rodriguez-Leon, J., Garrity, D. M., Fishman, M. C. *et al.* (2002) The limb identity gene Tbx5 promotes limb initiation by interacting with Wnt2b and Fgf10. *Development*, **129**, 5161-70.
 28. Niswander, L., Tickle, C., Vogel, A., Booth, I. and Martin, G. R. (1993) FGF-4 replaces the apical ectodermal ridge and directs outgrowth and patterning of the limb. *Cell*, **75**, 579-87.
 29. Kuhlman, J. and Niswander, L. (1997) Limb deformity proteins: role in mesodermal induction of the apical ectodermal ridge. *Development*, **124**, 133-9.
 30. Dimitrov, B. I., de Ravel, T., Van Driessche, J., de Die-Smulders, C., Toutain, A., Vermeesch, J. R., Fryns, J. P., Devriendt, K. and Debeer, P. Distal limb deficiencies, micrognathia syndrome, and syndromic forms of split hand foot malformation (SHFM) are caused by chromosome 10q genomic rearrangements. *J Med Genet*, **47**, 103-11.
 31. Wieczorek D, Pawlik B, Li Y, Akarsu NA, Caliebe A, May KJ, Schweiger B, Vargas FR, Balci S, Gillessen-Kaesbach G, Wollnik B (2009) A specific mutation in the distant sonic hedgehog (SHH) cis-regulator (ZRS) causes Werner mesomelic syndrome (WMS) while complete ZRS duplications underlie Haas type polysyndactyly and preaxial polydactyly (PPD) with or without triphalangeal thumb. *Human Mutation*, **31**, 81-9.

Figure Legends

Figure 1: Pathophysiological mechanism of p.R332W mutation in *Wnt10b*. (A) Results of Dual Luciferase assay after co-expression of Lrp6, Wnt1, wt *Wnt10b* and *Wnt10b* p.R332W variant. Expression and stability of mutant *Wnt10b* protein was analyzed by western blotting (B). The p.R332W variant is expressed but fails to activate canonical Wnt signalling. Each experiment was performed 3 times with each transfection measured in triplicate. (C) Anti-*Wnt10b* precipitates of HEK293T cells expressing Lrp6 alone or together with wt *Wnt10b* or the *Wnt10b* p.R332W variant were analyzed by anti-Lrp6-immunoblotting. (D) Lysates of HEK293T variant described in (C) were subjected to anti-Lrp6 immunoprecipitation and proteins so obtained were analyzed by anti-*Wnt10b* immunoblotting. (E) Western Blot analysis of Sulfo-SBED Biotin Label Transfer experiments. Whole cell lysates of cells expressing wild-type *Wnt10b* or p.R332W variant were incubated with labeled human LRP6 protein and separated by reducing SDS-PAGE. Following transfer to nitrocellulose membranes, proteins were analyzed using streptavidin-HRP. After membrane stripping detection of *Wnt10b* was verified by re-probing the membrane with antibodies against *Wnt10b*.

Figure 2: Fgf8 suppresses *Wnt10b*-mediated Wnt signalling. Result from Dual Luciferase assays after co-expression of Lrp6, *Wnt10b* (wt) and flag-tagged Fgf8. Comparable steady-state expression levels of Lrp6, *Wnt10b* and Fgf8 were verified by western blot analysis of total cell lysates. Each transfection (n=3) was measured in triplicate.

Figure 3: Dose-dependent suppression of *Wnt10b*-mediated Wnt/ β -catenin activation by Fgf8. Results from Dual Luciferase assay after co-expression of Lrp6, wild-type *Wnt10b*, and flag-tagged Fgf8 with different ratios of *Wnt10b*/Fgf8 plasmid concentrations (+ = 1:1, ++ = 10:1, +++ = 50:1). Fgf8-dependent suppression of canonical Wnt signalling could be reversed

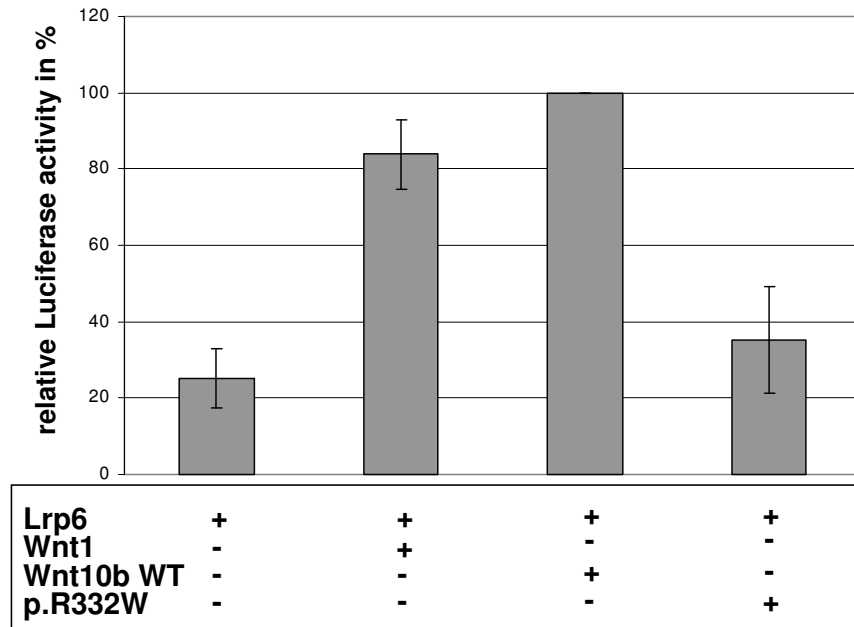
by increasing amounts of Wnt10b. Expression levels of were confirmed by western blot analysis of total cellular lysates and each experiment was performed 3 times with each transfection measured in triplicate.

Figure 4: FGF21 suppresses Wnt10b-mediated Wnt/ β -catenin activation while Bmp4 does not. (A) Dual Luciferase assay after co-expression of Lrp6, wt Wnt10b, GFP-tagged FGF21 and c-myc-tagged Bmp4. FGF21 has a similar effect as Fgf8 on Wnt10b-mediated Wnt signalling, whereas Bmp4 does not show any inhibition. Each transfection (n=3) was measured in triplicate. (B) HEK293T cells expressing Wnt10b and Flag-tagged Fgf8 were lysed and subjected to immunoprecipitations with antibodies to Fgf8 or Wnt10b. Purified proteins were analyzed by immunoblotting with antibodies to Flag peptide tag (left panel) or Wnt10b (right panel). (C) Anti-Lrp6 and anti-Fgf8 precipitates prepared from HEK293T cell expressing Lrp6 and Flag-tagged Fgf8 were analyzed by immunoblotting with antibodies to Lrp6 (left panel) or Flag peptide tag (right panel).

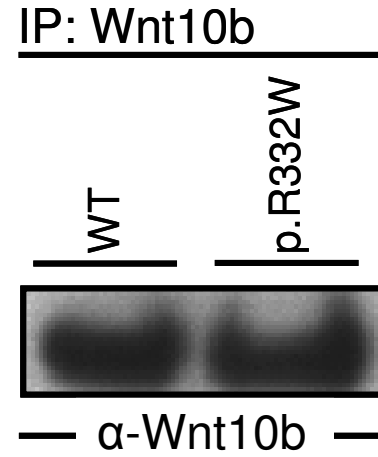
Figure 5: Model of Fgf8 inhibiting Wnt signalling. Both, Wnt1 and Wnt10b are known Wnt signalling agonists, which can bind to Lrp6 receptor. Lrp4 is a known Wnt antagonist acting in a so far unknown way. We propose that Fgf8 has an additional function and is a novel Wnt signalling antagonist via binding of Wnt10b and thereby repressing Wnt/ β -catenin activation.

Figure 1

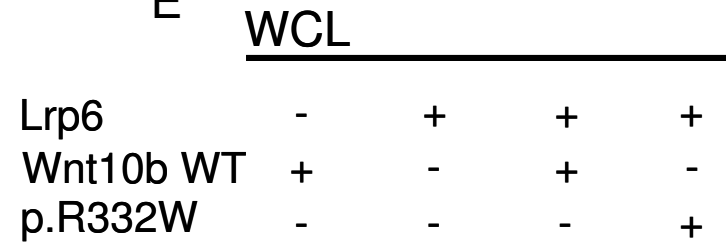
A



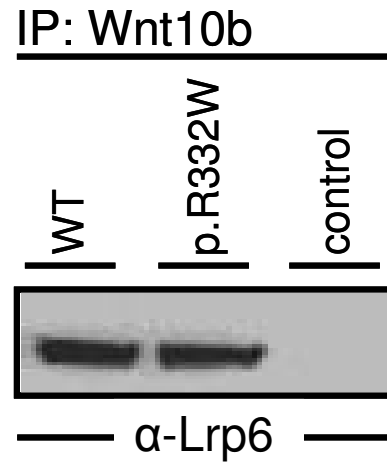
B



E



C



D

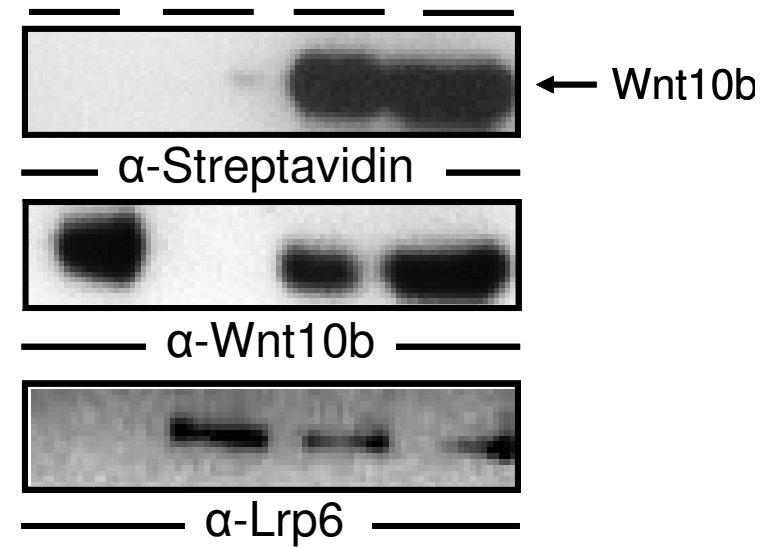
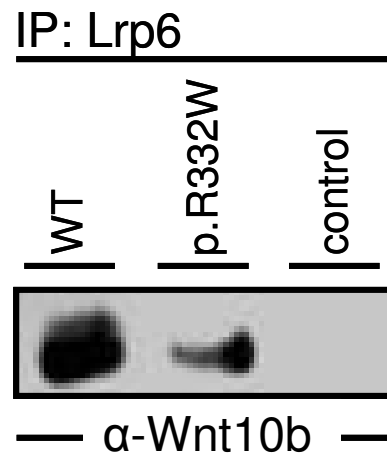
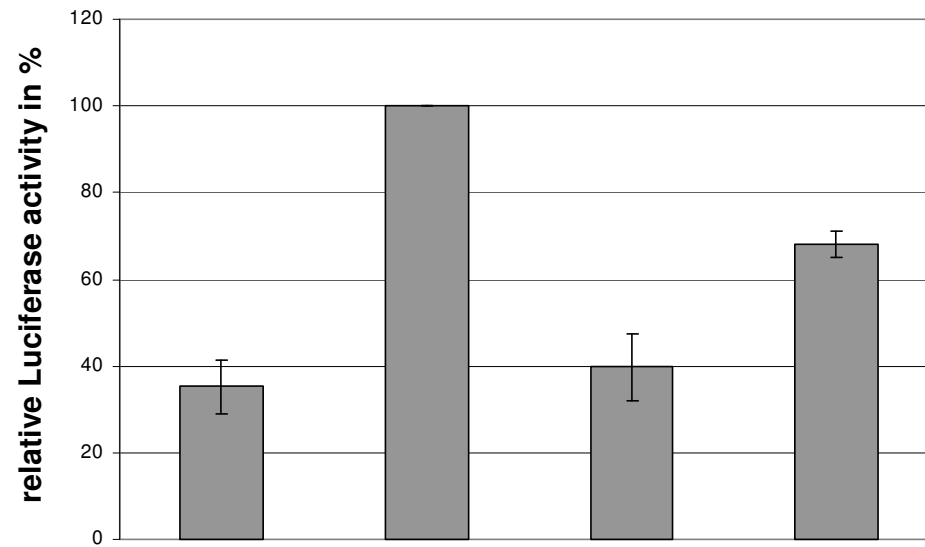
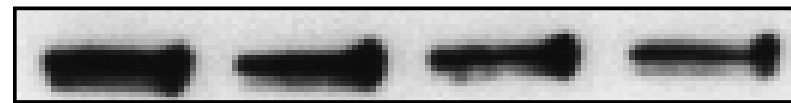


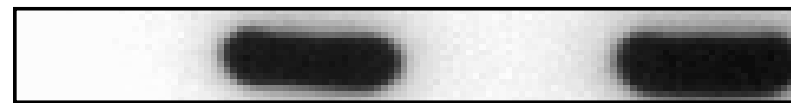
Figure 2



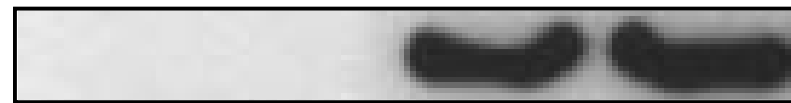
Lrp6	+	+	+	+
Wnt10b WT	-	+	-	+
Fgf8	-	-	+	+



α-Lrp6



α-Wnt10b



α-Fgf8

Figure 3

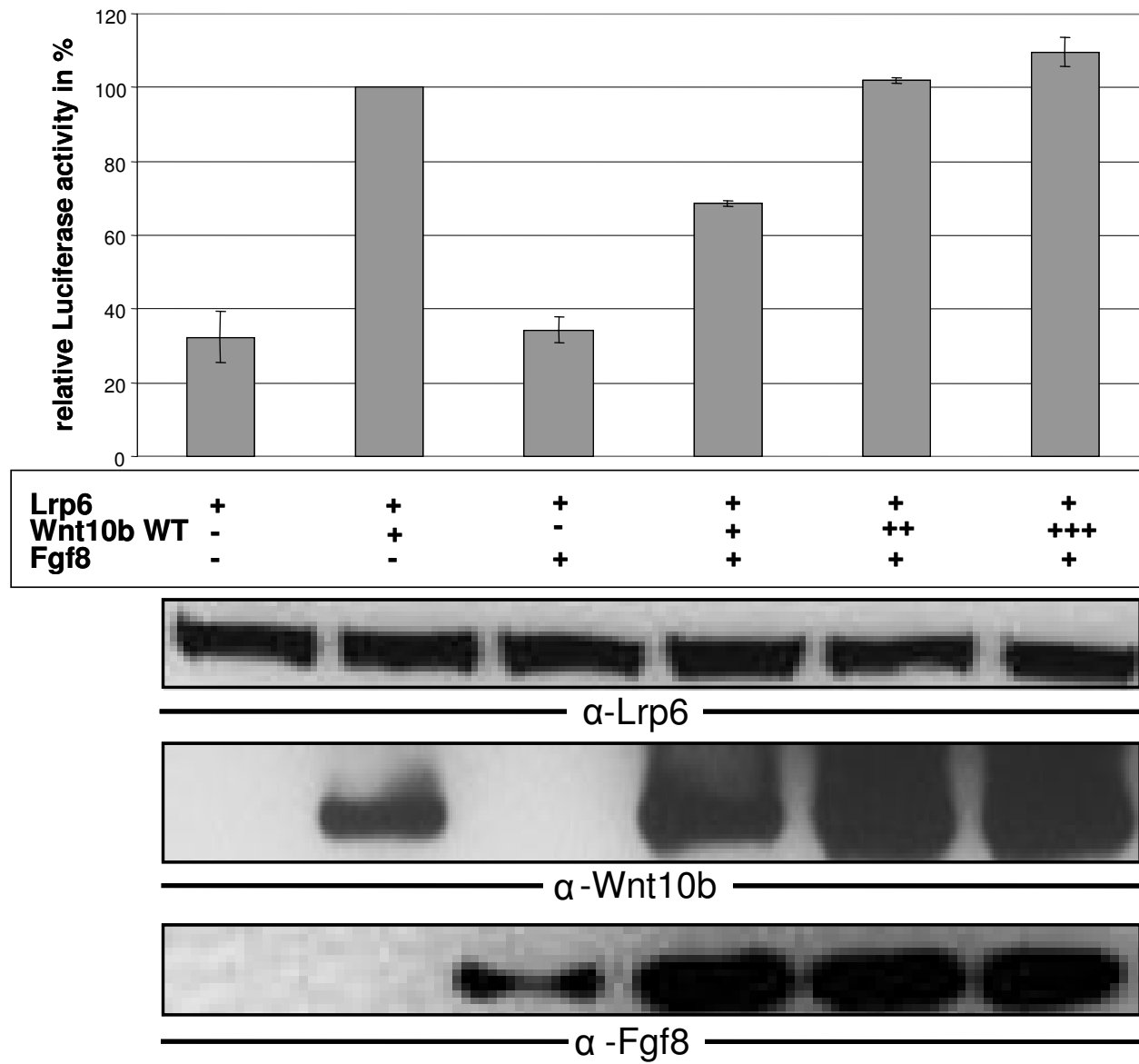
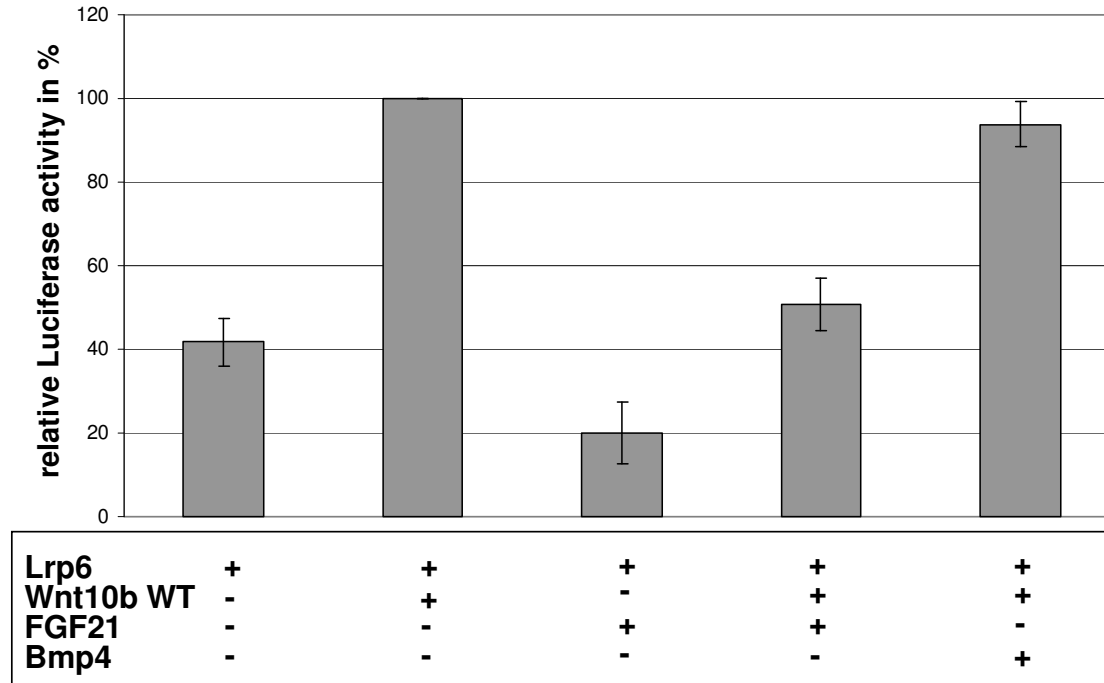
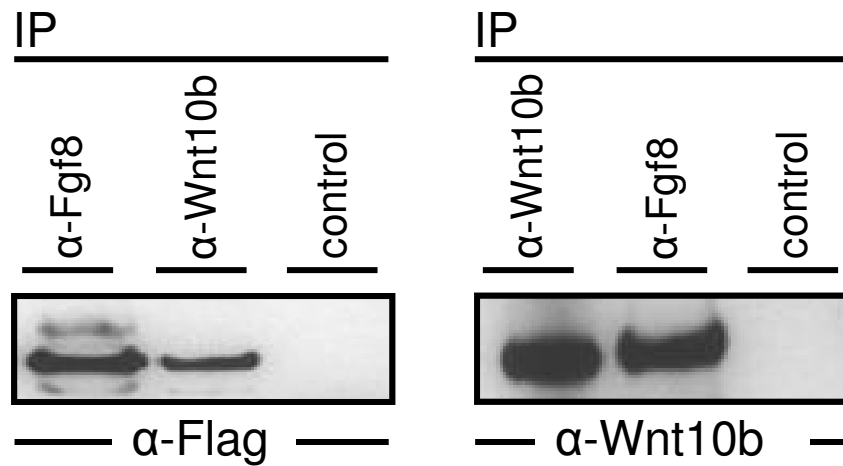


Figure 4

A



B



C

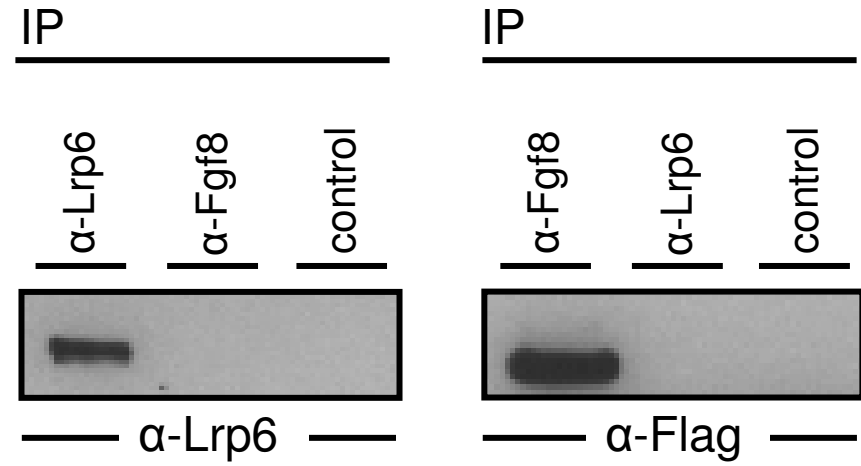
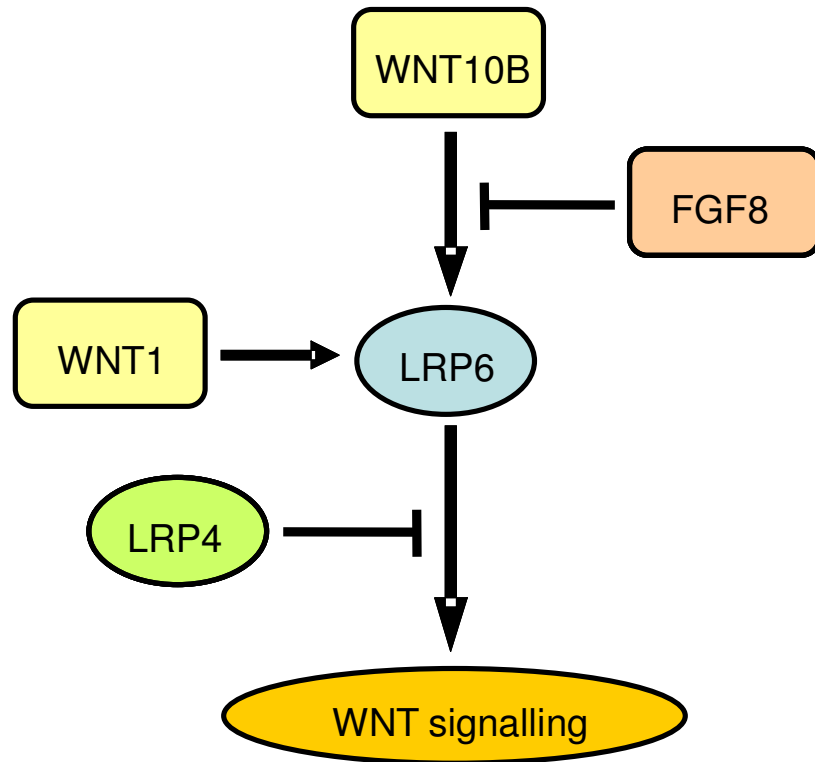


Figure 5



5.5 Li Y, Laue K, Temtamy S, Aglan M, Kotan L.D, Yigit G, Husniye C, Pawlik B, Nürnberg G, Wakeling EL, Quarrell OW, Baessmann I, Lanktree MB, Yilmaz M, Hegele RA, Amr K, May KW, Nürnberg P, Topaloglu AK, Hammerschmidt M, Wollnik B. Temtamy preaxial brachydactyly syndrome is caused by loss-of-function mutations in Chondroitin synthase 1, a potential target of BMP signalling (In Press, Am J Hum Genet (2010)).

Abstract of the publication:

The Temtamy preaxial brachydactyly syndrome (TPBS) is an autosomal recessively inherited congenital syndrome mainly characterized by bilateral, symmetric preaxial brachydactyly, facial dysmorphism, dental anomalies, sensorineural hearing loss, delayed motor and mental development as well as growth retardation. Brachydactyly can occur either as an isolated trait or as part of a syndrome and recent investigations have identified mutations in components of the Bone Morphogenetic Protein (BMP) signalling pathway in different types of brachydactyly, which is crucial for normal limb development, to be disease causing.

In this study we examined in total five TPBS families with a variable expression of clinical symptoms. In order to map the *TPBS* locus we first performed the Affymetrix GeneChip® Human Mapping 10K SNP Array (CCG, University of Cologne) with two TPBS families from Egypt. Two possibly linked loci on chromosomes 1p33 and 15q26 were identified with a combined parametric LOD score of 2.37 and 2.51, respectively. Extensive analysis of microsatellite markers of these regions finally mapped the *TPBS* locus to chromosome 15q26-qterm between SNPs rs1480952 and rs352744 defining a shared homozygous critical interval of approximately 3.8 Mb in affected individuals. Further mapping data of one additional TPBS family, TPB3, from Turkey, confirmed the *TPBS* locus. The critical region on 15q25 contained 20 annotated genes of which we tested *ADAMTS17*, *CHSY1*, *PCSK6*, and *SELS* as highly relevant candidate genes. Sequencing of the three coding exons of the chondroitin synthase 1 gene (*CHSY1*), revealed different homozygous mutations in affected individuals in each of the three linked families as well as in two additional families diagnosed with TPBS. We were able to detect three mutations in exon 1 of *CHSY1*, a 30-bp deletion, c.55-84del (p.G19_L28del, TPB1 family), a 1-bp deletion, c.14delG (p.G5AfsX29, TPB2 family), and the c.205C>T nonsense mutation (p.Q69X) in all three affected individuals of the TPB3 family. An acceptor splice site mutation, c.321-3C>G was identified in TPB4 family, while the only missense mutation, c.1616C>G (p.P539R, TPB5 family) was located in exon 3 of the

gene. All mutations co-segregated with the disease in the families and were not found in over 150 healthy control individuals.

Next we functionally characterized the mutant CHSY1 protein which is a key player in the biosynthesis of chondroitin sulfate (CS) by using different approaches and showed that complete or nearby complete loss of CHSY1 function causes brachydactyly, progressive skeletal anomalies, craniofacial dysmorphism, and hearing loss in humans.

In order to address the developmental functions of CHSY1 and CS, and their possible relation to BMP signalling, we turned to the zebrafish model system. Whole mount in situ hybridization revealed widespread expression of *chsy1* in the head and prominent expression in the floor plate of wild-type zebrafish embryos at 24 hours post fertilisation (hpf). Expression was also detected in the heart, distal regions of the pectoral fin buds, chondrocytes of the developing head skeleton, and epithelial protrusions of the inner ears.

Additional knock-down of *Chsy1* activity as well as gain-of-function studies displayed a significant reduction of body length, compromised pectoral fin formation, and severe midline deficiencies in the cartilage of the neurocranium. In the inner ears, formation of epithelial protrusions and semicircular canals was severely affected. To determine the effect of BMP signalling on the expression of *chsy1* we accomplished further co-expression analysis. We could show that at 56 hpf, *bmp2b* expression is strongest in the developing cristae of the inner ear, where *chsy1* expression is very weak. In contrast, the epithelial protrusions exhibit strong expression of *chsy1* and the BMP inhibitor *dan*, but weak *bmp2b* expression. Consistently, transgenic overexpression of *bmp2b* during the second day of development or MO-mediated knock-down of *dan* led to impaired semicircular canal formation similar to that caused by knock-down of *chsy1*. Furthermore, both treatments compromised *chsy1* expression in the epithelial protrusions.

Taken together, our data indicates that BMP signalling has a negative effect on *chsy1* expression, and that *Dan* is required to inhibit BMP signalling and to de-repress *chsy1* expression in epithelial protrusions, thereby allowing semicircular canal morphogenesis. We therefore conclude that both loss and gain of CHSY1 function lead to similar defects during various morphogenetic processes in the zebrafish, some of which might be equivalent to the distal limb malformations, craniofacial dysmorphism, shorter stature, and hearing loss caused by the homozygous loss of human CHSY1 function in Temtamy preaxial brachydactyly syndrome.

Own contributions:

Initially, the two TPB1 and TPB2 families from Egypt were subjected to a genome-wide scan using the Affymetrix GeneChip® Human Mapping 10K Array (CCG, University of Cologne, group of Prof. Dr. P. Nürnberg).

First of all I evaluated and interpreted the Affymetrix GeneChip data which showed linkage of the families to two possible different loci on chromosomes 1p33 and 15q26 (Data not shown). In order to map the *TPBS* locus I designed primers for microsatellite marker analysis for these loci and performed fine mapping analysis by using PCR technique. Finally, I interpreted the microsatellite marker analysis and established the corresponding haplotypes for the families (Figure 1a).

Temtamy Preaxial Brachydactyly Syndrome Is Caused by Loss-of-Function Mutations in Chondroitin Synthase 1, a Potential Target of BMP Signaling

Yun Li,^{1,2,15} Kathrin Laue,^{3,15} Samia Temtamy,⁴ Mona Aglan,⁴ L. Damla Kotan,⁵ Gökhan Yigit,^{1,2} Husniye Canan,⁶ Barbara Pawlik,^{1,2} Gudrun Nürnberg,^{1,7,8} Emma L. Wakeling,⁹ Oliver W. Quarrell,¹⁰ Ingelore Baessmann,⁷ Matthew B. Lanktree,¹¹ Mustafa Yilmaz,¹² Robert A. Hegele,¹¹ Khalda Amr,⁴ Klaus W. May,¹³ Peter Nürnberg,^{1,7,8} A. Kemal Topaloglu,¹⁴ Matthias Hammerschmidt,^{1,3,8,*} and Bernd Wollnik^{1,2,8,*}

Altered Bone Morphogenetic Protein (BMP) signaling leads to multiple developmental defects, including brachydactyly and deafness. Here we identify chondroitin synthase 1 (CHSY1) as a potential mediator of BMP effects. We show that loss of human CHSY1 function causes autosomal-recessive Temtamy preaxial brachydactyly syndrome (TPBS), mainly characterized by limb malformations, short stature, and hearing loss. After mapping the *TPBS* locus to chromosome 15q26-qterm, we identified causative mutations in five consanguineous TPBS families. In zebrafish, antisense-mediated *chsy1* knockdown causes defects in multiple developmental processes, some of which are likely to also be causative in the etiology of TPBS. In the inner ears of zebrafish larvae, *chsy1* is expressed similarly to the BMP inhibitor *dan* and in a complementary fashion to *bmp2b*. Furthermore, unrestricted *Bmp2b* signaling or loss of *Dan* activity leads to reduced *chsy1* expression and, during epithelial morphogenesis, defects similar to those that occur upon *Chsy1* inactivation, indicating that *Bmp* signaling affects inner-ear development by repressing *chsy1*. In addition, we obtained strikingly similar zebrafish phenotypes after *chsy1* overexpression, which might explain why, in humans, brachydactyly can be caused by mutations leading to either loss or to gain of BMP signaling.

Introduction

Brachydactyly is characterized by finger and toe shortening caused by short or absent metacarpus or metatarsus and/or phalanges. They can occur either as an isolated trait or as part of a syndrome in combination with other developmental malformations. Recent analyses have identified mutations in components of the Bone Morphogenetic Protein (BMP) signaling pathway or its modulators as the cause of different types of brachydactyly. According to current concepts, loss of BMP signaling, as for example caused by loss-of-function mutations in the BMP ligand GDF5 (MIM 601146) or the GDF5 high-affinity receptor BMPRI1 (MIM 603248), leads to reduced bone formation and brachydactyly type A2 (BDA2 [MIM 112600]) or type C (BDAC [MIM 113100]),¹ whereas gain of BMP signaling, as manifested by loss-of-function mutations in the BMP inhibitor Noggin (MIM 602991), can result in compromised joint formation between the different bony hand and foot elements and in the development of symphalangism (SYM1 [MIM 185800]) and/or multiple synostosis syndrome (SYNS1 [MIM 186500]).² However, the effects

of BMP signaling seem to be more complex and subject to intensive fine tuning. For instance, in addition to being caused by loss of GDF5 activity, BDA2 can also be caused by gain of BMP2 signaling, and brachydactyly type B2 (BDB2 [MIM 611377]) can be caused by missense mutations in Noggin (Mundlos¹ and references therein). Similarly, both GDF5 and Noggin mutations are linked to deafness in SYNS1.³ In light of this, the exact roles of BMP signaling and the nature of mediators accounting for the differential effects remain largely obscure.

The Temtamy preaxial brachydactyly syndrome (TPBS [MIM 605282]) is an autosomal-recessive congenital syndrome mainly characterized by bilateral, symmetric preaxial brachydactyly and hyperphalangism of digits, facial dysmorphism, dental anomalies, sensorineural hearing loss, delayed motor and mental development, and growth retardation.⁴

Here we mapped the *TPBS* locus to chromosome 15q26-qterm and identified causative mutations in *CHSY1* (MIM 608183) in five TPBS families. The zebrafish has recently emerged as a suitable animal model for human development and disease.⁵ We show that in developing zebrafish,

¹Center for Molecular Medicine Cologne, University of Cologne, Cologne, Germany; ²Institute of Human Genetics, University Hospital Cologne, University of Cologne, Cologne, Germany; ³Institute of Developmental Biology, University of Cologne, Cologne, Germany; ⁴Departments of Clinical and Molecular Genetics, Division of Human Genetics and Human Genome Research, National Research Centre, Cairo, Egypt; ⁵Department of Biotechnology, Institute of Sciences, Cukurova University, Adana, Turkey; ⁶Department of Forensic Medicine, Faculty of Medicine, Cukurova University, Adana, Turkey; ⁷Cologne Center for Genomics, University of Cologne, Cologne, Germany; ⁸Cologne Excellence Cluster on Cellular Stress Responses in Aging-Associated Diseases, University of Cologne, Cologne, Germany; ⁹North West Thames Regional Genetic Service, Harrow, London, UK; ¹⁰Sheffield Clinical Genetics Service, Sheffield Children's Hospital, Sheffield, UK; ¹¹Blackburn Cardiovascular Genetics Laboratory, Roberts Research Institute, University of Western Ontario, London, Ontario, Canada; ¹²Department of Pediatric Allergy and Immunology, Faculty of Medicine, Cukurova University, Adana, Turkey; ¹³Genomatix Software GmbH, München, Germany; ¹⁴Department of Pediatric Endocrinology, Faculty of Medicine, Cukurova University, Adana, Turkey

¹⁵These authors contributed equally to this work

*Correspondence: mhammers@uni-koeln.de (M.H.), bwollnik@uni-koeln.de (B.W.)

DOI 10.1016/j.ajhg.2010.10.003. ©2010 by The American Society of Human Genetics. All rights reserved.

loss and gain of *chsy1* function leads to defects similar to those in human TPBS patients. Such defects include reduced body length, compromised formation of the pectoral fin, severe midline deficiencies in the cartilage of the neurocranium, and compromised formation of epithelial protrusions and semicircular canals in the inner ear. Moreover, we demonstrate that Bmp signaling has a negative effect on *chsy1* expression and that Dan is required for inhibition of Bmp signaling and derepression of *chsy1* expression in epithelial protrusions, and it thereby allowing allows semicircular canal morphogenesis.

Material and Methods

Subjects

All subjects or their legal representatives gave written informed consent to the study. The study was performed in accordance to the Declaration of Helsinki protocols and approved by the local institutional review boards. Five families with the clinical diagnosis of Temtamy preaxial brachydactyly (TPBS) were included in the study. Clinical features of some of the families have been already published: TPB1,⁴ TPB4,⁶ and TPB5.⁷ Patients underwent general otological examinations and pure-tone audiometry with air and bone conduction at 250 Hz, 500 Hz, 1000 Hz, 2000 Hz, 4000 Hz, and 8000 Hz. Vestibular evaluation in affected individuals did not reveal any symptoms of vestibular dysfunction. Moderate to profound sensorineural hearing impairment was diagnosed in families TPB1 (individual II-2), TPB2 (individual II-2), TPB3 (individuals II-3 and II-5), TPB4 (individual II-2), and TPB5 (individuals II-5 and II-6). DNA from participating family members was extracted from peripheral blood lymphocytes by standard extraction procedures.

Linkage Analysis

Genome-wide linkage analysis in available members of the TB1 and TB2 families was performed with the Affymetrix GeneChip Human Mapping 10K SNP Array Xba142 (version 2.0). Genotypes were called by the GeneChip DNA Analysis Software (GDAS v3.0, Affymetrix). We verified sample genders by counting heterozygous SNPs on the X chromosome. Relationship errors were evaluated with the help of the program Graphical Relationship Representation.⁸ The program PedCheck detected Mendelian errors,⁹ and data for SNPs with such errors were removed from the data set. Non-Mendelian errors were identified with the program MERLIN,¹⁰ and unlikely genotypes for related samples were deleted. Linkage analysis was performed under the assumption of autosomal-recessive inheritance, full penetrance, consanguinity, and a disease gene frequency of 0.0001. Multipoint LOD scores were calculated with the program ALLEGRO.¹¹ Haplotypes were reconstructed with ALLEGRO and presented graphically with HaploPainter.¹² All data handling was performed with the graphical user interface ALOHOMORA.¹³ For the TPB3 family, an independent genome-wide 250K NspI Affymetrix SNP Array (Affymetrix, CA, USA) analysis was done on all members of the nuclear family at the Genome Sciences Laboratory of the Ankara University Biotechnology Institute. SNP Array data were analyzed by Genespring GT (Agilent, Santa Clara, CA, USA). For subsequent fine mapping, known and newly designed microsatellite markers for the critical region were genotyped (Table S2).

Mutation Screening

We searched databases to identify candidate genes in the critical region on chromosome 15q26-qterm (GeneDistiller, Ensemble Genome Server, and UCSC Genome Bioinformatics). Four candidate genes, *ADAMTS17* (MIM 607511), *CHSY1*, *SELS* (MIM 607918), and *PCSK6* (MIM 167405), were chosen for mutation screening on the basis of their expression pattern and presumed functional properties (OMIM and Unigene). Primers were designed according to the reference sequences. The coding exons and adjacent splice sites of these candidate genes were sequenced in the index patients of TPB1 and TPB2 families. We amplified the three exons of *CHSY1* (*CHSY1*, NC_000015.9; *CHSY1*, NP_055733.2; Table S2) from DNA of all affected members of the five families and sequenced the PCR products by BigDye Terminator method on an ABI 3100 sequencer. We resequenced all identified mutations in independent experiments and tested for cosegregation within the families. We tested 150 healthy control individuals from Turkey, 30 from Morocco, and 30 from Egypt for the mutations in exon 1 (c.55-84del30, c.14delG, and c.205C>T) by direct sequencing. One hundred twenty controls from Pakistan and 40 from Turkey were tested for the mutation of c.321-3C>G by PCR and restriction digestion, and 150 controls from Pakistan were tested for the mutation of p.P539R. *CHSY* protein sequence was analyzed with the server Pfam for protein domains. All primer sequences of designed polymorphic markers on 15qter and primer sequences for genomic and cDNA amplification of *CHSY1* can be found in Table S2.

CHSY1 cDNA Analysis

RNA was extracted from fresh blood with the Paxgene Blood RNA system (QIAGEN). Reverse-transcriptase polymerase chain reaction (RT-PCR) was performed with RevertAid First Strand cDNA synthesis Kit (Fermentas). The primers for amplification were designed according to the reference sequence and located in exon 1 and exon 3 (*CHSY1* mRNA, NM_014918.4; Table S2).

Histology

Whole-mount in situ hybridizations, immunostainings, and double in situ hybridizations were carried out as described.^{14,15} For *chsy1* probe synthesis, a 1030 bp fragment of zebrafish *chsy1* cDNA (GenBank accession number BC064670;¹⁶) was amplified via RT-PCR, cloned into pCRII (Invitrogen), linearized with HindIII, and transcribed with T7 RNA polymerase. Sense control probe was generated with NotI and SP6 RNA polymerase. The *bmp2b*, *msxc*, and *sox9a* probes were generated as described.¹⁷⁻¹⁹ Fluorescein-phalloidin staining of hair cells in sensory patches of inner ears was carried out as described.¹⁷

Morpholino Injection

Two sequence-independent antisense morpholino oligonucleotides (MOs) targeting the translational start codon (*chsy1*-ATG MO) or 5' untranslated region (*chsy1*-UTR MO) were purchased from GeneTools. Sequences were as follows: *chsy1*-ATG MO, 5'-AA GATCTGCGACTCCTTCCTGCCAT-3' (identical to MO in Zhang et al.¹⁶ and Peal et al.²⁰); and *chsy1*-UTR MO, 5'-CTAGTCGCTT TAATTTGTCAGAGTT-3'. MOs were injected into 1- to 4-cell-stage embryos, as described;²¹ per embryo, 1.5 nl was injected at concentrations ranging from 66-333 μ M (ATG MO) and from 333-500 μ M (UTR MO). To avoid unspecific toxicity, we coinjected the UTR MO with p53-MO.²² To control knockdown efficacy, we cloned the 5' UTR and the first 46 nucleotides of the coding region

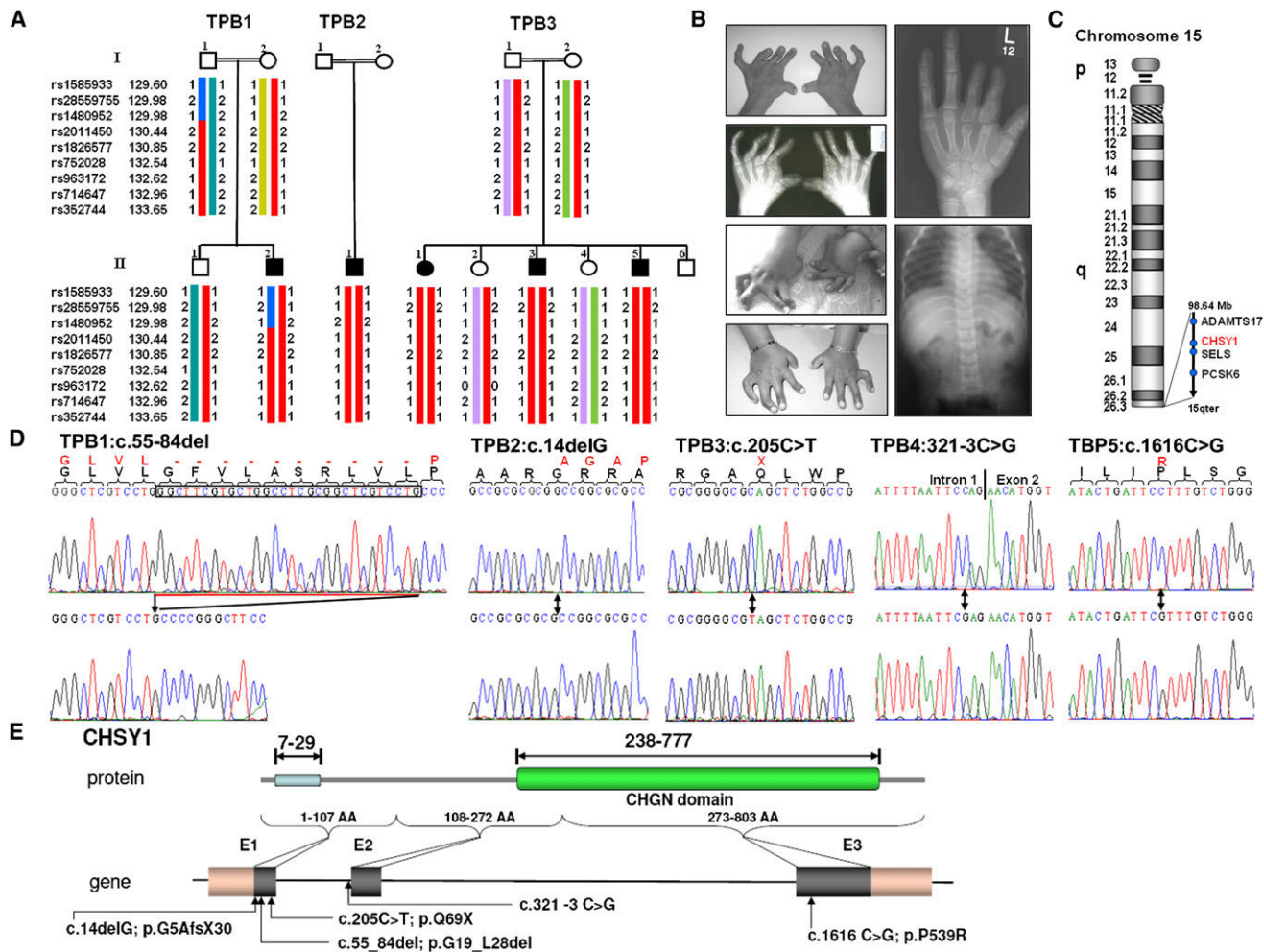


Figure 1. Clinical and Molecular Findings in Families with TPBS

(A) A haplotype analysis of the 15q26-qter critical region indicates homozygosity in affected individuals of the TPB1, TPB2, and TPB3 families.

(B) Typical hand anomalies and skeletal findings seen in our patients with TPBS.

(C) Genomic overview of the 15q26 critical region and genomic localization of the genes tested.

(D) Electropherograms of identified homozygous *CHSY1* mutations compared to wild-type sequences.

(E) Schematic view of *CHSY1* protein domains, coding exons, and localization of identified *CHSY1* mutations.

into pCS2+ vector²³ and fused it to GFP. The plasmid was linearized with NotI, and *chsy1-gfp* hybrid mRNA was generated with the SP6 MessageMachine Kit (Ambion, Austin, TX). Injection of this mRNA into zebrafish embryos yielded strong GFP fluorescence at late gastrula stages (Figure S3). However, fluorescence was completely suppressed upon subsequent coinjection of the mRNA with *chsy1*-ATG MO or *chsy1*-UTR MO (Figure S3). *dan* MO injections were done as described.²⁴

Overexpression Studies

For *chsy1* overexpression, the coding region of human *CHSY1* was cloned into the ClaI and XhoI sites of pCS2+.²³ The plasmid was linearized with NotI, and capped sense RNA was synthesized in vitro via the SP6 MessageMachine Kit (Ambion, Austin, TX). mRNA (1.5 nl) was injected into 1- to 4-cell-stage embryos at a concentration of 100 ng/μl. For temporally controlled *bmp2b* overexpression, the offspring of *Tg(hsp70l:bmp2b)fr13* transgenic fish were subjected to a 30 min heat shock (transfer from 28°C to 39°C) at 48 hpf, as described.²⁵

Results

Clinical Findings in CLS Families

We have examined five TPBS families presenting with a variable expression of clinical symptoms (Figure 1A, B, and Table 1). We observed mild facial dysmorphism, including round face and craniosynostosis, mild hypertelorism, and micrognathia, in the majority of TPBS cases (Table 1). Distal limb anomalies affected both hands and feet and were characterized by short and abducted thumbs, short and deviated halluces, and syndactyly. Typical preaxial brachydactyly of digits 1–3 was seen in all affected individuals and, in addition, hyper- and symphalangism, radio-ulnar synostosis, and carpal or tarsal fusions were observed in X-rays of some cases. Further skeletal anomalies showed a progressive course in TPBS patients and included growth retardation, kyphoscoliosis, and pectus excavatum. Interestingly, we found moderate

Table 1. Clinical Findings in TPBS Families Carrying *CHSY1* Mutations

Family Data	TB-1	TB-2	TB-3	TB-4	TB-5
Consanguinity	+	+	+	+	+
Number of affected individuals	1	2	3	1	3
Mutation (nucleotide change)	c.55-84del	c.14delG	c.205C>T	c.321-3C>G	c.1616C>G
Mutation (protein change)	G19_L28del	G5AfsX30	Q69X	–	P539R
Origin	Egypt	Egypt	Turkey	Sri Lanka	Pakistan
Facial Dysmorphism					
Plagiocephaly	+	+	+/-	–	–
Hypertelorism	+	+	–	+	–
Micro- or retrognathia	+	+	–	–	–
Dental Anomalies					
Microdontia	+	+	+	+	+
Talon cusps	+	+	+	+	–
Hearing loss					
Sensorineural	+	+	+	+	+
Conductive	–	–	–	–	+
Malformed ears	+	+	+	?	–
Hand or foot anomalies					
Short fingers or toes I, II, III	+	+	+	+	+
Syndactyly	+	+	+	+	+
Abducted thumbs	+	+	+	+	+
Lateral/medial deviations of fingers/toes	+	+	+	+	+
Clinodactyly	+	+	+	+	+
Radiological findings					
Preaxial brachydactyly	+	+	+	+	+
Short metacarpals/metatarsals	+	+	+	+	+
Hyperphalangism	+	+	+	+	+
Symphalangism	+	+	+	+	+
Phalangeal duplications	+	+	+	+	+
Radioulnar synostosis	–	–	–	+	–
Skeletal anomalies					
Kyphoscoliosis	+	+	+/-	–	–
Pectus excavatum	+	–	–	–	–
Generalized osteoporosis	+	+	+	n.a.	n.a.
Additional findings					
Developmental delay	+	+	+	?	–
Mental retardation	+	+	+	?	–
MRI findings	n.a.	partial agenesis of the cerebellar vermis	cerebellar degeneration, mild brain stem atrophy	n.a.	n.a.
Optic atrophy	–	–	–	+	–

to profound sensorineural hearing loss in almost 80% of the cases.

Mapping of the TPBS Locus and Identification of CHSY1 Mutations

Initially, we genotyped DNA samples from available family members of the originally described TPB1 family (4) and one additional family, TPB2, which both originated from Egypt, by using the Affymetrix GeneChip Human Mapping 10K SNP Array (version 2.0). Affected individuals were born to consanguineous parents in both families. Two possibly linked loci on chromosomes 1p33 and 15q26 were observed and had a combined parametric LOD score of 2.37 and 2.51, respectively (Figure S1). Extensive analysis of microsatellite markers of these regions mapped the TPBS locus to chromosome 15q26-qterm between SNPs rs1480952 and rs352744 (Figure 1A; see also Figure S2), defining a shared homozygous critical interval of approximately 3.8 Mb and excluding the 1p33 region (Figure 1C; see also Figure S2). Mapping data of one additional TPBS family, TPB3 from Turkey, confirmed TPBS locus without reducing the critical region (Figure 1A).

Among the 20 annotated genes within this region, we sequenced four of them as highly relevant positional candidate genes (*ADAMTS17*, *CHSY1*, *PCSK6*, and *SELS*; Table S1). Sequencing of the three coding exons of the chondroitin synthase 1, *CHSY1*, gene revealed different homozygous mutations in affected individuals in each of the three linked families as well as two additional families with TPBS, which were subsequently tested. *CHSY1* is transcribed to a 4549 bp transcript (NM_014918.4), which encodes a protein of 803 amino acids. All mutations cosegregated with the disease in the families and were not when more than 150 healthy control individuals were tested. We found three mutations in exon 1 of *CHSY1*: a 30 bp deletion, c.55-84del (p.G19_L28 del, TPB1 family); a 1 bp deletion, c.14delG (p.G5AfsX30, TPB2 family); and the c.205C>T nonsense mutation (p.Q69X) in all three affected individuals of the TPB3 family (Figures 1D and 1E). An acceptor splice-site mutation, c.321-3C>G, was identified in the TPB4 family, whereas the only missense mutation, c.1616C>G (p.P539R, TPB5 family), was located in exon 3 of the gene (Figures 1D and 1E).

The acceptor splice-site mutation c.321-3C>G is predicted to cause skipping of *CHSY1* exon 2 and lead to the loss of 496 bp on the transcript level and a thus frame shift and premature protein truncation. We confirmed skipping of exon 2 on cDNA of the affected individual (Figures S2A and S2B). The only missense mutation identified, p.P539R, affects a highly conserved proline (Figure 2C).

Expression of *chsy1* in Zebrafish

No *Chsy1* knockout mice have been reported yet. However, consistent with the phenotypic traits of TPBS, our in situ hybridization analysis revealed *Chsy1* expression in chondrocytes and the developing inner ear of e12.5 and e14.5 mouse embryos (data not shown). To address the develop-

mental functions of *CHSY1* and *CS*, and their possible relationship to BMP signaling, we turned to the zebrafish system. Whole-mount in situ hybridization revealed widespread expression of *chsy1* in the head (data not shown) and prominent expression in the floor plate (Figure 3A) and the fin epithelium (Figures 3B and 3D) of wild-type zebrafish embryos at 24 hr postfertilization (hpf). During the second day of development, prominent expression was also detected in the heart (data not shown), chondrocytes of the developing head skeleton (Figure 3E), pharyngeal endoderm of the branchial arches (Figure 3F,G), distal regions of the pectoral fin buds (Figure 3H), and epithelial protrusions of the inner ears (Figure 3I). These protrusions later fuse to form the semicircular canal ducts; the central components of the vestibular system contribute to angular motion sensing and body balancing.²⁶ After this fusion has occurred, *chsy1* transcript levels appear to drop (Figure 3J).

Phenotypes of Zebrafish after Loss and Gain of *chsy1* Activity and the Correlation of *chsy1* to *bmp2b* and *dan*

To knock down *Chsy1* activity, we injected zebrafish embryos with antisense morpholino oligonucleotides (MOs; for efficacy control; see Figure S3). In addition, for gain-of-function studies, we injected in vitro synthesized human *CHSY1* mRNA. Surprisingly, both treatments led to similar defects, including a significant reduction of body length (Figures 4A–4C), compromised pectoral fin formation (Figures 4D–4F), severe midline deficiencies in the cartilage of the neurocranium (Figures 4G and 4H), notochord undulation (Figures 4K and 4L), and later, notochord degeneration (Figures 4I and 4J), which could be correlated with the aforementioned *chsy1* expression in the overlying floorplate cells (see above; Figure 3A) and with the shorter body length (Figure 4B). Furthermore, *chsy1* morphants displayed reduced eye distances, as well as slight cyclopia in severe cases (Figures 4M–4O), which is linked with the neurocranial deficiencies (Figures 4G and 4H). In addition, the eyes developed colobomas (Figures 4P–4R).

In the inner ears, formation of epithelial protrusions and semicircular canals was severely compromised (Figures 5A–5D). However, according to *msxc* in situ hybridization and FITC-phalloidin staining of hair cells, the cristae and maculae, semicircular canal- and otolith-associated sensory patches of the ear, respectively, did not show major alterations in *chsy1* morphants (Figures 5K–5N). This suggests that, rather than being important for hair cell development itself, *Chsy1* might be instrumental for proper morphogenesis of the vestibular organ.

Positive and negative effects on semicircular canal development have also been reported for BMP signaling. Although according to genetic analysis, late loss of *Bmp2b* function leads to defective semicircular canal morphogenesis,²⁷ another report describes similar effects under *Bmp2b/4* gain-of-function conditions.²⁸ *bmp2b* and *chsy1* are expressed in a largely complementary manner.

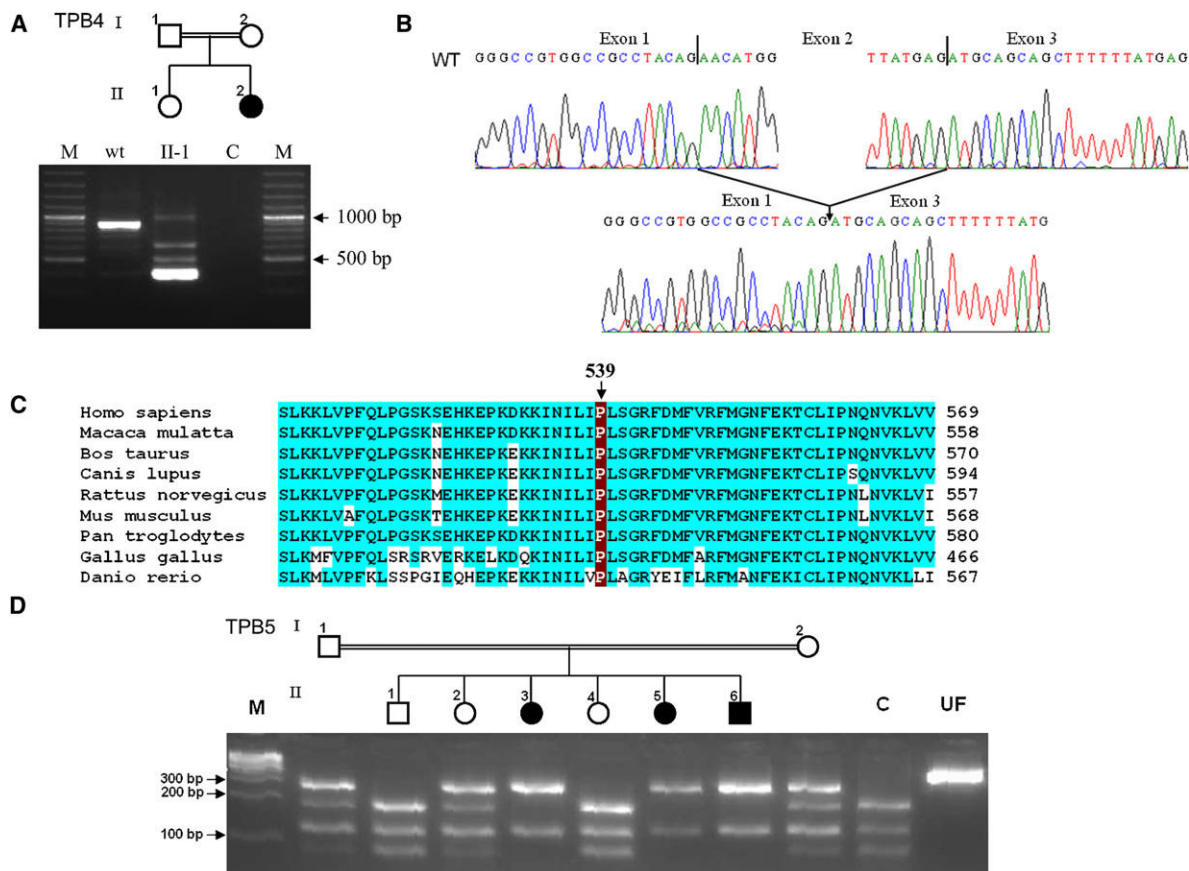


Figure 2. Additional Molecular Findings in TPBS

(A) Amplification of *CHSY1* cDNAs of the TPB4 patient carrying the c.321–3C>G splice-site mutation and of a healthy control. The forward primer was located in exon 1, and the reverse primer was located in exon 3. Complete loss of the normal amplicon size in the patient's cDNA was due to the skipping of exon 2. Abbreviations are as follows: M, marker; WT, wild-type control; Pat, patient; and C, water control without DNA.

(B) Electropherograms of *CHSY1* transcripts from the wild-type control and patient TPB4 show the skipping of exon 2 in the patient.

(C) An amino acid sequence alignment of *CHSY1* proteins of different species shows the highly conserved proline at position 539.

(D) A PCR and enzyme-digestion method was used as a second independent method of showing the cosegregation of the c.1616C>G (p.P539R) missense mutation in the TPB5 family. The mutation abolishes one of the two *Bsl*I restriction sites in the amplicon. Parents were heterozygotes, and all of three patients (II3, II5 and II6) were homozygotes for the mutation, whereas none of the three healthy siblings had the homozygous mutation. Abbreviations are as follows: M, Marker; C, healthy control individual; and UF, undigested PCR fragment.

At 56 hpf, *bmp2b* expression is strongest in the developing cristae of the inner ear (Figure 5J), where *chsy1* expression is very weak (Figure 5G). In contrast, the epithelial protrusions display strong expression of *chsy1* (Figure 5G) and the Bmp inhibitor *dan*²⁴ but weak *bmp2b* expression (Figure 5J). Consistently, transgenic overexpression of *bmp2b* during the second day of development or MO-mediated knockdown of *dan* led to impaired semicircular-canal formation similar to that caused by knockdown of *chsy1* (Figures 5E and 5F). Furthermore, both treatments compromised *chsy1* expression in the epithelial protrusions (Figures 5H and 5I). Together, this suggests that Bmp signaling has a negative effect on *chsy1* expression and that Dan is required for inhibition of Bmp signaling and derepression of *chsy1* expression in epithelial protrusions; Dan thereby allows semicircular canal morphogenesis. It is tempting to speculate that Bmp inhibition and

Chsy1 play a similar role during morphogenesis of the cochlea, the central auditory structure in mammals, and that they possibly underlie the hearing loss in human TPBS patients.

Discussion

In the present study we showed that congenital bilateral, symmetric preaxial brachydactyly and hyperphalangism of digits, facial dysmorphism, dental anomalies, sensorineural hearing loss, and growth retardation in the Temtamy preaxial brachydactyly syndrome (TPBS) is caused by recessive mutations in *CHSY1*. The encoded protein, chondroitin synthase 1, is a key protein in the biosynthesis of chondroitin sulfate (CS). It belongs to the glycosaminoglycans (GAGs) and is composed of alternating glucuronic

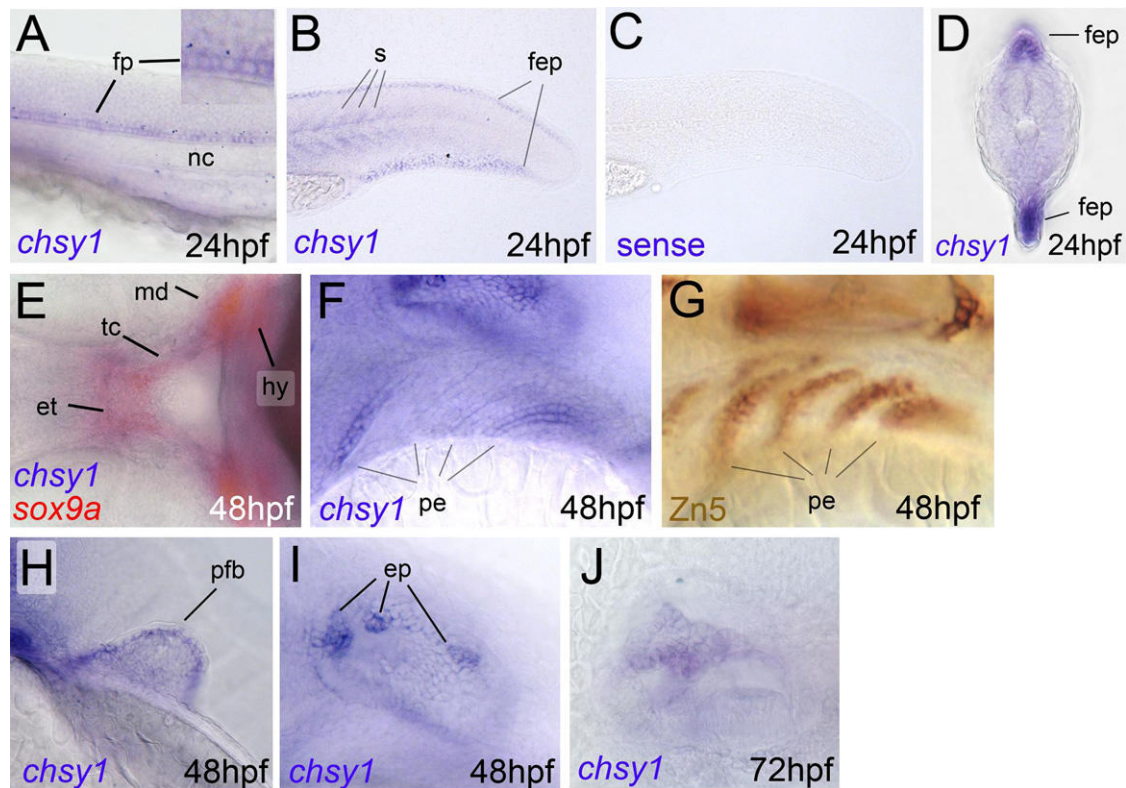


Figure 3. Expression of *chs1* during Zebrafish Development

Ages of embryos and larvae (in hpf) are indicated in the lower right corners, and the in situ hybridization probes (A–F and H–J) or antibody (G) are indicated in the lower left corners. (A–C, F–J) Lateral views. Anterior is to the left. (D) A transverse section through the tail. Dorsal is to the top. (E) A ventral view of the head region.

(A–F and H–J) Whole-mount in situ hybridization with a *chs1* antisense probe to detect *chs1* mRNA (A, B, D, E, F, H, I, and J), *sox9a* antisense probe¹⁹ to colabel chondrocytes (E, in red), and a *chs1* sense control probe (C). (G) Whole-mount anti-Zn5 immunostaining, marking the pharyngeal endoderm (compare with Piotrowski and Nüsslein-Volhard⁴⁰). *chs1* is expressed in the floor plate (fp), located between the spinal cord and the notochord (nc) (A), in the basal keratinocyte layer of the fin epithelium (B and D), in somatic cells close to the myosepta (B), in chondrocytes of the neurocranium and pharyngeal arches of the visceral skeleton (E), in the pharyngeal endoderm (pe) of the branchial arches (F), and in epithelial protrusions of forming semicircular canals in the inner ear (I). When these epithelial protrusions have fused in the center of the otic vesicle, *chs1* transcript levels drop (J).

Abbreviations are as follows: ep, epithelial protrusions; et, ethmoid plate (neurocranium); fep, fin epithelium; fp, floor plate; hy, hyoid (second pharyngeal arch); md, mandibular (first pharyngeal arch); nc, notochord; pe, pharyngeal endoderm; pfb, pectoral fin bud; s, somite; and tc, trabecula cranii (neurocranium).

acid (GlcUA) and N-acetyl galactosamine (GalNAc) residues.²⁹ CS can be synthesized in multistep processes as covalently bound side chains of proteins known as proteoglycans.³⁰ CHSY1 has both the glucuronyltransferase II and N-acetylgalactosaminyl-transferase II activities required for the synthesis of the repeating disaccharide unit of CS. Both deletions and the p.Q69X nonsense mutation, all located in exon 1 of *CHSY1*, can be expected to cause structural alterations and disruption of the CHSY1 protein structure. We also confirmed that the acceptor splice-site mutation c.321–3C>G causes skipping of *CHSY1* exon 2 and leads to the loss of 496 bp on the transcript level and a frame shift and premature protein truncation. Therefore, it is likely that the c.321–3C>G mutation also leads to a nonfunctional CHSY1 protein. We only identified one missense mutation, p.P539R, which affects a highly conserved proline within the functionally important chondroitin N-acetylgalactosaminyl-transferase (CHGN) domain of CHSY1 (Figure 1E). The

substitution of proline by arginine might interfere with the normal folding of this domain and thus prevent efficient protein function. Taken together, these findings demonstrate that complete or nearby complete loss of CHSY1 function underlies autosomal-recessive TPBS.

Our zebrafish study demonstrated that both loss and gain of *Chs1* function lead to similar defects during various morphogenetic processes in the zebrafish; some of these processes might be equivalent to the distal limb malformations, craniofacial dysmorphism, shorter stature, and hearing loss caused by the homozygous loss of human CHSY1 function in TPBS. The similarity of the zebrafish inner-ear phenotype after loss and gain of *Chs1* or *Bmp* activity, together with the loss of *chs1* transcription after gain of *Bmp* signaling, further suggests that a similar deregulation of CHSY1 might at least partly underlie the different defects caused by aberrant BMP signaling in mammals. Such defects include craniofacial and inner-ear dysmorphologies^{31–33} and the different types of

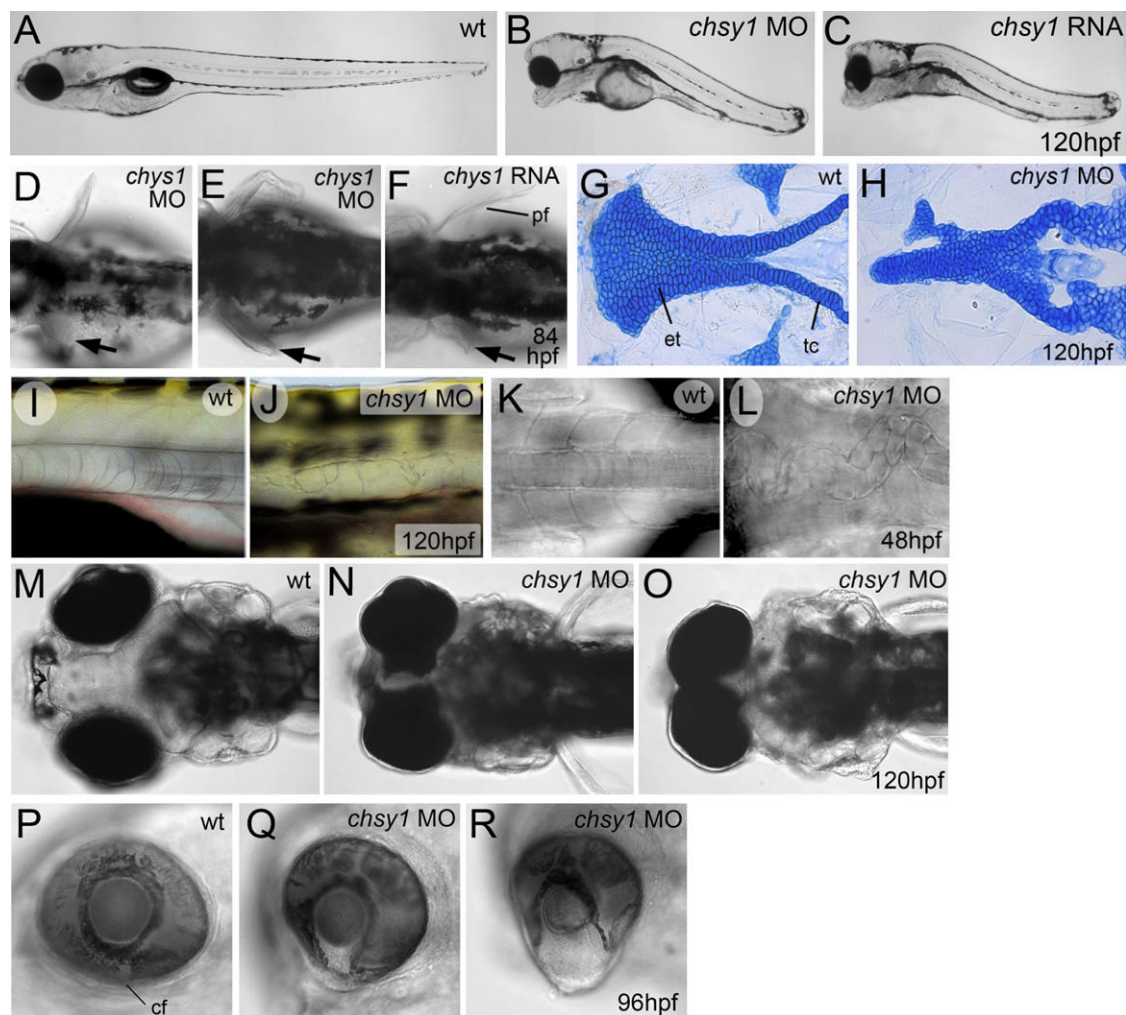


Figure 4. Phenotypes of Zebrafish Larvae after Loss and Gain of *chsy1* Function

Ages of zebrafish larvae (in hpf) are indicated in the lower right corners, and treatments are indicated in the upper right corners. Abbreviations are as follows: MO, embryo injected with antisense morpholino, loss of function; RNA, embryo injected with synthetic mRNA, gain of function; and wt, unjected wild-type control).

(A–C) Lateral views of live animals, displaying reduced body length and altered head morphology after *chsy1* loss and gain of function. (D–F) Dorsal views of the anterior trunk of live larvae, displaying pectoral fins with variably reduced outgrowth. Upper fin in (F) is of normal size and shape. Compared to the other phenotypic traits, impaired fin development was only moderately penetrant (approximately 30%), and it often occurred in a unilateral manner (as in F). (G and H) Alcian blue staining of cartilage of the neurocranium. For a better appreciation of the neurocranial deficiencies, the visceral skeleton was manually removed.

(I and J) Lateral view of the trunk of live animals, revealing degeneration of notochord cells in the morphant. In several zebrafish mutants, notochord degeneration is linked to and most likely causative of reduced body length,⁴¹ as also seen in the *chsy1* morphants described here.

(K and L) View of the trunk of live embryo. The notochord undulation of the morphant indicates that the shortened body length cannot be solely caused by notochord degeneration. Similar notochord undulation has been observed in several zebrafish mutants, e.g., those carrying loss-of-function mutations in *wnt5a*,³⁶ pointing to a possible additional role of Chsy1 in modulating noncanonical Wnt signaling.

(M–O) Dorsal view of the heads of live larvae. Medial expansion of the eyes and loss of midline forebrain tissue leads to partial cyclopia. Note that in the morphants shown here, the pectoral fins are not or only moderately affected.

(P–R) Lateral view of the eyes, revealing lack of dorsal retinal tissue and failed closure of the choroid fissure (coloboma). This phenotypic trait is linked to the above-described medial-forebrain deficiencies and shifts of the eyes to more medial positions, and it might be a secondary consequence of the overall alterations in head and head-skeleton morphology.

Abbreviations are as follows: cf, choroid fissure of eye; et, ethmoid plate (neurocranium); pf, pectoral fin bud; and tc, trabeluca crani (neurocranium).

human brachydactylies, caused by either gain or loss of BMP signaling.¹ Future studies will have to reveal the molecular mechanisms of *chsy1* repression by Bmp signaling and of Chsy1 and CS function. Computational

analysis of human *CHSY1* revealed the presence of several Smad transcription-factor binding sites (data not shown), suggesting that the effect of BMP signaling on *CHSY1* expression might be direct. CS, in turn, could have

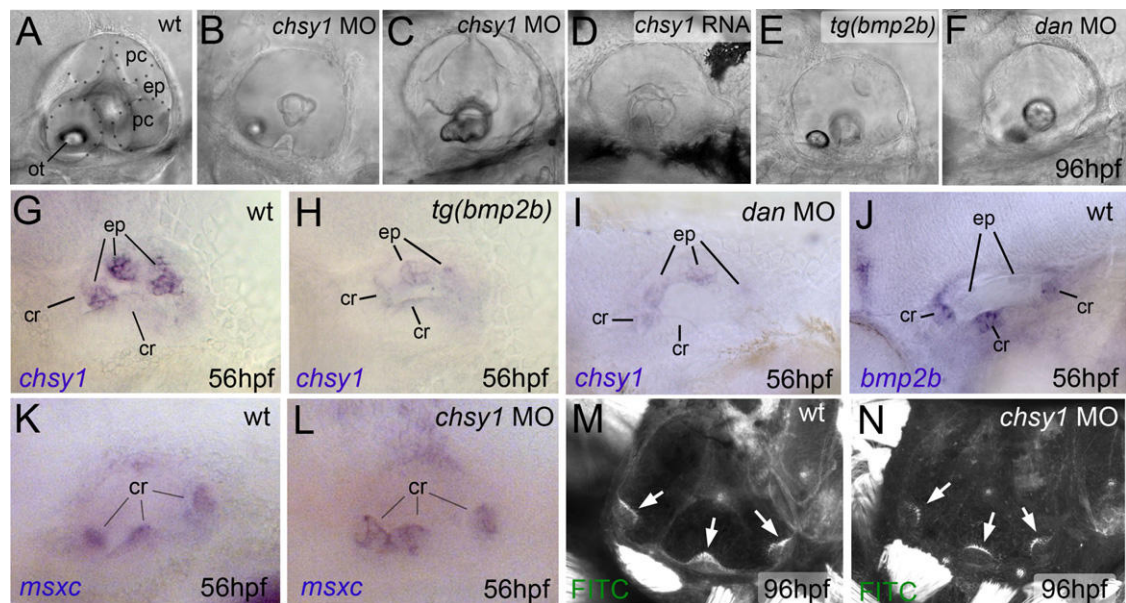


Figure 5. Interaction between *chs1*, *bmp2b*, and *dan* during Inner-Ear Morphogenesis.

Ages of larvae (in hpf) are indicated in lower right corners, and treatments are indicated in upper right corners. Abbreviations are as follows: MO, embryo injected with antisense morpholino; RNA, embryo injected with synthetic mRNA; *tg(bmp)*, transgenic after heat-shock induction of ubiquitous *bmp2b* expression;²⁵ and wt, unjected or nontransgenic wild-type control.

(A–F) Lateral views of the inner ear of live animals. In the wild-type control (A), the walls of the semicircular canals are outlined by dots. (G–H) Inner ears after whole-mount in situ hybridization for *chs1* (t-v) or *bmp2b* (w) mRNA. For details, see text.

(G–L) Lateral views of the inner ears after whole-mount in situ hybridization for *chs1* (G–I), *bmp2b* (J), or *msxc* (K and L). (G–I) *chs1* mRNA levels in epithelial protrusions (ep) are strongly reduced after overexpression of *bmp2b* (H) and after inactivation of the BMP inhibitor DAN (I). The much weaker expression in the cristae primordia (cr) remains unaltered (compare G and H). (J) In contrast to *chs1* (see G), *bmp2b* is strongly expressed in the cristae of the wild-type inner ear. (K and L) *msxc* expression in cristae of the *chs1* morphant is unaltered (L). Because *msx* genes are known transcriptional targets of BMP signaling, these data also suggest that, in contrast to the BMPs upstream of *chs1*, Chs1 does not act upstream of BMP signaling.

(M and N) Merged stacks of confocal images of inner ears after fluorescein (FITC)-phalloidin staining. Cristae (indicated by white arrows) of wild-type and morphant larvae contain hair cells of indistinguishable numbers and morphology.

Abbreviations are as follows: cr, crista (sensory patch of inner ear); ep, epithelial protrusions; o, otolith; and pc, posterior semicircular canal.

a structural role during morphogenetic processes, consistent with its expression in the tips of the epithelial projections of the forming semicircular canals and with the described role of other GAGs such as hyaluronic acid during zebrafish inner-ear morphogenesis.³⁴ In addition, as a component of proteoglycans-like aggrecan or versican, CS might feed back to BMP or other growth-factor signaling, consistent with the described activities of proteoglycans as growth-factor binding proteins and/or coreceptors.³⁵ For instance, an undulated notochord phenotype as in zebrafish *chs1* morphants is also displayed by *wnt5a* mutants,³⁶ pointing to a possible involvement of CHSY1 in noncanonical WNT signaling. Furthermore, as described in detail in the accompanying work by Tian et al.,³⁷ CHSY1 could modulate signaling through the Notch receptor. CHSY1 has a Fringe domain, which is possibly involved in glycosylation of Notch receptors and thus modifying their ligand specificity and signaling efficiency.³⁸ Consistent with a role of Chs1 in reducing Notch signaling, we found that conditional expression of the constitutively active intracellular domain of Notch in zebrafish causes compromised semicircular-canal formation, as

does loss of Chs1 activity (K.L. and M.H., unpublished data). Together, the negative role of Bmp signaling on *chs1* expression and the negative role of Chs1 on Notch signaling are in line with the synergistic effect of Notch function downstream of Bmp signaling as reported in many different developmental and physiological scenarios.³⁹

In conclusion, we show that loss of human CHSY1 function causes autosomal-recessive Temtamy preaxial brachydactyly syndrome and that antisense-mediated *chs1* knockdown in zebrafish causes similar defects in multiple developmental processes. In the inner ears of zebrafish larvae, unrestricted *Bmp2b* signaling or loss of *Dan* activity leads to reduced *chs1* expression and, during epithelial morphogenesis, defects similar to those that occur upon *Chs1* inactivation, indicating that Bmp signaling affects inner-ear development by suppressing *Chs1*.

Supplemental Data

Supplemental Data include three figures and two tables and are available with this article online at <http://www.cell.com/AJHG/>.

Acknowledgments

We are thankful to all family members who participated in this study, Esther Milz and Evelin Fahle for excellent technical assistance, and Karin Boss for critical reading of the manuscript. This work was supported by the German Federal Ministry of Education and Research (BMBF) by grant number 01GM0880 (SKELNET) and by 01GM0801 (E-RARE network CRANIRARE) to B.W. Work in M.H.'s laboratory was supported by the National Institutes of Health (grant 1R01 GM63904) and the German Research Foundation (SFB572).

Received: August 7, 2010

Revised: October 3, 2010

Accepted: October 7, 2010

Published online: December 2, 2010

Web Resources

The URLs for data presented herein are as follows:

ENSEMBL, <http://www.ensembl.org>

UCSC Genome Browser, <http://www.genome.ucsc.edu>

Online Mendelian Inheritance in Man (OMIM), <http://www.ncbi.nlm.nih.gov/omim>

PolyPhen, <http://coot.embl.de/PolyPhen>

Accession Numbers

CHSY1: MIM 608183. Temtamy preaxial brachydactyly syndrome: OMIM, MIM 605282.

References

- Mundlos, S. (2009). The brachydactylies: A molecular disease family. *Clin. Genet.* 76, 123–136.
- Gong, Y., Krakow, D., Marcelino, J., Wilkin, D., Chitayat, D., Babul-Hirji, R., Hudgins, L., Cremers, C.W., Cremers, F.P., Brunner, H.G., et al. (1999). Heterozygous mutations in the gene encoding noggin affect human joint morphogenesis. *Nat. Genet.* 21, 302–304.
- Dawson, K., Seeman, P., Sebald, E., King, L., Edwards, M., Williams, J., 3rd, Mundlos, S., and Krakow, D. (2006). GDF5 is a second locus for multiple-synostosis syndrome. *Am. J. Hum. Genet.* 78, 708–712.
- Temtamy, S.A., Meguid, N.A., Ismail, S.I., and Ramzy, M.I. (1998). A new multiple congenital anomaly, mental retardation syndrome with preaxial brachydactyly, hyperphalangism, deafness and orodental anomalies. *Clin. Dysmorphol.* 7, 249–255.
- Lieschke, G.J., and Currie, P.D. (2007). Animal models of human disease: Zebrafish swim into view. *Nat. Rev. Genet.* 8, 353–367.
- Race, H., Hall, C.M., Harrison, M.G., Quarrell, O.W., and Wakeling, E.L. (2010). A distinct autosomal recessive disorder of limb development with preaxial brachydactyly, phalangeal duplication, symphalangism and hyperphalangism. *Clin. Dysmorphol.* 19, 23–27.
- Abecasis, G.R., Cherny, S.S., Cookson, W.O., and Cardon, L.R. (2001). GRR: Graphical representation of relationship errors. *Bioinformatics* 17, 742–743.
- O'Connell, J.R., and Weeks, D.E. (1998). PedCheck: A program for identification of genotype incompatibilities in linkage analysis. *Am. J. Hum. Genet.* 63, 259–266.
- Abecasis, G.R., Cherny, S.S., Cookson, W.O., and Cardon, L.R. (2002). Merlin—Rapid analysis of dense genetic maps using sparse gene flow trees. *Nat. Genet.* 30, 97–101.
- Kruglyak, L., Daly, M.J., Reeve-Daly, M.P., and Lander, E.S. (1996). Parametric and nonparametric linkage analysis: A unified multipoint approach. *Am. J. Hum. Genet.* 58, 1347–1363.
- Strauch, K., Fimmers, R., Kurz, T., Deichmann, K.A., Wienker, T.F., and Baur, M.P. (2000). Parametric and nonparametric multipoint linkage analysis with imprinting and two-locus-trait models: application to mite sensitization. *Am. J. Hum. Genet.* 66, 1945–1957.
- Thiele, H., and Nürnberg, P. (2005). HaploPainter: A tool for drawing pedigrees with complex haplotypes. *Bioinformatics* 21, 1730–1732.
- Rüschendorf, F., and Nürnberg, P. (2005). ALOHOMORA: A tool for linkage analysis using 10K SNP array data. *Bioinformatics* 21, 2123–2125.
- Hammerschmidt, M., Pelegri, F., Mullins, M.C., Kane, D.A., van Eeden, F.J., Granato, M., Brand, M., Furutani-Seiki, M., Haffter, P., Heisenberg, C.P., et al. (1996). dino and mercedes, two genes regulating dorsal development in the zebrafish embryo. *Development* 123, 95–102.
- Herzog, W., Zeng, X., Lele, Z., Sonntag, C., Ting, J.W., Chang, C.Y., and Hammerschmidt, M. (2003). Adenohypophysis formation in the zebrafish and its dependence on sonic hedgehog. *Dev. Biol.* 254, 36–49.
- Zhang, J., Lefebvre, J.L., Zhao, S., and Granato, M. (2004). Zebrafish unplugged reveals a role for muscle-specific kinase homologs in axonal pathway choice. *Nat. Neurosci.* 7, 1303–1309.
- Mowbray, C., Hammerschmidt, M., and Whitfield, T.T. (2001). Expression of BMP signalling pathway members in the developing zebrafish inner ear and lateral line. *Mech. Dev.* 108, 179–184.
- Whitfield, T.T., Granato, M., van Eeden, F.J., Schach, U., Brand, M., Furutani-Seiki, M., Haffter, P., Hammerschmidt, M., Heisenberg, C.P., Jiang, Y.J., et al. (1996). Mutations affecting development of the zebrafish inner ear and lateral line. *Development* 123, 241–254.
- Yan, Y.-L., Miller, C.T., Nissen, R.M., Singer, A., Liu, D., Kirn, A., Draper, B., Willoughby, J., Morcos, P.A., Amsterdam, A., et al. (2002). A zebrafish *sox9* gene required for cartilage morphogenesis. *Development* 129, 5065–5079.
- Peal, D.S., Burns, C.G., Macrae, C.A., and Milan, D. (2009). Chondroitin sulfate expression is required for cardiac atrioventricular canal formation. *Dev. Dyn.* 238, 3103–3110.
- Nasevicius, A., and Ekker, S.C. (2000). Effective targeted gene 'knockdown' in zebrafish. *Nat. Genet.* 26, 216–220.
- Robu, M.E., Larson, J.D., Nasevicius, A., Beiraghi, S., Brenner, C., Farber, S.A., and Ekker, S.C. (2007). p53 activation by knockdown technologies. *PLoS Genet.* 3, e78.
- Rupp, R.A., Snider, L., and Weintraub, H. (1994). Xenopus embryos regulate the nuclear localization of XMyoD. *Genes Dev.* 8, 1311–1323.
- Petko, J.A., Kabbani, N., Frey, C., Woll, M., Hickey, K., Craig, M., Canfield, V.A., and Levenson, R. (2009). Proteomic and functional analysis of NCS-1 binding proteins reveals novel

- signaling pathways required for inner ear development in zebrafish. *BMC Neurosci.* 10, 27.
25. Chocron, S., Verhoeven, M.C., Rentzsch, F., Hammerschmidt, M., and Bakkers, J. (2007). Zebrafish *Bmp4* regulates left-right asymmetry at two distinct developmental time points. *Dev. Biol.* 305, 577–588.
 26. Whitfield, T.T., Riley, B.B., Chiang, M.-Y., and Phillips, B. (2002). Development of the zebrafish inner ear. *Dev. Dyn.* 223, 427–458.
 27. Hammond, K.L., Loynes, H.E., Mowbray, C., Runke, G., Hammerschmidt, M., Mullins, M.C., Hildreth, V., Chaudhry, B., and Whitfield, T.T. (2009). A late role for *bmp2b* in the morphogenesis of semicircular canal ducts in the zebrafish inner ear. *PLoS ONE* 4, e4368.
 28. Omata, Y., Nojima, Y., Nakayama, S., Okamoto, H., Nakamura, H., and Funahashi, J. (2007). Role of Bone morphogenetic protein 4 in zebrafish semicircular canal development. *Dev. Growth Differ.* 49, 711–719.
 29. Kitagawa, H., Uyama, T., and Sugahara, K. (2001). Molecular cloning and expression of a human chondroitin synthase. *J. Biol. Chem.* 276, 38721–38726.
 30. Sugahara, K., Mikami, T., Uyama, T., Mizuguchi, S., Nomura, K., and Kitagawa, H. (2003). Recent advances in the structural biology of chondroitin sulfate and dermatan sulfate. *Curr. Opin. Struct. Biol.* 13, 612–620.
 31. Bok, J., Brunet, L.J., Howard, O., Burton, Q., and Wu, D.K. (2007). Role of hindbrain in inner ear morphogenesis: Analysis of *Noggin* knockout mice. *Dev. Biol.* 311, 69–78.
 32. Nie, X., Luukko, K., and Kettunen, P. (2006). BMP signalling in craniofacial development. *Int. J. Dev. Biol.* 50, 511–521.
 33. Chang, W., Lin, Z., Kulesa, H., Hebert, J., Hogan, B.L., and Wu, D.K. (2008). *Bmp4* is essential for the formation of the vestibular apparatus that detects angular head movements. *PLoS Genet.* 4, e1000050.
 34. Busch-Nentwich, E., Söllner, C., Roehl, H., and Nicolson, T. (2004). The deafness gene *dfna5* is crucial for *ugdh* expression and HA production in the developing ear in zebrafish. *Development* 131, 943–951.
 35. Domowicz, M.S., Cortes, M., Henry, J.G., and Schwartz, N.B. (2009). Aggrecan modulation of growth plate morphogenesis. *Dev. Biol.* 329, 242–257.
 36. Rauch, G.-J., Hammerschmidt, M., Blader, P., Schauerte, H.E., Strähle, U., Ingham, P.W., McMahon, A.P., and Haffter, P. (1997). *Wnt5* is required for tail formation in the zebrafish embryo. *Cold Spring Harb. Symp. Quant. Biol.* 62, 227–234.
 37. Tian, J., Ling, L., Shboul, M., Lee, H., O'Connor, B., Merriman, B., Nelson, F., Cool, S., Ababneh, O.H., Al-Hadidy, A., et al. (2010). Loss of *CHSY1*, a secreted *FRINGE* enzyme, causes syndromic brachydactyly and increased *NOTCH* signaling in humans. *Am. J. Hum. Genet.* 87, ■■■–■■■.
 38. Yin, L. (2005). Chondroitin synthase 1 is a key molecule in myeloma cell-osteoclast interactions. *J. Biol. Chem.* 280, 15666–15672.
 39. Guo, X., and Wang, X.F. (2009). Signaling cross-talk between TGF-beta/BMP and other pathways. *Cell Res.* 19, 71–88.
 40. Piotrowski, T., and Nüsslein-Volhard, C. (2000). The endoderm plays an important role in patterning the segmented pharyngeal region in zebrafish (*Danio rerio*). *Dev. Biol.* 225, 339–356.
 41. Stemple, D.L., Solnica-Krezel, L., Zwartkuis, F., Neuhaus, S.C., Schier, A.F., Malicki, J., Stainier, D.Y., Abdelilah, S., Rangini, Z., Mountcastle-Shah, E., and Driever, W. (1996). Mutations affecting development of the notochord in zebrafish. *Development* 123, 117–128.

6. Publications derived from additional projects during this Ph.d

6.1 Elçioglu NH, Pawlik B, Colak B, Beck M, Wollnik B. A novel loss-of-function mutation in the GNS gene causes Sanfilippo syndrome type D. Genet Couns (2009); 20(2):133-9.

Abstract of the publication:

Mucopolysaccharidosis type IIID (MPS3D) is the least common form of the four subtypes of Sanfilippo Syndrome which is a rare autosomal recessive lysosomal disorder mainly characterized by progressive neurodegeneration and caused by a deficiency of the N-acetylglucosamine-6- sulphatase (GlcNAc-6S sulphatase, GNS), a hydrolase, which is one of the enzymes involved in heparan sulphate catabolism leading to lysosomal storage. So far only twenty patients have been described in the literature and only seven causative mutations in the *GNS* gene encoding GlcNAc-6S sulphatase have been reported to date.

In this study we report on 10 year old boy of Turkish origin with mental retardation of unknown aetiology. Phenotypically he had relative macrocephaly with a long, coarse facies, thick lips and eyebrows mild synophrys, low nasal bridge, high palate and an open mouth with salivary overproduction. Diagnostic analyses from serum, leucocyte and cultured fibroblast regarding the different Mucopolysaccharide groups were performed and displayed that the GlcNAc-6S sulphatase activity in cultured skin fibroblast cells was nearly zero. Therefore the diagnosis of MPS3D was established.

In order to confirm diagnosis we sequenced all 14 exon/introns boundaries of the *GNS* gene and identified the novel homozygous single base pair insertion, c.1226insG, which leads to a frame-shift and a premature truncation of the GNS protein (p.R409Rfs21X). In addition, we analyzed 100 controls individuals for the mutation by PCR /restriction digestion and the mutation was not detected. In conclusion we provide further evidence that loss-of-function of the *GNS* gene is the underlying pathophysiological mechanism of the rare Sanfilippo phenotype.

Own contributions:

In order to sequence the GNS gene, I first designed and ordered primers for PCR amplification for all 14 coding exons. Then I established PCR conditions and sequenced all exon and introns boundaries of the GNS gene.

I identified a novel homozygous base pair insertion, c.1226insG in exon 11, which leads to a frame-shift and a premature truncation of the GNS protein (Figure 2a, p.137). This mutation was re-sequenced in the patient and also in both parents.

In addition, I established an enzyme restriction method with Hpy 1881 to detect the mutation and performed restriction with 100 healthy control individuals (Figure 2b, p.137).

Finally, I completed the study by preparing the mutation and enzyme restriction pictures (Figure 2, p.137) for the submission to Genetic Counselling.

A NOVEL LOSS-OF-FUNCTION MUTATION IN THE GNS GENE CAUSES SANFILIPPO SYNDROME TYPE D

BY N.H. ELÇIOĞLU¹, B. PAWLIK², B. ÇOLAK¹, M. BECK³ AND B. WOLLNIK²

Summary: *A novel loss-of-function mutation in the GNS gene causes Sanfilippo syndrome type D: Mucopolysaccharidosis type IIID (MIM 252940) is the least common form of the four subtypes of Sanfilippo syndrome. It is an autosomal recessive lysosomal disorder caused by a deficiency of the N-acetylglucosamine-6-sulphatase (GlcNAc-6S sulphatase, GNS), a hydrolase, which is one of the enzymes involved in heparan sulfate catabolism leading to lysosomal storage. The clinical features of this disorder are progressive neurodegeneration with relatively mild somatic symptoms. Twenty patients have been described in the literature and only seven causative mutations in the GNS gene encoding GlcNAc-6S sulphatase have been reported to date. We present the clinical and molecular results of a newly diagnosed Turkish patient with MPS IIID. We identified the novel homozygous single base pair insertion, c.1226GinsG, which leads to a frame-shift and a premature truncation of the GNS protein (p.R409Rfs21X). Conclusion: This novel mutation provides further evidence that loss-of-function is the underlying pathophysiological mechanism of this rare phenotype.*

Key-words: MPS type 3D – Sanfilippo-D – N-acetylglucosamine-6-sulfatase – GNS gene

INTRODUCTION

The mucopolysaccharidoses (MPS) are a family of lysosomal storage diseases caused by deficiencies of several enzymes required for the catabolism of glycosaminoglycans (GAG). The defects result in accumulation of excessive intralysosomal GAG in various tissues, causing distended lysosomes to accumulate in the cell and interfere with cell function. Multiple types with subgroups caused by different enzyme defect have been characterized (10).

The four deficient enzymes in Sanfilippo disease (MPS-3), which inhibit the catabolism of heparan sulphate and resulting an indistinguishable clinical picture, are heparan N-sulphatase (type-A), alpha-N-acetylglucosaminidase (type-B), acetyl-CoA-glucosaminide acetyltransferase (type-C) and N-acetylglucosamine-6-sulphatase (type-D). Type A is the most common form and type D is the less common one. All four enzymes are involved with the stepwise degradation of heparan sulphate. Heparan sulphate (HS) is primarily found in the central nervous system whereas the storage of HS is also abundant in connective tissue and liver. There is little clinical difference among the four types of Sanfilippo syndrome, since all four types accumulate the same GAG, heparan sulphate. In contrast to the other mucopolysaccharidoses, typical physical features are not apparent and Sanfilippo patients

(1) Department of Pediatric Genetics, Marmara University Hospital, Istanbul, Turkey.

(2) Institute of Human Genetics & Center for Molecular Medicine (CMMC), University of Cologne, Cologne, Germany.

(3) Center of Lysosomal Storage Disorders, University Children Hospital, Mainz, Germany.

reach almost normal body height. The only clinical sign seen early might be thick and coarse hair and synophrys of the eye brows. The first symptoms may be observed earlier or later during the development, regardless of the type of enzyme deficiency. Although pathological findings may be absent until the children reach early school age, some affected children with an age of 2 to 4 years may already attract attention by restless behavior, sleeping problems, speech disorders and slowing of learning abilities. Later, body temperature irregularity, seizures and spasticity may develop. Major issues in the care of patients with MPS-IIID include behavioral problems, sleep problems, recurrent infections, dysphagia, and pain from orthopedic complications. To date there is no enzyme treatment for MPS-III and life expectancy is variable, but less than one decade (1, 3-5, 9, 10).

We present here the clinical, biochemical findings of a newly identified MPS IIID patient with a novel homozygous mutation. This will be the twenty-first patient and the eighth mutation reported for this lysosomal disorder so far.

CASE REPORT

Patient MSC is a 10 years old boy with mental retardation of unknown origin and has been referred for genetic counseling and diagnostic assistance. He was the second child from unrelated parents originating from a small region of Turkey. He was born after uncomplicated pregnancy and delivery at term with a birth weight 3050 gr. He had an operation to correct an inguinal hernia at 2 years of age. Early motor development was normal. He was able to sit up without support at 6 months, walk independently at 12 months and started to talk at 12 months with nearly normal speech development. Toilet training was successful in time. He was able to read and write adequately about the age of six years and followed the mainstream school program, although with some learning difficulties and short attention span. By the age of 7 years, his fine motor and language skills slowly began to deteriorate, 'clumsiness' was reported and he tended to walk on tiptoe. A progressive dementing encephalopathy followed and, as mental decline, motor deterioration and deafness developed, he required specialist care. Currently, he has moderate mental retardation, sleep disturbances, temper tantrums and hyperactivity with attention deficit disorder, which was treated with Risperidol.

Physical examination at the age of 10 yrs revealed weight 37 kg (25-50th percentile), length 137 cm (25-50th percentile), head circumference 51.5 cm (50th percentile).

Phenotypically he had relative macrocephaly with a long, coarse facies, thick lips and eyebrows mild synophrys, low nasal bridge, high palate, open mouth with salivary overproduction (Fig.1a). Hypertrichosis was present on the back. Lordosis was absent from the lumbar region, and the patient exhibited increased tendon reflexes with flexion contractures of the ankle and hammershaped toes with mild equinovarus deformity on feet. Visceral examination was normal without organomegaly or any heart murmur. No corneal opacities were present. He was hyperactive with short attention span and difficult to control. He understood simple verbal instructions but his speech was not clearly understandable and his fine motor activity was severely impaired.

Skeletal survey revealed mild dysostosis multiplex. There was a thickened diploe, ground glass opacity, sclerosis on basis cranii, wide ribs, ovoid vertebrae on the thoracal region, irregular end plates on the lumbar vertebrae region with enlargement and mild irregular shapes on the spinal processes (Figs.1b-c). Cranial MRI was normal. Hearing test confirmed sensorineural deafness with the right ear more severely affected than the left ear. Biochemical and metabolic screening, tandem MS, serum ammonia and lactate level, were normal except a strong positive urine MPS screening test.

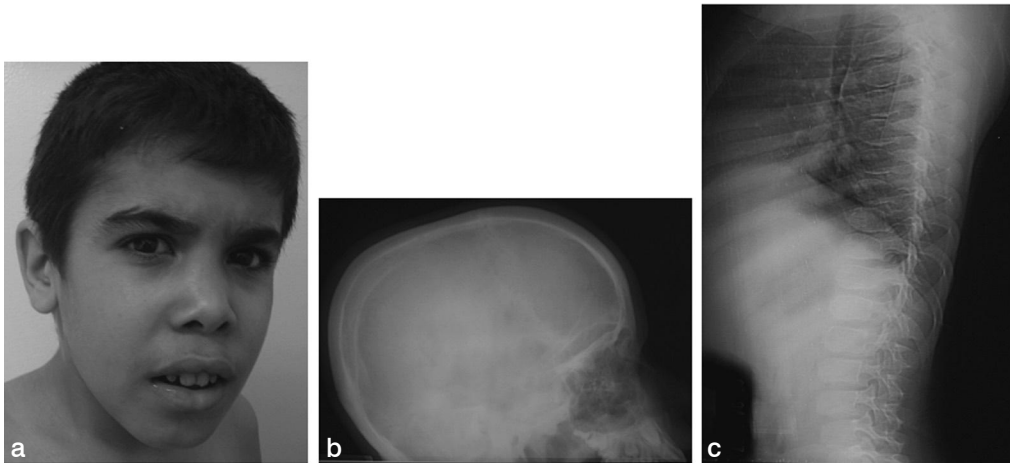


Figure 1: Phenotype of the patient. (a) Face: coarse facial structures and hirsutism; (b) Craniography: thick calvaria, ground glass opacity; (c) Thoracolumbar graphy: wide ribs and ovoid vertebral bodies.

Enzymatic results on urine analyses revealed negative oligosaccharides and free neuraminic acid by thin layer chromatography, but positive Berry test, elevated GAG (glycosaminoglycans) excretion as 21.41mg/mmol Cre ($N < 5.6$). GAG electrophoresis showed elevated heparan sulphate and chondroitin sulphate what indicated MPS-3 group. Enzymatic analyses from serum, leucocyte and cultured fibroblast regarding

the different MPS group were performed. The GlcNAc-6S sulphatase activity in cultured skin fibroblast cells was nearly zero confirming the diagnosis MPS 3D, in contrast to different enzymes related to other types of MPS which were normal (Table I).

The family received genetic counseling and after informed consent molecular studies were performed. Primers to amplify the promoter and all 14 exons and intron/exon boundaries of the *GNS* gene (MIM 607664) in the index case were designed (primer sequences are available upon request). After PCR amplification of all exons, sequencing was performed from both strands. In the patient, the homozygous single base pair insertion c.1226GinsG in exon 11 (Fig. 2) was identified. This mutation was resequenced in the patient and also in both parents and found the parents heterozygous for the c.1226GinsG mutation. In addition, 100 controls were analyzed for the mutation by PCR/restriction digestion and the mutation was not detected. The c.1226GinsG mutation is predicted to cause a frame-shift and a premature truncation of the protein (p.R409Rfs21X). Therefore, the mutant protein lacks the C-terminal part and is likely to cause loss of protein function.

Table I: Results of Lysosomal enzymes related to mps group

Sample	ENZYME	Results		Normal ranges	Related Disorder
Serum	Iduronate-Sulfatase	572.9	nM/ml/4h	300- 800	MPS- 2
Serum	B-Glucuronidase	0.8968	mU/ml	0.281-1.99	MPS- 7
Serum	N-Ac- α -Glucosamine	1.911	mU/ml	0.320-2.64	MPS- 3B
Leucocyte	Sulfamidase	2.299	nmol/mg/17h	3-9	MPS- 3A
Leucocyte	N-Ac-Transferase	12.89	nmol/mg/17h	8-32	MPS- 3C
Fibroblast	GlcNAc-6S sulphatase	0.2	nmol/mg/17h	31-135	MPS- 3D
Fibroblast	α -Iduronidase	4.89	mU/mg	1.36-4.40	MPS- 1

DISCUSSION

Sanfilippo syndrome type D is an autosomal recessive lysosomal storage disease that is caused by a deficiency of the activity of N-acetylglucosamine-6-sulphatase (GNS), which is required for degradation of heparan sulphate. The clinical features include an initial period of hyperactivity and aggressive behavior, followed by progressive neurodegeneration, with relatively mild somatic symptoms and skeletal involvement. Biochemical features of type D include accumulation

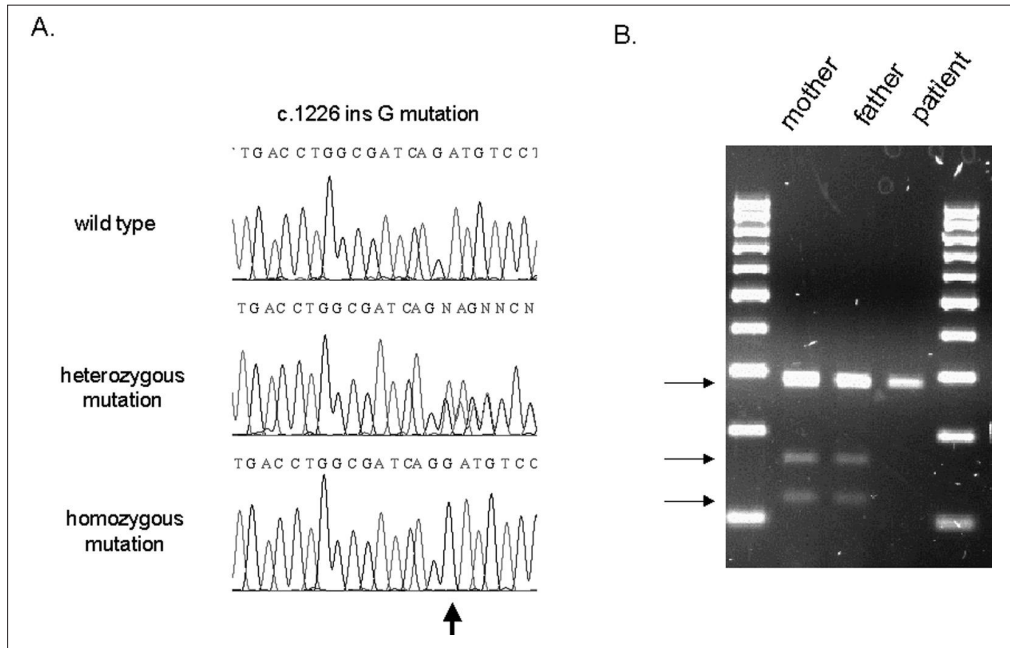


Figure 2: Mutations identified in the *GNS* gene. (A) Sequence chromatograms showing the mutations identified in the homozygous state in the patient and heterozygous state in the parents, compared to wild-type sequence. (B) Results of the enzyme restriction method established for mutation detection. As seen, the mutation abolishes a *Hpy1881* site leading to an uncut amplicon in the patient, while both parents show the pattern for a heterozygous carrier (bands indicated by arrows).

of HS and N-acetylglucosamine-6-sulphate in the brain and viscera. Diagnosis of this rare condition requires a specific enzyme assay for lysosomal *GNS* activity in cultured fibroblasts. MPS IIID is the least common of the four subtypes of Sanfilippo syndrome with only 20 patients have been described in the literature (1-7, 9, 11, 12).

The causative *GNS* gene (MIM 607664) is located on chromosome 12q14 extending 46kb and including 14 exons, which encode a protein of 552 amino acids. To date, only seven mutations have been described in seven Sanfilippo-D families: c.1169delA, R355X, Q277X, c.1168C>T, c.1138_1139insGTCCT, c.876-2A>G, and large intragenic deletion of exon 2 and exon 3. All individual mutations are predicted to cause a premature truncation of the protein (1, 2, 5, 9).

The present case is the first reported Turkish patient and has been found to be homozygous for a single base pair insertion, c.1226GinsG leading to a frame-shift and also premature truncation of the protein (p.R409Rfs21X). This novel mutation is the eighth mutation described in the *GNS* gene and the present finding provides further evidence that loss-of-function is the underlying molecular mechanism.

Sanfilippo syndrome type D is known as the rarest form of Sanfilippo syndrome with a population frequency of 1 in 1.000.000 (8). Interestingly, 60% of the patients have been of Italian origin suggesting a common founder mutation; however, since 8 different mutations were found in 8 different families including the present one, this does not appear to be true.

Although few families have been analyzed at the molecular level to date, MPS-IIID syndrome seems as heterogeneous at the genetic level as other Sanfilippo subtypes without any predictable genotype-phenotype correlation. Thus in clinically and genetically heterogeneous storage disorders like the MPS groups, it is important to confirm the diagnosis through both enzyme analysis and molecular studies in order to allow appropriate genetic counseling, family planning and prenatal diagnosis.

REFERENCES

1. BEESLEY C.E., BURKE D., JACKSON M., VELLODI A., WINCHESTER B.G., YOUNG E.P.: Sanfilippo syndrome type D: identification of the first mutation in the N-acetylglucosamine-6-sulfatase gene. *J. Med. Genet.*, 2003, 40, 192-194.
2. BEESLEY C.E., CONCOLINO D., FILOCAMO M., WINCHESTER B.G., STRISCIUGLIO P.: Identification and characterisation of an 8.7 kb deletion and a novel nonsense mutation in two Italian families with Sanfilippo syndrome type D (mucopolysaccharidosis IIID). *Mol. Genet. Metab.*, 2007, 90, 77-80.
3. COPPA G.V., GIORGI P.L., FELICIL, GABRIELLI O., DONTI E., BERNASCONI S., KRESSE H., PASCHKE E., MASTROPAOLO C.: Clinical heterogeneity in Sanfilippo disease (mucopolysaccharidosis III) type D: presentation of two new cases. *Eur. J. Pediatr.*, 1983, 140, 130-133.
4. GATTI R., BORRONE C., DURAND P., DE VIRGILIS S., SANNA G., CAO A., VON FIGURA K., KRESSE H., PASCHKE E.: Sanfilippo type D disease: clinical findings in two patients with a new variant of mucopolysaccharidosis III. *Eur. J. Pediatr.*, 1982, 138, 168-171.
5. JANSEN A.C., CAO H., KAPLAN P., SILVER K., LEONARD G., DE MEIRLEIR L., LISSENS W., LIEBAERS I., VEILLEUX M., ANDERMANN F., HEGELE R.A., ANDERMANN E.: Sanfilippo syndrome type D. natural history and identification of 3 novel mutations in the GNS Gene. *Arch. Neurol.*, 2007, 64, 1629-1634.
6. KAPLAN P., WOLFE L.S.: Sanfilippo syndrome type D. *J. Pediatr.*, 1987, 110, 267-271.
7. KRESSE H., PASCHKE E., VON FIGURA K., GILBERG W., FUCHS W.: Sanfilippo disease type D: deficiency of N-acetylglucosamine-6-sulfate sulfatase required for heparan sulfate degradation. *Proc. Natl. Acad. Sci.*, 1980, 77, 6822-6826.
8. MEIKLE P.J., HOPWOOD J.J., CLAGUE A.E., CAREY W.F.: Prevalence of lysosomal storage disorders. *JAMA*, 1999, 281, 249-254.
9. MOK A., CAO H., HEGELE R.A.: Genomic basis of mucopolysaccharidosis type IIID (MIM 252940) revealed by sequencing of GNS encoding N-acetylglucosamine-6-sulfatase. *Genomics*, 2003, 81, 1-5.
10. *Online Mendelian Inheritance in Man*, OMIM (252900, 252920, 252930, 252940, 607664). McKusick-Nathans Institute for Genetic Medicine, John Hopkins University (Baltimore, MD) and National Center for Biotechnology Information, National Library of Medicine (Bethesda, MD), 18.11.2008. World Wide Web URL: www.ncbi.nlm.nih.gov/omim/

11. OZAND P.T., THOMPSON J.N., GASCON G.G., SARVEPALLI S.B., RAHBEENI Z., NESTER M.J., BRISMAR J.: Sanfilippo type D presenting with acquired language disorder but without features of mucopolysaccharidosis. *J. Child. Neurol.*, 1994, 9, 408-411.
12. SICILIANOL., FIUMARAA., PAVONE L., FREEMAN C., ROBERTSON D., MORRIS C.P., HOPWOOD J.J., DI NATALE P, MUSUMECIS., HORWITZ A.L.: Sanfilippo syndrome type D in two adolescent sisters. *J. Med. Genet.*, 1991, 28, 402-405.

ADDRESS FOR CORESSPONDENCE:

Dr. Nursel H Elçioglu
Department of Pediatric Genetics
Marmara University Hospital
Tophanelioglu cad 15
Altunizade - Istanbul
34 660 Turkey
Fax: +90216 325 0323
E-mail: nelcioglu3@yahoo.com

6.2 Hilgert N, Alasti F, Dieltjens N, Pawlik B, Wollnik B, Uyguner O, Delmaghani S, Weil D, Petit C, Danis E, Yang T, Pandelia E, Petersen MB, Goossens D, Favero JD, Sanati MH, Smith RJ, Van Camp G. Mutation analysis of TMC1 identifies four new mutations and suggests an additional deafness gene at loci DFNA36 and DFNB7/11. Clin Genet. (2008); 74(3):223-32.

Abstract of the paper:

Hearing loss (HL) is the most common sensory disorder in humans and affects one in 1000 newborns. About 30% of hereditary hearing loss (HHL) is associated with co-inherited clinical abnormalities and therefore classified as syndromic HL. In the remaining 70% of cases, newborns have nonsyndromic HHL, which is characterized by hearing problems and mostly due to cochlear defects. Non-syndromic HHL is further classified by mode of inheritance. It is almost exclusively monogenic and inherited as an autosomal recessive trait (autosomal recessive non-syndromic hearing loss, ARNSHL) in about 70% of cases. HHL is a very heterogeneous trait and many gene localizations and causing genes have already been identified for non-syndromic hearing loss. One of these genes is Transmembrane channel-like gene 1 (*TMC1*) which has been identified as the disease-causing gene for autosomal dominant and autosomal recessive non-syndromic hearing loss at the DFNA36 and DFNB7/11 loci, respectively.

In this study, we investigated one family with dominant and 10 families with recessive non-syndromic sensorineural hearing loss (ARNSHL) plus additional 51 familial Turkish patients with autosomal recessive hearing loss. We amplified and sequenced all 24 intron/exon boundaries of the *TMC1* gene located on chromosome 9. In seven families with ARNSHL, we identified the two known *TMC1* c.100C>T and c.1165C>T mutations as well as the four novel c.2350C>T, c.77611G>A, c.767delT and c.1166G>A mutations. No proven disease causing mutation could be found in *TMC1* or in 15 other genes in the remaining families and isolated cases.

Own contributions:

First of all, I designed primers for the *TMC1* gene by using genome databases and established the test conditions for PCR amplification and sequencing. Then I screened 70 Turkish patients with autosomal recessive hearing loss (ARNSHL) for all 24 coding exons of *TMC1*.

I identified the novel homozygous deletion c.767delT in exon 13 in a patient as well as another novel c.1166G>A missense mutation in exon 15 in another deafness patient (Table 2, p. 4).

Furthermore, I evaluated the sequencing results by using database analysis and performed control studies of 100 control individuals either by an enzyme restriction method or by direct sequencing (data not shown).

Original Article

Mutation analysis of *TMC1* identifies four new mutations and suggests an additional deafness gene at loci DFNA36 and DFNB7/11

Hilgert N, Alasti F, Dieltjens N, Pawlik B, Wollnik B, Uyguner O, Delmaghani S, Weil D, Petit C, Danis E, Yang T, Pandelia E, Petersen MB, Goossens D, Favero JD, Sanati MH, Smith RJH, Van Camp G. Mutation analysis of *TMC1* identifies four new mutations and suggests an additional deafness gene at loci DFNA36 and DFNB7/11. Clin Genet 2008. © Blackwell Munksgaard, 2008

Hearing loss is the most frequent sensorineural disorder affecting 1 in 1000 newborns. In more than half of these babies, the hearing loss is inherited. Hereditary hearing loss is a very heterogeneous trait with about 100 gene localizations and 44 gene identifications for non-syndromic hearing loss. Transmembrane channel-like gene 1 (*TMC1*) has been identified as the disease-causing gene for autosomal dominant and autosomal recessive non-syndromic hearing loss at the DFNA36 and DFNB7/11 loci, respectively. To date, 2 dominant and 18 recessive *TMC1* mutations have been reported as the cause of hearing loss in 34 families. In this report, we describe linkage to DFNA36 and DFNB7/11 in 1 family with dominant and 10 families with recessive non-syndromic sensorineural hearing loss. In addition, mutation analysis of *TMC1* was performed in 51 familial Turkish patients with autosomal recessive hearing loss. *TMC1* mutations were identified in seven of the families segregating recessive hearing loss. The pathogenic variants we found included two known mutations, c.100C>T and c.1165C>T, and four new mutations, c.2350C>T, c.776+1G>A, c.767delT and c.1166G>A. The absence of *TMC1* mutations in the remaining six linked families implies the presence of mutations outside the coding region of this gene or alternatively at least one additional deafness-causing gene in this region. The analysis of copy number variations in *TMC1* as well as DNA sequencing of 15 additional candidate genes did not reveal any proven pathogenic changes, leaving both hypotheses open.

**N Hilgert^a, F Alasti^{a,b},
N Dieltjens^a, B Pawlik^{c,d},
B Wollnik^{c,d}, O Uyguner^e,
S Delmaghani^f, D Weil^f, C Petit^f,
E Danis^a, T Yang^g, E Pandelia^h,
MB Petersen^h, D Goossensⁱ,
JD Faveroⁱ, MH Sanati^j,
RJH Smith^g and G Van Camp^a**

^aDepartment of Medical Genetics, University of Antwerp, Antwerp, Belgium, ^bDepartment of Molecular Genetics, National Institute for Genetic Engineering and Biotechnology, Tehran, Iran, ^cCenter for Molecular Medicine Cologne, ^dInstitute of Human Genetics, University of Cologne, Cologne, Germany, ^eMedical Genetics Department, Istanbul Medical Faculty, Istanbul University, Istanbul, Turkey, ^fUnité de Génétique et Physiologie Auditive, INSERM U587, Institut Pasteur, Paris, France, ^gDepartment of Otolaryngology – Head and Neck Surgery, University of Iowa, Iowa city, IA, USA, ^hDepartment of Genetics, Institute of Child Health, 'Aghia Sophia' Children's Hospital, Athens, Greece, ⁱApplied Molecular Genomics Group, Department of Molecular Genetics, Flemish Institute for Biotechnology, University of Antwerp, Antwerp, Belgium, and ^jDepartment of Medical Genetics, National Institute for Genetic Engineering and Biotechnology, Tehran, Iran

Key words: DFNA36 – DFNB7/11 – sensorineural hearing loss – *TMC1*

Corresponding author: Professor Dr Guy Van Camp, Department of Medical Genetics, University of Antwerp, Universiteitsplein 1, B-2610 Antwerp, Belgium.

Tel.: +32-3-820-24-91;
fax: +32-3-820-25-66;
e-mail: guy.vancamp@ua.ac.be

Received 21 March 2008, revised and accepted for publication 9 May 2008

Hearing loss is the most common sensory disorder affecting 1 in 1000 newborns. In more than half of these babies, the cause is hereditary (hereditary hearing loss, HHL) (1). About 30% of HHL is associated with co-inherited clinical abnormalities and therefore classified as syndromic HL. In the remaining 70% of cases, newborns have non-syndromic HHL, which is solely characterized by hearing problems and mostly due to cochlear defects. Non-syndromic HHL is further classified by mode of inheritance. It is almost exclusively monogenic and inherited as an autosomal recessive trait (autosomal recessive non-syndromic hearing loss, ARNSHL) in about 70% of cases. Post-lingual hearing loss, in contrast, is often multifactorial, the most prevalent example being age-related hearing loss or presbycusis, which affects about half of octogenarians. Families segregating monogenic post-lingual autosomal dominant non-syndromic hearing loss (ADNSHL) are well described but rare compared with presbycusis.

The genetic heterogeneity of HHL is reflected by the mapping of 43 dominant, 52 recessive and 4 X-linked non-syndromic loci and the identification of 44 genes (Hereditary hearing Loss Homepage, <http://webh01.ua.ac.be/hhh/>). One example is transmembrane channel-like gene 1 (*TMC1*) (GenBank ID NT_023935 position 4301249–4615799), mutations of which are a cause of both ADNSHL and ARNSHL at the DFNA36 and DFNB7/11 loci, respectively. The gene has been implicated as the cause of deafness in 34 families: 2 dominant families from North America and 32 recessive families from Pakistan, India, Turkey, Sudan and Tunisia (2–8) (Table 1). In the mouse ortholog *Tmc1*, mutations have been identified in both the recessive mutant *deafness* (*dn*) and the dominant mutant *Beethoven* (*Bth*) (2, 9).

The genomic structure of *TMC1* consists of 24 exons that encode a full-length mRNA of 3201 bp. Its sequence is highly similar to *TMC2* and to the corresponding mouse orthologs *Tmc1* and *Tmc2*. These genes, together with six other orthologs, belong to the new *TMC* gene family, which has been created as none of the genes shows nucleotide sequence similarity to other known genes or domains. Two members of the gene family, *TMC6* and *TMC8*, are identical to the long isoforms of *EVER1* and *EVER2*, respectively. Mutations in both genes have been found to be associated with epidermodysplasia verruciformis (MIM 226400). The exact function of the transmembrane proteins encoded by this gene family remains to be determined. Based upon their structure, they may act as ion channels, ion pumps or transporters (10, 11). Studies of the recessive mutant *dn* and the dominant mutant *Bth* have

given some clues about the possible function of *Tmc1* (12). In mice, the protein is expressed before the onset of hearing in the pericuticular necklace and the endoplasmic reticulum of mature hair cells as well as during early postnatal development. Therefore, *Tmc1* might play a role in normal maturation of the hair cells. It has been suggested that the protein may be responsible for the upregulation or downregulation of ion channels or molecules of the exocytotic machinery during development. Alternatively, it could be involved in intracellular trafficking. The expression pattern of *TMC1* is very specific: apart from its expression in inner and outer hair cells of the cochlea and in neurosensory epithelia of the vestibular end organs, very low levels of transcript are also found in human placenta and testis but in no other tissues (2).

In this study, we report mutation analysis in 1 DFNA36 family, 10 DFNB7/11 families and 51 Turkish index patients of families with ARNSHL (Table 2). In seven families with ARNSHL, we identified two known and four novel mutations in *TMC1*. In the remaining five DFNB7/11 families and in the DFNA36 family, no proven disease-causing mutation could be found in *TMC1* or in 15 other genes in the overlap of all candidate regions defined by the significantly linked families.

Materials and methods

Family data

In this study, different approaches were used to collect families and perform mutation analysis. Eleven families of different origin segregating ADNSHL or ARNSHL were collected and analysed (Table 2) (Fig. S1, supplementary material online). Family 101 has been reported before (13). In addition, genetic analysis was performed in 51 Turkish index patients from families with ARNSHL containing 2 or more affected patients. All these patients were seen personally and completed a questionnaire to exclude syndromic hearing loss. All participants signed an informed consent form. For family PE, audiometry was performed by measuring air conduction thresholds at frequencies ranging from 125 to 8000 Hz. In family GRE, auditory evoked potentials were measured in two affected individuals.

Linkage analysis

DNA was isolated from blood samples of participating subjects using a standard salting-out protocol. In a first part of the study, the information

Table 1. Overview of all *TMC1* mutations identified to date

Family name	Origin	Sequence variant		Exon	Type of sequence variant	Inheritance pattern	Reference
		cDNA level	Protein level				
LMG128	North America	c.1714 G>A	p.D572N	19	Missense mutation	ad	(2)
LMG248	North America	c.1714 G>C	p.D572H	19	Missense mutation	ad	(7)
PKSR9, PKSN9, PKSN24, PKDF7, PKDF75, PKDF69, PKDF178, PKDF243, PKDF319, PKDF401, and three Tunisian cases	Pakistan and Tunisia	c.100 C>T	p.R34X	7	Nonsense mutation	ar	(2, 5, 6)
PKDF22	Pakistan	c.IVS3_IVS5del27kb		5	Deletion	ar	(2)
IN-DKB6	India	c.295_296delA		8	Deletion	ar	(2)
PKSR25 and 4090	Pakistan	c.IVS10-8T>A		Intron 10: -8	Splice site mutation	ar	(2, 4)
PKSR1a	Pakistan	c.IVS13+1G>A		Intron 13: +1	Splice site mutation	ar	(2)
TR56	Turkey	c.776 A>G	p.Y259C	13	Missense mutation	ar	(8)
TR47	Turkey	c.821 C>T	p.P274L	13	Missense mutation	ar	(8)
TR50	Turkey	c.1083_1087delCAGAT	p.R362PfsX6	15	Deletion	ar	(8)
TR63	Turkey	c.1334 G>A	p.R445H	16	Missense mutation	ar	(8)
PKSR20a	Pakistan	c.1534 C>T	p.R512X	17	Nonsense mutation	ar	(2)
IN-M17	India	c.1960 A>G	p.M654V	20	Missense mutation	ar	(2)
4049	Pakistan	c.830 A>G	p.Y277C	13	Missense mutation	ar	(4)
DFNB7/11 Sudanese family and Tunisian family	Sudan and Tunisia	c.1165 C>T	p.R389X	15	Nonsense mutation	ar	(3, 6)
DFNB7/11 Sudanese family	Sudan	c.IVS19+5G>A		Intron 19: +5	Splice site mutation	ar	(3)
PKDF431	Pakistan	c.1541C>T	p.P514L	17	Missense mutation	ar	(5)
PKDF329 and PKDF511	Pakistan	c.1543T>C	p.C515R	17	Missense mutation	ar	(5)
PKDF274	Pakistan	c.IVS5+1G>T		Intron 5: +1	Splice site mutation	ar	(5)
Tunisian family	Tunisia	c.1764G>A	p.W588X	19	Nonsense mutation	ar	(6)

ad, autosomal dominant; ar, autosomal recessive.

Table 2. Overview of the families linked to DFNA36 and DFNB7/11 and the Turkish index patients with *TMC1* mutations described in this report^a

Family	Origin	Inheritance pattern	SLINK score	Maximal LOD score	Sequence variant <i>TMC1</i>		Exon	Type of sequence variant
					Genomic/cDNA level	Protein level		
PE	Guatemala/Mexico	ad	4.78	4.44				
GRE	Greece	ar	4.41	3.96	c.2350C>T	p.R604X	20	Nonsense mutation
TM	India	ar	3.99	3.5				
101 ^b	India	ar	4.82	3.6				
G9	Iran	ar	2.91	2.91	g.94615A>C		3	Variant in non-coding exon
M28	Iran	ar	1.78	1.66				
M13	Iran	ar	2.9	2.55				
M36	Iran	ar	2.78	2.24	c.776+1G>A		7	Splice site mutation
935	Iran	ar	3.46	2.46	c.100C>T	p.R34X	7	Nonsense mutation
Nias	Lebanon/Jordan	ar	3.86	1.79	c.100C>T	p.R34X	7	Nonsense mutation
Fay	Lebanon/Jordan	ar	2.45	1.94	c.1165C>T	p.R389X	15	Nonsense mutation
DF139	Turkey	ar			c.767delT	p.F255FfsX14	13	Deletion
DF135	Turkey	ar			c.1166G>A	p.R389Q	15	Missense mutation

ad, autosomal dominant; ar, autosomal recessive.

^aFor all families, the SLINK score and maximal LOD scores obtained are listed. For families in which sequence variants in *TMC1* were identified by DNA sequencing, the variant, its position and the protein change are listed. All variants were homozygous in patients. For families 935, Nias, Fay, GRE, and M36 and index patients of families DF139 and DF135, the nucleotide changes found were judged to be pathogenic.

^bThe family has previously been reported (13).

content for linkage of 11 hearing loss families was estimated based on SLINK simulations using the program EASYLINKAGE (version 4.01) (14). Fixed linkage parameters were used for all LOD score calculations with an allele frequency of 0.001 and a phenocopy rate of 0%. For the dominant family, the penetrance was 0% for the wild-type/wild-type (wt/wt) genotype and 100% for the wild-type/mutant (wt/mt) and mutant/mutant (mt/mt) genotypes. For the recessive families, penetrance was 0% for wt/wt and wt/mt and 100% for mt/mt.

Different strategies were used for linkage analysis. If the SLINK score had a value of 3.3 or higher, the family was considered informative enough for genome-wide linkage analysis (15). For families in which the LOD score was below 3.3, linkage analysis was performed for known deafness loci and LOD score calculations were combined with haplotype analysis to confirm or exclude linkage. For families 935, Nias and Fay, DFNB1 was excluded by direct sequencing. Next, a genome-wide scan was performed for these families as well as for families PE, TM and 101. Linkage analysis on family 101 has been reported before (13). In families GRE, G9 and M28, nine of the more common recessive loci were checked for linkage (DFNB1, DFNB2, DFNB3, DFNB4, DFNB7/11, DFNB9, DFNB12, DFNB21 and DFNB23). In families M13 and M36, only DFNB1 and DFNB7/11 were screened to find additional *TMC1* families. Linkage analysis was performed by calculating two-point and multipoint LOD scores using the EASYLINKAGE program. All genotyping was performed by polymerase chain reaction (PCR) amplification of fluorescently labelled microsatellite markers and fragment analysis on an ABI 3130 automated DNA sequencer (Applied Biosystems, Foster City, CA) using standard procedures.

DNA sequence analysis

To screen candidate genes, non-coding and coding exons including the intron–exon boundaries were PCR amplified. Subsequent DNA sequencing of both strands was carried out on an ABI 3130 automated DNA sequencer (Applied Biosystems) using the Big-Dye Terminator Cycle Sequencing Kit, Version 3.1 (Applied Biosystems). DNA sequencing of *TMC1* was performed in 2 patients of 11 hearing loss families and in 51 Turkish index patients of ARNSHL families. In affected subjects from larger families in which no *TMC1* mutation was identified, additional candidate genes were sequenced. Most of these genes localize to the

minimal shared candidate region defined by the three significantly linked families negative for *TMC1* mutations and include *TJP2*, *MIRN204*, *TMEM2*, *LOC729027*, *C9ORF77*, *C9ORF85*, *LOC653553*, *C9ORF57*, *LOC392350*, *GDA*, *ZFAND5*, *ALDH1A1*, *ANXA1*, *LOC138971* and *LOC138972* (Fig. 2). In addition, DNA sequencing of *TRPM3* was performed in families TM and 101. In all Turkish index patients, the coding exon of *GJB2* was sequenced.

We used the ConSeq Server to check the conservation of amino acids affected by the identified *TMC1* mutations (16). A BLAST analysis of the human *TMC1* protein sequence showed 61 sequences with an e-value below 0.001 of which all hits with a sequence identity below 20% were excluded. With the remaining 27 sequences, a multiple sequence alignment was made, which was subsequently used as an input at the ConSeq Server. The same strategy was used for calculating the conservation scores for *TJP2*. ConSeq scores that are obtained using this procedure vary from 1 (variable) to 9 (conserved).

The I-MUTANT2.0 program was used to predict the effect of the *TJP2* variant on the protein stability (17). A $\Delta\Delta G$ value is calculated from the unfolding Gibbs free energy value of the mutated protein minus the unfolding Gibbs free energy value of the wild-type protein (kcal/mol). The calculation was performed at pH 7.0 and at temperatures of 25°C (*in vitro* conditions) and 37°C (*in vivo* conditions). $\Delta\Delta G$ values below zero indicate a reduced stability of the mutant protein. A

reliability index (RI) is computed if a negative $\Delta\Delta G$ value is present, indicating how reliable the prediction is.

Multiplex amplicon quantification

TMC1 was screened for copy number variations (CNVs) using the multiplex amplicon quantification (MAQ) technique (18, 19). This technique consists of a multiplex PCR amplification of several fluorescently labelled test and reference amplicons, followed by fragment analysis. Twelve test amplicons located in *TMC1* and eight reference amplicons located at randomly selected genomic positions outside known CNVs were simultaneously PCR amplified in samples from two affected subjects and one control from each of six families (PE, G9, M13, M28, TM and 101). The primer sequences of the test and reference amplicons are given in Table 3. Unlabelled and FAM-labelled primers were ordered from Eurogentec (Seraing, Belgium). The multiplex PCR reactions were performed on 40 ng genomic DNA in a 15 µl reaction containing 1× Titanium™ Taq PCR buffer (Clontech, Palo Alto, CA) with a final concentration of 2.5 mM for each dNTP (Invitrogen, Carlsbad, CA) and a total of 0.075 µl of Titanium™ Taq DNA Polymerase (Clontech). PCR cycle conditions were 2 min at 98°C, followed by 23 cycles of 45 s at 95°C, 45 s at 60°C and 2 min at 68°C. After a final extension step of 10 min at 72°C, samples were cooled to 8°C. Subsequently, fragment analysis was performed on an

Table 3. Primer sequences of the test and reference amplicons used for MAQ analysis of *TMC1*

Amplicon name	Forward primer sequence (3'-5')	Reversed primer sequence (3'-5')
<i>TMC1</i> -Amp01	CTTCAATCAAGTCCCAGTTTCCT	TCAAACACACAGTAGTGCCTTCTA
<i>TMC1</i> -Amp02	GATTCAGTTTCAATAAATGCTTCCT	CTGTATCAGCCCAGCTTCCT
<i>TMC1</i> -Amp03	TATCTCTTCTTGGATTTCCCTTTGCT	CTCATACCATTCTCACATTCATCC
<i>TMC1</i> -Amp04	GGGTAGTTTCCCTTTGTTTCCT	CAACAATAGGGTTTGATGTCTCCT
<i>TMC1</i> -Amp05	TTGAGGGTAACTTATGTGTCAACAAC	TAAACCCAGTGCTCAAAGTACACTAA
<i>TMC1</i> -Amp06	TGCCACATTCTCATTCTTCCT	CTGTCTTGAAAGCCTTCTGATCTA
<i>TMC1</i> -Amp07	TCACTGGCCCCACTCTTCC	CAGTCAGGTCAACCACATTCC
<i>TMC1</i> -Amp08	TAAATCAAAGGGCATTTCACG	CAAACCCGTAAAATCCAAGAAC
<i>TMC1</i> -Amp09	CGTCCACTTGATCAGATTCCT	GATCTTGCTGTGCAAATTCCT
<i>TMC1</i> -Amp10	TTGGTCAGTCTCCTCTGATTCTCTA	ATTCAATGTCCAGTCTCCATGTC
<i>TMC1</i> -Amp11	GCCAATAACTGTGTGTTCCACG	GAACCAAATCCTTTGCATCAAC
<i>TMC1</i> -Amp12	GTGAAAGGGTGAAAGTCAATTC	TTCAACCACCTCATCTTCTGC
<i>TMC1</i> -Contr01	TTCAATATGTATACCCAACCTTCG	TAACTTCAAGGCTACGCTTCTC
<i>TMC1</i> -Contr02	CAGTATCTAAGACCAGGGTGATTCT	AAAGATTTCTTCTCCAGGCTA
<i>TMC1</i> -Contr04	CTTTGTATCCGAGCTCCATTCT	TCATCCTGTCTGCTTTCACAAC
<i>TMC1</i> -Contr05	TGAAATTCTCCAAACACCTGTC	TTTCCAAAGCCAGATTATTCCTAA
<i>TMC1</i> -Contr06	CATACCCTTAATGGCTCTTCTTTCT	TTCTGGTTCTCAGCTCTGC
<i>TMC1</i> -Contr08	TCAGGGTAAACAAGGGCAAC	TGACTGCCACCATCTTTTCG
<i>TMC1</i> -Contr09	CAAGCTCCTCCTCTCCTTCC	TGCACACCCATGCATAATAAC
<i>TMC1</i> -Contr11	ACCGGATTCACACACTACCAC	AACCACAGCGAGGGATTCT

MAQ, multiplex amplicon quantification.

Applied Biosystems 3730 DNA analyzer with the GeneScan™ 500 LIZ™ Size Standard (Applied Biosystems). The experiment was performed in duplicate. Peak areas of the test amplicons were normalized to those of the reference amplicons. Chromatogram files were analysed with the MAQS software (<http://www.vibgeneticservicefacility.be/soft/maqs.php>). The dosage quotient (DQ) of every amplicon is calculated as described by Suls et al. (19). DQ values below 0.75 were considered indicative of a deletion and values above 1.25 indicative of a duplication.

Results

Clinical data

The Guatemalan family PE segregates ADNSHL characterized by hearing impairment that starts in the mid frequencies during the first decade of life and progresses to involve all frequencies. The rate of progression is faster in the higher frequencies, leading to a downward-sloping audiogram after several decades (Fig. 1). Five subjects in the Greek family GRE were diagnosed as affected. For the two youngest patients (3 and 7 years old), auditory evoked potentials were available, which showed no response at equipment limits, consistent with profound pre-lingual ARNSHL. Affected subjects in the other families as well as the Turkish index patients were reported to have congenital severe-to-profound sensorineural hearing impairment. By completing questionnaires, syndromic hearing loss could be excluded in all cases.

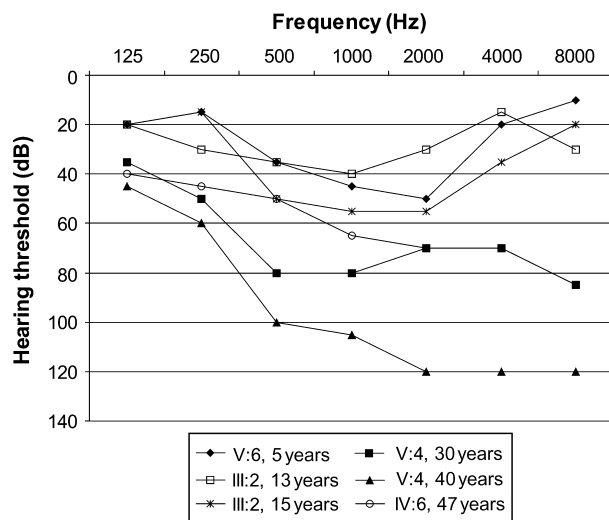


Fig. 1. Air conduction thresholds of the better ear of four patients of family PE at different ages. There is clear progression of the hearing loss for individuals III:2 and V:4. For all patients, mainly the mid and high frequencies are affected.

Linkage analysis

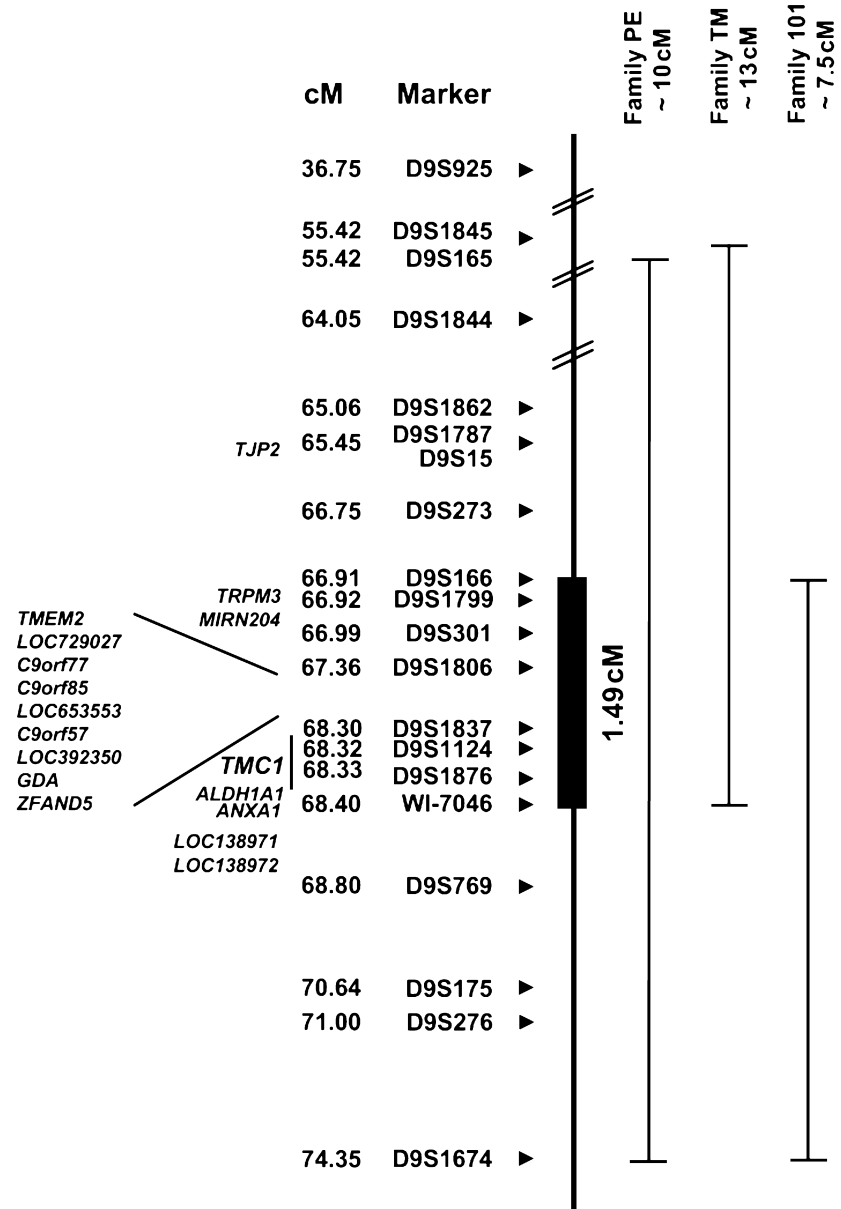
Genome-wide linkage analysis in family PE revealed linkage to DFNA36 with a maximal LOD score of 4.44. About 80% of the total genome was excluded with LOD scores below -2 . Apart from the region on chromosome 9q, no other linked regions were found. In the recessive family GRE, linkage to locus DFNB7/11 was identified by linkage analysis of known loci, showing a LOD score of 3.96. We tried to identify additional families that link to this genomic region in different ways. A series of Iranian families segregating ARNSHL had been collected before and although their SLINK scores were not above the genome-wide significance level, we chose to perform linkage analysis for a set of known loci. This screening revealed suggestive linkage at DFNB7/11 in four families, G9, M28, M13 and M36, all having LOD scores between 1.66 and 2.91. Three more families, 935, Nas and Fay, were identified with probable linkage having LOD scores between 1.79 and 2.46. All other genomic regions were excluded. For one additional family, TM, significant DFNB7/11 linkage was found with a LOD score of 3.5, while no linkage to other genomic regions was identified. Family 101 was previously reported to show significant linkage to DFNB7/11 and was also included in our analysis (13). For all families, candidate regions were defined by polymorphic marker analysis and linkage was checked by both haplotype reconstruction (Fig. S1, supplementary material online) and LOD score calculation (Table 2). The linked regions of the families included *TMCI*.

Candidate gene analysis

DNA sequencing of *TMCI*

Mutation screening of *TMCI* was completed by direct DNA sequencing in 2 patients of each family with suggestive and significant linkage and in 51 Turkish index patients with ARNSHL. All sequence variants segregating with the hearing loss phenotype are listed in Table 2. In families 935 and Nas, the known mutation c.100C>T was identified in homozygous condition in all affected subjects. This change predicts the nonsense mutation p.R34X. Similarly, in family Fay, affected subjects were homozygous for the known mutation c.1165C>T, which causes the nonsense mutation p.R389X. In the Greek family GRE, a new nonsense mutation was identified in exon 20, which segregates with the hearing loss. The identified nucleotide change c.2350C>T causes a nonsense mutation p.R604X, leading to

Fig. 2. Candidate regions of three families significantly linked to DFNA36 or DFNB7/11, without *TMC1* mutation identified. All analysed markers and their corresponding positions from the Decode genetic map are indicated. At the left, all candidate genes located in the common linked region are listed containing eight genes and six gene predictions. The common region is 1.49 cM large and includes the *TMC1* gene.



a premature termination codon (PTC). In the Iranian family M36, a new splice site mutation was identified in all affected subjects. The mutation c.776+1G>A is located at the splice donor site of exon 7 and changes the 5' splice site from GT to AT. This change was not identified in 100 Iranian control samples. In an index patient of family DF139, a 1-bp deletion c.767delT was identified in exon 13 of *TMC1*. The deletion changes the highly conserved leucine at position 255 (ConSeq score 9) and leads to a frameshift p.F255FfsX14. In a patient of family DF135, a new missense mutation c.1166G>A was identified, causing the amino acid change p.R389Q. The mutation was not found in 100 ethnically matched control samples, and the amino acid at position 389 has a Con-

Seq score of 8. In family G9, a nucleotide change g.94615A>C was identified in exon 3 (non coding) of *TMC1* and was found to segregate with the hearing loss. The variant was not found in 100 Iranian and 100 Belgian control samples.

MAQ of *TMC1*

In the six families in which no pathogenic *TMC1* changes were found, MAQ analysis was completed using 12 amplicons covering *TMC1*. Family G9 was also analysed as we could not prove that the variant we found was pathogenic. No differences in peak area were observed between normalized chromatograms of affected subjects and controls. This result indicates that no deletion or duplication is present at the regions of these amplicons.

DNA sequencing of other candidate genes

Other candidate genes were also selected for DNA sequencing under the hypothesis that mutations in another gene in this region also cause HHL. To narrow the interval, we assumed that the same gene was mutated in the three families that were significantly linked to the *TMC1* locus (PE, TM and 101), thereby defining a shared interval of 1.49 cM (2596 Mb) common to all families (Fig. 2). This region contains eight genes and six gene predictions, including *TMC1*. The coding exons and intron–exon boundaries of all 13 candidate genes in this region were sequenced in the three families with significant linkage as well as in the remaining three families with suggestive linkage, but no mutations could be identified. *LOC138971* and *LOC138972* were also sequenced because they were located in the shared region in an earlier phase of the project when fewer families had been collected, but no possible pathogenic change was found in these two genes. In addition to these genes chosen on the basis of location, *TJP2* (*ZO-2*) was considered a good candidate due to its interesting function as a tight junction protein and its expression in the cochlea. In exon 19 of the gene, a new sequence variant c.2971A>T was identified, segregating with the hearing loss phenotype in family PE and causing the amino acid change p.D924V. This aspartic acid residue has a ConSeq score of 7 and belongs to a conserved acidic domain of the protein. The Grantham score of the amino acid change was 152, while scores above 100 indicate radical amino acid changes (20). The I-MUTANT2.0 program predicted a decreased stability of the mutant protein ($\Delta\Delta G = -1.84$ at 25°C and -1.65 at 37°C with RI = 2). The change was not found in any of the non-affected family members or in 104 independent Belgian control samples and 103 ethnically matched controls. The gene was sequenced in two affected subjects from 26 additional small families segregating deafness, but no variants were identified (data not shown). The DNA sequencing of *GJB2* in all Turkish index patients revealed the presence of 35delG in heterozygous state in the index patient of family DF139.

Discussion

Twenty different mutations in *TMC1* have been reported as the cause of hearing loss in 2 families segregating ADNSHL and 32 families segregating ARNSHL. A literature search allowed making an estimate of the most frequent causes of ARNSHL based on the reported numbers of mutations. *GJB2* is without any doubt the most frequent cause of ARNSHL carrying over 220 different

mutations. The other more frequent genes, ranked according to their reported frequency, are *SLC26A4*, *MYO15A*, *OTOF*, *CDH23* and *TMC1*. The literature data together with the data from this report indicate that *TMC1* is one of the more frequent causes of ARNSHL. In this study, we have reported 1 additional dominant family linked to the DFNA36 locus and 10 additional recessive families linked to the DFNB7/11 locus. We were able to identify disease-causing *TMC1* mutations in 5 of these 11 families. In two families, putative mutations were identified, one in *TMC1* and one in *TJP2*, but for none of them, the pathogenicity could be confirmed. In addition, we found two new *TMC1* mutations in an index patient of two Turkish families segregating ARNSHL.

In families 935, Nas and Fay, known recessive mutations c.100C>T and c.1165C>T were identified in *TMC1*. Both are nonsense mutations leading to a PTC. As the mRNA contains a PTC, it may be detected and degraded by nonsense-mediated decay, a eukaryotic mRNA surveillance mechanism (21). Including this study, c.100C>T has been identified in 16 families segregating ARNSHL, accounting for 47% of all recessive *TMC1* mutations.

In four families with ARNSHL, we detected new pathogenic changes in *TMC1*. In family GRE, a nonsense mutation c.2350C>T was found to cause a PTC at nucleotide position 47 of exon 20. In the Iranian family M36, a novel splice site mutation c.776+1G>A was found to change the 5' splice donor site of exon 7 from GT to AT. The effect of this splice site mutation depends on the adjacent sequence. Use of a cryptic splice site will lead to partial exon skipping or partial intron retention. Alternatively, if no cryptic splice site is used, then, either exon skipping or a greatly reduced production of normal transcript will be the predominant outcome (22). Experimental study of this effect using patient mRNA is not possible as *TMC1* is not expressed in lymphocytes. In two Turkish families with ARNSHL, new *TMC1* mutations were identified in an index patient. The first mutation c.767delT is a 1-bp deletion causing a frameshift. As a result, 14 amino acids are altered and followed by a stop codon. The second mutation, c.1166G>A, causes the highly conserved amino acid arginine to change into glutamine at position 389 of the protein, causing a shift from a positively charged into a neutral residue. In addition, the variant was not found in 100 Turkish control samples. Therefore, we believe that this new variant may be pathogenic.

In family G9, a putative pathogenic change was found in the third non-coding exon of *TMC1* segregating with the hearing loss and absent in 200

control samples. The variant may be located in the promoter region or in a regulatory region of the gene, but none of these regions has been identified so far. Functional studies should be performed to further investigate the effect of the variant on the protein.

In family PE, a putative mutation in *TJP2* was found to segregate with the hearing loss. Different arguments support the hypothesis that the variation may be a true pathogenic change. The amino acid is highly conserved and belongs to a conserved acidic protein domain, it has a high Grantham score, the mutant protein is predicted to have a decreased stability and the variant was absent in 207 control samples. However, no conclusive evidence could be given as it is a missense mutation, and no *TJP2* mutations were identified in other hearing loss families. A mutation in *TJP2* has already been suggested to be associated with familial hypercholanaemia (OMIM 607709) (23). However, the inheritance may be oligogenic, only causing the disease in combination with a mutation in a second gene. It is possible that the *TJP2* variant is a pathogenic variant involved in familial hypercholanaemia or another autosomal recessive disease and that the occurrence in the current family is correlated to the hearing impairment.

In previous reports, patients of six families with significant linkage to DFNB7/11 did not carry *TMCI* mutations (4). In addition, we found three significantly linked families and three families with possible linkage that also lack pathogenic changes in *TMCI*. To screen for possible disease-causing mutations, we tested three hypotheses.

First, we hypothesized that *TMCI* is the disease-causing gene in these families but that the pathogenic change could not be detected by DNA sequencing. Therefore, MAQ of *TMCI* was performed in six hearing loss families to determine whether CNVs could be observed. While this screen failed to identify any deletions or duplication of the amplicons we used, it should be noted that smaller CNVs could have been missed as *TMCI* is large and only 12 amplicons were studied. Complete CNV analysis of *TMCI* may allow detecting smaller rearrangements. This could be performed either by using a fine-tiling array comparative genomic hybridization with oligonucleotides or by using a high-density single nucleotide polymorphism microarray. Assaying for other pathogenic changes in *TMCI* at the transcription level using mRNA from blood is not feasible because *TMCI* is not expressed in white blood cells. It should be noted, however, that this type of change is infrequent, making it somewhat implausible that all families would carry this type of pathogenic mutation. For family PE, we compared the hearing loss phenotype with two other

families, LMG128 and LMG248, segregating ADNSHL and carrying *TMCI* mutations (Fig. 1) (2, 7). The hearing loss of patients from all three families is comparable, starting in the first to second decade and affecting mainly the mid-to-high frequencies. Later on, the hearing loss becomes profound across most frequencies, showing some variation in the low-frequency thresholds. In family LMG128, the rate of progression seems to be faster compared with families LMG248 and PE. This phenotypic similarity may be an additional support to the hypothesis that *TMCI* is the disease-causing gene in family PE.

The second hypothesis we tested stated that a second deafness gene lies near *TMCI* and is the cause of the hearing loss in the families lacking a *TMCI* mutation. The common candidate region shared by all families with significant linkage includes only 14 genes. No single pathogenic change could be identified in any of these genes. However, our screen does not definitively exclude these genes as a possible new deafness gene. We may have missed mutations not detectable by DNA sequence analysis of exons. In addition, the LOC and c9orf genes might have additional exons, which have not been annotated yet.

In a third hypothesis, we considered that some families carry an undetected *TMCI* mutation, while others carry mutations in one or more new deafness genes. As a corollary to this hypothesis, the candidate region that contains this new gene(s) is much larger and many more candidate genes must therefore be screened for mutations.

In conclusion, we have shown that *TMCI* mutations are one of the more frequent causes of ARNSHL. Our data also show that a subset of families linked to the DFNA36-DFNB7/11 loci do not carry mutations in *TMCI* exons, suggesting either a remarkably high proportion of mutations outside of the exons or an additional deafness gene in this region.

Supplementary material

Fig. S1. Pedigrees of all families analysed, with the linked haplotypes at loci DFNA36 and DFNB7/11. All individuals with hearing loss are indicated with black symbols, the open symbols are individuals with normal hearing and symbols with question marks indicate individuals with an uncertain phenotype. The analysed markers are listed at the left, and the linked haplotype is indicated with a box.

Supplementary materials are available as part of the online article at <http://www.blackwell-synergy.com>

Acknowledgements

We are very grateful to Gilad Wainreb for helping us to score the conservation of amino acids using the ConSeq Server. This study

was supported by grants from EUROHEAR (LSHG-CT-2004-512063), the Fund for Scientific Research Flanders (FWO-F, grant G.0138.07), the National Institutes of Health (1RO1DC02842, R. J. H. S.) and the Oticon Foundation (M. B. P.). N. H. is a fellow of the Fund for Scientific Research Flanders (FWO-F).

References

1. Parving A. The need for universal neonatal hearing screening – some aspects of epidemiology and identification. *Acta Paediatr Suppl* 1999; 88: 69–72.
2. Kurima K, Peters LM, Yang Y et al. Dominant and recessive deafness caused by mutations of a novel gene, TMC1, required for cochlear hair-cell function. *Nat Genet* 2002; 30: 277–284.
3. Meyer CG, Gasmelseed NM, Mergani A et al. Novel TMC1 structural and splice variants associated with congenital nonsyndromic deafness in a Sudanese pedigree. *Hum Mutat* 2005; 25: 100.
4. Santos RL, Wajid M, Khan MN et al. Novel sequence variants in the TMC1 gene in Pakistani families with autosomal recessive hearing impairment. *Hum Mutat* 2005; 26: 396.
5. Kitajiri SI, McNamara R, Makishima T et al. Identities, frequencies and origins of TMC1 mutations causing DFNB7/B11 deafness in Pakistan. *Clin Genet* 2007; 72: 546–550.
6. Tlili A, Rebeh IB, Aifa-Hmani M et al. TMC1 but not TMC2 is responsible for autosomal recessive nonsyndromic hearing impairment in Tunisian families. *Audiol Neurootol* 2008; 13: 213–218.
7. Kitajiri S, Makishima T, Friedman T et al. A novel mutation at the DFNA36 hearing loss locus reveals a critical function and potential genotype-phenotype correlation for amino acid-572 of TMC1. *Clin Genet* 2007; 71: 148–152.
8. Kalay E, Karaguzel A, Caylan R et al. Four novel TMC1 (DFNB7/DFNB11) mutations in Turkish patients with congenital autosomal recessive nonsyndromic hearing loss. *Hum Mutat* 2005; 26: 591.
9. Vreugde S, Erven A, Kros CJ et al. Beethoven, a mouse model for dominant, progressive hearing loss DFNA36. *Nat Genet* 2002; 30: 257–258.
10. Kurima K, Yang Y, Sorber K et al. Characterization of the transmembrane channel-like (TMC) gene family: functional clues from hearing loss and epidermodysplasia verruciformis. *Genomics* 2003; 82: 300–308.
11. Keresztes G, Mutai H, Heller S. TMC and EVER genes belong to a larger novel family, the TMC gene family encoding transmembrane proteins. *BMC Genomics* 2003; 4: 24.
12. Marcotti W, Erven A, Johnson SL et al. Tmc1 is necessary for normal functional maturation and survival of inner and outer hair cells in the mouse cochlea. *J Physiol* 2006; 574: 677–698.
13. Jain PK, Fukushima K, Deshmukh D et al. A human recessive neurosensory nonsyndromic hearing impairment locus is potential homologue of murine deafness (dn) locus. *Hum Mol Genet* 1995; 4: 2391–2394.
14. Lindner TH, Hoffmann K. easyLINKAGE: a PERL script for easy and automated two-/multi-point linkage analyses. *Bioinformatics* 2005; 21: 405–407.
15. Lander E, Kruglyak L. Genetic dissection of complex traits: guidelines for interpreting and reporting linkage results. *Nat Genet* 1995; 11: 241–247.
16. Berezin C, Glaser F, Rosenberg J et al. ConSeq: the identification of functionally and structurally important residues in protein sequences. *Bioinformatics* 2004; 20: 1322–1324.
17. Capriotti E, Fariselli P, Casadio R. I-Mutant2.0: predicting stability changes upon mutation from the protein sequence or structure. *Nucleic Acids Res* 2005; 33: W306–W310.
18. Slegers K, Brouwers N, Gijssels I et al. APP duplication is sufficient to cause early onset Alzheimer's dementia with cerebral amyloid angiopathy. *Brain* 2006; 129: 2977–2983.
19. Suls A, Claeys KG, Goossens D et al. Microdeletions involving the SCN1A gene may be common in SCN1A-mutation-negative SMEI patients. *Hum Mutat* 2006; 27: 914–920.
20. Grantham R. Amino acid difference formula to help explain protein evolution. *Science* 1974; 185: 862–864.
21. Linde L, Boelz S, Neu-Yilik G et al. The efficiency of nonsense-mediated mRNA decay is an inherent character and varies among different cells. *Eur J Hum Genet* 2007; 15: 1156–1162.
22. Krawczak M, Reiss J, Cooper DN. The mutational spectrum of single base-pair substitutions in mRNA splice junctions of human genes: causes and consequences. *Hum Genet* 1992; 90: 41–54.
23. Carlton VE, Harris BZ, Puffenberger EG et al. Complex inheritance of familial hypercholanemia with associated mutations in TJP2 and BAAT. *Nat Genet* 2003; 34: 91–96.

7. Conclusions

The identification and analysis of altered gene function in inherited forms of limb malformations can provide essential information, not only concerning the pathogenesis of the disease, but also for understanding physiological processes during limb development. The present Ph.D thesis aimed to identify novel key factors and new molecular mechanisms involved in physiological and pathophysiological mechanisms during limb development. In order to identify novel genes and types of mutations, we wanted to focus on different human inherited limb malformations, such as Cenani-Lenz syndrome (CLS), Werner mesomelic syndrome (WMS), or Temtamy preaxial brachydactyly syndrome (TPBS).

During the Ph.D project, new genes and novel types of mutations were identified demonstrating that different components of evolutionary highly conserved pathways are important key factors during developing limb, each with specific function in limb patterning and outgrowth. In this respect, we identified (i) LRP4 as an essential component of Wnt signalling during limb formation, (ii) specific alterations in the long-range limb-specific enhancer of the *sonic hedgehog* (*SHH*) gene, *ZRS*, to cause a defined limb malformation, and (iii) mutations in *CHSY1* that alter chondroitin sulphate chain synthesis. Furthermore, we pointed out that the ciliary protein BBS12 is important in the pathogenesis of limb malformations seen in Bardet-Biedl syndrome, though the specific role in the context of limb bud initiation and patterning is yet unknown.

Additional results from this Ph.D thesis showed new pathogenic mechanisms underlying impaired limb development. We showed that LRP4 mutations in CLS cause a loss of LRP4 antagonistic function on Wnt signalling, which subsequently leads to an increased activation of LRP6-mediated Wnt signalling. Moreover, we elucidated the functional consequence of the described *WNT10B* mutation in SHFM and showed that the analyzed missense mutation causes a loss of WNT10B function and possibly a reduced LRP6-mediated Wnt signalling. In this context it is a highly interesting finding that we could provide first evidence for a putative direct cross-talk between the Wnt and Fgf signalling pathways by demonstrating the ability of Fgf8 to bind Wnt10b. As a consequence, Wnt10b loses its ability to activate Wnt signalling. In conclusion, this Ph.D thesis provides novel insights into the pathogenesis of limb malformations by the identification of new genes and mutations, the elucidation of underlying pathophysiological mechanisms, and the finding of a putative direct cross-talk between major signalling pathways involved in orchestrating physiological limb development.

8. References

- Adaimy L, Chouery E, Megarbane H, Mroueh S, Delague V et al. (2007) Mutation in WNT10A is associated with an autosomal recessive ectodermal dysplasia: the odontonycho-dermal dysplasia. *Am J Hum Genet* 81(4): 821-828.
- Agarwal P, Wylie JN, Galceran J, Arkhitko O, Li C et al. (2003) Tbx5 is essential for forelimb bud initiation following patterning of the limb field in the mouse embryo. *Development* 130(3): 623-633.
- Ahmad M, Abbas H, Haque S, Flatz G (1987) X-chromosomally inherited split-hand/split-foot anomaly in a Pakistani kindred. *Hum Genet* 75(2): 169-173.
- Anakwe K, Robson L, Hadley J, Buxton P, Church V et al. (2003) Wnt signalling regulates myogenic differentiation in the developing avian wing. *Development* 130(15): 3503-3514.
- Bacchelli C, Goodman FR, Scambler PJ, Winter RM (2001) Cenani-Lenz syndrome with renal hypoplasia is not linked to FORMIN or GREMLIN. *Clin Genet* 59(3): 203-205.
- Barrow JR, Thomas KR, Boussadia-Zahui O, Moore R, Kemler R et al. (2003) Ectodermal Wnt3/beta-catenin signaling is required for the establishment and maintenance of the apical ectodermal ridge. *Genes Dev* 17(3): 394-409.
- Basson CT, Bachinsky DR, Lin RC, Levi T, Elkins JA et al. (1997) Mutations in human TBX5 [corrected] cause limb and cardiac malformation in Holt-Oram syndrome. *Nat Genet* 15(1): 30-35.
- Beales PL, Elcioglu N, Woolf AS, Parker D, Flintner FA (1999) New criteria for improved diagnosis of Bardet-Biedl syndrome: results of a population survey. *J Med Genet* 36(6): 437-446.
- Bennett CN, Longo KA, Wright WS, Suva LJ, Lane TF et al. (2005) Regulation of osteoblastogenesis and bone mass by Wnt10b. *Proc Natl Acad Sci U S A* 102(9): 3324-3329.
- Bouwmeester T, Kim S, Sasai Y, Lu B, De Robertis EM (1996) Cerberus is a head-inducing secreted factor expressed in the anterior endoderm of Spemann's organizer. *Nature* 382(6592): 595-601.
- Brown SD, Twells RC, Hey PJ, Cox RD, Levy ER et al. (1998) Isolation and characterization of LRP6, a novel member of the low density lipoprotein receptor gene family. *Biochem Biophys Res Commun* 248(3): 879-888.
- Cadigan KM, Liu YI (2006) Wnt signaling: complexity at the surface. *J Cell Sci* 119(Pt 3): 395-402.
- Cenani A, Lenz W (1967) [Total syndactylia and total radioulnar synostosis in 2 brothers. A contribution on the genetics of syndactylia]. *Z Kinderheilkd* 101(3): 181-190.
- Charite J, de Graaff W, Shen S, Deschamps J (1994) Ectopic expression of Hoxb-8 causes duplication of the ZPA in the forelimb and homeotic transformation of axial structures. *Cell* 78(4): 589-601.
- Chen WJ, Goldstein JL, Brown MS (1990) NPXY, a sequence often found in cytoplasmic tails, is required for coated pit-mediated internalization of the low density lipoprotein receptor. *J Biol Chem* 265(6): 3116-3123.
- Chiang AP, Beck JS, Yen HJ, Tayeh MK, Scheetz TE et al. (2006) Homozygosity mapping with SNP arrays identifies TRIM32, an E3 ubiquitin ligase, as a Bardet-Biedl syndrome gene (BBS11). *Proc Natl Acad Sci U S A* 103(16): 6287-6292.
- Choi HY, Dieckmann M, Herz J, Niemeier A (2009) Lrp4, a novel receptor for Dickkopf 1 and sclerostin, is expressed by osteoblasts and regulates bone growth and turnover in vivo. *PLoS One* 4(11): e7930.
- Clevers H (2006) Wnt/beta-catenin signaling in development and disease. *Cell* 127(3): 469-480.

- Crackower MA, Scherer SW, Rommens JM, Hui CC, Poorkaj P et al. (1996) Characterization of the split hand/split foot malformation locus SHFM1 at 7q21.3-q22.1 and analysis of a candidate gene for its expression during limb development. *Hum Mol Genet* 5(5): 571-579.
- Dailey L, Ambrosetti D, Mansukhani A, Basilico C (2005) Mechanisms underlying differential responses to FGF signaling. *Cytokine Growth Factor Rev* 16(2): 233-247.
- Dealy CN, Roth A, Ferrari D, Brown AM, Kosher RA (1993) Wnt-5a and Wnt-7a are expressed in the developing chick limb bud in a manner suggesting roles in pattern formation along the proximodistal and dorsoventral axes. *Mech Dev* 43(2-3): 175-186.
- Duchesne A, Gautier M, Chadi S, Grohs C, Floriot S et al. (2006) Identification of a doublet missense substitution in the bovine LRP4 gene as a candidate causal mutation for syndactyly in Holstein cattle. *Genomics* 88(5): 610-621.
- Duijf PH, van Bokhoven H, Brunner HG (2003) Pathogenesis of split-hand/split-foot malformation. *Hum Mol Genet* 12 Spec No 1: R51-60.
- Elliott AM, Reed MH, Evans JA, Cross HG, Chudley AE (2004) Cenani-Lenz syndactyly in a patient with features of Kabuki syndrome. *Clin Dysmorphol* 13(3): 143-150.
- Faiyaz-Ul-Haque M, Zaidi SH, King LM, Haque S, Patel M et al. (2005) Fine mapping of the X-linked split-hand/split-foot malformation (SHFM2) locus to a 5.1-Mb region on Xq26.3 and analysis of candidate genes. *Clin Genet* 67(1): 93-97.
- Farag TI, Teebi AS (1988) Bardet-Biedl and Laurence-Moon syndromes in a mixed Arab population. *Clin Genet* 33(2): 78-82.
- Galceran J, Farinas I, Depew MJ, Clevers H, Grosschedl R (1999) Wnt3a-/- like phenotype and limb deficiency in Lef1(-/-)Tcf1(-/-) mice. *Genes Dev* 13(6): 709-717.
- Glinka A, Wu W, Delius H, Monaghan AP, Blumenstock C et al. (1998) Dickkopf-1 is a member of a new family of secreted proteins and functions in head induction. *Nature* 391(6665): 357-362.
- Gong Y, Slee RB, Fukai N, Rawadi G, Roman-Roman S et al. (2001) LDL receptor-related protein 5 (LRP5) affects bone accrual and eye development. *Cell* 107(4): 513-523.
- Goodman FR, Majewski F, Collins AL, Scambler PJ (2002) A 117-kb microdeletion removing HOXD9-HOXD13 and EVX2 causes synpolydactyly. *Am J Hum Genet* 70(2): 547-555.
- Gordon MD, Nusse R (2006) Wnt signaling: multiple pathways, multiple receptors, and multiple transcription factors. *J Biol Chem* 281(32): 22429-22433.
- Gul D, Oktenli C (2002) Evidence for autosomal recessive inheritance of split hand/split foot malformation: a report of nine cases. *Clin Dysmorphol* 11(3): 183-186.
- Hartmann C, Tabin CJ (2001) Wnt-14 plays a pivotal role in inducing synovial joint formation in the developing appendicular skeleton. *Cell* 104(3): 341-351.
- He X, Semenov M, Tamai K, Zeng X (2004) LDL receptor-related proteins 5 and 6 in Wnt/beta-catenin signaling: arrows point the way. *Development* 131(8): 1663-1677.
- Huangfu D, Anderson KV (2006) Signaling from Smo to Ci/Gli: conservation and divergence of Hedgehog pathways from Drosophila to vertebrates. *Development* 133(1): 3-14.
- Ianakev P, Kilpatrick MW, Toudjarska I, Basel D, Beighton P et al. (2000) Split-hand/split-foot malformation is caused by mutations in the p63 gene on 3q27. *Am J Hum Genet* 67(1): 59-66.
- Itasaki N, Jones CM, Mercurio S, Rowe A, Domingos PM et al. (2003) Wise, a context-dependent activator and inhibitor of Wnt signalling. *Development* 130(18): 4295-4305.
- Jena N, Martin-Seisdedos C, McCue P, Croce CM (1997) BMP7 null mutation in mice: developmental defects in skeleton, kidney, and eye. *Exp Cell Res* 230(1): 28-37.
- Jiang J, Struhl G (1998) Regulation of the Hedgehog and Wingless signalling pathways by the F-box/WD40-repeat protein Slimb. *Nature* 391(6666): 493-496.

- Johnson EB, Hammer RE, Herz J (2005) Abnormal development of the apical ectodermal ridge and polysyndactyly in *Megf7*-deficient mice. *Hum Mol Genet* 14(22): 3523-3538.
- Kang S, Graham JM, Jr., Olney AH, Biesecker LG (1997) *GLI3* frameshift mutations cause autosomal dominant Pallister-Hall syndrome. *Nat Genet* 15(3): 266-268.
- Kano H, Kurosawa K, Horii E, Ikegawa S, Yoshikawa H et al. (2005) Genomic rearrangement at 10q24 in non-syndromic split-hand/split-foot malformation. *Hum Genet* 118(3-4): 477-483.
- Katsanis N, Ansley SJ, Badano JL, Eichers ER, Lewis RA et al. (2001) Triallelic inheritance in Bardet-Biedl syndrome, a Mendelian recessive disorder. *Science* 293(5538): 2256-2259.
- Kazanskaya O, Glinka A, del Barco Barrantes I, Stannek P, Niehrs C et al. (2004) *R-Spondin2* is a secreted activator of Wnt/beta-catenin signaling and is required for *Xenopus* myogenesis. *Dev Cell* 7(4): 525-534.
- Kelly OG, Pinson KI, Skarnes WC (2004) The Wnt co-receptors *Lrp5* and *Lrp6* are essential for gastrulation in mice. *Development* 131(12): 2803-2815.
- Klint P, Claesson-Welsh L (1999) Signal transduction by fibroblast growth factor receptors. *Front Biosci* 4: D165-177.
- Laufer E, Nelson CE, Johnson RL, Morgan BA, Tabin C (1994) Sonic hedgehog and *Fgf-4* act through a signaling cascade and feedback loop to integrate growth and patterning of the developing limb bud. *Cell* 79(6): 993-1003.
- Lettice LA, Heaney SJ, Purdie LA, Li L, de Beer P et al. (2003) A long-range *Shh* enhancer regulates expression in the developing limb and fin and is associated with preaxial polydactyly. *Hum Mol Genet* 12(14): 1725-1735.
- Lettice LA, Horikoshi T, Heaney SJ, van Baren MJ, van der Linde HC et al. (2002) Disruption of a long-range cis-acting regulator for *Shh* causes preaxial polydactyly. *Proc Natl Acad Sci U S A* 99(11): 7548-7553.
- Li H, Wang CY, Wang JX, Wu GS, Yu P et al. (2009) Mutation analysis of a large Chinese pedigree with congenital preaxial polydactyly. *Eur J Hum Genet* 17(5): 604-610.
- Logan CY, Nusse R (2004) The Wnt signaling pathway in development and disease. *Annu Rev Cell Dev Biol* 20: 781-810.
- Lyle R, Radhakrishna U, Blouin JL, Gagos S, Everman DB et al. (2006) Split-hand/split-foot malformation 3 (*SHFM3*) at 10q24, development of rapid diagnostic methods and gene expression from the region. *Am J Med Genet A* 140(13): 1384-1395.
- MacDonald BT, Tamai K, He X (2009) Wnt/beta-catenin signaling: components, mechanisms, and diseases. *Dev Cell* 17(1): 9-26.
- Mani A, Radhakrishnan J, Wang H, Mani A, Mani MA et al. (2007) *LRP6* mutation in a family with early coronary disease and metabolic risk factors. *Science* 315(5816): 1278-1282.
- Mao B, Wu W, Li Y, Hoppe D, Stannek P et al. (2001a) LDL-receptor-related protein 6 is a receptor for Dickkopf proteins. *Nature* 411(6835): 321-325.
- Mao J, Wang J, Liu B, Pan W, Farr GH, 3rd et al. (2001b) Low-density lipoprotein receptor-related protein-5 binds to Axin and regulates the canonical Wnt signaling pathway. *Mol Cell* 7(4): 801-809.
- Marshall WF, Nonaka S (2006) Cilia: tuning in to the cell's antenna. *Curr Biol* 16(15): R604-614.
- May P, Woldt E, Matz RL, Boucher P (2007) The LDL receptor-related protein (LRP) family: an old family of proteins with new physiological functions. *Ann Med* 39(3): 219-228.
- McDonald MT, Gorski JL (1993) Nager acrofacial dysostosis. *J Med Genet* 30(9): 779-782.

- Niemann S, Zhao C, Pascu F, Stahl U, Aulepp U et al. (2004) Homozygous WNT3 mutation causes tetra-amelia in a large consanguineous family. *Am J Hum Genet* 74(3): 558-563.
- Niswander L, Jeffrey S, Martin GR, Tickle C (1994) A positive feedback loop coordinates growth and patterning in the vertebrate limb. *Nature* 371(6498): 609-612.
- Niswander L, Tickle C, Vogel A, Booth I, Martin GR (1993) FGF-4 replaces the apical ectodermal ridge and directs outgrowth and patterning of the limb. *Cell* 75(3): 579-587.
- Odent S, Atti-Bitach T, Blayau M, Mathieu M, Aug J et al. (1999) Expression of the Sonic hedgehog (SHH) gene during early human development and phenotypic expression of new mutations causing holoprosencephaly. *Hum Mol Genet* 8(9): 1683-1689.
- Ohazama A, Johnson EB, Ota MS, Choi HY, Porntaveetus T et al. (2008) Lrp4 modulates extracellular integration of cell signaling pathways in development. *PLoS One* 3(12): e4092.
- Ornitz DM, Itoh N (2001) Fibroblast growth factors. *Genome Biol* 2(3): REVIEWS3005.
- Ozen RS, Baysal BE, Devlin B, Farr JE, Gorry M et al. (1999) Fine mapping of the split-hand/split-foot locus (SHFM3) at 10q24: evidence for anticipation and segregation distortion. *Am J Hum Genet* 64(6): 1646-1654.
- Parr BA, McMahon AP (1995) Dorsalizing signal Wnt-7a required for normal polarity of D-V and A-P axes of mouse limb. *Nature* 374(6520): 350-353.
- Parr BA, Shea MJ, Vassileva G, McMahon AP (1993) Mouse Wnt genes exhibit discrete domains of expression in the early embryonic CNS and limb buds. *Development* 119(1): 247-261.
- Pepinsky RB, Zeng C, Wen D, Rayhorn P, Baker DP et al. (1998) Identification of a palmitic acid-modified form of human Sonic hedgehog. *J Biol Chem* 273(22): 14037-14045.
- Pinson KI, Brennan J, Monkley S, Avery BJ, Skarnes WC (2000) An LDL-receptor-related protein mediates Wnt signalling in mice. *Nature* 407(6803): 535-538.
- Radhakrishna U, Wild A, Grzeschik KH, Antonarakis SE (1997) Mutation in GLI3 in postaxial polydactyly type A. *Nat Genet* 17(3): 269-271.
- Rallis C, Bruneau BG, Del Buono J, Seidman CE, Seidman JG et al. (2003) Tbx5 is required for forelimb bud formation and continued outgrowth. *Development* 130(12): 2741-2751.
- Riddle RD, Johnson RL, Laufer E, Tabin C (1993) Sonic hedgehog mediates the polarizing activity of the ZPA. *Cell* 75(7): 1401-1416.
- Rodriguez-Esteban C, Tsukui T, Yonei S, Magallon J, Tamura K et al. (1999) The T-box genes Tbx4 and Tbx5 regulate limb outgrowth and identity. *Nature* 398(6730): 814-818.
- Roessler E, Belloni E, Gaudenz K, Jay P, Berta P et al. (1996) Mutations in the human Sonic Hedgehog gene cause holoprosencephaly. *Nat Genet* 14(3): 357-360.
- Rohmann E, Brunner HG, Kayserili H, Uyguner O, Nurnberg G et al. (2006) Mutations in different components of FGF signaling in LADD syndrome. *Nat Genet* 38(4): 414-417.
- Roscioli T, Taylor PJ, Bohlken A, Donald JA, Masel J et al. (2004) The 10q24-linked split hand/split foot syndrome (SHFM3): narrowing of the critical region and confirmation of the clinical phenotype. *Am J Med Genet A* 124A(2): 136-141.
- Ross AJ, May-Simera H, Eichers ER, Kai M, Hill J et al. (2005) Disruption of Bardet-Biedl syndrome ciliary proteins perturbs planar cell polarity in vertebrates. *Nat Genet* 37(10): 1135-1140.
- Rudnicki JA, Brown AM (1997) Inhibition of chondrogenesis by Wnt gene expression in vivo and in vitro. *Dev Biol* 185(1): 104-118.

- Saunders JW, Jr. (1948) The proximo-distal sequence of origin of the parts of the chick wing and the role of the ectoderm. *J Exp Zool* 108(3): 363-403.
- Saxena R, Voight BF, Lyssenko V, Burt NP, de Bakker PI et al. (2007) Genome-wide association analysis identifies loci for type 2 diabetes and triglyceride levels. *Science* 316(5829): 1331-1336.
- Scherer SW, Poorkaj P, Allen T, Kim J, Geshuri D et al. (1994) Fine mapping of the autosomal dominant split hand/split foot locus on chromosome 7, band q21.3-q22.1. *Am J Hum Genet* 55(1): 12-20.
- Schwabe GC, Mundlos S (2004) Genetics of congenital hand anomalies. *Handchir Mikrochir Plast Chir* 36(2-3): 85-97.
- Semenov M, Tamai K, He X (2005) SOST is a ligand for LRP5/LRP6 and a Wnt signaling inhibitor. *J Biol Chem* 280(29): 26770-26775.
- Stoetzel C, Muller J, Laurier V, Davis EE, Zaghoul NA et al. (2007) Identification of a novel BBS gene (BBS12) highlights the major role of a vertebrate-specific branch of chaperonin-related proteins in Bardet-Biedl syndrome. *Am J Hum Genet* 80(1): 1-11.
- Stone DM, Hynes M, Armanini M, Swanson TA, Gu Q et al. (1996) The tumour-suppressor gene patched encodes a candidate receptor for Sonic hedgehog. *Nature* 384(6605): 129-134.
- Sun M, Ma F, Zeng X, Liu Q, Zhao XL et al. (2008) Triphalangeal thumb-polysyndactyly syndrome and syndactyly type IV are caused by genomic duplications involving the long range, limb-specific SHH enhancer. *J Med Genet* 45(9): 589-595.
- Sun X, Mariani FV, Martin GR (2002) Functions of FGF signalling from the apical ectodermal ridge in limb development. *Nature* 418(6897): 501-508.
- Takeuchi JK, Koshihara-Takeuchi K, Matsumoto K, Vogel-Hopker A, Naitoh-Matsuo M et al. (1999) Tbx5 and Tbx4 genes determine the wing/leg identity of limb buds. *Nature* 398(6730): 810-814.
- Tamai K, Semenov M, Kato Y, Spokony R, Liu C et al. (2000) LDL-receptor-related proteins in Wnt signal transduction. *Nature* 407(6803): 530-535.
- Temtam SA, Ismail S, Nemat A (2003) Mild facial dysmorphism and quasidominant inheritance in Cenani-Lenz syndrome. *Clin Dysmorphol* 12(2): 77-83.
- Ugur SA, Tolun A (2008) Homozygous WNT10b mutation and complex inheritance in Split-Hand/Foot Malformation. *Hum Mol Genet* 17(17): 2644-2653.
- Villavicencio EH, Walterhouse DO, Iannaccone PM (2000) The sonic hedgehog-patched-gli pathway in human development and disease. *Am J Hum Genet* 67(5): 1047-1054.
- Vortkamp A, Gessler M, Grzeschik KH (1991) GLI3 zinc-finger gene interrupted by translocations in Greig syndrome families. *Nature* 352(6335): 539-540.
- Wallingford JB, Habas R (2005) The developmental biology of Dishevelled: an enigmatic protein governing cell fate and cell polarity. *Development* 132(20): 4421-4436.
- Weston AD, Hoffman LM, Underhill TM (2003) Revisiting the role of retinoid signaling in skeletal development. *Birth Defects Res C Embryo Today* 69(2): 156-173.
- Williams KP, Rayhorn P, Chi-Rosso G, Garber EA, Strauch KL et al. (1999) Functional antagonists of sonic hedgehog reveal the importance of the N terminus for activity. *J Cell Sci* 112 (Pt 23): 4405-4414.
- Witte F, Dokas J, Neuendorf F, Mundlos S, Stricker S (2009) Comprehensive expression analysis of all Wnt genes and their major secreted antagonists during mouse limb development and cartilage differentiation. *Gene Expr Patterns* 9(4): 215-223.
- Wodarz A, Nusse R (1998) Mechanisms of Wnt signaling in development. *Annu Rev Cell Dev Biol* 14: 59-88.
- Wu L, Liang D, Niikawa N, Ma F, Sun M et al. (2009) A ZRS duplication causes syndactyly type IV with tibial hypoplasia. *Am J Med Genet A* 149A(4): 816-818.

- Xu Q, Wang Y, Dabdoub A, Smallwood PM, Williams J et al. (2004) Vascular development in the retina and inner ear: control by Norrin and Frizzled-4, a high-affinity ligand-receptor pair. *Cell* 116(6): 883-895.
- Yamaguchi TP (2001) Heads or tails: Wnts and anterior-posterior patterning. *Curr Biol* 11(17): R713-724.
- Yamaguchi YL, Tanaka SS, Kasa M, Yasuda K, Tam PP et al. (2006) Expression of low density lipoprotein receptor-related protein 4 (Lrp4) gene in the mouse germ cells. *Gene Expr Patterns* 6(6): 607-612.
- Yang Y (2003) Wnts and wing: Wnt signaling in vertebrate limb development and musculoskeletal morphogenesis. *Birth Defects Res C Embryo Today* 69(4): 305-317.
- Yang Y, Topol L, Lee H, Wu J (2003) Wnt5a and Wnt5b exhibit distinct activities in coordinating chondrocyte proliferation and differentiation. *Development* 130(5): 1003-1015.
- Yashiro K, Zhao X, Uehara M, Yamashita K, Nishijima M et al. (2004) Regulation of retinoic acid distribution is required for proximodistal patterning and outgrowth of the developing mouse limb. *Dev Cell* 6(3): 411-422.
- Zaghloul NA, Katsanis N (2009) Mechanistic insights into Bardet-Biedl syndrome, a model ciliopathy. *J Clin Invest* 119(3): 428-437.
- Zakany J, Duboule D (2007) The role of Hox genes during vertebrate limb development. *Curr Opin Genet Dev* 17(4): 359-366.
- Zeng X, Huang H, Tamai K, Zhang X, Harada Y et al. (2008) Initiation of Wnt signaling: control of Wnt coreceptor Lrp6 phosphorylation/activation via frizzled, dishevelled and axin functions. *Development* 135(2): 367-375.
- Zou H, Niswander L (1996) Requirement for BMP signaling in interdigital apoptosis and scale formation. *Science* 272(5262): 738-741.
- Zuniga A, Haramis AP, McMahon AP, Zeller R (1999) Signal relay by BMP antagonism controls the SHH/FGF4 feedback loop in vertebrate limb buds. *Nature* 401(6753): 598-602.

9. Appendix: Acknowledgements and Academic Curriculum Vitae

Acknowledgements

The preparation of this Ph.D thesis would not have been possible without the support, hard work and endless efforts of a large number of individuals and institutions. Therefore it is a pleasure for me to thank those who made this thesis feasible and enjoyable.

First of all I would like to thank my supervisor Dr. Bernd Wollnik, who gave me the opportunity to conduct this Ph.D thesis within his group. Bernd always supported me with good advices, great motivation, inspiration and excellent scientific knowledge. He taught me how to ask questions in the research world and how to express my ideas. Furthermore he showed me different ways to approach a research problem and the need to be persistent to accomplish any goal.

Next I am grateful to Prof. Dr. Gabriele Pfitzer and Prof. Dr. Peter Nürnberg for supervising my thesis and my lectures during the MD-PhD program. They always displayed great interest and helpfulness for my work.

I am especially indebted to my colleges from the AG Wollnik who supported me in many different ways. Special thank to Dr. Yun Li for introducing me into the field of molecular genetics, for endless scientific discussions and always kind assistance. In particular I want to express my gratitude to Nadine Plume, who became one of my best friends also outside the lab, for her open mind for scientific and technical problems, her mentally support and encouragement. Finally I also want to thank Dr. Gökhan Yigit for his useful comments and suggestions for my experimental work and Esther Pohl, Katharina Keupp, Esther Milz and Martin Rachwalski for their daily humour, laugh and fun in the lab. You all made my Ph.D time enjoyable and unforgettable.

Last but no least, I want to thank my parents and the most important person at my side, Manuel Stollfuß, for their understanding, support, love and care. Thank you for believing in me and escorting me through this important time of my life.

Academic Curriculum Vitae

Personal Data

Surname Pawlik

Forename Barbara

Titel Master of Science
(Dipl.Biol.)

Date of birth 28. March 1982

Birthplace Ratibor (Poland)

Adress Arnulfstr.14

City 50937 Cologne, Germany

Phone +49 1784 765044

Email bpawlik@web.de

Nationality German

Office Adress Center for Molecular
Medicine Cologne (CMMC)
Institute of Human Genetics
University of Cologne,
Robert-Kochst.21,
NRW, Cologne
D-50931, Germany
Tel.: +49 221 478-89558



Education

15.10.2001-June 2006

Study of Biology, University of Cologne, Germany
Key classes: medical Genetics, Biochemistry,
Pharmacology

1992-2001

Secondary school, Hölderlin Gymnasium, Cologne,
qualification for University entrance

1988-1992

Elementary school, Gebrüder Grimm Grundschule
Leverkusen, Germany

Work experience

January 2007 to date

Interdisciplinary Postgraduate Programm in Molecular
Medicine at the Institute of Human Genetics,
University of Cologne, Study of molecular medicine
Dissertation at the Department of Human Genetics,
Group of Dr. Bernd Wollnik.
Dissertation thesis: Molecular mechanisms of congenital limb
malformations

October 2006

-December 2006

Traineeship at the Institute for Human Genetics, Group
of Dr. Bernd Wollnik, University of Cologne

July 2006-Oktober 2006

Scientific Stay at the University of Oxford, England,
UK, Wellcome Trust Centre for Human Genetics,
Group of Prof. Dr. Dominique Gauguier

June 2005-July 2006

Diploma thesis in Pharmacology, Institute for
Pharmacology, University of Cologne, Group of
Prof. Dr. Dirk Gründemann
Diploma thesis: Physiological substrate search
for the human Organic Cation Transporter 2 (OCT2h)
Academic degree: Master of Science (Dipl.Biol)

Publications

Pawlik B, Mir A, Iqbal H, Li Y, Nürnberg G, Becker C, Qamar R, Nürnberg P, Wollnik B. **A Novel Familial *BBS12* Mutation Associated with a Mild Phenotype: Implications for Clinical and Molecular Diagnostic Strategies.** *Mol Syndromol* (2010); 1:27-34.

Li Y*, **Pawlik B***, Elcioglu N, Aglan M, Kayserili H, Yigit G, Percin F, Goodman F, Nürnberg G, Cenani A, Urquhart J, Chung B, Ismail S, Amr K, Aslanger AD, Becker C, Netzer C, Scambler P, Eyaid W, Hamamy H, Clayton-Smith Y, Hennekam R, Nürnberg P, Herz J, Temtamy SA, Wollnik B. **LRP4 Mutations Alter Wnt/b-Catenin Signalling and Cause Limb and Kidney Malformations in Cenani-lenz Syndrome.** *Am J Hum Genet* (2010);86(5):696-706.

* These authors contributed equally to this work

Wieczorek D, **Pawlik B**, Li Y, Akarsu NA, Caliebe A, May KJ, Schweiger B, Vargas FR, Balci S, Gillessen-Kaesbach G, Wollnik B. **A specific mutation in the distant sonic hedgehog cis-regulator (ZRS) causes Werner mesomelic syndrome while complete ZRS duplications underlie Haas type polysyndactyly and preaxial polydactyly with or without triphalangeal thumb.** *Hum Mutat.* (2010); 31(1):81-9.

Pawlik B, Yigit G, Wollnik B. **Reduced LRP6-mediated WNT10B signalling in the pathogenesis of SHFM6.** (submitted)

Li Y, Laue K, Temtamy S, Aglan M, Kotan L.D, Yigit G, Husniye C, **Pawlik B**, Nürnberg G, Wakeling EL, Quarrell OW, Baessmann I, Lanktree MB, Yilmaz M, Hegele RA, Amr K, May KW, Nürnberg P, Topaloglu AK, Hammerschmidt M, Wollnik B. **Temtamy preaxial brachydactyly syndrome is caused by loss-of-function mutations in Chondroitin synthase 1, a potential target of BMP signalling.** In Press, *Am J Hum Genet* (2010).

Elçioglu NH, **Pawlik B**, Colak B, Beck M, Wollnik B. **A novel loss-of-function mutation in the GNS gene causes Sanfilippo syndrome type D.** *Genet Couns* (2009); 20(2):133-9.

Hilgert N, Alasti F, Dieltjens N, **Pawlik B**, Wollnik B, Uyguner O, Delmaghani S, Weil D, Petit C, Danis E, Yang T, Pandelia E, Petersen MB, Goossens D, Favero JD, Sanati MH, Smith RJ, Van Camp G. **Mutation analysis of TMC1 identifies four new mutations and**

suggests an additional deafness gene at loci DFNA36 and DFNB7/11. Clin Genet. (2008); 74(3):223-32.

Bach M, Grigat S, **Pawlik B**, Fork C, Utermöhlen O, Pal S, Banczyk D, Lazar A, Schömig E, Gründemann D. **Fast set-up of doxycycline-inducible protein expression in human cell lines with a single plasmid based on Epstein-Barr virus replication and the simple tetracycline repressor.**; FEBS J. (2007);274(3):783-90.

Congresses

Participation at the 18th Annual Meeting of the German Society of Human Genetics March 7 –10, 2007, Bonn.

Wieczorek D, **Pawlik B**, Li Y, Akarsu NA, Caliebe A, May KJ, Schweiger B, Vargas FR, Balci S, Gillessen-Kaesbach G, Wollnik B. Oral presentation: Hypoplasia of tibia with polysyndactyly (Werner syndrome) is allelic to preaxial polydactyly II (PPD2) and caused by a point mutation in the distant Sonic Hedgehog (SHH) cis-regulator (ZRS). 19th Annual Meeting of the German Society of Human Genetics, April 8-10, 2008, Hannover.

Pawlik B, Wollnik B, Poster Presentation: The p.R332W mutation in WNT10b causes split hand/foot malformation by a reduced activation of LRP6-mediated WNT signalling. 20th Annual Meeting of the German Society of Human Genetics, April 1-3, 2009, Aachen.

Li Y, Kaue K, Yigit G, Temtamy SA, Aglam M, **Pawlik B**, Nürnberg G, Wakeling EL, Quarrel OW, Nürnberg P, Topaloglu KA, Hammerschmidt M, Wollnik B, Oral presentation: Homozygous disruption of an extracellular matrix component cause Temtamy preaxial brachydactyly syndrome. 21th Annual Meeting of the German Society of Human Genetics, March 2-4, 2010, Hamburg.

Erklärung

Ich versichere, dass ich die von mir vorgelegte Dissertation selbständig angefertigt, die benutzten Quellen und Hilfsmittel vollständig angegeben und die Stellen der Arbeit - einschließlich Tabellen, Karten, und Abbildungen - , die anderen Werken im Wortlaut oder dem Sinn nach entnommen sind, in jedem Einzelfall als Entlehnung kenntlich gemacht habe; dass diese Dissertation noch keiner anderen Fakultät oder Universität zur Prüfung vorgelegen hat; dass sie – abgesehen von unten angegebenen Teilpublikationen – noch nicht veröffentlicht worden ist sowie, dass ich eine solche Veröffentlichung vor Abschluss des Promotionsverfahrens nicht vornehmen werde. Die Bestimmungen dieser Promotionsordnung sind mir bekannt. Die von mir vorgelegte Dissertation ist von Dr. med. Bernd Wollnik betreut worden.

Teilpublikationen:

Ich versichere, dass ich alle Angaben wahrheitsgemäß nach bestem Wissen und Gewissen gemacht habe und verpflichte mich, jedmögliche, die obigen Angaben betreffenden Veränderungen, dem Promotionsausschuss unverzüglich mitzuteilen.

Köln, den 23.11.2010

Ort, Datum

.....

Unterschrift